The thalamocortcal symphony : how thalamus and cortex play together in schizophrenia and plastcity

Yi Qin

Université de Strasbourg

UNIVERSITÉ DE STRASBOURG

École doctorale
Sciences de la vie et de la santé | ED 414
Université de Strasbourg

ÉCOLE DOCTORALE DES SCIENCES DE LA VIE ET DE LA SANTÉ

Inserm, U1114

THÈSE présentée par :

Yi QIN

soutenue le : **18.12. 2023**

pour obtenir le grade de : **Docteur de l'université de Strasbourg** Discipline/ Spécialité : Neurosciences

La symphonie thalamocorticale : comment le thalamus et le cortex s'accordent ensemble dans la schizophrénie et la plasticité

THÈSE dirigée par :

M. PINAULT Didier	Chargé de recherche HDR
M. ROELFSEMA Pieter	Professeur University of Amsterdam
M. LEVELT Christiaan	Professeur Netherland Institute for Neurosciencee

RAPPORTEURS :

M. UHLHAAS Peter	Professeur Charité – Universitätsmedizin Berlin
Mme. WIERINGA Corette	Professeur Radboud University Nijmegen

AUTRES MEMBRES DU JURY :

M. VEINANTE Pierre	Professeur Université de Strasbourg
M. PENNARTZ Cyriel	Professeur University of Amsterdam
M. OLCESE Umberto	Associate Professor University of Amsterdam

---

INVITÉS : (le cas échéant)

The Thalamocortical Symphony

How Thalamus and Cortex Play Together in Schizophrenia and Plasticity

Yi Qin

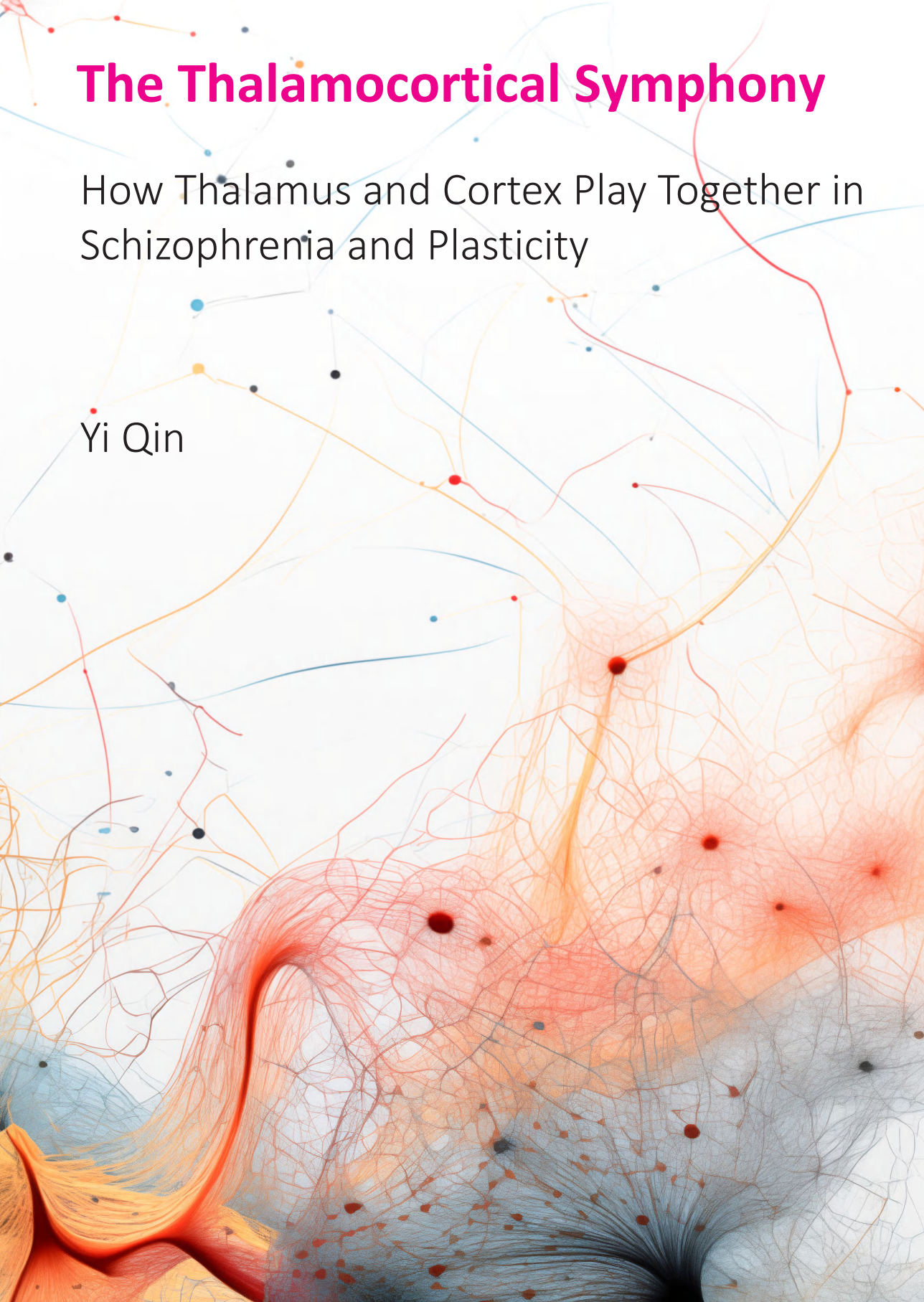

The Thalamocortical Symphony: How Thalamus and Cortex Play Together in Schizophrenia and Plasticity

Yi Qin

ISBN/EAN: 978-94-6473-300-6

The research described in this thesis was carried out at the Netherlands Institue for Neuroscience, an Institute of the Royal Netherlands Academy for Arts and Sciences (KNAW), Amsterdam, The Netherlands and Inserm, U1114, Université de Strasbourg, Strasbourg, France.

Cover design: Yi Qin

Layout and design: Yi Qin

The Thalamocortical Symphony: How Thalamus and Cortex Play Together in Schizophrenia and Plasticity

ACADEMISCH PROEFSCHRIFT

ter verkrijging van de graad van doctor
aan de Universiteit van Amsterdam
op gezag van de Rector Magnificus
prof. dr. ir. P.P.C.C. Verbeek
ten overstaan van een door het College voor Promoties ingestelde commissie,
in het openbaar te verdedigen in de Agnietenkapel
op maandag 18 december 2023, te 16.00 uur

door Yi Qin
geboren te Sichuan

Table of Contents

Chapter 1

Introduction

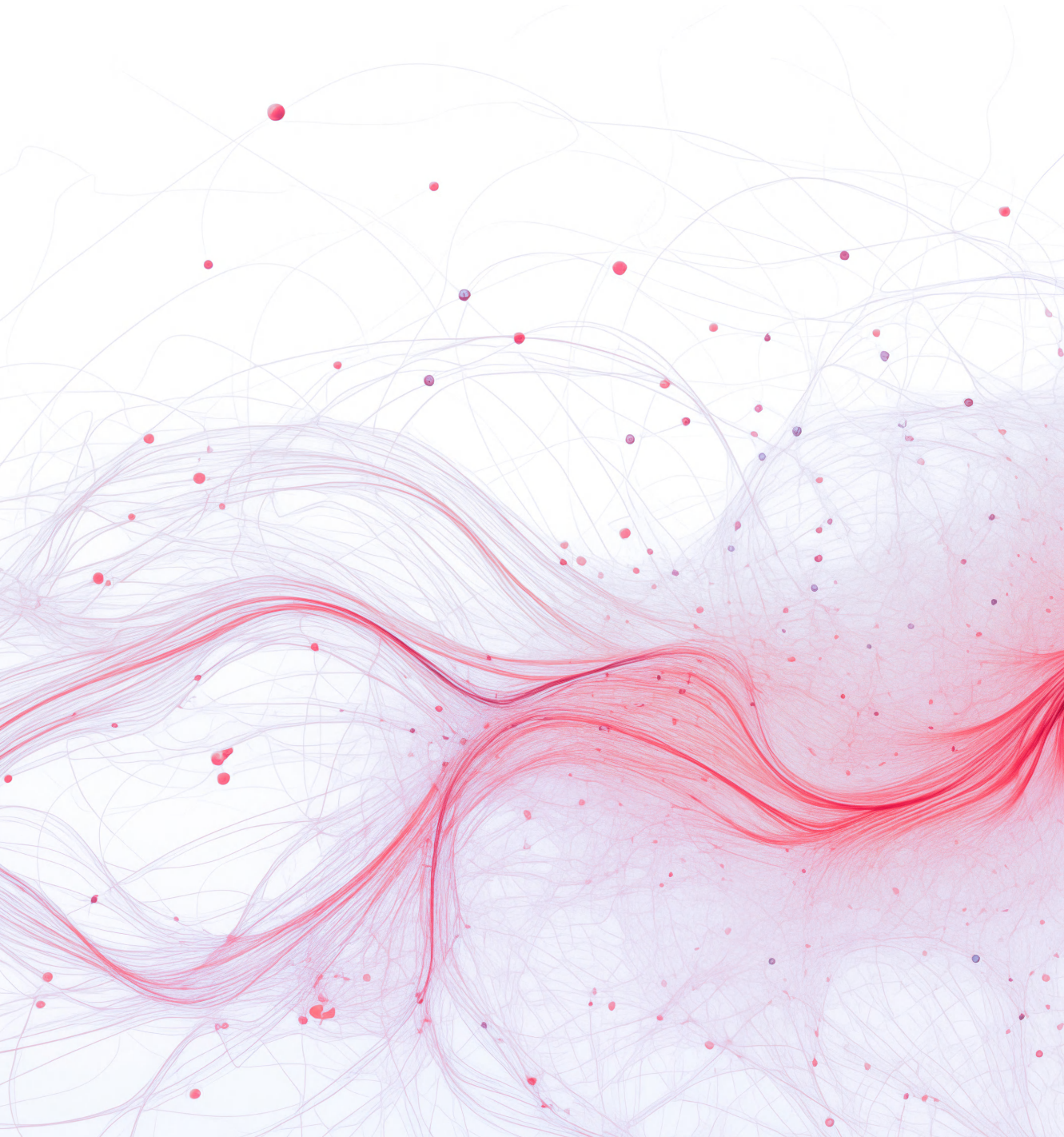

Chapter 1

Perceiving the world through our senses

When we interact with the outside world, we continuously need to adapt and adjust our behavior to this complex and dynamic environment. Through more than 500 million years of brain evolution, we are capable of perceiving complex external signals through six basic senses: vision, audition, smell, taste, touch and proprioception. Among all these senses, vision is probably the most complex and important one for humans and the visual system is the largest system in the human brain. Like other senses, the visual system has a hierarchical organization that consists of multiple brain areas. Three types of connections can be differentiated in this network: ascending feedforward projections, descending feedback projections and horizontal projections within a hierarchical level.

This organization enables the processing of visual information at increasing levels of complexity, with the lower levels (thalamus, primary visual cortex (V1)) specialized at detecting dots and lines in particular orientations, and higher cortical regions recognizing object categories, faces, movement in space, etc. Importantly, the extensive feedback connections send the complex information processed in the higher cortical regions back to lower visual areas, thus providing contextual information about the feedforward inputs they are receiving. This allows the visual system to be highly efficient by continuously predicting what happens in our environment and updating these predictions with visual inputs.

Anatomy of visual circuits

The visual information processing begins with photoreceptors in the retina, which detect light. There are two types of primary photoreceptor cells: rods and cones. Rods and cones convert photoreceptor binding signals to changes in neurotransmitter release and transfer visual information to the horizontal, bipolar, and amacrine cells of the retina. The network of these cells serves as an initial information integrator and regulator. Then, retinal ganglion cells (RGCs) that receive this processed information, deliver the outputs of the eyes to the ~46 retinorecipient brain areas in mouse, including basal forebrain, hypothalamus, bed nucleus, thalamus, midbrain, and accessory optic nuclei[1]. More than 30 different subtypes of RGCs are involved; each type has unique functional and physiological characteristics[2]. All those circuits can be divided into image-related and non-image-related circuits. Image-related circuits generally involve visual perception, while non-image-related circuits support unconscious sight-related functions, such as pupil reflexes and involuntary eye movements. By far the most RGCs from retina target the

image-related targets: dorsal geniculate nucleus (dLGN, ~30-40%) and the superior colliculus (SC, ~90%). Here, the initial information detecting, diverting, filtering and delivering takes place.

Thalamus

As a "first-order nucleus" of the thalamus, the dLGN serves as an information relay station between the eyes and visual cortex. Recent studies show that dLGN neurons receive inputs from on average 2-6 types of RGCs[3,4], but only about two of those play a functional role in each relay neuron[4]. Unlike like primate dLGN, mouse dLGN is a homogenous structure and does not have cytoarchitectural lamination. By using specific transgenic mice, RGC tracing shows that no distinct layers were present. However, mouse dLGN does have functional areas that are innervated by distinct types of retinogeniculate cells. The shell region of dLGN receives more ON-OFF direction-selective RGCs (DSRGCs) and non-canonical DSRGCs, whereas ON sustained retinogeniculate cells (ONsRGCs), OFF sustained retinogeniculate cells (OFFsRGCs), OFF transient RGCs (OFFtRGCs), and also Suppressed-by-Contrast (SbC-) RGCs (SbC-RGCs) show strong projections to the core part of dLGN[5–7]. By this functional segregation, the vast amount of complex visual information is efficiently divided and processed. In mouse (and human) dLGN, the segregation of RGCs axons is not only defined by cell types, but also by the eye in which they are situated. Previous studies with tracer injections showed that axons from the contralateral and ipsilateral eye have different destinations. The ipsilateral projections are restricted to a small dorsomedial part of dLGN, while most of the contralateral RGCs innervate the rest of dLGN[8,9]. However, a recent study using monosynaptic rabies tracing showed that many dLGN neurons receive anatomic inputs from both eyes[3]. Although more than half of dLGN neurons in the ipsilateral projection zone receive binocular inputs, the strengths of the inputs from the two eyes are inequal[10]. Thus, with functional and eye segregation of RGCs in dLGN, visual information is well organized in the visual thalamus.

The thalamus plays the role of logistic center of sensory information. In the mouse, the majority of dLGN cells are excitatory glutamatergic relay cells (~90%). These can be subdivided in three types of region-specific thalamic relay cells (TC): X-like (biconical), Y-like (symmetrical), and W-like (hemispheric), similarly to the X-, Y-, W- cells of cats[11]. Those cell types have different region preferences: X- like cells predominate at the ventrolateral part of dLGN, while Y- like and W- like cells are most abundant in the core and shell of dLGN. Moreover, the targets of W-like projections are cortex layer 1-3, while X-like and Y-like TCs mainly innervate layer 4-6. Although those cells are quite different in morphology, their electrophysiological properties are very similar in vitro[11]. Different from other dorsal

thalamic nuclei, the dLGN also has GABAergic interneurons (~10%)[12]. Previous work shows that interneurons in mouse dLGN can be clustered in two major populations, based on morphology, cell size, and electrophysiological properties[13]. However, the actual functional differences between the two types of interneurons are still unknown. Since in the dLGN both TC and interneurons receive inputs from RGCs, a local inhibitory circuit is formed which can dynamically improve information encoding efficiency through a classic push-pull mechanism[14] and increase signal-noise ratios.

Thalamic inhibition

Interestingly, dLGN interneurons are quite unique in having two very different ways of inhibiting thalamocortical neurons: classical axonal (F1) terminals and presynaptic dendritic (F2) terminals. Unlike classic F1 terminals, the F2 terminal is organized in a triadic structure, which consists of an inhibitory synapse between the interneuron dendrite and a TC cell, and a glutamatergic retinogeniculate synapse which provides excitation. Therefore, when thalamocortical neurons are excited by RGCs, the interneuron dendrite will also be activated via glutamate receptors (AMPARs, NMDARs, and mGluRs), which leads to very rapid GABA release and inhibition of the TC neuron. Moreover, multiple neuromodulators, such as 5-HT, dopamine, and muscarinic acetylcholine can cause slow and lasting GABA release at F2 terminals[15–17] (Fig. 1). The activation of F2 terminals is dynamic, and can be trigged by dendritic back-propagating action potentials[18], or independently by action potential firing at the soma. Although the role of F2 in information processing is not fully understood, it is believed that the combination of F1 and F2 is involved with a push-pull or same-sign mechanism, which may improve temporal precision[19–21] .

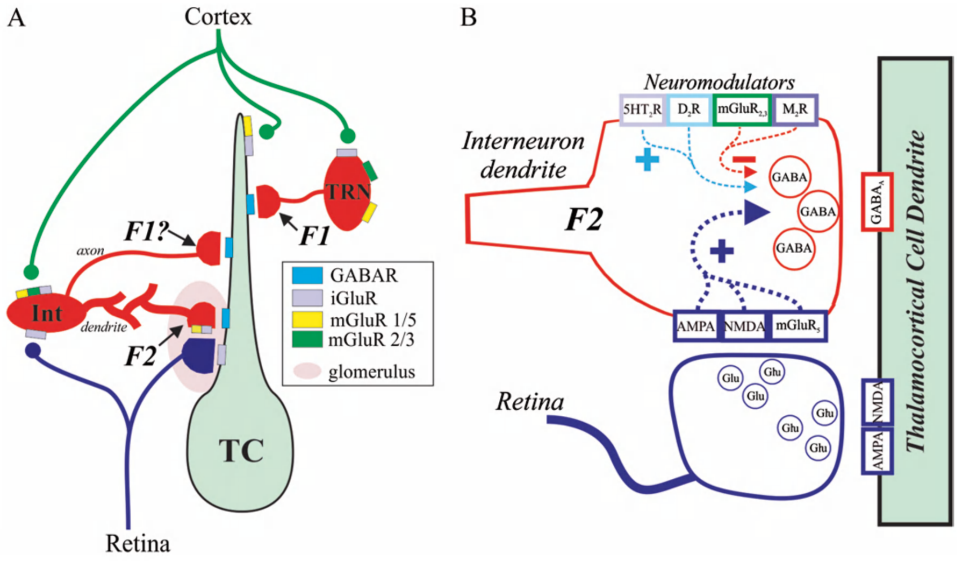

Fig. 1. (A) Schematic of thalamic inhibitory inputs. F1 terminals are traditional inhibitory synapses. Unlike F1, meanwhile innervating thalamic relay cells, the F2 terminals are also innervated by retinogeniculate axons. (B) Schematic of a F2 triad. The output of F2 terminals are manipulated by various neuromodulators and retinogeniculate glumatergic inputs. Adopted from Cox and Beatty (2017).

Primary visual cortex

After initial visual input arrives in dLGN, information is sent to primary visual cortex (V1). In V1, layers 2/3 and 4 receive most dLGN input, and layer 5/6 receive less abundant inputs[22]. Different V1 cells vary strongly in their responses to visual inputs. Based on their orientation-selectivity, V1 cells can be categorized into two different classes, 'simple (linear)' and 'complex (nonlinear)' cells. For simple cells, the classical receptive field (RFs) is spatially segregated by ON and OFF stimuli. Complex cells, in contrast, have overlapping ON and OFF subregions. By applying a Fourier transform, the ratio of neural responses at the drift frequency (F1, first harmonic) to the mean response (F0, 0^{th} harmonic) can be computed. Thus, the cell type can be predicted based on the ratio F1/F0 ratio. Simple cells show strong modulation to sinusoidal stimuli, as reflected by a F1/F0 > 1. In contrast, the ON/OFF RFs of complex cells are partially overlapping, and the F1/F0 ratio is not necessarily larger than 1[23] (Fig. 2). Also, in mouse V1, the complex cells are significantly less orientation tuned than simple cells[23]. Thus, V1 neurons can pass on different types of feedforward information to particular downstream areas due to the functional differences between simple and complex cells[24,25].

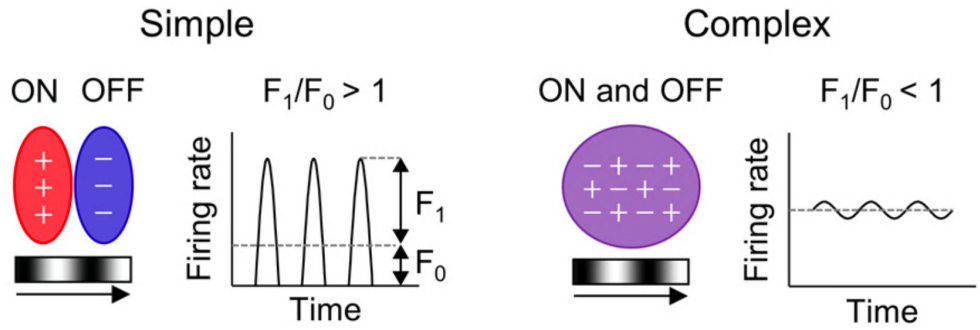

Fig. 2. Illustration of simple and complex cells. +: ON subregion; -:OFF subregion; +&-: both ON and OFF subregion. Adopted from Kim et al., 2020.

Inhibitory neurons in V1

Except excitatory neurons, inhibitory interneurons in V1 also have an essential role in information processing. GABAergic interneurons only make up 10-20% of the neuronal population in the cortex. Despite their relative sparsity, interneurons are a diverse set of neurons that provide various types of inhibition to pyramidal neurons and other interneurons. There are four major subtypes of interneuron in cortex: parvalbumin (PV)-positive, somatostatin (SST)-positive, vasoactive intestinal peptide (VIP)-positive and neuron-derived neurotrophic factor (NDNF)-positive interneurons. The main developmental sources of cortical interneurons are the caudal ganglionic eminence (CGE) and medial ganglionic eminence (MGE). Among all sources, the MGE is origin of around 60% of cortical interneurons in the mouse[26], from which most of PV+ and SST+ cells are derived. The CGE produces around 30%-40% cortical neurons, which includes most of VIP+ interneurons and NDNF+ neurogliaform cells. Each subtype has its unique role and feature. In cortex around 40% of GABAergic are PV+ cells[27], and most of them are fast-spiking basket cells. PV+ cells are normally located in all layers except layer 1. PV+ basket cells strongly innervate proximal dendrites and somata of local neurons. They receive thalamic input and input from local pyramidal cells. They are believed to broadly integrate the activity of these inputs, making them ideal for mediating gain control through feedforward inhibition. Moreover, PV basket cells are thought to generate cortical gamma oscillations (20-80Hz)[28] through inhibitory-inhibitory (I-I) and excitatory -inhibitory (E-I) loops. This activity pattern is highly related to sensory perception[28]. SST+ cells are accounting for 30% of cortical GABAergic interneurons. Most SST+ cells are located in layer 2/3 and 5. They mostly receive major inputs from local or more remotely localized pyramidal cells in V1, but lack thalamic feedforward inputs. Because SST+ interneurons become increasingly active when a larger part of V1 is stimulated, they are thought to be involved in feature coding, like surround suppression. When visual stimuli of increasing size are presented,

V1 neurons initially respond more strongly. However, if the stimulus is enlarged further, the response of the neuron will decrease. This phenomenon is called surround suppression. Surround suppression enhances apparent contrast and underlies visual pop-out. Another interesting feature of SST+ cells is that they predominantly innervate distal dendrites of pyramidal cells, in particular the dendritic tufts in layer 1 where feedback projections from higher cortical areas or thalamic nuclei form their synapses. This may allow SST+ interneurons to efficiently control feedback-driven activity in V1. Unlike PV+ interneurons, SST+ cells do not innervate each other, but they do inhibit other types of interneurons, such as PV+ cells[29]. Therefore, SST+ cells might disinhibit thalamic feedforward information, by inhibiting PV+ neurons (Fig. 3).

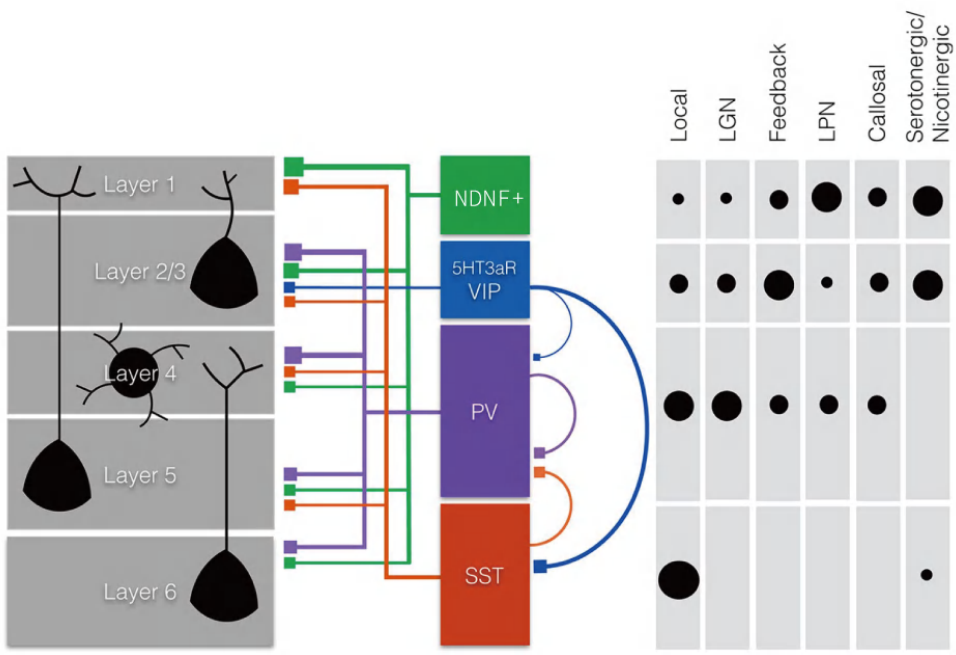

Fig. 3. Cortical main subtypes of interneurons and their main inputs/ outputs in visual cortext. Green, blue, purple and red indicate NDNF (Reelin) cells, VIP cells, PV cells and SST cells. Color lines indicate projections from each neuron type. Right panel indicate source of inputs for each subtype. Black circle sizes indicate the strength level of inputs. Adopted from Versendaal and Levelt, 2016.

The third largest group of interneurons are VIP+ cells, which predominantly inhibit other interneurons such as SST+ and PV+ cells[30,31]. VIP+ interneurons also receive higher order cortical and thalamic feedback inputs. Due to the interconnectedness of VIP+, SST+ and PV+ interneurons, they form an effective switch controlling the relative influence of feedforward and feedback inputs to V1. When VIP+ interneurons are active, they will suppress SST+ interneurons thus strengthening the influence of feedback inputs. Reduced

SST+ interneuron activity may also increase PV+ basket cell activity, thus reducing responses driven by feedforward inputs.

The last subtype of interneurons is NDNF+ neurogliaform cells. They can provide strong inhibition through volume release of GABA, resulting in the activation of metabotropic $GABA_{B}$- and extrasynaptic $GABA_{A}$ receptors. This can cause strong and prolonged inhibition. Neurogliaform cells receive thalamic and local cortical inputs and feedback from higher visual areas. Like SST+ interneurons, neurogliaform cells inhibit both pyramidal and PV+ interneurons[32]. Therefore, they might also be involved in switching between feedforward and feedback inputs. In conclusion, interneurons regulate local, feedforward and feedback information, which is critical for visual perception.

V1 feedforward to higher visual areas

V1 innervates a variety of brain areas with distinct functions, and most V1 neurons project to more than one area. At least 9 visual areas of neocortex receive V1 projections. These are anterolateral (AL), lateromedial (LM), rostrolateral (RL), lateral intermediate (LI), posteromedial (PM), posterior (P), anteromedial (AM), postrhinal (POR) and anterior visual area (A) (Fig. 4). The information sent to each higher visual area is biased to the functions of these areas. Among all higher areas, AL and LM receive the strongest input from V1 and contain moreneurons with direction preference[33]. A large part of RL encodes the lower nasal visual field[34] and also responds to movement[33]. LI neurons prefer high spatial frequencies[24]. PM neurons have large receptive fields[35] and consist of two subpopulations: one prefers high spatial frequencies while the other prefers low spatial frequencies[36]. However, these preferences per brain region are not absolute; there are many functional overlaps in the response properties of neurons in different visual areas. Through these widespread V1-to-higher visual area connections, visual information from V1 can spread to different regions of neocortex and participate in cognition and behavior of the animal.

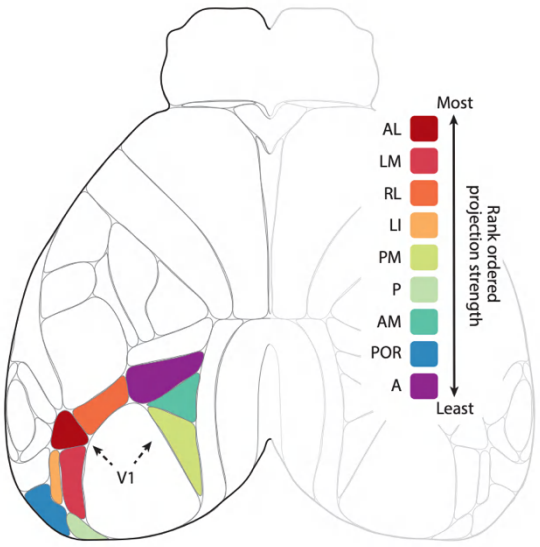

Fig. 4. Feedforward projections from V1. Different colors indicate higher visual regions. Adopted from Froudarakis et al., 2019.

Anticipation/contextual information plays a crucial role through feedback

The cortex has an abundance of feedback projections. In fact, cortical feedback connections are more abundant than feedforward connections. Generally speaking, feedforward projections tend to originate from superficial cortical layers and target layer 4 and to a lesser extent other superficial layers. Feedback projections can start from deep or superficial layers, and innervate layers 1 and 5.

Cortical feedback may add broader contextual information to relevant sensory signals. One example is figure-ground modulation. This is a feature that can already be detected in V1 and underlies pop-out of the key elements (figures) in a visual scene from the background. A recent study demonstrates that higher visual areas mediate figure-ground modulation by providing feedback to V1 neurons whose receptive fields match the figure[37]. In this study, optogenetic silencing of the higher visual areas strongly reduced figure-ground modulation in V1, but had no effect on the initial visual responses. It proves that V1 figure-ground segregation requires feedback from higher visual areas.

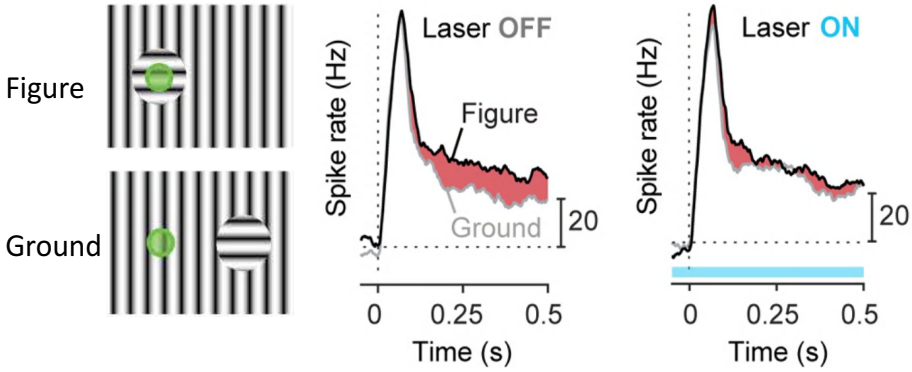

Fig. 5. V1 figure-ground depends on higher visual area. Left top, figure condition stimuli, the green circle is the receptive field. Right bottom, ground condition stimuli. Mid, The example of V1 figure (black curve) and ground (gray curve) responses to figure-ground stimuli. Right, optogenetically inhibited HVAs while recording V1 activity. V1 figure-ground activity is reduced when HVAs are inhibited. Adopted from Kirchberger et al., 2021.

Another example of feedback providing contextual information is predictive processing. In predictive processing, the brain forecasts the expected sensory input in higher-level areas and sends this prediction to lower areas through feedback projections. Lower level areas compute the differences between the prediction and actual inputs as a prediction error. This prediction error in the lower level areas is then sent to the higher-level area again through feedforward projections to update the prediction. Predictive coding is hard to study, because it is difficult to differentiate between predictive and sensory inputs. However, mismatch between motor and visual input can be readily observed in rodents[38,39]. Two-photon calcium imaging in mice has demonstrated that secondary motor cortex sends feedback to V1, conveying body movement-based prediction of visual information[38]. A related study has shown that mouse V1 layer 2/3 neurons respond to mismatch between actual and predicted visual feedback[39].

Apart from direct corticocortical feedback, transcortical communication can also be delivered through the thalamus. Many studies have shown that pulvinar (a higher-order visual thalamic nucleus, equivalent to the lateral posterior thalamic nucleus in rodents) plays a significant role in predictive processing and attention[40,41]. Pulvinar lesions can interfere with new learning and attention shifts[42–45].

Anatomy of whisker somatosensory system

Like the visual system, the facial whisker sensory system is also important for rodents. It offers tactile information of the immediate surroundings. Whiskers on the snout of rodents are arranged in a matrix structure. The matrix also exists in the primary somatosensory cortex (S1), and each element of them is termed a 'barrel'. These barrels are arranged in a similar map layout to the whiskers on the snout. Like the visual system, the somatosensory pathway involves multiple layers of hierarchy.

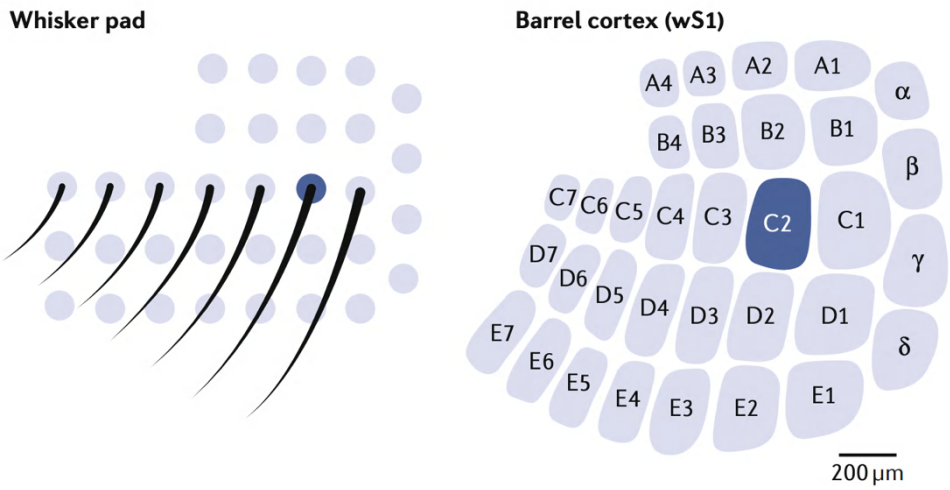

Fig. 6. Organization of 'barrel' structure on the snout and somatosensory cortex. Each of barrels in cortex represents an individual whisker and is somatotopically organized. Adopted from Petersen, 2019.

Sensory information is first detected in the whisker follicle, which is connected with trigeminal afferent neurons. Each follicle is connected to around 100-200 trigeminal neurons through mostly fast-conducting sensory fibers[46]. With each whisker stimulus, whisker motion transmits mechanical energy to the follicle. These analog signals are then translated into action potentials by follicle-connected trigeminal ganglion cells. The brainstem trigeminal nuclei are the first nuclei in the brain relaying and processing this tactile information. They are complex nuclei with multiple substructures. Within them, two neural compartments are highly related with whisker somatosensation: The principal (PrV) sensory nucleus for high-resolution mechanoreceptive aspects of touch and the spinal nucleus (SpV) for low-resolution touch.

Based on the target differences of trigeminal ganglion cells, they either project to PrV or to SpV. The whisker-cortex pathway is thus divided in two parallel pathways: the lemniscal pathway and paralemniscal pathway. In the lemniscal pathway, the PrV has an obvious whisker map, similar to the barrel cortex and whiskers on the snout. However, in the SpV, which forms the paralemniscal pathway, only some parts show a similar topographic organization. In PrV, most neurons only respond to a single whisker (70%)[47] and transvey both touch and movement information[48]. It is still unclear which specific whisker information is transferred by SpV.

The next hierarchical layer of the somatosensory pathway is thalamus. The ventral posteromedial nucleus (VPM) and posteromedial complex (PoM) are the major thalamic nuclei that receive trigeminal complex inputs. Like the visual thalamic nucleus dLGN, VPM is the first order nucleus of the somatosensory pathway[49]. As part of lemniscal pathway, VPM predominantly receives ascending excitatory inputs from PrV, thus inheriting a clear barreloid whisker map. The size of the barreloids is highly correlated with the length of the whiskers[50]. Except feedforward inputs from the trigeminal nuclei, VPM also receives excitatory and inhibitory feedback from primary somatosensory cortex and the thalamic reticular nucleus (TRN), respectively. In contrast to dLGN, rodent VPM barely has interneurons[51]. Therefore, the only GABAergic inputs are provided by TRN. Afferents from VPM mostly innervate layer 4, lower layer 2/3 and layer 5/6 of primary somatosensory cortex, forming a one-to-one connection between the VPM barreloid map and cortical barrels[52]. TRN and layer 6 of the barrel cortex also receive feedforward projections from VPM.

PoM, like LP of the visual thalamus, is a higher order nucleus of the somatosensory system[49]. It is also the thalamic part of the paralemniscal pathway, which means it mostly receives inputs from SpV. Although there is evidence suggesting PoM has a topographical organization, it is more homogeneous and without a barreloid type of structure[53]. Unlike VPM, the receptive fields of PoM are large, and each neuron can respond to 6-8 whiskers[54]. However, responses to single whisker stimuli are much weaker. Like VPM, PoM also receives feedback from TRN and cortical layer 6. However, the TRN-VPM projection is topographically organized, while no somatotopic map is found in TRN-PoM projections[55]. Compared to VPM, PoM has much wider innervation areas, which includes the primary somatosensory, secondary somatosensory, insular and motor cortices and TRN[56]. Most PoM-cortex projections terminate in layers 1 and 5.

In barrel cortex, neurons are structured in 200 to 300 um cortical columns, each representing a whisker on the snout. Each cortical barrel column contains around 6500 neurons that include ~85% excitatory and ~15% inhibitory cells[57]. Like visual cortex, barrel cortex also has various types of interneurons, including VIP+, SST+, PV+ and NDNF+ cells and all of them also take part in regulating feedback and feedforward information. In conclusion, although the cortex and thalamic nuclei processing whisker inputs have some differences when compared to the visual system, the principle of thalamo-cortico-thalamic networks for each system are quite similar.

Development of thalamocortical and intracortical circuits

The general development of neuronal connections arises through many steps. The development of thalamus and cortex occurs in a synchronized way. Before birth, shortly after thalamic neurogenesis, the thalamic and cortical projections start to growth towards each other. At around embryonic day (E) E14 to E16, guided by guidepost cells, thalamocortical and corticothalamic axons connect and reach their destination areas. After birth, development can be described in three major phases: before the critical period, the critical period, and after the critical period.

Spontaneous activity

One of the most essential features driving early postnatal development of the thalamocortical network is spontaneous activity. In the mouse visual system, spontaneous waves of activity start in the retina around embryonic day 16. Here, we focus on postnatal activity. Based on the time and features of the waves, the postnatal spontaneous activity periods can be divided into two stages. The first stage begins at ~P1 and lasts until ~P10, whereas the second stage begin at ~P10 and lasts until around eye opening. The first stage waves are slow and propagating and depend on cholinergic signaling[58,59], while the second stage waves are faster and depend on glutamatergic signaling[60,61]. It is worth noting that retinal spontaneous waves can also drive wave-like activities in the visual thalamus, superior colliculus, and V1.

Spontaneous activity in the rodent somatosensory and visual thalamus contains two categories: early gamma oscillations (30-50) and spindle bursts (8-20 Hz)[62,62,63]. These activities are mainly triggered by spontaneous activity in the upstream sensory organs[62] and have an essential role in shaping thalamocortical projections[64]. Since thalamus receives corticothalamic feedback, the thalamic spontaneous activities will also be affected by cortical activity[62,65].

Electrophysiological recordings show that sensory cortex also has spontaneous spindle bursts in newborn rodents. It has been shown that impairments of sensory organs or thalamus causes defects in cortical spontaneous activity and the organization of cortical network. This suggests that most early spontaneous cortical activities underlying corticothalamic circuits depend on subcortical inputs.

Experience-dependent plasticity: critical periods

The second phase of postnatal development starts with experience-dependent plasticity during a critical period. Critical periods have been widely observed in many brain systems. The most used model for studying critical periods (CP) is ocular dominance (OD) plasticity in V1[66]. In mammals, after eye opening, V1 cells fire more action potentials when the same visual stimuli are shown to one eye vs the other. This property is defined as OD. If one eye is experimentally closed for several days (monocular deprivation, MD), a shift in OD is induced, which means that V1 becomes less responsive to eye that was closed and more responsive to the open eye. This change in visual responsiveness is termed OD plasticity.

In juvenile mice, a few days of MD induces a significant OD shift in V1. This effect is the strongest between P21 and P35, which is considered the critical period for OD plasticity. The peak of the critical period is around P28. The onset of the critical period depends on the development of inhibitory innervation[67]. In mice lacking the GABA synthetic enzyme glutamic acid decarboxylase (GAD) 65 KO, the critical period does not start, unless the animals are treated with the GABA-A receptor agonist diazepam[68]. Treating P19 wild-type animals with benzodiazepines was found to induce a premature critical period[68].

Interestingly, in mice in which the GABA receptor alpha1 subunit was genetically rendered insensitive to benzodiazepine, an early onset of the critical period could not be induced with diazepam[69]. This effect was not observed when the GABA receptor alpha2 subunit was made insensitive to benzodiazepine. As GABA receptor alpha1-containing synapses are mostly innervated by PV+ basket cells, it is thought that these interneurons are the most important regulators of critical period onset.

These experiments directly show that GABAergic innervation is essential for critical period onset. Interestingly, other factors that were found to influence critical period onset often affect inhibitory innervation of V1. Overexpression of brain-derived neurotropic factor (BDNF) in mice, for example, causes an early onset of the critical period due to accelerated development of inhibitory synapses[70–72]. Moreover, IGF-1, a protein with a molecular

structure similar to insulin, can speed up the development of inhibitory innervation, also causing an early onset of the critical period[73]. Also, in mice lacking polysialic acid (PSA) of neural cell-adhesion molecule before critical period onset, GABAergic synapse maturation is expedited, and results in a premature critical period onset[74]. Together, these findings support the idea that the development of inhibitory innervation underlies the onset of the critical period.

Like the onset of the critical period of OD plasticity, its closure is also thought to involve inhibition by PV+ interneurons. In mice treated with chondroitinase, an enzyme that degrades the extracellular matrix (ECM), OD plasticity can readily be induced in adult mice. Interestingly, PV+ interneurons are encapsulated by perineuronal nets (PNNs), a densely organized ECM structure. PNNs are partially removed upon chondroitinase treatment. This suggests that PNNs may contribute to PV+ interneuron function involved in critical period closure. Indeed, more recently, it was discovered that PV+ interneurons rapidly lose excitatory input upon MD during the critical period, but not in adulthood. The reduced activity of PV+ interneurons caused by loss of excitatory inputs was found to be essential for OD plasticity to occur. It is therefore thought that PNNs stabilize excitatory inputs onto PV+ interneurons, thus reducing the potential of V1 to undergo OD plasticity.

Since the discovery of OD plasticity by Hubel and Wiesel, it was considered a cortical process, regulated by cortical mechanisms. However, a recent study has demonstrated that thalamic relay neurons in mouse dLGN also undergo OD plasticity during the critical period, and that this plasticity depends on thalamic inhibitory synapses containing the GABA receptor alpha1 subunit[75]. This study also showed that OD plasticity in V1 during the critical period was also dependent on thalamic inhibition and plasticity.

Adult plasticity in the visual system

Although OD plasticity can be induced most readily during the critical period, it still can be induced in adult mice. Compared to juvenile mice, OD plasticity in adult mice requires a longer period of MD[76–78], and the OD shift is smaller and less sustained than in juvenile mice. The contribution of inhibition in the regulation of adult OD plasticity is less well understood. However, it was found that inhibitory boutons are lost during OD plasticity in adulthood as are inhibitory synapses on dendritic spines of pyramidal cells[79–81]. Moreover, there are indications suggesting that SST+ interneurons are also involved in facilitating OD plasticity in adult mice[82,83]. Interestingly, also in adult mice, OD plasticity does not only take place in V1 but also in dLGN. Using in vivo two-photon imaging of calcium responses

in dLGN afferents in binocular V1, it was shown that a significant OD shift could be induced in thalamic neurons upon monocular deprivation[84].

Disorders involving the thalamocortical network

One of the most common disorders of the thalamocortical network is amblyopia, also known as “lazy eye”. About 1-5% of people suffer from it, and is caused by OD plasticity. If the two eyes do not provide strongly overlapping inputs, as is the case in children that are cross-eyed or when the refractory index of the two eyes differ strongly, plasticity in V1 will occur resulting in reduced responsiveness to the eye that provides the least reliable input. Treatment of this disorder has to happen before the critical period for OD plasticity in children closes, which occurs around 8 years of age.

The typical treatment of amblyopia is occlusion therapy, which involves depriving the good eye with a patch in order to induce an ocular dominance shift and thereby providing the lazy eye with an advantage. Of course, this also requires correction of vision in this eye using glasses or surgery. The treatment for most of children requires a total of 150-250 hours of patching, approximately 3 months of 3 hours per day[85]. Overall, earlier intervention results in better recovery, and a later onset of therapy will require a longer period of occlusion[85]. Although clinical trials show that occlusion can still improve amblyopia in untreated children as old as 17 years old[86], the visual benefits of occlusion in children that are older than 10 years are considered to be marginal[87]. Unfortunately, the vision loss in a child may not be noticed until vision is tested by an ophthalmologist, which does not always happen in time in all countries. Many studies suggest that it is possible to restore visual function using perceptual learning tasks in adults with amblyopia, although it remains unclear how persistent these improvements are. Studies on critical period regulation may help to develop novel approaches to improve amblyopia in adulthood.

A very different type of disorder also thought to involve the thalamocortical network is schizophrenia. Schizophrenia is a mental illness characterized by a broad variety of symptoms divided into three categories: positive, negative and cognitive symptoms[88]. Positive symptoms include delusions, hallucinations, thinking abnormalities, disordered speech and motor impairments, among other things. Motivation loss, decreased initiative and energy, anhedonia and social retreat are all negative effects. Patients with cognitive impairments perform poorly on a variety of cognitive activities, including working memory, attention, reasoning and social interaction. Currently, schizophrenia is diagnosed using the Diagnostic and Statistical Manual of Mental Disorders, Fifth Edition (DSM-V) and the

11th International Classification of Diseases (ICD-11), both of which lack strong and precise biological markers.

Schizophrenia normally starts in late adolescence or early twenties, rarely in childhood or adulthood[89]. Although no satisfactory etiological explanation exists for schizophrenia, research on twins or family members reveals a substantial connection between environmental and genetic variables[90]. Prenatal stress during pregnancy is one of the most researched environmental risk factors. Evidence shows that children from moms who have maternal hemorrhage, diabetes or infections during pregnancy are at a higher risk of developing schizophrenia[91]. Furthermore, there is some evidence that perinatal vitamin D insufficiency is a risk factor for schizophrenia[92], with newborns born in the winter and spring, or at higher latitudes, having a greater chance of developing schizophrenia in the future. All the various environmental variables outlined above raise the possibility that schizophrenia is the outcome of abnormal neurodevelopment and maturation[92]. A variety of genetic loci have also been linked to schizophrenia[90,93,94]. Most genetic changes in schizophrenia are thought to be connected to neurotransmitters and their receptors; however, current investigations suggest a substantial association with aberrant structures[95].

An important theory about the pathogenesis of schizophrenia states that the symptoms of schizophrenia could be caused by N-methyl-D-aspartate receptor (NMDAR) malfunction. This theory is based on the discovery that NMDAR antagonists such phencyclidine (PCP) and ketamine can cause psychotic symptoms in healthy people[96,97]. This concept is supported in various ways by a large body of molecular and genetic research. Genes linked to schizophrenia include genes encoding for the endogenous NMDAR metabolizer flavoenzyme DAO[98], glutamate signaling protein GRM3[99] and neuregulin 1, which are all associated with NMDAR driven synaptic signaling[100,101]. Moreover, there is evidence for low glutamate levels in schizophrenia patients' cerebral spinal fluid[102]. Reduced NMDAR binding has been observed in the hippocampus of schizophrenia patients, which can be reversed by antipsychotic medications[102], as well as reductions in NMDAR subunit proteins in multiple brain areas, including the prefrontal cortex[103], temporal lobe[104] and thalamus[105–107].

Since systemically administered NMDAR antagonists can cause multiple schizophrenia-like behavioral deficits in rodents[108–118], as well as in humans[97,119], ketamine was proposed as an inducer of schizophrenia-like symptoms. Indeed, a study found that an intravenous infusion of ketamine can cause both sensory-motor and cognitive problems, akin to the

early stages of schizophrenia[120]. This finding lends credence to the notion that acute ketamine could be viewed as a model of psychosis transition[121]. Antipsychotic medications have been shown in preclinical trials to diminish the effects of NMDA receptor antagonists[122–124]. Although ketamine does not induce all symptoms of schizophrenia, it is a validated and well-recognized pharmacological model across the illness course of schizophrenia[120,125–127].

Ketamine interferes with NMDAR function by binding inside the receptor's channel, which normally allows inwards currents of Ca^{2+} and Na^{+} upon binding of glutamate. Ketamine will thus block NMDAR-mediated neuronal depolarization. As intracellular Ca^{2+} also plays an important part in long-term potentiation (LTP), long-term depression (LTD), and multiple metabolic activities, ketamine may also interfere with these processes too. Apart from acting on NMDARs, considered as ketamine's primary target, it also affects other aspects of neural function. It was found to inhibit dopamine release[128,129], as well as serve as a partial agonist on GABA(A), dopamine D(2) and serotonin 5-HT(2)receptors[130,131]. It thus remains unclear whether ketamine causes various positive symptoms of schizophrenia through modulating NMDARs or through other mechanisms.

It has long been debated whether schizophrenia is caused by malfunction of certain isolated brain circuits or by dysfunction of whole brain networks. According to the dopamine hypothesis, schizophrenia may be induced by changes in dopaminergic circuits, notably in the substantia nigra and ventral tegmental areas. Several investigations have shown deficits in the prefrontal cortex, hippocampus, striatum, substantia nigra and ventral tegmental area[132–135]. However, due to the widespread presence of glutamatergic neurons (80% of all neurons in the brain)[136] and the evidence for glutamate/NMDAR-related alterations, it seems improbable that schizophrenia is the consequence of a change in one or two brain areas. Furthermore, numerous studies have found immune response modifications, such as higher cytokine levels in the blood and cerebral fluid[137], indicating whole-brain changes. Increasing evidence shows that schizophrenia is caused by a breakdown in communication across multiple brain areas, rather than by distinct and localized neurological impairments[138–142]. Imaging studies have revealed structural changes in schizophrenia patients, including changes in cerebral ventricle size (~130% of normal control), grey matter volume and white matter size. The hippocampus[143], amygdala[143], thalamus[144], anterior cingulate[145] and corpus callosum also show changes in schizophrenia patients[146]. Moreover, various aberrant brain network oscillatory activities are widely found in schizophrenia patients and animal models, from low delta[147,148], theta[149,150], alpha[151,152] and beta[153–155] frequencies to high gamma frequencies.

One of the key features of schizophrenia is irregular gamma oscillatory activity. Various studies have described schizophrenia-related deficits in attention-related sensorimotor and cognitive processes associated with dysfunctional corticocortical and corticothalamic (CT) networks [156–160] showing disturbances of gamma (γ, 30-80 Hz) frequency oscillations. Under normal circumstances, two types of gamma frequency oscillations are involved in sensory/perceptual processes: sensory-evoked gamma oscillations, defined as phase-locked to the stimulus[161,162] and perception-induced gamma oscillation, defined as not phase-locked to the stimulus[163,164]. Clinical studies found that gamma disruptions are associated with cognitive impairments in schizophrenia, in both resting and task-related gamma oscillations. Some studies noted that baseline gamma power was increased in schizophrenia patients[165,166], while others demonstrated a decrease in sensory-evoked gamma oscillations[141,167].

The schizophrenia-related disturbances in brain rhythms found in patients can be reproduced in schizophrenia animal models. NMDAR antagonists, such as ketamine or PCP, can dose-dependently increase the power of ongoing gamma oscillations in rodents[168–171]. This is consistent with ketamine upregulating gamma activities in humans during task performance[172,173] or resting state[127].

Many lines of evidence indicate that the thalamocortical network is altered in schizophrenia. Postmortem studies show lower cell counts in thalamus of schizophrenia patients[174,175]. N-acetyl aspartate, a brain metabolite associated with ischemic brain injury and dementia, is also frequently reduced in the thalamus of schizophrenia patients, as determinded by proton magnetic resonance spectroscopy (1H-MRS)[176]. Also an MRS study reported significant elevations of glutamine level in the thalamus of schizophrenia patients[177]. Several magnetic resonance imaging (MRI) studies in schizophrenia patients revealed aberrant structural and functional activity during cognitive tasks[178–180]. Notably, altered thalamocortical functional connectivity has been consistently reported in schizophrenia fMRI studies, including clinical high psychosis risk individuals[126,181], first-episode patients[182] and patients with established disease .

Thesis outline

In this thesis, we examine the function of the corticothalamic-thalamocortical (CTC) network from the perspectives of schizophrenia and neural plasticity. We build on previous research suggesting that a dysfunctional corticothalamic network plays a significant role in mental and developmental disorders.

In **Chapter 2**, we investigate the mechanism of spindle activity deficits in the CTC network in schizophrenia using *in vivo* electrophysiology in the thalamus and cortex of rats. We induce psychotomimetic states using low-dose ketamine and demonstrate that this reproduces spindle and delta oscillation deficits observed in human patients. To gain a better understanding of the impact of ketamine on thalamic neurons, we analyze the firing patterns of TRN and TC neurons.

In **Chapter 3**, we investigate the effects of ketamine on sensory responses. We hypothesize that ketamine-induced dysfunction in the CTC network could result in sensory information chaos. To test this, we measure sensory information using multi-scale entropy analysis in both the thalamus and cortex. Additionally, we investigate the functional network connectivity of the CTC.

In **Chapter 4**, we explore the role of the corticothalamic network in experience-dependent plasticity. We investigate how plasticity in the thalamus and cortex interact in the adult visual system. To assess the influence of thalamic plasticity on V1 plasticity in adult animals, we use multielectrode recordings in both V1 and dLGN in adult WT and thalamic GABA alpha1 subunit KO mice. We also silence V1 during thalamic recordings to investigate the role of V1 in thalamic OD plasticity.

In **Chapter 5**, we investigate the role of endocannabinoids in experience-dependent neural plasticity. Previous studies have highlighted the unexpected role of astrocytic CB1Rs in plasticity, so we examine the impact of removing CB1Rs from interneurons or astrocytes during the critical period of OD plasticity in V1. To explore how cell type-specific loss of CB1Rs affects inhibitory synaptic maturation, we assess the dynamics of short-term transmission and long-term depression in acute brain slices. Additionally, we assess OD plasticity per layer in mice with and without astrocytic CB1Rs.

In **Chapter 6**, we discuss the results of this thesis and provide an outlook on future research.

References

1. Lawrence, P. M. & Studholme, K. M. Retinofugal projections in the mouse. *Journal of Comparative Neurology* **522**, 3733–3753 (2014).
2. Baden, T. *et al.* The functional diversity of retinal ganglion cells in the mouse. *Nature* **529**, 345–350 (2016).
3. Rompani, S. B. *et al.* Different Modes of Visual Integration in the Lateral Geniculate Nucleus Revealed by Single-Cell-Initiated Transsynaptic Tracing. *Neuron* **93**, 767-776.e6 (2017).
4. Román Rosón, M. *et al.* Mouse dLGN Receives Functional Input from a Diverse Population of Retinal Ganglion Cells with Limited Convergence. *Neuron* **102**, 462-476.e8 (2019).
5. Cruz-Martín, A. *et al.* A dedicated circuit linking direction selective retinal ganglion cells to primary visual cortex. *Nature* **507**, 358–361 (2014).
6. Zhu, Y., Xu, J., Hauswirth, W. W. & DeVries, S. H. Genetically Targeted Binary Labeling of Retinal Neurons. *J Neurosci* **34**, 7845–7861 (2014).
7. Ellis, E. M., Gauvain, G., Sivyer, B. & Murphy, G. J. Shared and distinct retinal input to the mouse superior colliculus and dorsal lateral geniculate nucleus. *J Neurophysiol* **116**, 602–610 (2016).
8. Reese, B. E. & Jeffery, G. Crossed and uncrossed visual topography in dorsal lateral geniculate nucleus of the pigmented rat. *J Neurophysiol* **49**, 877–885 (1983).
9. Reese, B. E. 'Hidden lamination' in the dorsal lateral geniculate nucleus: the functional organization of this thalamic region in the rat. *Brain Res* **472**, 119–137 (1988).
10. Bauer, J. *et al.* Limited functional convergence of eye-specific inputs in the retinogeniculate pathway of the mouse. *Neuron* **109**, 2457-2468.e12 (2021).
11. Krahe, T. E., El-Danaf, R. N., Dilger, E. K., Henderson, S. C. & Guido, W. Morphologically distinct classes of relay cells exhibit regional preferences in the dorsal lateral geniculate nucleus of the mouse. *Journal of Neuroscience* **31**, 17437–17448 (2011).
12. Arcelli, P., Frassoni, C., Regondi, M. C., De Biasi, S. & Spreafico, R. GABAergic neurons in mammalian thalamus: a marker of thalamic complexity? *Brain Res Bull* **42**, 27–37 (1997).
13. Leist, M. *et al.* Two types of interneurons in the mouse lateral geniculate nucleus are

characterized by different h-current density. *Sci Rep* **6**, 24904 (2016).

14. Hirsch, J. A., Wang, X., Sommer, F. T. & Martinez, L. M. How Inhibitory Circuits in the Thalamus Serve Vision. *Annual Review of Neuroscience* **38**, 309–329 (2015).
15. Cox, C. L. & Sherman, S. M. Control of dendritic outputs of inhibitory interneurons in the lateral geniculate nucleus. *Neuron* **27**, 597–610 (2000).
16. Munsch, T., Freichel, M., Flockerzi, V. & Pape, H.-C. Contribution of transient receptor potential channels to the control of GABA release from dendrites. *Proc Natl Acad Sci U S A* **100**, 16065–16070 (2003).
17. Munsch, T., Yanagawa, Y., Obata, K. & Pape, H.-C. Dopaminergic control of local interneuron activity in the thalamus. *European Journal of Neuroscience* **21**, 290–294 (2005).
18. Acuna-Goycolea, C., Brenowitz, S. D. & Regehr, W. G. Active dendritic conductances dynamically regulate GABA release from thalamic interneurons. *Neuron* **57**, 420–431 (2008).
19. Butts, D. A., Weng, C., Jin, J., Alonso, J.-M. & Paninski, L. Temporal Precision in the Visual Pathway through the Interplay of Excitation and Stimulus-Driven Suppression. *J. Neurosci.* **31**, 11313–11327 (2011).
20. Babadi, B., Casti, A., Xiao, Y., Kaplan, E. & Paninski, L. A generalized linear model of the impact of direct and indirect inputs to the lateral geniculate nucleus. *Journal of Vision* **10**, 22 (2010).
21. Casti, A., Hayot, F., Xiao, Y. & Kaplan, E. A simple model of retina-LGN transmission. *J Comput Neurosci* **24**, 235–252 (2008).
22. Antonini, A., Fagiolini, M. & Stryker, M. P. Anatomical correlates of functional plasticity in mouse visual cortex. *J Neurosci* **19**, 4388–4406 (1999).
23. Li, Y., Liu, B., Chou, X., Zhang, L. I. & Tao, H. W. Strengthening of Direction Selectivity by Broadly Tuned and Spatiotemporally Slightly Offset Inhibition in Mouse Visual Cortex. *Cerebral Cortex* **25**, 2466–2477 (2015).
24. Andermann, M. L., Kerlin, A. M., Roumis, D. K., Glickfeld, L. L. & Reid, R. C. Functional specialization of mouse higher visual cortical areas. *Neuron* **72**, 1025–1039 (2011).
25. Glickfeld, L. L., Andermann, M. L., Bonin, V. & Reid, R. C. Cortico-cortical projections in mouse visual cortex are functionally target specific. *Nat Neurosci* **16**, 219–226 (2013).

26. Gelman, D. M., Marín, O. & Rubenstein, J. L. R. The Generation of Cortical Interneurons. in *Jasper's Basic Mechanisms of the Epilepsies* (eds. Noebels, J. L., Avoli, M., Rogawski, M. A., Olsen, R. W. & Delgado-Escueta, A. V.) (National Center for Biotechnology Information (US), 2012).
27. Butt, S. J. *et al.* The temporal and spatial origins of cortical interneurons predict their physiological subtype. *Neuron* **48**, 591–604 (2005).
28. Buzsáki, G. & Wang, X.-J. Mechanisms of Gamma Oscillations. *Annual Review of Neuroscience* **35**, 203–225 (2012).
29. Xu, H., Jeong, H.-Y., Tremblay, R. & Rudy, B. Neocortical Somatostatin-Expressing GABAergic Interneurons Disinhibit the Thalamorecipient Layer 4. *Neuron* **77**, 155–167 (2013).
30. Jiang, X. *et al.* Principles of connectivity among morphologically defined cell types in adult neocortex. *Science* **350**, aac9462 (2015).
31. Pi, H.-J. *et al.* Cortical interneurons that specialize in disinhibitory control. *Nature* **503**, 521–524 (2013).
32. Chittajallu, R., Pelkey, K. A. & McBain, C. J. Neurogliaform cells dynamically regulate somatosensory integration via synapse-specific modulation. *Nat Neurosci* **16**, 13–15 (2013).
33. Juavinett, A. L. & Callaway, E. M. Pattern and Component Motion Responses in Mouse Visual Cortical Areas. *Current Biology* **25**, 1759–1764 (2015).
34. Garrett, M. E., Nauhaus, I., Marshel, J. H. & Callaway, E. M. Topography and Areal Organization of Mouse Visual Cortex. *J. Neurosci.* **34**, 12587–12600 (2014).
35. Murgas, K. A., Wilson, A. M., Michael, V. & Glickfeld, L. L. Unique Spatial Integration in Mouse Primary Visual Cortex and Higher Visual Areas. *J Neurosci* **40**, 1862–1873 (2020).
36. Roth, M. M., Helmchen, F. & Kampa, B. M. Distinct Functional Properties of Primary and Posteromedial Visual Area of Mouse Neocortex. *J Neurosci* **32**, 9716–9726 (2012).
37. Kirchberger, L. *et al.* The Essential Role of Feedback Processing for Figure-Ground Perception in Mice. *SSRN Electronic Journal* (2019) doi:10.2139/ssrn.3441074.
38. Leinweber, M., Ward, D. R., Sobczak, J. M., Attinger, A. & Keller, G. B. A Sensorimotor Circuit in Mouse Cortex for Visual Flow Predictions. *Neuron* **95**, 1420-1432.e5 (2017).
39. Attinger, A., Wang, B. & Keller, G. B. Visuomotor Coupling Shapes the

Functional Development of Mouse Visual Cortex. *Cell* **169**, 1291-1302.e14 (2017).

40. Bennett, C. *et al.* Higher-Order Thalamic Circuits Channel Parallel Streams of Visual Information in Mice. *Neuron* **102**, 477-492.e5 (2019).
41. Saalmann, Y. B., Pinsk, M. A., Wang, L., Li, X. & Kastner, S. The pulvinar regulates information transmission between cortical areas based on attention demands. *Science* **337**, 753–756 (2012).
42. Zhou, H., Schafer, R. J. & Desimone, R. Pulvinar-Cortex Interactions in Vision and Attention. *Neuron* **89**, 209–220 (2016).
43. Purushothaman, G., Marion, R., Li, K. & Casagrande, V. A. Gating and control of primary visual cortex by pulvinar. *Nat Neurosci* **15**, 905–912 (2012).
44. Robinson, D. L. & Petersen, S. E. The pulvinar and visual salience. *Trends in Neurosciences* **15**, 127–132 (1992).
45. Chalupa, L. M. A review of cat and monkey studies implicating the pulvinar in visual function. *Behavioral Biology* **20**, 149–167 (1977).
46. Waite, P. M. E. CHAPTER 26 - Trigeminal Sensory System. in *The Rat Nervous System (Third Edition)* (ed. Paxinos, G.) 817–851 (Academic Press, 2004). doi:10.1016/B978-012547638-6/50027-4.
47. Veinante, P. & Deschênes, M. Single- and multi-whisker channels in the ascending projections from the principal trigeminal nucleus in the rat. *J Neurosci* **19**, 5085–5095 (1999).
48. Moore, J. D. *et al.* Hierarchy of orofacial rhythms revealed through whisking and breathing. *Nature* **497**, 205–210 (2013).
49. Sherman, S. M. & Guillery, R. W. On the actions that one nerve cell can have on another: Distinguishing "drivers" from "modulators". *Proceedings of the National Academy of Sciences* **95**, 7121–7126 (1998).
50. Ahissar, E., Sosnik, R., Bagdasarian, K. & Haidarliu, S. Temporal frequency of whisker movement. II. Laminar organization of cortical representations. *J Neurophysiol* **86**, 354–367 (2001).
51. Harris, R. M. Morphology of physiologically identified thalamocortical relay neurons in the rat ventrobasal thalamus. *J Comp Neurol* **251**, 491–505 (1986).
52. Lu, S.-M. & Lin, R. C.-S. Thalamic Afferents of the Rat Barrel Cortex: A Light-and Electron-Microscopic Study Using Phaseolus vulgaris Leucoagglutinin as an Anterograde Tracer.

Somatosensory & Motor Research **10**, 1–16 (1993).

53. Friedberg, M. H., Lee, S. M. & Ebner, F. F. Modulation of Receptive Field Properties of Thalamic Somatosensory Neurons by the Depth of Anesthesia. *Journal of Neurophysiology* **81**, 2243–2252 (1999).
54. Diamond, M. E., Armstrong-James, M. & Ebner, F. F. Somatic sensory responses in the rostral sector of the posterior group (POm) and in the ventral posterior medial nucleus (VPM) of the rat thalamus. *J Comp Neurol* **318**, 462–476 (1992).
55. Pinault, D., Bourassa, J. & Deschênes, M. The Axonal Arborization of Single Thalamic Reticular Neurons in the Somatosensory Thalamus of the Rat. *European Journal of Neuroscience* **7**, 31–40 (1995).
56. Deschênes, M., Veinante, P. & Zhang, Z.-W. The organization of corticothalamic projections: reciprocity versus parity. *Brain Research Reviews* **28**, 286–308 (1998).
57. Lefort, S., Tomm, C., Floyd Sarria, J.-C. & Petersen, C. C. H. The Excitatory Neuronal Network of the C2 Barrel Column in Mouse Primary Somatosensory Cortex. *Neuron* **61**, 301–316 (2009).
58. Ford, K. J., Félix, A. L. & Feller, M. B. Cellular Mechanisms Underlying Spatiotemporal Features of Cholinergic Retinal Waves. *J. Neurosci.* **32**, 850–863 (2012).
59. Wong, R. O. L., Meister, M. & Shatz, C. J. Transient period of correlated bursting activity during development of the mammalian retina. *Neuron* **11**, 923–938 (1993).
60. Blankenship, A. G. *et al.* Synaptic and extrasynaptic factors governing glutamatergic retinal waves. *Neuron* **62**, 230–241 (2009).
61. Maccione, A. *et al.* Following the ontogeny of retinal waves: pan-retinal recordings of population dynamics in the neonatal mouse. *J Physiol* **592**, 1545–1563 (2014).
62. Murata, Y. & Colonnese, M. T. An excitatory cortical feedback loop gates retinal wave transmission in rodent thalamus. *eLife* **5**, 1–19 (2016).
63. Wosniack, M. E. *et al.* Adaptation of spontaneous activity in the developing visual cortex. *eLife* **10**, e61619.
64. Minlebaev, M., Colonnese, M., Tsintsadze, T., Sirota, A. & Khazipov, R. Early γ oscillations synchronize developing thalamus and cortex. *Science* **334**, 226–229 (2011).
65. Yang, J.-W. *et al.* Thalamic Network Oscillations Synchronize

Ontogenetic Columns in the Newborn Rat Barrel Cortex. *Cerebral Cortex* **23**, 1299–1316 (2013).

66. Wiesel, T. N. & Hubel, D. H. SINGLE-CELL RESPONSES IN STRIATE CORTEX OF KITTENS DEPRIVED OF VISION IN ONE EYE. *J Neurophysiol* **26**, 1003–1017 (1963).
67. Hensch, T. K. *et al.* Local GABA circuit control of experience-dependent plasticity in developing visual cortex. *Science* **282**, 1504–1508 (1998).
68. Fagiolini, M. & Hensch, T. K. Inhibitory threshold for critical-period activation in primary visual cortex. *Nature* **404**, 183–186 (2000).
69. Fagiolini, M. *et al.* Specific GABAA circuits for visual cortical plasticity. *Science* **303**, 1681–1683 (2004).
70. Huang, Z. J. Activity-dependent development of inhibitory synapses and innervation pattern: Role of GABA signalling and beyond. in *Journal of Physiology* vol. 587 1881–1888 (2009).
71. Hanover, J. L., Huang, Z. J., Tonegawa, S. & Stryker, M. P. Brain-derived neurotrophic factor overexpression induces precocious critical period in mouse visual cortex. *The Journal of neuroscience : the official journal of the Society for Neuroscience* **19**, (1999).
72. Gianfranceschi, L. *et al.* Visual cortex is rescued from the effects of dark rearing by overexpression of BDNF. *Proc Natl Acad Sci U S A* **100**, 12486–12491 (2003).
73. Ciucci, F. *et al.* Insulin-like growth factor 1 (IGF-1) mediates the effects of enriched environment (EE) on visual cortical development. *PLoS One* **2**, e475 (2007).
74. Di Cristo, G. *et al.* Activity-dependent PSA expression regulates inhibitory maturation and onset of critical period plasticity. *Nature Neuroscience* **10**, 1569–1577 (2007).
75. Sommeijer, J. P. *et al.* Thalamic inhibition regulates critical-period plasticity in visual cortex and thalamus. *Nature Neuroscience* **20**, 1716–1721 (2017).
76. Pham, T. A. *et al.* A semi-persistent adult ocular dominance plasticity in visual cortex is stabilized by activated CREB. *Learn Mem* **11**, 738–747 (2004).
77. Tagawa, Y., Kanold, P. O., Majdan, M. & Shatz, C. J. Multiple periods of functional ocular dominance plasticity in mouse visual cortex. *Nature Neuroscience* **8**, 380–388 (2005).
78. Sawtell, N. B. *et al.* NMDA receptor-dependent ocular dominance plasticity in adult visual cortex. *Neuron* **38**, 977–985 (2003).

79. Keck, T. *et al.* Synaptic Scaling and Homeostatic Plasticity in the Mouse Visual Cortex In Vivo. *Neuron* **80**, 327–334 (2013).
80. van Versendaal, D. *et al.* Elimination of Inhibitory Synapses Is a Major Component of Adult Ocular Dominance Plasticity. *Neuron* **74**, 374–383 (2012).
81. Chen, J. L. & Nedivi, E. Highly Specific Structural Plasticity of Inhibitory Circuits in the Adult Neocortex. *Neuroscientist* **19**, 384–393 (2013).
82. Kaneko, M. & Stryker, M. P. Sensory experience during locomotion promotes recovery of function in adult visual cortex. *Elife* **3**, e02798 (2014).
83. Fu, Y., Kaneko, M., Tang, Y., Alvarez-Buylla, A. & Stryker, M. P. A cortical disinhibitory circuit for enhancing adult plasticity. *eLife* **2015**, 1–12 (2015).
84. Jaepel, J., Hübener, M., Bonhoeffer, T. & Rose, T. Lateral geniculate neurons projecting to primary visual cortex show ocular dominance plasticity in adult mice. *Nature Neuroscience* **20**, 1708–1714 (2017).
85. Stewart, C. E., Stephens, D. A., Fielder, A. R., Moseley, M. J., & ROTAS Cooperative. Objectively monitored patching regimens for treatment of amblyopia: randomised trial. *BMJ* **335**, 707 (2007).
86. Scheiman, M. *et al.* A randomized clinical trial of treatments for convergence insufficiency in children. *Arch Ophthalmol* **123**, 14–24 (2005).
87. Astle, A. T., McGraw, P. V. & Webb, B. S. Recovery of stereo acuity in adults with amblyopia. *BMJ Case Rep* **2011**, bcr0720103143 (2011).
88. Kahn, R. S. & Sommer, I. E. The neurobiology and treatment of first-episode schizophrenia. *Mol Psychiatry* **20**, 84–97 (2015).
89. Gogtay, N., Vyas, N. S., Testa, R., Wood, S. J. & Pantelis, C. Age of onset of schizophrenia: Perspectives from structural neuroimaging studies. *Schizophrenia Bulletin* **37**, 504–513 (2011).
90. Ripke, S. *et al.* Genome-wide association study identifies five new schizophrenia loci. *Nature Genetics* **43**, 969–978 (2011).
91. Van Lieshout, R. J. & Voruganti, L. P. Diabetes mellitus during pregnancy and increased risk of schizophrenia in offspring: A review of the evidence and putative mechanisms. *Journal of Psychiatry and Neuroscience* **33**, 395–404 (2008).
92. McGrath, J. J., Féron, F. P., Burne, T. H. J., Mackay-Sim, A. & Eyles, D. W. The neurodevelopmental

hypothesis of schizophrenia: A review of recent developments. *Annals of Medicine* **35**, 86–93 (2003).

93. Shi, W. *et al.* Aberrant expression of serum miRNAs in schizophrenia. *Journal of Psychiatric Research* **46**, 198–204 (2012).
94. Yue, W., Yu, X. & Zhang, D. Progress in genome-wide association studies of schizophrenia in Han Chinese populations. *npj Schizophrenia* **3**, 24 (2017).
95. Harari, J. H. *et al.* The association between gene variants and longitudinal structural brain changes in psychosis: A systematic review of longitudinal neuroimaging genetics studies. *npj Schizophrenia* **3**, 40 (2017).
96. Javitt, D. C. & Zukin, S. R. Recent advances in the phencyclidine model of schizophrenia. *American Journal of Psychiatry* **148**, 1301–1308 (1991).
97. Krystal, J. H. *et al.* Subanesthetic Effects of the Noncompetitive NMDA Antagonist, Ketamine, in Humans: Psychotomimetic, Perceptual, Cognitive, and Neuroendocrine Responses. *Archives of General Psychiatry* **51**, 199–214 (1994).
98. Verrall, L., Burnet, P. W. J., Betts, J. F. & Harrison, P. J. The neurobiology of D-amino acid oxidase and its involvement in schizophrenia. *Molecular Psychiatry* **15**, 122–137 (2010).
99. Ripke, S. *et al.* Biological insights from 108 schizophrenia-associated genetic loci. *Nature* **511**, 421–427 (2014).
100. Harrison, P. J. & Law, A. J. Neuregulin 1 and Schizophrenia: Genetics, Gene Expression, and Neurobiology. *Biological Psychiatry* **60**, 132–140 (2006).
101. Kotzadimitriou, D. *et al.* Neuregulin 1 Type I Overexpression Is Associated with Reduced NMDA Receptor–Mediated Synaptic Signaling in Hippocampal Interneurons Expressing PV or CCK. *eneuro* **5**, ENEURO.0418-17.2018 (2018).
102. Kim, J. S., Kornhuber, H. H., Schmid-Burgk, W. & Holzmüller, B. Low cerebrospinal fluid glutamate in schizophrenic patients and a new hypothesis on schizophrenia. *Neuroscience Letters* **20**, 379–382 (1980).
103. Catts, V. S., Lai, Y. L., Weickert, C. S., Weickert, T. W. & Catts, S. V. A quantitative review of the postmortem evidence for decreased cortical N-methyl-d-aspartate receptor expression levels in schizophrenia: How can we link molecular abnormalities to mismatch negativity deficits? *Biological Psychology* **116**, 57–67 (2016).

104. Beneyto, M., Kristiansen, L. V., Oni-Orisan, A., McCullumsmith, R. E. & Meador-Woodruff, J. H. Abnormal glutamate receptor expression in the medial temporal lobe in schizophrenia and mood disorders. *Neuropsychopharmacology* **32**, 1888–1902 (2007).

105. Gao, X. M. *et al.* Ionotropic glutamate receptors and expression of N-methyl-D-aspartate receptor subunits in subregions of human hippocampus: Effects of schizophrenia. *American Journal of Psychiatry* **157**, 1141–1149 (2000).

106. Law, A. J. & Deakin, J. F. W. Asymmetrical reductions of hippocampal NMDAR1 glutamate receptor mRNA in the psychoses. *Neuroreport* **12**, 2971–2974 (2001).

107. Stan, A. D. *et al.* Magnetic resonance spectroscopy and tissue protein concentrations together suggest lower glutamate signaling in dentate gyrus in schizophrenia. *Molecular Psychiatry* **20**, 433–439 (2015).

108. David Sturgeon, R., Fessler, R. G. & Meltzer, H. Y. Behavioral rating scales for assessing phencyclidine-induced locomotor activity, stereotypes behavior and ataxia in rats. *European Journal of Pharmacology* **59**, 169–179 (1979).

109. Sams-Dodd, F. Automation of the social interaction test by a video-tracking system: behavioural effects of repeated phencyclidine treatment. *Journal of Neuroscience Methods* **59**, 157–167 (1995).

110. Martinez, Z. A., Ellison, G. D., Geyer, M. A. & Swerdlow, N. R. Effects of sustained phencyclidine exposure on sensorimotor gating of startle in rats. *Neuropsychopharmacology* **21**, 28–39 (1999).

111. Noda, A. *et al.* Phencyclidine impairs latent learning in mice: Interaction between glutamatergic systems and sigma1receptors. *Neuropsychopharmacology* **24**, 451–460 (2001).

112. Marquis, J. P., Goulet, S. & Doré, F. Y. Schizophrenia-like syndrome inducing agent phencyclidine failed to impair memory for temporal order in rats. *Neurobiology of Learning and Memory* **80**, 158–167 (2003).

113. Nagai, T. *et al.* Effect of AD-5423 on animal models of schizophrenia: Phencyclidine-induced behavioral changes in mice. *NeuroReport* **14**, 269–272 (2003).

114. Campbell, U. C. *et al.* The mGluR5 antagonist 2-methyl-6-

(phenylethynyl)-pyridine (MPEP) potentiates PCP-induced cognitive deficits in rats. *Psychopharmacology* **175**, 310–318 (2004).

115. Egerton, A., Reid, L., McKerchar, C. E., Morris, B. J. & Pratt, J. A. Impairment in perceptual attentional set-shifting following PCP administration: A rodent model of set-shifting deficits in schizophrenia. *Psychopharmacology* **179**, 77–84 (2005).
116. Wang, D. *et al.* Synergistic effect of galantamine with risperidone on impairment of social interaction in phencyclidine-treated mice as a schizophrenic animal model. *Neuropharmacology* **52**, 1179–1187 (2007).
117. Mouri, A. *et al.* Involvement of a Dysfunctional Dopamine-D1/N-Methyl-D-aspartate-NR1 and Ca2+/Calmodulin-Dependent Protein Kinase II Pathway in the Impairment of Latent Learning in a Model of Schizophrenia Induced by Phencyclidine. *Molecular Pharmacology* **71**, 1598–1609 (2007).
118. Tanaka, D. H., Toriumi, K., Kubo, K. -i., Nabeshima, T. & Nakajima, K. GABAergic Precursor Transplantation into the Prefrontal Cortex Prevents Phencyclidine-Induced Cognitive Deficits. *Journal of Neuroscience* **31**, 14116–14125 (2011).
119. Newcomer, J. W. *et al.* Ketamine-induced NMDA receptor hypofunction as a model of memory impairment and psychosis. *Neuropsychopharmacology* **20**, 106–118 (1999).
120. Hetem, L. A. B., Danion, J. M., Diemunsch, P. & Brandt, C. Effect of a subanesthetic dose of ketamine on memory and conscious awareness healthy volunteers. *Psychopharmacology* **152**, 283–288 (2000).
121. Kantrowitz, J. T. & Javitt, D. C. N-methyl-d-aspartate (NMDA) receptor dysfunction or dysregulation: The final common pathway on the road to schizophrenia? *Brain Research Bulletin* **83**, 108–121 (2010).
122. Bakshi, V. P. & Geyer, M. A. Antagonism of phencyclidine induced deficits in prepulse inhibition by the putative atypical antipsychotic olanzapine. *Psychopharmacology* **122**, 198–201 (1995).
123. Lieberman, J. A. *et al.* Serotonergic basis of antipsychotic drug effects in schizophrenia. *Biological Psychiatry* **44**, 1099–1117 (1998).
124. Jones, N. C. *et al.* Acute administration of typical and atypical antipsychotics reduces

EEG gamma power, but only the preclinical compound LY379268 reduces the ketamine-induced rise in gamma power. *International Journal of Neuropsychopharmacology* **15**, 657–668 (2012).

125. Abram, S. V. *et al.* Validation of ketamine as a pharmacological model of thalamic dysconnectivity across the illness course of schizophrenia. *Mol Psychiatry* **27**, 2448–2456 (2022).
126. Anticevic, A. *et al.* Association of Thalamic Dysconnectivity and Conversion to Psychosis in Youth and Young Adults at Elevated Clinical Risk. *JAMA Psychiatry* **72**, 882–891 (2015).
127. Rivolta, D. *et al.* Ketamine dysregulates the amplitude and connectivity of high-frequency oscillations in cortical-subcortical networks in humans: Evidence from resting-state magnetoencephalography-recordings. *Schizophrenia Bulletin* **41**, 1105–1114 (2015).
128. Smith, G. S. *et al.* Glutamate modulation of dopamine measured in vivo with positron emission tomography (PET) and 11C-raclopride in normal human subjects. *Neuropsychopharmacology* **18**, 18–25 (1998).
129. Kegeles, L. S. *et al.* NMDA antagonist effects on striatal dopamine release: Positron emission tomography studies in humans. *Synapse* **43**, 19–29 (2002).
130. Irifune, M. *et al.* Evidence for GABA(A) receptor agonistic properties of ketamine: Convulsive and anesthetic behavioral models in mice. *Anesthesia and Analgesia* **91**, 230–236 (2000).
131. Kapur, S. & Seeman, P. NMDA receptor antagonists ketamine and PCP have direct effects on the dopamine D2 and serotonin 5-HT2 receptors - Implications for models of schizophrenia. *Molecular Psychiatry* **7**, 837–844 (2002).
132. Perez-Costas, E., Melendez-Ferro, M. & Roberts, R. C. Basal ganglia pathology in schizophrenia: Dopamine connections and anomalies. *Journal of Neurochemistry* **113**, 287–302 (2010).
133. Lodge, D. J. & Grace, A. A. Hippocampal dysregulation of dopamine system function and the pathophysiology of schizophrenia. *Trends in Pharmacological Sciences* **32**, 507–513 (2011).
134. Yoon, J. H., Minzenberg, M. J., Raouf, S., D'Esposito, M. & Carter,

C. S. Impaired prefrontal-basal ganglia functional connectivity and substantia nigra hyperactivity in schizophrenia. *Biological Psychiatry* **74**, 122–129 (2013).

135. Brisch, R. *et al.* The role of dopamine in schizophrenia from a neurobiological and evolutionary perspective: Old fashioned, but still in vogue. *Frontiers in Psychiatry* **5**, 47 (2014).
136. Meldrum, B. S. Glutamate as a neurotransmitter in the brain: review of physiology and pathology. *The Journal of nutrition* **130**, 1007S–15S (2000).
137. Miller, B. J., Buckley, P., Seabolt, W., Mellor, A. & Kirkpatrick, B. Meta-analysis of cytokine alterations in schizophrenia: Clinical status and antipsychotic effects. *Biological Psychiatry* **70**, 663–671 (2011).
138. Friston, K. J. & Friston, K. J. Schizophrenia and the disconnection hypothesis. *Acta psychiatrica Scandinavica. Supplementum* **395**, 68–79 (1999).
139. Liu, J. *et al.* Dysfunctional connectivity patterns in chronic heroin users: An fMRI study. *Neuroscience Letters* **460**, 72–77 (2009).
140. Stephan, K. E., Friston, K. J. & Frith, C. D. Dysconnection in Schizophrenia: From abnormal synaptic plasticity to failures of self-monitoring. *Schizophrenia Bulletin* **35**, 509–527 (2009).
141. Uhlhaas, P. J. Dysconnectivity, large-scale networks and neuronal dynamics in schizophrenia. *Current Opinion in Neurobiology* **23**, 283–290 (2013).
142. Kambeitz, J. *et al.* Aberrant Functional Whole-Brain Network Architecture in Patients with Schizophrenia: A Meta-analysis. *Schizophrenia Bulletin* **42**, S13–S21 (2016).
143. Wong, A. H. C. & Van Tol, H. H. M. Schizophrenia: From phenomenology to neurobiology. *Neuroscience and Biobehavioral Reviews* **27**, 269–306 (2003).
144. Konick, L. C. & Friedman, L. Meta-analysis of thalamic size in schizophrenia. *Biological Psychiatry* **49**, 28–38 (2001).
145. Baiano, M. *et al.* Anterior cingulate volumes in schizophrenia: A systematic review and a meta-analysis of MRI studies. *Schizophrenia Research* **93**, 1–12 (2007).
146. Woodruff, P. W. R., McManus, I. C. & David, A. S. Meta-analysis of corpus callosum size in schizophrenia. *Journal of Neurology, Neurosurgery and Psychiatry* **58**, 457–461 (1995).
147. SPONHEIM, S. R., CLEMENTZ, B. A., IACONO, W. G. & BEISER, M. Resting EEG in first-episode and

chronic schizophrenia. *Psychophysiology* **31**, 37–43 (1994).

148. Keshavan, M. S. *et al.* Delta sleep deficits in schizophrenia: Evidence from automated analyses of sleep data. *Archives of General Psychiatry* **55**, 443–448 (1998).
149. Kirihara, K., Rissling, A. J., Swerdlow, N. R., Braff, D. L. & Light, G. A. Hierarchical organization of gamma and theta oscillatory dynamics in schizophrenia. *Biological Psychiatry* **71**, 873–880 (2012).
150. Barr, M. S. *et al.* Impaired theta-gamma coupling during working memory performance in schizophrenia. *Schizophrenia Research* **189**, 104–110 (2017).
151. Howells, F. M. *et al.* Electroencephalographic delta/alpha frequency activity differentiates psychotic disorders: A study of schizophrenia, bipolar disorder and methamphetamine-induced psychotic disorder. *Translational Psychiatry* **8**, 1–11 (2018).
152. Jia, S. *et al.* Abnormal Alpha Rhythm During Self-Referential Processing in Schizophrenia Patients. *Frontiers in Psychiatry* **10**, 691 (2019).
153. Hudson, M. R. *et al.* High-Frequency Neuronal Oscillatory Abnormalities in the Phospholipase C-β1 Knockout Mouse Model of Schizophrenia. doi:10.1093/ijnp/pyy097.
154. Rebollo, B., Perez-Zabalza, M., Ruiz-Mejias, M., Perez-Mendez, L. & Sanchez-Vives, M. V. Beta and Gamma Oscillations in Prefrontal Cortex During NMDA Hypofunction: An In Vitro Model of Schizophrenia Features. *Neuroscience* **383**, 138–149 (2018).
155. Moran, J. K., Michail, G., Heinz, A., Keil, J. & Senkowski, D. Long-range temporal correlations in resting state beta oscillations are reduced in schizophrenia. *Frontiers in Psychiatry* **10**, (2019).
156. Zhang, L. I. & Poo, M. M. Electrical activity and development of neural circuits. *Nature neuroscience* **4 Suppl**, 1207–1214 (2001).
157. Pinault, D. Dysfunctional thalamus-related networks in schizophrenia. *Schizophrenia Bulletin* **37**, 238–243 (2011).
158. Cronenwett, W. J. & Csernansky, J. Thalamic pathology in schizophrenia. *Current Topics in Behavioral Neurosciences* **4**, 509–528 (2010).
159. Clinton, S. M. & Meadow-Woodruff, J. H. Abnormalities of the NMDA receptor and associated intracellular molecules in the thalamus in schizophrenia and

bipolar disorder. *Neuropsychopharmacology* **29**, 1353–1362 (2004).

160. Cox, C. L. & Sherman, S. M. Glutamate Inhibits Thalamic Reticular Neurons. *J Neurosci* **19**, 6694–6699 (1999).
161. Pantev, C. *et al.* Human auditory evoked gamma-band magnetic fields. *Proceedings of the National Academy of Sciences* **88**, 8996–9000 (1991).
162. Spencer, K. M., Niznikiewicz, M. A., Nestor, P. G., Shenton, M. E. & McCarley, R. W. Left auditory cortex gamma synchronization and auditory hallucination symptoms in schizophrenia. *BMC neuroscience* **10**, 85 (2009).
163. Gray, C. M., König, P., Engel, A. K. & Singer, W. Oscillatory responses in cat visual cortex exhibit inter-columnar synchronization which reflects global stimulus properties. *Nature* **338**, 334–337 (1989).
164. Joliot, M., Ribary, U. & Llinás, R. Human oscillatory brain activity near 40 Hz coexists with cognitive temporal binding. *Proceedings of the National Academy of Sciences of the United States of America* **91**, 11748–51 (1994).
165. Kissler, J., Müller, M. M., Fehr, T., Rockstroh, B. & Elbert, T. MEG gamma band activity in schizophrenia patients and healthy subjects in a mental arithmetic task and at rest. *Clinical Neurophysiology* **111**, 2079–2087 (2000).
166. Krishnan, G. P. *et al.* Steady state visual evoked potential abnormalities in schizophrenia. *Clinical Neurophysiology* **116**, 614–624 (2005).
167. Gandal, M. J., Edgar, J. C., Klook, K. & Siegel, S. J. Gamma synchrony: Towards a translational biomarker for the treatment-resistant symptoms of schizophrenia. *Neuropharmacology* **62**, 1504–1518 (2012).
168. Pinault, D. N-Methyl d-Aspartate Receptor Antagonists Ketamine and MK-801 Induce Wake-Related Aberrant γ Oscillations in the Rat Neocortex. *Biological Psychiatry* **63**, 730–735 (2008).
169. Ehrlichman, R. S. *et al.* N-methyl-d-aspartic acid receptor antagonist-induced frequency oscillations in mice recreate pattern of electrophysiological deficits in schizophrenia. *Neuroscience* **158**, 705–712 (2009).
170. Hakami, T. *et al.* NMDA receptor hypofunction leads to generalized and persistent aberrant γ oscillations independent of hyperlocomotion and the state of consciousness. *PLoS ONE* **4**, e6755 (2009).
171. Lazarewicz, M. T. *et al.* Ketamine modulates theta and gamma

oscillations. *Journal of Cognitive Neuroscience* **22**, 1452–1464 (2010).

172. Hong, L. E. *et al.* Gamma and delta neural oscillations and association with clinical symptoms under subanesthetic ketamine. *Neuropsychopharmacology* **35**, 632–640 (2010).
173. Shaw, A. D. *et al.* Ketamine amplifies induced gamma frequency oscillations in the human cerebral cortex. *European Neuropsychopharmacology* **25**, 1136–1146 (2015).
174. Dorph-Petersen, K.-A. & Lewis, D. A. Postmortem structural studies of the thalamus in schizophrenia. *Schizophrenia Research* **180**, 28–35 (2017).
175. Steullet, P. Thalamus-related anomalies as candidate mechanism-based biomarkers for psychosis. *Schizophrenia Research* **226**, 147–157 (2020).
176. Brugger, S., Davis, J. M., Leucht, S. & Stone, J. M. Proton magnetic resonance spectroscopy and illness stage in schizophreniaa systematic review and meta-analysis. *Biological Psychiatry* **69**, 495–503 (2011).
177. Merritt, K., Egerton, A., Kempton, M. J., Taylor, M. J. & McGuire, P. K. Nature of glutamate alterations in schizophrenia a meta-analysis of proton magnetic resonance spectroscopy studies. *JAMA Psychiatry* **73**, 665–674 (2016).
178. Pergola, G., Selvaggi, P., Trizio, S., Bertolino, A. & Blasi, G. The role of the thalamus in schizophrenia from a neuroimaging perspective. *Neuroscience and Biobehavioral Reviews* **54**, 57–75 (2015).
179. Giraldo-Chica, M. & Woodward, N. D. Review of thalamocortical resting-state fMRI studies in schizophrenia. *Schizophrenia Research* **180**, 58–63 (2017).
180. Huang, A. S., Rogers, B. P. & Woodward, N. D. Disrupted modulation of thalamus activation and thalamocortical connectivity during dual task performance in schizophrenia. *Schizophrenia Research* **210**, 270–277 (2019).
181. Cao, H. *et al.* Cerebello-thalamo-cortical hyperconnectivity as a state-independent functional neural signature for psychosis prediction and characterization. *Nat Commun* **9**, 3836 (2018).
182. Woodward, T. S., Leong, K., Sanford, N., Tipper, C. M. & Lavigne, K. M. Altered balance of functional brain networks in Schizophrenia. *Psychiatry Res Neuroimaging* **248**, 94–104 (2016).
183. Avram, M., Brandl, F., Bäuml, J. & Sorg, C. Cortico-thalamic hypo- and hyperconnectivity extend consistently to basal ganglia in

schizophrenia.
Neuropsychopharmacology **43**,
2239–2248 (2018).

Chapter 2

A single psychotomimetic dose of ketamine decreases thalamocortical spindles and delta oscillations in the sedated rat

A. Mahdavi[1], **Y. Qin[1]**, A.-S. Aubry, D. Cornec, S. Kulikova, D. Pinault

[1]Co-first author

Schizophrenia Research, 2020 Aug; 222:362-374

Abstract

Background: In patients with psychotic disorders, sleep spindles are reduced, supporting the hypothesis that the thalamus and glutamate receptors play a crucial etio-pathophysiological role, whose underlying mechanisms remain unknown. We hypothesized that a reduced function of NMDA receptors is involved in the spindle deficit observed in schizophrenia.

Methods: An electrophysiological multisite cell-to-network exploration was used to investigate, in pentobarbitalsedated rats, the effects of a single psychotomimetic dose of the NMDA glutamate receptor antagonist ketamine in the sensorimotor and associative/cognitive thalamocortical (TC) systems.

Results: Under the control condition, spontaneously-occurring spindles (intra-frequency: 10–16 waves/s) and delta-frequency (1–4 Hz) oscillations were recorded in the frontoparietal cortical EEG, in thalamic extracellular recordings, in dual juxtacellularly recorded GABAergic thalamic reticular nucleus (TRN) and glutamatergic TC neurons, and in intracellularly recorded TC neurons. The TRN cells rhythmically exhibited robust high frequency bursts of action potentials (7 to 15 APs at 200–700 Hz). A single administration of low-dose ketamine fleetingly reduced TC spindles and delta oscillations amplified ongoing gamma-(30–80 Hz) and higher frequency oscillations and switched the firing pattern of both TC and TRN neurons from a burst mode to a single AP mode. Furthermore, ketamine strengthened the gamma-frequency band TRN-TC connectivity. The antipsychotic clozapine consistently prevented the ketamine effects on spindles, delta- and gamma−/higher-frequency TC oscillations.

Conclusion: The present findings support the hypothesis that NMDA receptor hypofunction is involved in the reduction in sleep spindles and delta oscillations. The ketamine-induced swift conversion of ongoing TC-TRN activities may have involved at least both the ascending reticular activating system and the corticothalamic pathway.

1. Introduction

Sleep abnormalities are detected not only during the early course of complex mental health diseases, such as schizophrenia (Kamath et al., 2015; Monti and Monti, 2005; Wamsley et al., 2012) but also in individuals having a high-risk mental state for developing a transition to psychotic and bipolar disorders (Zanini et al., 2015). Cortical EEG studies conducted in such patients have revealed a reduction in sleep spindles (Castelnovo et al., 2017; Ferrarelli et al., 2007; Ferrarelli et al., 2010; Manoach et al., 2014; Manoach et al., 2016) and slow-wave activity (Kaskie and Ferrarelli, 2018). The underlying neural mechanisms are unknown.

Sleep spindles have a thalamic origin with the GABAergic thalamic reticular nucleus (TRN) being a leading structure in their generation by exerting a powerful rhythmic inhibitory modulation of thalamocortical (TC) activities (Pinault, 2004; Steriade et al., 1985; Steriade et al., 1993). The TRN, the principal inhibitory structure of the dorsal thalamus, is innervated by two major glutamatergic inputs, TC and layer VI corticothalamic (CT) axon collaterals, which mediate most of their excitatory effects through the activation of glutamate receptors (Crandall et al., 2015; Deschênes and Hu, 1990; Gentet and Ulrich, 2003). Importantly, layer VI CT axons innervate simultaneously TC and TRN neurons (Bourassa et al., 1995), together forming a 3- neuron circuit robustly involved in the generation of sleep spindles (Bal et al., 2000; Bonjean et al., 2011). The specific, sensory and motor TC systems receive cortical inputs only from layer VI CT neurons, whereas the non-specific, associative/limbic/cognitive TC systems receive cortical inputs from both layer V and layer VI CT neurons (Guillery and Sherman, 2002). In contrast to layer VI CT neurons, layer V CT neurons do not innervate the TRN.

There is accumulating evidence that dysfunction of thalamusrelated systems is a core pathophysiological hallmark for psychosisrelated disorders (Andreasen, 1997; Clinton and Meador-Woodruff, 2004b; Cronenwett and Csernansky, 2010; Pinault, 2011; Steullet, 2019). NMDA receptors are also essential in the generation of thalamic spindles (Deleuze and Huguenard, 2016; Jacobsen et al., 2001), and a reduced function of these receptors is thought to play a critical role in the etio-pathophysiology of schizophrenia (Clinton and Meador-Woodruff, 2004a; Coyle, 2012; Krystal et al., 1994; Snyder and Gao, 2019; Vukadinovic, 2014). Furthermore, the NMDA receptor antagonist ketamine models a transition to a psychosis-relevant state in both healthy humans (Anticevic et al., 2015; Baran et al., 2019; Hoflich et al., 2015; Rivolta et al., 2015) and rodents (Chrobak et al.,

2008; Ehrlichman et al., 2009; Hakami et al., 2009; Kocsis, 2012a; Pinault, 2008; Pitsikas et al., 2008). Therefore, we hypothesized that a reduced function of NMDA receptors is implicated in the reduction of the density of sleep spindles recorded in patients having or about to have psychotic disorders. In an attempt to test this hypothesis, the effects of a single low-dose of ketamine on sleep oscillations were investigated using network and cellular recordings in the dorsal thalamus and TRN along with an EEG of the frontoparietal cortex in the pentobarbitalsedated rat.

2. Methods and materials

2.1. Animals and drugs

Sixty-nine Wistar adult male rats (285–370 g) were used with procedures performed under the approval of the Ministère de l'Education Nationale, de l'Enseignement Supérieur et de la Recherche. Ketamine was provided from Merial (Lyon, France); clozapine, MK-801, apomorphine, and physostigmine, from SigmaAldrich (Saint-Quentin Fallavier, France), pentobarbital from Sanofi (Libourne, France), and Fentanyl from Janssen-CILAG (Issy-LesMoulineaux, France).

2.2. Surgery under general anesthesia

Deep general anesthesia was initiated with an intraperitoneal injection of pentobarbital (60 mg/kg). An additional dose (10–15 mg/kg) of pentobarbital was administered when necessary. Analgesia was achieved with a subcutaneous injection of fentanyl (10 μg/kg) every 30 min. The anesthesia depth was continuously monitored using an electrocardiogram, watching the rhythm and breathing, and measuring the withdrawal reflex. The rectal temperature was maintained at 36.5 °C (peroperative and protective hypothermia) using a thermoregulated pad. The trachea was cannulated and connected to a ventilator (50% air–50% O2, 60 breaths/min). The anesthesia lasted about 2 h, the time necessary to perform the stereotaxic implantation of the electrodes (Pinault, 2005).

2.3. Cortical EEG and thalamic cell-to-network recordings under sedation

To understand how ketamine could influence ongoing sleep oscillations, cortical EEG and cell-to-network recordings were performed in the TC system of pentobarbital sedated rats, a rodent model of slow-wave sleep with spindles (Connor et al., 2003; Ganes and Andersen, 1975; Pinault et al., 2006). At the end of the surgery, the rectal temperature was set to

and maintained at 37.5 °C. The analgesic pentobarbital-induced sedation was initiated about 2 h after the induction of the deep anesthesia and maintained by a continuous intravenous infusion of the following regimen (average quantity given per kg and per hour): Pentobarbital (4.2 ± 0.1 mg), fentanyl (2.4 ± 0.2 µg), and glucose (48.7 ± 1.2 mg). To help maintain a stable mechanical ventilation and to block muscle tone and tremors, a neuromuscular blocking agent was used (d-tubocurarine chloride: 0.64 ± 0.04 mg/kg/h). The cortical EEG and heart rate were under continuous monitoring to adjust the infusion rate to maintain the sedation.

For the cortical EEG recordings (28 rats), a recording silver wire (diameter: 200 µm) sheathed with Teflon was implanted in the parietal bone over the primary somatosensory cortex (from bregma: 2.3 mm posterior and 5 mm lateral).

The network and cellular recordings and labellings were done with glass micropipettes filled with a saline solution (potassium acetate, 0.5 M) and a neuronal tracer (Neurobiotin, 1.5%). Three series of experiments were carried out: 1) The first (16 rats) was designed to perform, along with the cortical EEG, extracellular (field potential and single/multiunit) recordings in specific and non-specific thalamic nuclei. The regions of interest were stereotaxically (Paxinos and Watson, 1998) located behind the bregma (2.3 to 3.6 mm posterior). 2) To consolidate the ketamine-induced effects on the extracellular recordings (population activities), a second series (8 rats) consisting paired juxtacellular TC and TRN recordings were performed in the somatosensory system. The diameter of the micropipette tip was about 1 µm (15–30 MΩ) (Pinault, 1996). 3) In an attempt to understand the cellular membrane potential oscillations underlying the firing patterns, a third series of experiments (11 rats) was designed to record intracellularly TC neurons. The diameter of the micropipette tip was inferior to 1 µm (30–70 MΩ). The extracellular and juxtacellular signals (0.1–6000 Hz), and the intracellular signal (0–6000 Hz) were acquired using a low-noise differential amplifier (DPA-2FL, npi electronic, GmbH) and an intracellular recording amplifier (NeuroData IR-283; Cygnus Technology Inc.), respectively. All signals were sampled at 20 kHz 16-bit (Digidata 1440A with pCLAMP10 Software, Molecular Devices). At the end of the recording session, the target neurons were individually labeled with Neurobiotin using the extra- or juxtacellular nano-iontophoresis technique (Pinault, 1996) to identify formally both the recording site and the structure of the recorded neurons (Fig. 1B). Then the animal was humanely killed with an intravenous overdose of pentobarbital, transcardially perfused with a fixative containing 4% paraformaldehyde in 10 mM phosphate buffer saline, and the brain tissue was processed using standard histological techniques for anatomical documentation.

2.4. Data analysis

Analysis software packages Clampfit v10 (Molecular Devices) and SciWorks v10 (Datawave Technologies) were used. The spindle density was estimated by the number per 10 s of detected bouts filtered at the sigma-frequency (10–16 Hz) oscillations. Spectral analysis of EEG and network oscillations was performed with fast Fourier transformation (FFT, 2-Hz resolution). The power of baseline activity was analyzed in 4 frequency bands: delta-(1–4 Hz), sigma-(10–16 Hz, spindles), gamma-(30–80 Hz), and higher-(81–200 Hz) frequency oscillations. For each band, the total power was the sum of all FFT values. In single-unit juxtacellular recordings, single action potentials (APs) were detected using a voltage threshold and an inter-AP interval superior to 10 ms. High-frequency bursts (hfBursts) were identified based on a voltage threshold and an inter-AP interval inferior to 4 ms. A TC or TRN burst had a minimum of 1 inter-AP interval. Inter-AP time and autocorrelogram histograms, and the density (number per minute) of single APs and hfBursts were computed. To apprehend the time relationship between the network or cellular gamma waves and the cellular firing of a single TC or TRN neuron, a 25–55 Hz filter was used to make gamma waves detectable, to create a peri-event time histogram of the TC or TRN firings. Standard interAP interval (resolution 1 ms) histograms were computed. Each drug effect was measured relative to the vehicle condition with each rat being its control. Statistical significance of the observed effects was evaluated with the Student's paired t-test (significant when $p \leqslant 0.05$).

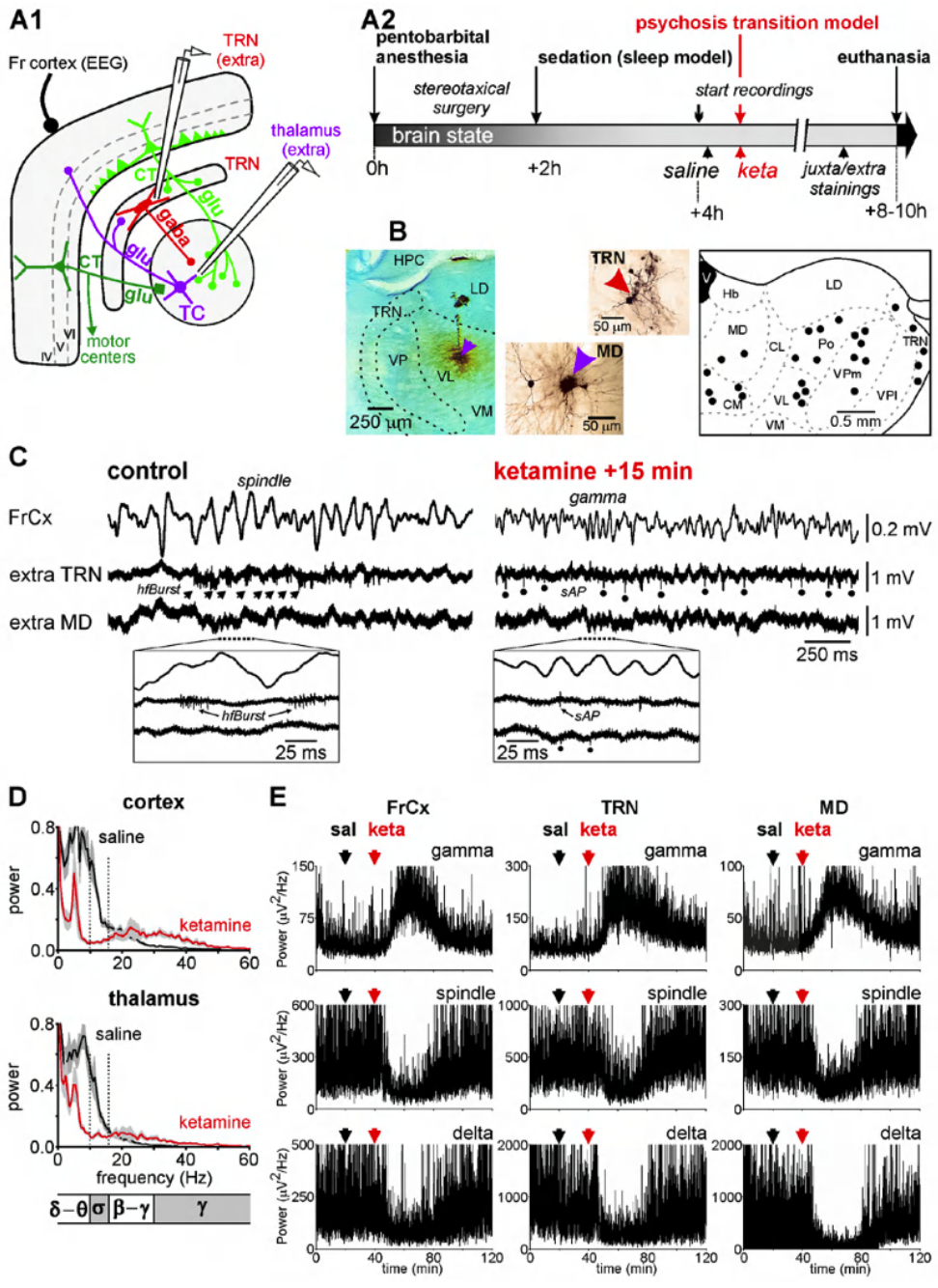

Fig. 1. Ketamine reduces sleep oscillations in the thalamocortical systems. (A1) Experimental design showing the location of the two glass micropipettes designed to record the extracellular activities in the thalamic reticular nucleus (TRN) and in a dorsal thalamic nucleus along with the EEG of the frontal cortex. The hodology of the 4-

neuron CT-TRN-TC circuit is also shown. The corticothalamic (CT) and thalamocortical (TC) neurons are glutamatergic while the TRN neuron is GABAergic. The cortical inputs of the specific thalamic nuclei (like the ventral posterior, VP (somatosensory), and the ventral lateral, VL (motor)) originate from layer VI whereas the cortical inputs of the associative/cognitive thalamic nuclei (like the posterior group, Po, or intralaminar/midline nuclei) originate from layers V and VI. In contrast to the layer V CT neurons, the layer VI CT neurons do innervate the TRN. The intrathalamic innervation pattern of layer VI CT neurons is regional whereas that of the layer V CT neurons, these latter CT neurons targeting only associative/limbic/cognitive thalamic nuclei, is more punctual. The layer V CT axon, which does not innervate the TRN, is a branch of the corticofugal main axon that targets the lower motor centers (brainstem and spinal cord). (A2) Design timeline illustrating the principal steps of the experiment. The color code of the brain state is dark gray for anesthesia, light gray for sedation and dark for death. (B) The left microphotograph shows, at low-magnification, the track left by the electrode and the extracellular labeling of the neurons located at and close to the recording site (here in the VL); the middle microphotograph shows, at higher-magnification, the recording site in the thalamic medial dorsal nucleus (MD, indicated by the arrowhead) and the somatodendritic complex of a couple of MD neurons; the left microphotograph shows the recording site with a few neural elements labeled in the TRN. On the right is presented, into a coronal plane, a mapping of the recording sites (black dots) into the TRN and the dorsal thalamic nuclei. The coronal plane represents a block of brain of about 3.6 mm thick posterior to the bregma (from −2.3 to −3.6 mm) in which recordings were performed. (C) Under the saline (control) condition, the cortex, the TRN and the dorsal thalamic nuclei exhibit a synchronized state, characterized by the occurrence of low-frequency (1–16 Hz) oscillations, including spindles. The extracellular TRN recordings can contain high-frequency (200–700 Hz) bursts of APs (hfBurst, indicated by arrows). The framed expanded trace shows a couple of hfBursts associated with TC spindle waves. Under the ketamine condition, the TC system displays a more desynchronized state, characterized by the prominent occurrence of fast activities (N16 Hz), which include gamma-frequency oscillations. And the TRN cell fires more in the single AP (sAP) mode than in the hfBurst mode. Extracellular sAPs are indicated by the dots. Below, the expanded trace reveals sAPs associated with TC gamma waves. Single APs are also identifiable (indicated by dots) in the extracellular recording of the MD under the ketamine condition. (D) Spectral analysis of the cortical EEG (top) and of the thalamic extracellular activities (bottom) recorded under the saline then the ketamine conditions. Each value is a grand average (±SEM) from 6 rats, each rat being its control (per value: 23 epochs of 2 s/rat (hamming, resolution: 0.5 Hz)). In each chart, the part delimited by 2 dotted lines indicates the sigma-frequency band, which corresponds predominantly to spindles. (E) Time course of the power of, from top to bottom, gamma oscillations, spindles, and delta oscillations recorded simultaneously in the frontal cortex (FrCx), the TRN and in the medial dorsal (MD) nucleus before and after subcutaneous administrations of saline and ketamine (at 20 and 40 min, respectively).

3. Results

3.1. Ketamine reduces thalamocortical spindles and delta-frequency oscillations

The recordings started about 2 h after the onset of the infusion of the pentobarbital containing regimen (Fig. 1A2), that is when the on-line spectral analysis revealed a stationary amount of spindles and slower oscillations (Fig. S2, Fig. 1C), which were qualitatively similar to those recorded during the natural non-REM sleep (Fig. S1B2). Multisite extra- cellular recordings were performed in the TRN, in midline, posterior, and ventral thalamic nuclei. From ~5 min after a subcutaneous administration of ketamine (2.5

mg/kg), the pattern of the cortical and thalamic baseline sleep activities was dramatically reduced in amplitude, supplanted by a more desynchronized pattern (Fig. 1C). Indeed, keta- mine significantly decreased the spindle density (Fig. S3A), and the power (synchronization index) of the spindles and delta oscillations (Figs. 1D,E, S3B). It also decreased the amount of theta-frequency (5–9 Hz) oscillations (Fig. 1D), a CT theta activity that is a hallmark of drowsiness (Pinault et al., 2001). Concomitantly, ketamine significantly increased the power of ongoing gamma- and higher-frequency oscillations. The ketamine effects, observed in all recorded regions ($n \geqslant 4$ rats/region; Fig. 2), were transient (peaking at $15-20$ min) with partial recovery at $60-80$ min after the administration (Fig. 1E). In contrast to drugs modulating dopaminergic and cholinergic transmitter systems, dizocilpine (MK-801), a more specific NMDA receptor antagonist, well mimicked the ketamine effects on spindles and higher-frequency oscillations (S4). And the cholinomimetic physostigmine simulated the ketamine effects on delta oscillations and spindles, not on gamma and higher-frequency oscillations (Fig. S4a,b).

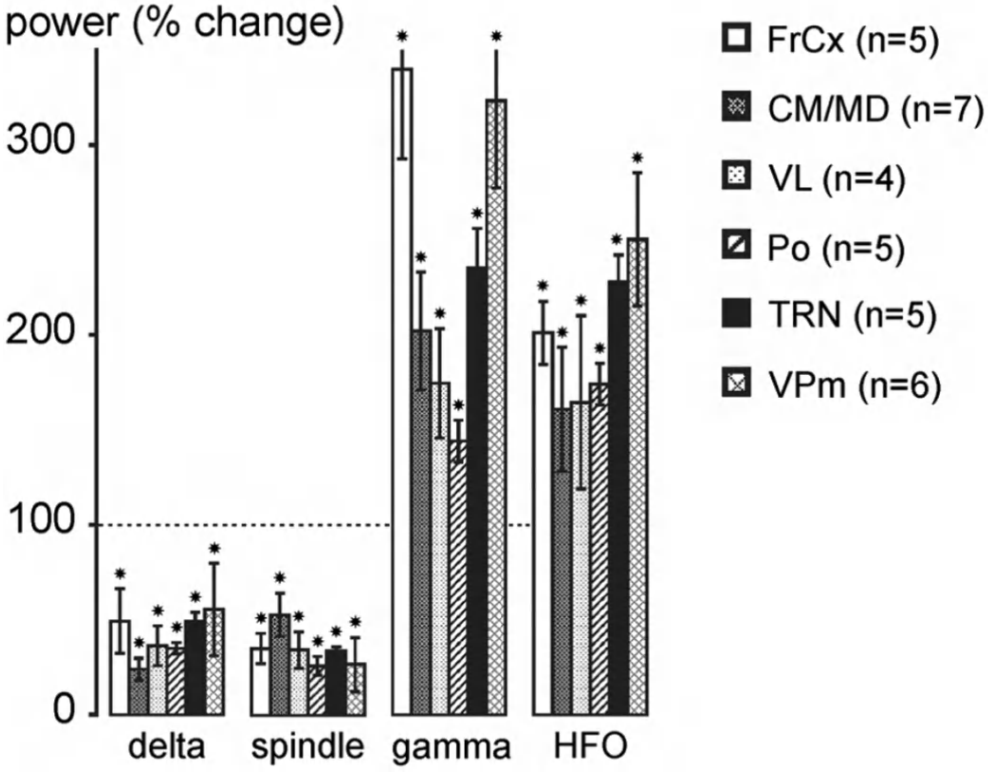

Fig. 2. Ketamine reduces delta-frequency oscillations and spindles and increases gamma and higher-frequency oscillations. The histogram shows the ketamine-induced percent changes (±SEM, relative to the saline condition, each rat being its control; post ketamine: 20 to 30 min) in power of delta oscillations, spindles, gamma- and

higher frequency oscillations recorded in the frontal cortex, in the TRN and in sensorimotor (VPm, VL) and in association/cognitive (CM/MD, Po) thalamic nuclei. Number of rats given in parentheses. Paired t-test relative to saline condition (star when p b 0.05). For abbreviations, see Fig. 1 legend.

3.2. Ketamine switches the firing pattern of thalamic relay and reticular neurons from the burst mode to the tonic mode

In the following, all data are from the somatosensory system as it contains b1% of local-circuit neurons (Harris and Hendrickson, 1987) and its 3-neuron layer VI CT-TRN-TC circuit, common to all nuclei of the dorsal thalamus, is the leading circuit in the generation of spindles. The location of the recording sites was identified based on electrophysiological and anatomical features (Fig. S5). From 11 extracellular thalamic recordings, 6 (from 6 rats) contained at least two TC units that were detectable using an automated spike sorting procedure (Fig. S6). Five out of 8 dual juxtacellular TC-TRN recordings (5 rats) had a duration long enough for data analyses under control and ketamine conditions, and 8 out of 15 TC cells met the intracellular requirements (Pinault et al., 2006).

3.2.1. Thalamic relay neurons

During the sedation, the extracellularly recorded TC units presented an irregular firing pattern consisting in hfBursts and single APs (Fig. S6A). It was extremely rare to see series of rhythmic hfBursts at the spindle frequency, suggesting that most of the TC spindle oscillations were subthreshold (Pinault et al., 2006), as demonstrated by the dual juxtacellular TRN-TC recordings (Fig. 3A1) and by the intracellular recordings of TC neurons (Fig. 3D). From ~5 min after the ketamine administration (16 TC units from 6 rats), the density of hfBursts significantly decreased whereas that of single APs increased for at least 60 min (Fig. S6B). The spike sorting method may, however, not be precise and reliable as the amplitude and shape of the APs might not be stationary over time (Lewicki, 1998). For instance, in TC hfBursts, the AP amplitude became progressively smaller (Fig. S6A).

Therefore, to better validate the ketamine effects observed in the extracellular TC recordings, we performed dual juxtacellular recordings of thalamic relay and reticular neurons. The juxtacellular single-unit recording-labeling technique allows the formal identification of the recorded neuron (Fig. 3A1, B1, C1) (Pinault, 1996). Ketamine, transiently and significantly, decreased the density of TC hfBursts and increased that of single APs (Fig. 3A1, A2 and B3). However, the decrease in the hfBurst density was ~50%, meaning that AP bursts still occurred under the ketamine condition. Embedded in the irregular tonic AP trains, a lot of them were doublets and triplets, whose intrafrequency

was lower (inter-AP interval peak at 5–6 ms, Fig. 4A1, A2) than that of typical hfBursts (interval peak at 2–3 ms, Fig. 4A1). A partial recovery was noticeable 60–80 min after the ketamine administration (Fig. S6B, and Fig. 3B3). Of importance, ketamine increased the firing frequency band of TC neurons from, on average, 5–20 Hz (10.8 ± 2.9 Hz, N = 5 from 5 rats) to 15–30 Hz (21.7 ± 3.5 Hz, N = 5) (Fig. 3E). Furthermore, in one of the experiments, designed to record in the posterior group (equivalent to the pulvinar in humans) of the thalamus, 2 nearby (100 µm apart) TC cells were simultaneously recorded in the juxtacellular configuration (Fig. S7). Ketamine consistently augmented their firing frequency band in a similar way (from 0 to 10 Hz to 0–35 Hz).

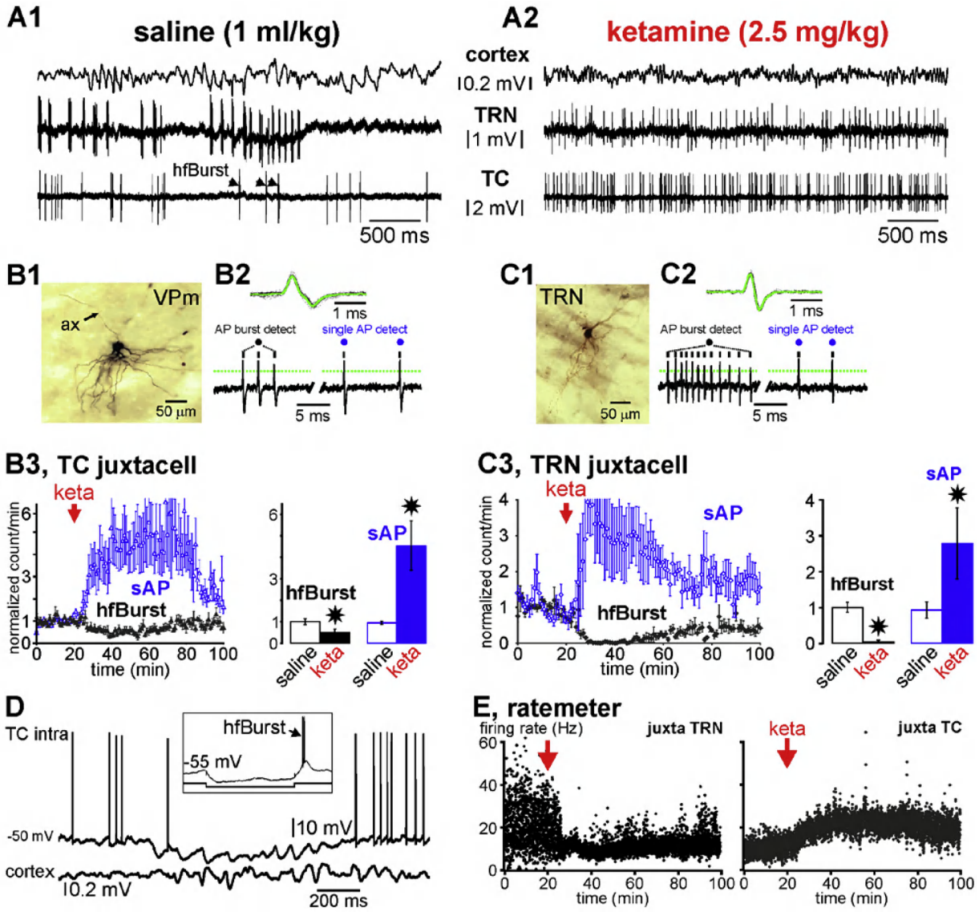

Fig. 3. Ketamine switches the firing pattern from a burst mode to a single action potential mode in thalamic relay (glutamatergic) and reticular (GABAergic) neurons. (A1, A2) Typical simultaneous recordings of the cortex (EEG), and of two single TRN and TC neurons (juxtacellular configuration) of the somatosensory system. Under the saline (A1, control) condition, the cortex displays a synchronized state, characterized by the occurrence of medium-voltage (N0.1 mV) low-frequency (1–16 Hz) oscillations, the TRN cell exhibits a typical series of rhythmic

robust high-frequency bursts of action potentials (hfBursts, 300–500 APs/s), and the TC neuron exhibits single action potentials (sAPs) and, during the TRN burst series, a few bursts. A few minutes after the systemic administration of ketamine (A2, here: +20 min), the cortex displays a more desynchronized state, characterized by the prominent occurrence of lower voltage (b0.1 mV) and faster activities (N16 Hz), which include gamma-frequency oscillations. Under the ketamine condition, both the TC and the TRN cells exhibit much more sAPs than hfBursts. (B1–B3) Data from juxtacellularly recorded TC neurons. (B1) Photomicrography of parts of the somatodendritic complex and of the main axon (ax) of a juxtacellularly recorded and labeled (with Neurobiotin) TC neuron of the somatosensory thalamus. (B2, top) Average and superimposition of 50 action potentials. (B2, below): Detection (from a voltage threshold, indicated by a dotted line) of a typical hfBurst of 3 APs and of 2 successive single APs. (B3) The density (number per minute, ±SEM, 5 TC cells from 5 rats) of hfBursts and of sAPs under the saline and ketamine conditions. Paired t-test (star when p b 0.05). (C1–C3) Data from juxtacellularly recorded TRN neurons. (C1) Photomicrography of part of the somatodendritic complex of a juxtacellularly recorded and labeled (with Neurobiotin) TRN cell. (C2, top) Average and superimposition of 50 APs. (C2, below): Detection (from a voltage threshold, indicated by a dotted line) of a typical hfBurst of 12 APs and of 2 successive single APs. (C3) The density (number per minute, ±SEM, 5 TRN cells from 5 rats) of hfBursts and of sAPs under the saline and ketamine conditions. Paired t-test (star when p b 0.05). (D) Representative trace of an intracellularly recorded TC neuron showing the occurrence of subthreshold oscillations, including spindle-frequency rhythmic waves, which are concomitant with a synchronized EEG state in the related cortex. Note that the subthreshold oscillations occur during the through of a long-lasting hyperpolarization. In the frame is shown the occurrence of a low-threshold potential topped by a high-frequency burst of APs (hfBurst) at the offset of a 200-ms hyperpolarizing pulse. (E) Ratemeter of simultaneously juxtacellularly recorded TRN and TC neurons under saline then ketamine conditions. Each dot is the average (n = 5 neurons from 5 rats) of the number of inter-AP intervals per second.

Curiously, under the ketamine condition, the mean firing frequency of TC neurons (b30 Hz) was lower than the network gamma-frequency oscillations (frequency at maximal power: 33.6 ± 1.1 Hz, n = 7), raising the question whether or not TC single APs were related to the juxta- and extracellular gamma oscillations. In an attempt to address this question, firstly we looked at the raw juxtacellular recordings, in which we notice that TC neurons did not emit an AP at every wave of the gamma oscillations, which were not perfectly regular in waveform and timing (Figs. 4B1, S8), suggesting that the juxtacellular field potential variations reflected more membrane potential oscillations than APs. Secondly, a substantial number of single APs were phase-related to both the juxtacellular and the extracellular (100 µm apart) gamma waves (Fig. S8, Fig. 4B2). However, the temporal link was stronger with the juxtacellular (cellular activity) than the extracellular (nearby network activity) wave. In contrast to layer-organized cortical structures, the weak relation between the juxtacellular APs and the extracellular gamma waves seen in the somatosensory thalamus might have been due to an anarchic overlap of the current sinks and sources generated by the neural activities. On the other hand, there was no apparent relation between the TC firing and the cortical gamma waves (Fig. 4B2), which is not surprising as the EEG integrates the activities of interweaved large-scale networks.

3.2.2. Thalamic reticular neurons

During sedation, all extracellularly (Fig. 1C) or juxtacellularly (Fig. 3 A1) recorded TRN cells exhibited sequences of rhythmic hfBursts in relation to the sleep TC oscillations. The burst sequence naturally recurred at a low frequency (b1 Hz) (Figs. S2B1 and S5B), during which rhythmic hfBursts occurred at the sigma (spindle)- and lower-frequency bands, including the delta band. The rhythmic character of spindle burst patterns was identifiable with an autocorrelation histogram (Fig. S2D). In TRN neurons, such sustained rhythmic burst activity involves the activation of NMDA receptors (Jacobsen et al., 2001). From ~5 min after a single ketamine administration, all juxtacellularly recorded TRN cells suddenly and transiently switched their ongoing rhythmic burst firing pattern to a sustained tonic, single AP firing pattern (Fig. 3A1,A2,C3). Furthermore, ketamine decreased their firing frequency band from 0 to 60 Hz (16.5 ± 2.5 Hz) to 5–25 Hz (8.1 ± 1.8 Hz; n = 5 from 5 rats) (Fig. 3E). Remarkably and significantly, the single AP density increased whereas the hfBurst density decreased (Fig. 3C3, 5A2, B1–B2). In the inter-AP interval histogram, the first peak at 2–4 ms, a marker of hfBursts, disappeared almost completely. Under the ketamine condition, the first peak (3–6 ms) reflects longer inter-AP intervals which, like in TC neurons, are the signature of doublets and triplets embedded in the irregular tonic AP trains (Fig. 5B2).

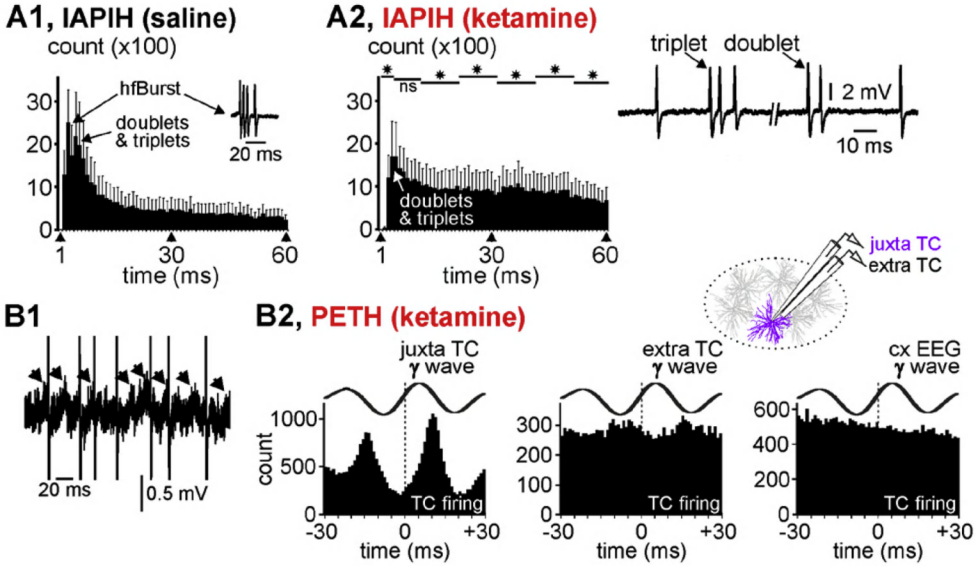

Fig. 4. Thalamocortical firing related to gamma-frequency oscillations. (A1, A2) Averaged cumulated inter-AP interval histograms (IAPIH) from 5 juxtacellularly recorded TC cells (from 5 rats) under the control (A1) then the ketamine (A2) conditions (keta +15–25 min). Note the ketamine-induced diminution in the number of the short-lasting IAPIs, especially those composing high-frequency bursts of APs (IAPI = 2–10 ms). A typical TC hfBurst (IAPI

at 2–3 ms) is shown in the control histogram. The remaining bursts were slower (IAPI at 5–6 ms) and shorter (e.g, especially doublets and triplets, like those shown on the right). Star when significant (paired t-test, p b 0.05). (B1) A typical short-lasting trace of a juxtacellularly recorded TC cell showing low-amplitude gamma-frequency oscillations in the field potential and the AP occurrence at some cycles of the gamma oscillation. Each arrow indicates a juxtacellular gamma wave. The APs are truncated. (B2) Peri-event (gamma wave) time histogram (1-ms resolution) of the TC firing (cumulative count) under the ketamine condition (5 TC cells from 5 rats). Every gamma wave (juxta TC, extra TC (inter-tip distance = 100 µm, see drawing), and cxEEG) is an average of 100 filtered (25–55 Hz) individual gamma (γ) waves. Time "0" corresponds to the time at which gamma waves were detected.

Interestingly, the interval histogram reveals a second peak at ~30–50 ms. We predicted that the 30–50-ms peak represents a marker of juxtacellular gamma oscillations. Indeed, when looking closely at the juxtacellular recordings, it is obvious that the TRN cells fired at a certain proportion of gamma waves during their positive-going component (Fig. 5B1), meaning that the juxtacellular oscillations reflected threshold/suprathreshold and subthreshold membrane potential gamma oscillations. This observation is supported by a peri-gamma wave time histogram of the AP distribution (Fig. 5B2), which shows that the probability of firing reached a maximum at (virtually 0 ms) the positivegoing component of the gamma wave. Furthermore, a substantial number of TRN APs was also phase-related to gamma waves recorded extracellularly in the related somatosensory thalamic nucleus, suggesting a certain degree of functional connectivity. Moreover, using the partial correlation coefficient (S9), the strength of the gamma-frequency band TRN-TC connectivity was significantly increased by ketamine (Fig. 6). On the other hand, in the same way as TC neurons, there was no apparent relation between the TRN firing and the cortical gamma waves (Fig. 5B2).

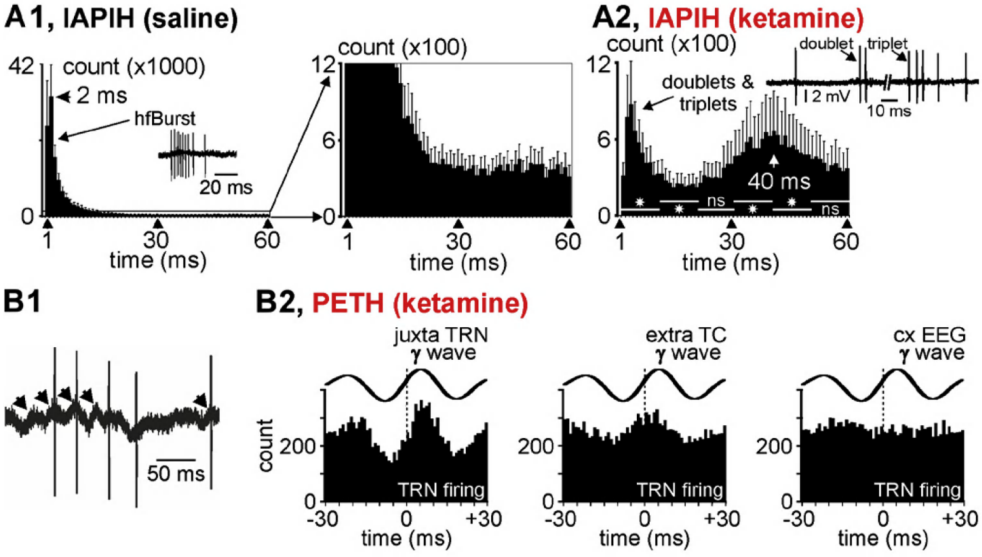

Fig. 5. Thalamic reticular nucleus firing related to gamma-frequency oscillations. (A1, A2) Averaged cumulated inter-AP interval histograms (IAPIH) from 5 juxtacellularly recorded TRN cells (from 5 rats) under the control (A1) then the ketamine (A2) conditions (keta +15–25 min). In (A1), are shown the control (saline) IAPIH in full (left) and partial (right) Y scales. Note the ketamine-induced dramatic diminution in the number of the short-lasting IAPIs, especially those composing high-frequency bursts of APs (IAPI = 2–10 ms). A typical TRN hfBurst is shown in the control histogram. The remaining bursts were slower (increase in IAPIs) and shorter (e.g, especially doublets and triplets, like those shown). Star when significant (paired ttest, p b 0.05). (B1) A typical short-lasting trace of a juxtacellularly recorded TRN cell showing low-amplitude gamma-frequency oscillations in the field potential and that the AP occurrence at some cycles of the gamma oscillation. Each arrow indicates a juxtacellular gamma wave. (B2) Peri-event (gamma wave) time histogram of the TRN firing (cumulative count) under the ketamine condition (5 TRN cells from 5 rats). Every gamma wave (juxta TRN, extra TC, and cxEEG) is an average of 100 filtered (25–55 Hz) individual gamma (γ) waves. Time "0" corresponds to the time at which gamma waves were detected.

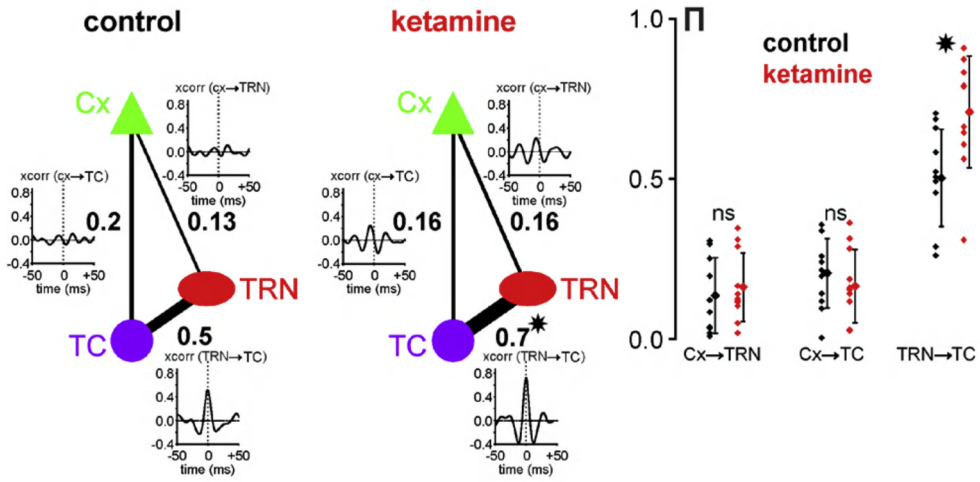

Fig. 6. Ketamine strengthens the functional gamma TRN-TC connectivity. Direct interaction strength between two different sites is given by a partial correlation coefficient written (bold font) next to the edge connecting these sites. The plots presented next to these edges are cross-correlograms of 400 ms-epochs from signals recorded at the corresponding sites and filtered in the gamma-range (25-55 Hz). Under control condition, the strength of gamma interactions between TRN and TC sites was more than twice higher than for CT-TRN and CT-TC interactions, which was also reflected by a high peak in the TRN-TC cross-correlogram. When ketamine was applied, the strength of TRN-TC gamma interactions was significantly increased (paired t-test, p b 0.001), resulting in a higher partial correlation coefficient and a higher peak in the average cross-correlogram. Although after ketamine application, correlations between CT and TRN and between CT and TC were higher in the cross-correlograms, the strength of CT-TRN and CT-TC interactions given by partial correlation coefficients did not change significantly (paired t-test, p N 0.4). The plot on the right shows distributions of partial correlation coefficients Π for CT⟶TRN, CT⟶TC and TRN⟶TC gamma interactions in all experiments (N = 11) under both control (black) and ketamine (red) conditions. (*) indicates significant difference revealed with a paired t-test with p b 0.001; ns, non-significant.

3.3. Clozapine prevents the ketamine effects

Clozapine is one of the most effective antipsychotic drugs against treatment-resistant schizophrenia (Kane et al., 1988). Its clinical effects are thought to be related to interactions with a variety of receptors, including the glutamatergic receptors and more specifically NMDA receptors via the glycine site (Hunt et al., 2015; Lipina et al., 2005; Schwieler et al., 2008). Also, clozapine is well-known to modulate sleep spindles (Tsekou et al., 2015), possibly due to the activation of GABAergic TRN neurons via a specific action on D4 dopamine receptors (Mrzljak et al., 1996), which would exert a tonic influence on the TRN activity (Barrientos et al., 2019). Therefore, it was interesting to probe whether a single systemic administration of clozapine could prevent the ketamine effects on TC oscillations. To address this issue, clozapine was subcutaneously administered at a dose

(5 mg/kg) that durably decreases the power of spontaneously-occurring cortical gamma oscillations in the naturally-behaving rat (Jones et al., 2012) 20 or 120 min before the ketamine challenges. In all rats (n = 7), clozapine consistently prevented the ketamine peak (at ~15–20 min) effect on spindles, delta- and gamma−/higher-frequency oscillations (Fig. S10 and Fig. 7). When administered alone, clozapine significantly increased the power of delta oscillations (Fig. 7).

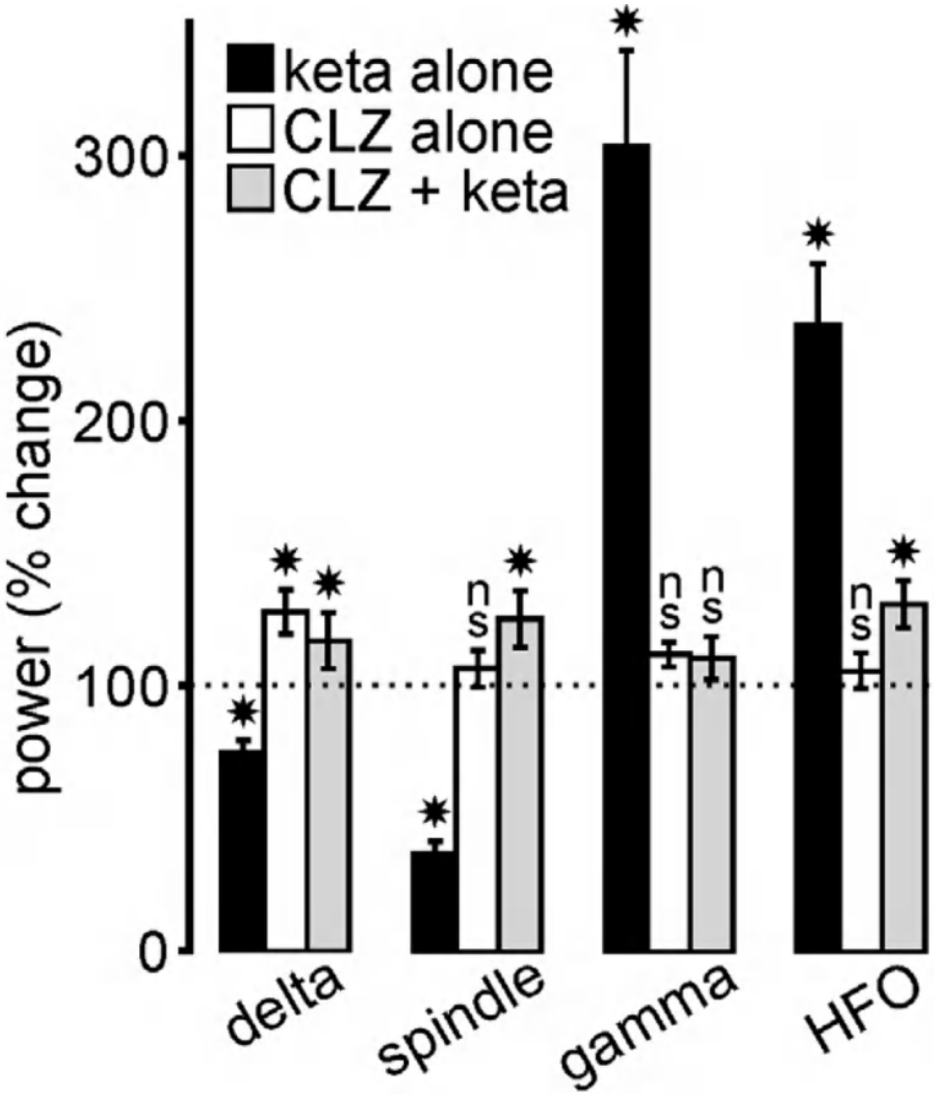

Fig. 7. Clozapine (CLZ) prevents the ketamine effects. The histogram illustrates the druginduced percent changes (mean ± SEM; relative to their respective vehicle (saline for ketamine, saline/HCl 0.1 N for clozapine) condition (100%, indicated by dotted line); 5 rats/condition) in power of all frequency bands in the cortical EEG. Student

paired t-test: (*) $p < 0.05$; ns, not significant. In the CLZ + keta condition, ketamine (2.5 mg/kg) was administered 20 min after the CLZ (5 mg/kg) administration.

4. Discussion

In the present study conducted in the sedated rat, the psychotomimetic ketamine induced a transient dramatic decrease in ongoing thalamic and cortical spindles and slower oscillations, and a concomitant increase in gamma−/higher-frequency oscillations, which is reminiscent of an arousal effect. These new preclinical findings support the hypothesis of a reduced function of NMDA receptors in the reduction of spindles and slow-waves in schizophrenia. They also support the hypothesis that the spindle reduction observed in patients with schizophrenia is due to deficient TRN inhibition (Baran et al., 2019; Ferrarelli and Tononi, 2011; Manoach and Stickgold, 2019; Pratt and Morris, 2015; Young and Wimmer, 2017). However, because ketamine impacted simultaneously and similarly the cellular and network activity patterns of both the GABAergic TRN and the glutamatergic TC neurons (present study), and because ketamine disrupts the function of the CT pathway (Anderson et al., 2017) and forces the brain to generate persistent and generalized aberrant gamma oscillations in cortical and subcortical structures (Hakami et al., 2009; Slovik et al., 2017), nonexclusive alternative theories will be discussed in the following in an attempt to understand the possible underlying mechanisms.

4.1. The arousal promoting effect of low-dose ketamine

Interestingly, the present findings are in agreement with a previous study performed in the awake rat demonstrating that, in a subpopulation of cortical neurons, NMDA receptor hypofunction produces a sustained increase in the firing rate (sAP mode) and a concomitant reduction of burst activity associated with a psychosis-relevant behavior (Jackson et al., 2004).

The arousal promoting effect of a single psychotomimetic dose of ketamine has been well documented in awake, free-behaving rats (Ahnaou et al., 2017; Hakami et al., 2009; Pinault, 2008). The ketamine-induced transient arousal effect is characterized by an abnormal, erratic behavior with hyperlocomotion, ataxias and stereotypies associated with deficits in cognitive performances (Chrobak et al., 2008; Pitsikas et al., 2008), and an excessive amplification of gammafrequency oscillations (Ehrlichman et al., 2009; Hakami et al., 2009; Pinault, 2008). These transient, behavioral, cognitive and electrophysiological abnormalities are reminiscent of a psychosis-relevant behavior, during which not a single

sleep episode was observed during the time dedicated to sleep (S1). Moreover, a comprehensive study demonstrated that ketamine delays the sleep onset latency (Ahnaou et al., 2017).

Clinical investigation showed that patients with psychosis have difficulties initiating sleep (Poulin et al., 2003). Abnormal levels of arousal may be a predictor of psychotic disorders (Lee et al., 2012; Tieges et al., 2013). Here, it is further shown that, in the sedated rat, ketamine elicited a fleeting arousal-like reaction, at least in the TC-TRN system, which is electrophysiologically reminiscent of REM sleep, a brain state considered as a natural model of psychosis (Dresler et al., 2015; Hobson, 1997; Mason and Wakerley, 2012; Mota et al., 2016; Scarone et al., 2008). Moreover, the NMDA receptor hypofunction-related increase in gamma−/higher-frequency oscillations observed in sedated rats is also recorded during the natural REM sleep (Kocsis, 2012b). So, we interpret the ketamine-induced desynchronized state as uncharacteristic REM-like sleep phenomena or a pathological persistent UP state (Fig. 8). During the ketamine-induced pathological UP state, expected to occur within diverse cortical and subcortical structures (Hakami et al., 2009), cortical and thalamic neurons would be more depolarized than during the DOWN state to generate more threshold (for AP initiation) and supra-threshold membrane potential oscillations (Destexhe and Pare, 1999). In thalamic neurons, the burst mode is a reliable hallmark of sleep oscillations, every hfBurst occurring at the top of a low-threshold Ca++ potential mediated by the activation of T-type channels, which are de-inactivated via membrane hyperpolarization (b−60 mV) (Crunelli et al., 2006). Both the synaptic interactions between TC and TRN neurons and the intrinsic pacemaker properties of TRN cells are well-known to play leading roles in the generation of thalamic spindles (Steriade et al., 1985; Steriade et al., 1993). Under the ketamine condition, the substantial increase in the single AP density suggests that the membrane potential of TC and TRN neurons was more often depolarized. This is supported first by the occurrence of gamma oscillations and single AP firing in our juxtacellular TC and TRN recordings and, second, by an increase in the gamma band TRNTC connectivity. The single AP mode is usually recorded when T-type Ca++ channels are inactivated via membrane depolarization (N−60 mV) (Mulle et al., 1986). Disruption of the CaV3.3 Ca++ channel, which encodes the low-threshold T channels (Astori et al., 2011), may be involved in the etio-pathophysiology of schizophrenia (Andrade et al., 2016).

4.2. Contribution of the corticothalamic pathway

In the thalamus, ketamine would act principally on both the glutamatergic TC and the GABAergic TRN neurons. How did ketamine convert the firing from burst to the tonic mode simultaneously in both TC and TRN neurons? During sleep, sustained hyperpolarization would be the result of either excess inhibition or disfacilitation. Under the ketamine condition, a likely effect would be a sustained excitation of these two types of neurons by common afferent input. In addition to the influence of neuromodulatory inputs (see below), the CT pathway seems an excellent candidate (Lam and Sherman, 2010; Landisman and Connors, 2007). Indeed, the primary axon of the CT neurons splits into two branches, one innervating TRN neurons, the other TC neurons (Bourassa et al., 1995; Golshani et al., 2001). Furthermore, it is known that cortical GABAergic interneurons are highly sensitive to NMDA receptor antagonists (Grunze et al., 1996). The ketamine-induced NMDA receptor-mediated disfacilitation of the GABAergic cortical interneurons would be responsible for the disinhibition (or excitation) of glutamatergic pyramidal neurons (Homayoun and Moghaddam, 2007), including CT neurons. So, the disinhibition of CT neurons would lead to the generation of a sustained thalamic AMPA-mediated gamma hyperactivity (Anderson et al., 2017; Crandall et al., 2015; Golshani et al., 2001). And the ketamine-induced hyperactivation of layer VI CT neurons could in addition promote the gamma-frequency pacemaker properties of the GABAergic TRN cells (Pinault and Deschênes, 1992a, 1992b). NMDA receptors are more critical for the CT-mediated excitation of TRN than TC neurons (Deleuze and Huguenard, 2016). Furthermore, the long-lasting kinetics of NMDA receptors in the GABAergic TRN neurons are essential to promote rhythmic Ca++-mediated burst firing, which then cyclically hyperpolarizes the postsynaptic TC neurons through the activation of GABA receptors. Importantly, in TRN neurons, the NMDA-mediated effects of CT transmission can work across a wide range of voltages so as the voltage-dependent blockade by Mg++ is incomplete and that NMDA receptors can be activated by synaptically released glutamate even in the absence of AMPA receptor-mediated activation (Deleuze and Huguenard, 2016). Thus, because CT neurons outnumber by a factor of ~10 TC neurons (Sherman and Koch, 1986), the ketamine NMDA-mediated effects are expected to be stronger on TRN than on TC neurons in reducing burst activity, which, in fact, was indeed observed in the present study (Fig. 3B3,C3). The NMDA receptor hypofunction-related spindle reduction and gamma increase in the TRN-TC system may help to understand the increased TC connectivity correlated with spindle deficits in schizophrenia (Baran et al., 2019).

Ketamine, at a psychotomimetic dose, is expected to affect almost, if not all, brain neurons. In the thalamus, it would impact at least TC and TRN neurons, which work together because of reciprocal connections through open and closed-loop circuits (Pinault and

Deschenes, 1998). Interestingly, under the ketamine condition, both TRN and TC neurons fired in the single AP mode, and the TRN cells on average 2.7 times less than TC neurons. This finding is in line with an intra-cortical study showing that NMDA receptor hypofunction decreases the firing of GABAergic neurons and increases that of glutamatergic neurons (Homayoun and Moghaddam, 2007). Thus, NMDA receptor hypofunction would lead to TC and cortical excitations by disinhibition of the glutamatergic neurons, which would lead to an excessive accumulation of synaptic glutamate and subsequently to activation of AMPA receptors (Moghaddam et al., 1997). Such a psychosis-relevant state may be the source for the generation of abnormal internallygenerated information (Gandal et al., 2012; Hakami et al., 2009).

4.3. Contribution of the ascending reticular activating system and basal forebrain

The likely mechanisms underlying the effects of ketamine remain debatable as it acts in all brain structures and at many receptors (Dorandeu, 2013; Sleigh et al., 2014; Zanos et al., 2018). The ketamine-induced acute arousal-like effect may involve, among many others, cholinergic, monoaminergic, and orexinergic arousal systems (Ahnaou et al., 2017; Dawson et al., 2013; Lu et al., 2008). We should not exclude that, under our experimental conditions, the observed physostigmine effects (decrease in spindles and slower waves) suggest that ketamine could have acted also at acetylcholine receptors. Interestingly, the fact that a single low-dose of ketamine simultaneously affected, in an opposite manner, spindle−/delta-frequency and gamma−/higherfrequency TC oscillations is reminiscent of the seminal finding of Moruzzi and Magoun (Moruzzi and Magoun, 1949). Indeed, these pioneering investigators demonstrated that electrical stimulation of the reticular formation, a complex set of interconnected circuits within the brainstem, evokes in the TC system a switch of the EEG pattern from a synchronized to a desynchronized state, an effect interpreted as an EEG arousal reaction. Moreover, activation of the mesencephalic reticular formation effectively desynchronizes the cortical EEG in lightly anesthetized animals (Munk et al., 1996). Thus, the present findings give further support to the hypothesis of a dysregulation of the ascending reticular activating system, which includes the pedunculopontine nucleus, the basal forebrain, and the thalamus, in the etiopathophysiology of psychotic disorders (Dawson et al., 2013; GarciaRill et al., 2015; Heimer, 2000; Howland, 1997). Moreover, in a previous investigation we demonstrated that NMDA receptor hypofunction leads to a persistent increase in gamma oscillations in the basalis, a cholinergic structure with widespread axonal projections well-known to modulate the neocortex and the TC-TRN system (Hakami et al., 2009; Pinault and Deschenes, 1992).

Also, for the observed ketamine effects, we should not exclude a contribution of the ascending GABAergic pathways (originating from the brainstem, midbrain, ventral tegmental area, zona incerta, basal ganglia, and from the basal forebrain), which play a critical role in promoting TC activation, arousal and REM sleep (Brown and McKenna, 2015; Kim et al., 2015). In the present study, interestingly, physostigmine, known to promote REM sleep (Sitaram et al., 1976) and a cortical EEG arousal (Kenny et al., 2016; Roy and Stullken, 1981), exerted a ketamine-like effect on delta oscillations and spindles (Fig. S4a,b) and on the firing pattern of TRN neurons (Fig. S4c). The atypical antipsychotic clozapine consistently prevented the foremost ketamine-induced acute effects on sleep oscillations. The fact that clozapine alone increased delta oscillations, but did not enhance sleep spindles or reduce gamma activity may indicate a general slowing of the EEG power, which may counteract the arousal effects of ketamine and help keeping the rats in the slow wave sleep (Hinze-Selch et al., 1997). The fact that, in contrast to ketamine, clozapine alone did not affect the cortical gamma power suggests that ketamine and clozapine exerted their action via distinct neural/molecular targets, which does not discredit the hypothesis of a dysregulation of the reticular activating system (Dawson et al., 2013; Garcia-Rill et al., 2015; Heimer, 2000; Howland, 1997), the TC system being nothing but its downstream part (Fig. 8).

Further investigation is required to better understand, in the thalamus, the mechanisms underlying the relative contribution of the topdown and bottom-up effects of low-dose ketamine.

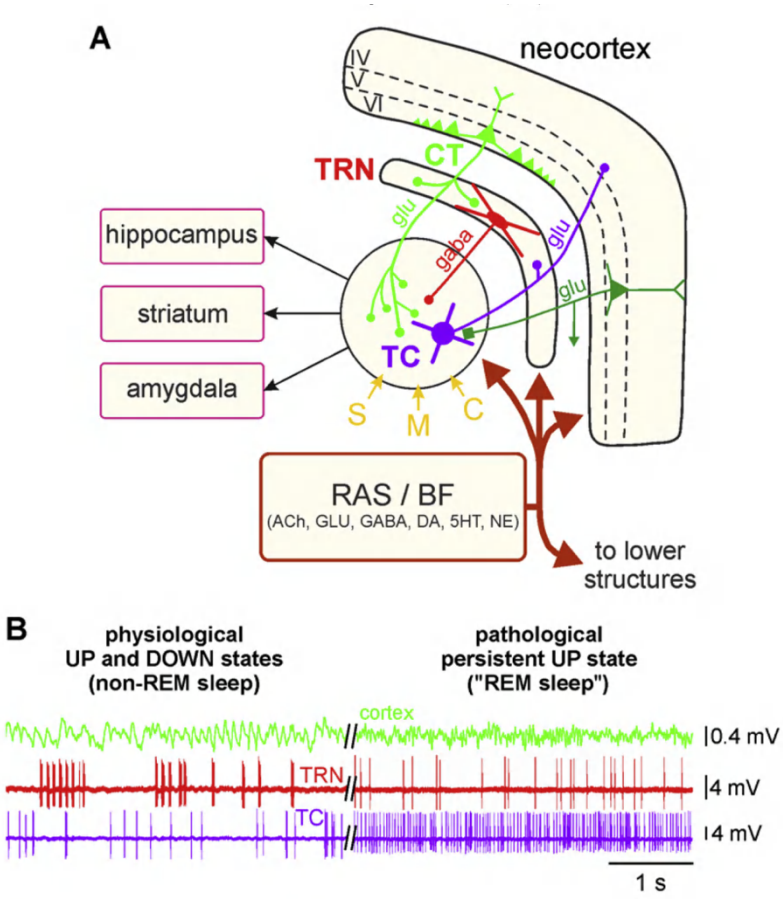

Fig. 8. Theoretical prediction of the ketamine action in both the ascending reticular activating system and the corticothalamic pathway. (A) Simplified drawing of the hodology of the 4- neuron CT-TRN-TC circuit, which is considered as being the upper part of the ascending reticular activating system (RAS). See main text and Fig. 1 legend for detailed description of the circuit, which receives sensory (S), motor (M) and cognitive/associative (C) inputs. It is important to specify that the layer VI CT neurons outnumber by a factor of about 10 the TC neurons. The thalamic nuclei are under the neuromodulatory influence of the various inputs from the ascending RSA and the basal forebrain (BF). (B, left) Physiological UP and DOWN states: During the non-REM sleep, the TC system displays principally a synchronized state, characterized by the occurrence of delta oscillations and spindles; the TRN cell exhibits mainly rhythmic (at the delta-, theta- and spindle-frequency bands) hfBursts of action potentials. The synchronized state includes two sub-states, UP and DOWN, which are usually associated with active and quiescent cellular firings, respectively. (B, right) Pathological persistent UP state: This ketamine-induced persistent UP state is assumed to be an abnormal REM sleep. After a single systemic administration of a subanesthetizing low-dose of ketamine, the TC system displays a more desynchronized state (peak effect at about +15–20 min) characterized by the prominent occurrence of lower voltage and faster activities (N16 Hz), which include beta-, gamma- and higher-frequency oscillations. Under the ketamine condition, both the TC and the TRN neurons exhibit a persistent irregular and tonic firing containing more single APs than hfBursts. ACh, acetylcholine; GLU, glutamate; 5HT, serotonin; DA, dopamine; NE, norepinephrine.

4.4. Conclusions and significance

The present preclinical investigation with its limitations (S11) demonstrates that the acute effects of ketamine result in fast onset arousal promoting effect, suggesting that it acts like a rapid-acting inducer of REM sleep-associated cognitive processes, which is reminiscent of its ability to induce hallucinatory and delusional symptoms (Baldeweg et al., 1998; Becker et al., 2009; Behrendt, 2003; Ffytche, 2008; Spencer et al., 2004). Low-dose ketamine not only disturbs brain rhythms, but also disrupts attention-related sensorimotor and cognitive processes (Grent-'t-Jong et al., 2018; Hoflich et al., 2015; Hong et al., 2010), supporting the notion that schizophrenia is a cognitive disorder with psychosis as a subsequent consequence (Cohen and Insel, 2008; Huang et al., 2019; Woodward and Heckers, 2016). The ketamineinduced changes in rodent EEG oscillations are reminiscent of those observed in at-risk mental state individuals (Fleming et al., 2019; Ramyead et al., 2015) and during the first episode of schizophrenia (Andreou et al., 2015; Flynn et al., 2008). Taken together, the present findings support more strongly the whole brain-networks hypothesis than the isolated brain circuit theory of schizophrenia (Kambeitz et al., 2016).

The neural mechanisms underlying the ketamine-induced fleeting arousal-like effect may be, in part, those responsible for the initial stage of the rapid-acting antidepressant action of ketamine in patients with drug-resistant major depressive disorders (Duncan Jr. et al., 2019; Krystal et al., 2019; Nugent et al., 2019), leading us to think that the ketamine effects are state-dependent. In addition, the present results suggest that the combined sleep and ketamine models have some predictive validity for the first-stage development of innovative therapies against psychotic, bipolar, and depressive disorders.

Acknowledgements

The present work was supported by INSERM, the French National Institute of Health and Medical Research (Institut National de la Santé et de la Recherche Médicale, 2013-), Université de Strasbourg, Unistra (2013-), and Neurex. This project has been funded with support from the NeuroTime Erasmus+ program of the European Commission (2015–2020: AM and YQ). This publication reflects the views only of the authors, and the Commission cannot be held responsible for any use which may be made of the information contained therein. ASA is a graduate student from the Euridol Graduate School of Pain. Data of the present study were presented in 2018 at both the FENS Forum (Berlin) and the SFN

meeting (San Diego). The authors thank Yoland Smith and Martin Deschênes for critical reading of the manuscript.

Authors' contribution

AM, YQ, SK, DP: Design, data acquisition & analysis, and writing; ASA: Data acquisition & analysis; DC: Animal well-being, surgery and technical aspects.

References

Ahnaou, A., Huysmans, H., Biermans, R., Manyakov, N.V., Drinkenburg, W.H.I.M., 2017. Ketamine: Differential Neurophysiological Dynamics In Functional Networks In The Rat Brain. TRANSLATIONAL PSYCHIATRY 7.

Anderson, P.M., Jones, N.C., O'Brien, T.J., Pinault, D., 2017. The N-Methyl D-Aspartate Glutamate Receptor Antagonist Ketamine Disrupts The Functional State Of The Corticothalamic Pathway. CEREBRAL CORTEX 27, 3172–3185.

Andrade, A., Hope, J., Allen, A., Yorgan, V., Lipscombe, D., Pan, J.Q., 2016. A Rare Schizophrenia Risk Variant Of CACNA1I Disrupts Ca(V)3.3 Channel Activity. SCIENTIFIC REPORTS 6.

Andreasen, N., 1997. The Role Of The Thalamus In Schizophrenia. CANADIAN JOURNAL OF PSYCHIATRY-REVUE CANADIENNE DE PSYCHIATRIE 42, 27–33.

Andreou, C., Nolte, G., Leicht, G., Polomac, N., Hanganu-Opatz, I.L., Lambert, M., Engel, A.K., Mulert, C., 2015. Increased Resting-State Gamma-Band Connectivity In First-Episode Schizophrenia. SCHIZOPHRENIA BULLETIN 41, 930–939.

Astori, S., Wimmer, R.D., Prosser, H.M., Corti, C., Corsi, M., Liaudet, N., Volterra, A., Franken, P., Adelman, J.P., Luethi, A., 2011. The Ca(V)3.3 Calcium Channel Is The Major Sleep Spindle Pacemaker In Thalamus. PROCEEDINGS OF THE NATIONAL ACADEMY OF SCIENCES OF THE UNITED STATES OF AMERICA 108, 13823–13828.

Bal, T., Debay, D., Destexhe, A., 2000. Cortical Feedback Controls The Frequency And Synchrony Of Oscillations In The Visual Thalamus. JOURNAL OF NEUROSCIENCE 20, 7478–7488.

Baldeweg, T., Spence, S., Hirsch, S., Gruzelier, J., 1998. Gamma-Band Electroencephalographic Oscillations In A Patient With Somatic Hallucinations. LANCET 352, 620–621.

Baran, B., Karahanoglu, F.I., Mylonas, D., Demanuele, C., Vangel, M., Stickgold, R., Anticevic, A., Manoach, D.S., 2019. Increased Thalamocortical Connectivity In Schizophrenia Correlates With Sleep Spindle Deficits: Evidence For A Common Pathophysiology. BIOLOGICAL PSYCHIATRY-COGNITIVE NEUROSCIENCE AND NEUROIMAGING 4, 706–714.

Barrientos, R., Alatorre, A., Martinez-Escudero, J., Garcia-Ramirez, M., Oviedo-Chavez, A., Delgado, A., Querejeta, E., 2019. Effects Of Local Activation And Blockade Of Dopamine D4 Receptors In The Spiking Activity Of The Reticular Thalamic Nucleus In Normal And In Ipsilateral Dopamine-Depleted Rats. BRAIN RESEARCH 1712, 34–46.

Becker, C., Gramann, K., Mueller, H.J., Elliott, M.A., 2009. Electrophysiological Correlates Of Flicker-Induced Color Hallucinations. CONSCIOUSNESS AND COGNITION 18, 266–276.

Behrendt, R., 2003. Hallucinations: Synchronisation Of Thalamocortical Gamma Oscillations Underconstrained By Sensory Input. CONSCIOUSNESS AND COGNITION 12, 413–451.

Bonjean, M., Baker, T., Lemieux, M., Timofeev, I., Sejnowski, T., Bazhenov, M., 2011. Corticothalamic Feedback Controls Sleep Spindle Duration In Vivo. JOURNAL OF NEUROSCIENCE 31, 9124–9134.

BOURASSA, J., PINAULT, D., DESCHENES, M., 1995. Corticothalamic Projections From The Cortical Barrel Field To The Somatosensory Thalamus In Rats - A Single-Fiber Study Using Biocytin As An Anterograde Tracer. EUROPEAN JOURNAL OF NEUROSCIENCE 7, 19–30.

Brown, R.E., Mckenna, J.T., 2015. Turning A Negative Into A Positive: Ascending Gabaergic Control Of Cortical Activation And Arousal. FRONTIERS IN NEUROLOGY 6.

Castelnovo, A., Graziano, B., Ferrarelli, F., D'Agostino, A., 2018. Sleep Spindles And Slow Waves In Schizophrenia And Related Disorders: Main Findings, Challenges And Future Perspectives. EUROPEAN JOURNAL OF NEUROSCIENCE 48, 2738–2758.

Chrobak, J.J., Hinman, J.R., Sabolek, H.R., 2008. Revealing Past Memories: Proactive Interference And Ketamine-Induced Memory Deficits. JOURNAL OF NEUROSCIENCE 28, 4512–4520.

Clinton, S., Meador-Woodruff, J., 2004a. Abnormalities Of The NMDA Receptor And Associated Intracellular Molecules In The Thalamus In Schizophrenia And Bipolar Disorder. NEUROPSYCHOPHARMACOLOGY 29, 1353–1362.

Clinton, S., Meador-Woodruff, J., 2004b. Thalamic Dysfunction In Schizophrenia: Neurochemical, Neuropathological, And In Vivo Imaging Abnormalities. SCHIZOPHRENIA RESEARCH 69, 237–253.

Cohen, J.D., Insel, T.R., 2008. Cognitive Neuroscience And Schizophrenia: Translational Research In Need Of A Translator. BIOLOGICAL PSYCHIATRY 64, 2–3.

Connor, L., Burrows, P., Zurakowski, D., Bucci, K., Gagnon, D., Mason, K., 2003. Effects Of Iv Pentobarbital With And Without Fentanyl On End-Tidal Carbon Dioxide Levels During Deep Sedation Of Pediatric Patients Undergoing MRI. AMERICAN JOURNAL OF ROENTGENOLOGY 181, 1691–1694.

Coyle, J.T., 2012. NMDA Receptor And Schizophrenia: A Brief History. SCHIZOPHRENIA BULLETIN 38, 920–926.

Crandall, S.R., Cruikshank, S.J., Connors, B.W., 2015. A Corticothalamic Switch: Controlling The Thalamus With Dynamic Synapses. NEURON 86, 768–782.

Cronenwett, W.J., Csernansky, J., 2010. Thalamic Pathology In Schizophrenia, In: Swerdlow, N. (Ed.), BEHAVIORAL NEUROBIOLOGY OF SCHIZOPHRENIA AND ITS TREATMENT, Current Topics In Behavioral Neurosciences. Pp. 509–528.

Crunelli, V., Cope, D.W., Hughes, S.W., 2006. Thalamic T-Type Ca2+ Channels And NREM Sleep. CELL CALCIUM 40, 175–190.

Dawson, N., Morris, B.J., Pratt, J.A., 2013. Subanaesthetic Ketamine Treatment Alters Prefrontal Cortex Connectivity With Thalamus And Ascending Subcortical Systems. SCHIZOPHRENIA BULLETIN 39, 366–377.

Deleuze, C., Huguenard, J.R., 2016. Two Classes Of Excitatory Synaptic Responses In Rat Thalamic Reticular Neurons. JOURNAL OF NEUROPHYSIOLOGY 116, 995–1011.

DESCHENES, M., HU, B., 1990. Electrophysiology And Pharmacology Of The Corticothalamic Input To Lateral Thalamic Nuclei - An Intracellular Study In The Cat. EUROPEAN JOURNAL OF NEUROSCIENCE 2, 140–152.

Destexhe, A., Pare, D., 1999. Impact Of Network Activity On The Integrative Properties Of Neocortical Pyramidal Neurons In Vivo. JOURNAL OF NEUROPHYSIOLOGY 81, 1531–1547.

Dorandeu, F., 2013. Happy 50th Anniversary Ketamine. CNS NEUROSCIENCE & THERAPEUTICS 19, 369.

Dresler, M., Wehrle, R., Spoormaker, V.I., Steiger, A., Holsboer, F., Czisch, M.,

Hobson, J.A., 2015. Neural Correlates Of Insight In Dreaming And Psychosis. SLEEP MEDICINE REVIEWS 20, 92–99.

Duncan, W.C., Jr., Ballard, E.D., Zarate, C.A., 2019. Ketamine-Induced Glutamatergic Mechanisms Of Sleep And Wakefulness: Insights For Developing Novel Treatments For Disturbed Sleep And Mood, In: Landolt, H., Dijk, D. (Eds.), SLEEP-WAKE NEUROBIOLOGY AND PHARMACOLOGY, Handbook Of Experimental Pharmacology. Pp. 337–358.

Ehrlichman, R.S., Gandal, M.J., Maxwell, C.R., Lazarewicz, M.T., Finkel, L.H., Contreras, D., Turetsky, B.I., Siegel, S.J., 2009. N-Methyl-D-Aspartic Acid Receptor Antagonist-Induced Frequency Oscillations In Mice Recreate Pattern Of Electrophysiological Deficits In Schizophrenia. NEUROSCIENCE 158, 705–712.

Ferrarelli, F., Huber, R., Peterson, M.J., Massimini, M., Murphy, M., Riedner, B.A., Watson, A., Bria, P., Tononi, G., 2007. Reduced Sleep Spindle Activity In Schizophrenia Patients. AMERICAN JOURNAL OF PSYCHIATRY 164, 483–492.

Ferrarelli, F., Peterson, M.J., Sarasso, S., Riedner, B.A., Murphy, M.J., Benca, R.M., Bria, P., Kalin, N.H., Tononi, G., 2010. Thalamic Dysfunction In Schizophrenia Suggested By Whole-Night Deficits In Slow And Fast Spindles. AMERICAN JOURNAL OF PSYCHIATRY 167, 1339–1348.

Ferrarelli, F., Tononi, G., 2011. The Thalamic Reticular Nucleus And Schizophrenia. SCHIZOPHRENIA BULLETIN 37, 306–315.

Ffytche, D.H., 2008. The Hodology Of Hallucinations. CORTEX 44, 1067–1083.

Fleming, L.M., Javitt, D.C., Carter, C.S., Kantrowitz, J.T., Girgis, R.R., Kegeles, L.S., Ragland, J.D., Maddock, R.J., Lesh, T.A., Tanase, C., Robinson, J., Potter, W.Z., Carlson, M., Wall, M.M., Choo, T.-H., Grinband, J., Lieberman, J., Krystal, J.H., Corlett, P.R., 2019. A Multicenter Study Of Ketamine Effects On Functional Connectivity: Large Scale Network Relationships, Hubs And Symptom Mechanisms. NEUROIMAGE-CLINICAL 22.

Flynn, G., Alexander, D., Harris, A., Whitford, T., Wong, W., Galletly, C., Silverstein, S., Gordon, E., Williams, L.M., 2008. Increased Absolute Magnitude Of Gamma Synchrony In First-Episode Psychosis. SCHIZOPHRENIA RESEARCH 105, 262–271.

Gandal, M.J., Edgar, J.C., Klook, K., Siegel, S.J., 2012. Gamma Synchrony: Towards A Translational Biomarker For The Treatment-Resistant Symptoms Of

Schizophrenia. NEUROPHARMACOLOGY 62, 1504–1518

GANES, T., ANDERSEN, P., 1975. BARBITURATE SPINDLE ACTIVITY IN FUNCTIONALLY CORRESPONDING THALAMIC AND CORTICAL SOMATO-SENSORY AREAS IN CAT. BRAIN RESEARCH 98, 457–472.

Garcia-Rill, E., D'Onofrio, S., Mahaffey, S., Bisagno, V., Urbano, F.J., 2015. Pedunculopontine Arousal System Physiology-Implications For Schizophrenia. SLEEP SCIENCE 8, 82–91.

Gentet, L., Ulrich, D., 2003. Strong, Reliable And Precise Synaptic Connections Between Thalamic Relay Cells And Neurones Of The Nucleus Reticularis In Juvenile Rats. JOURNAL OF PHYSIOLOGY-LONDON 546, 801–811.

Golshani, P., Liu, X., Jones, E., 2001. Differences In Quantal Amplitude Reflect Glur4-Subunit Number At Corticothalamic Synapses On Two Populations Of Thalamic Neurons. PROCEEDINGS OF THE NATIONAL ACADEMY OF SCIENCES OF THE UNITED STATES OF AMERICA 98, 4172–4177.

Grunze, H., Rainnie, D., Hasselmo, M., Barkai, E., Heam, E., Mccarley, R., Greene, R., 1996. NMDA-Dependent Modulation Of CA1 Local Circuit Inhibition. JOURNAL OF NEUROSCIENCE 16, 2034–2043.

Guillery, R., Sherman, S., 2002. Thalamic Relay Functions And Their Role In Corticocortical Communication: Generalizations From The Visual System. NEURON 33, 163–175.

Hakami, T., Jones, N.C., Tolmacheva, E.A., Gaudias, J., Chaumont, J., Salzberg, M., O'Brien, T.J., Pinault, D., 2009. NMDA Receptor Hypofunction Leads To Generalized And Persistent Aberrant Gamma Oscillations Independent Of Hyperlocomotion And The State Of Consciousness. PLOS ONE 4.

HARRIS, R., HENDRICKSON, A., 1987. Local Circuit Neurons In The Rat Ventrobasal Thalamus - A Gaba Immunocytochemical Study. NEUROSCIENCE 21, 229–236.

Heimer, L., 2000. Basal Forebrain In The Context Of Schizophrenia. BRAIN RESEARCH REVIEWS 31, 205–235.

Hinzeselch, D., Mullington, J., Orth, A., Lauer, C., Pollmacher, T., 1997. Effects Of Clozapine On Sleep: A Longitudinal Study. BIOLOGICAL PSYCHIATRY 42, 260–266.

Hobson, J., 1997. Dreaming As Delirium: A Mental Status Analysis Of Our Nightly Madness. SEMINARS IN NEUROLOGY 17, 121–128.

Homayoun, H., Moghaddam, B., 2007. NMDA Receptor Hypofunction Produces Opposite Effects On

Prefrontal Cortex Interneurons And Pyramidal Neurons. JOURNAL OF NEUROSCIENCE 27, 11496–11500

Hong, L.E., Summerfelt, A., Buchanan, R.W., O'Donnell, P., Thaker, G.K., Weiler, M.A., Lahti, A.C., 2010. Gamma And Delta Neural Oscillations And Association With Clinical Symptoms Under Subanesthetic Ketamine. NEUROPSYCHOPHARMACOLOGY 35, 632–640.

Howland, R., 1997. Sleep-Onset Rapid Eye Movement Periods In Neuropsychiatric Disorders: Implications For The Pathophysiology Of Psychosis. JOURNAL OF NERVOUS AND MENTAL DISEASE 185, 730–738.

Huang, A.S., Rogers, B.P., Woodward, N.D., 2019. Disrupted Modulation Of Thalamus Activation And Thalamocortical Connectivity During Dual Task Performance In Schizophrenia. SCHIZOPHRENIA RESEARCH 210, 270–277.

Hunt, M.J., Olszewski, M., Piasecka, J., Whittington, M.A., Kasicki, S., 2015. Effects Of NMDA Receptor Antagonists And Antipsychotics On High Frequency Oscillations Recorded In The Nucleus Accumbens Of Freely Moving Mice. PSYCHOPHARMACOLOGY 232, 4525–4535.

Jackson, M., Homayoun, H., Moghaddam, B., 2004. NMDA Receptor Hypofunction Produces Concomitant Firing Rate Potentiation And Burst Activity Reduction In The Prefrontal Cortex. PROCEEDINGS OF THE NATIONAL ACADEMY OF SCIENCES OF THE UNITED STATES OF AMERICA 101, 8467–8472.

Jacobsen, R., Ulrich, D., Huguenard, J., 2001. GABA(B) And NMDA Receptors Contribute To Spindle-Like Oscillations In Rat Thalamus In Vitro. JOURNAL OF NEUROPHYSIOLOGY 86, 1365–1375.

Jones, N.C., Reddy, M., Anderson, P., Salzberg, M.R., O'Brien, T.J., Pinault, D., 2012. Acute Administration Of Typical And Atypical Antipsychotics Reduces EEG Gamma Power, But Only The Preclinical Compound LY379268 Reduces The Ketamine-Induced Rise In Gamma Power. INTERNATIONAL JOURNAL OF NEUROPSYCHOPHARMACOLOGY 15, 657–668.

Kamath, J., Virdi, S., Winokur, A., 2015. Sleep Disturbances In Schizophrenia. PSYCHIATRIC CLINICS OF NORTH AMERICA 38, 777+.

Kambeitz, J., Kambeitz-Ilankovic, L., Cabral, C., Dwyer, D.B., Calhoun, V.D., Van Den Heuvel, M.P., Falkai,

P., Koutsouleris, N., Malchow, B., 2016. Aberrant Functional Whole-Brain Network Architecture In Patients With Schizophrenia: A Meta-Analysis. SCHIZOPHRENIA BULLETIN 42, S13–S21

KANE, J., HONIGFELD, G., SINGER, J., MELTZER, H., 1988. Clozapine In Treatment-Resistant Schizophrenics. PSYCHOPHARMACOLOGY BULLETIN 24, 62–67.

Kaskie, R.E., Ferrarelli, F., 2018. Investigating The Neurobiology Of Schizophrenia And Other Major Psychiatric Disorders With Transcranial Magnetic Stimulation. SCHIZOPHRENIA RESEARCH 192, 30–38.

Kenny, J.D., Chemali, J.J., Cotten, J.F., Van Dort, C.J., Kim, S.-E., Ba, D., Taylor, N.E., Brown, E.N., Solt, K., 2016. Physostigmine And Methylphenidate Induce Distinct Arousal States During Isoflurane General Anesthesia In Rats. ANESTHESIA AND ANALGESIA 123, 1210–1219.

Kim, T., Thankachan, S., Mckenna, J.T., Mcnally, J.M., Yang, C., Choi, J.H., Chen, L., Kocsis, B., Deisseroth, K., Strecker, R.E., Basheer, R., Brown, R.E., Mccarley, R.W., 2015. Cortically Projecting Basal Forebrain Parvalbumin Neurons Regulate Cortical Gamma Band Oscillations. PROCEEDINGS OF THE NATIONAL ACADEMY OF SCIENCES OF THE UNITED STATES OF AMERICA 112, 3535–3540.

Kocsis, B., 2012a. Differential Role Of NR2A And NR2B Subunits In N-Methyl-D-Aspartate Receptor Antagonist-Induced Aberrant Cortical Gamma Oscillations. BIOLOGICAL PSYCHIATRY 71, 987–995.

Kocsis, B., 2012b. State-Dependent Increase Of Cortical Gamma Activity During REM Sleep After Selective Blockade Of NR2B Subunit Containing NMDA Receptors. SLEEP 35, 1011–1016.

KRYSTAL, J., KARPER, L., SEIBYL, J., FREEMAN, G., DELANEY, R., BREMNER, J., HENINGER, G., BOWERS, M., CHARNEY, D., 1994. Subanesthetic Effects Of The Noncompetitive Nmda Antagonist, Ketamine, In Humans - Psychotomimetic, Perceptual, Cognitive, And Neuroendocrine Responses. ARCHIVES OF GENERAL PSYCHIATRY 51, 199–214.

Lam, Y.-W., Sherman, S.M., 2010. Functional Organization Of The Somatosensory Cortical Layer 6 Feedback To The Thalamus. CEREBRAL CORTEX 20, 13–24.

Landisman, C.E., Connors, B.W., 2007. VPM And Pom Nuclei Of The Rat Somatosensory Thalamus:

Intrinsic Neuronal Properties And Corticothalamic Feedback. CEREBRAL CORTEX 17, 2853–2865.

Lee, Y.J., Cho, S.-J., Cho, I.H., Jang, J.H., Kim, S.J., 2012. The Relationship Between Psychotic-Like Experiences And Sleep Disturbances In Adolescents. SLEEP MEDICINE 13, 1021–1027.

Lewicki, M., 1998. A Review Of Methods For Spike Sorting: The Detection And Classification Of Neural Action Potentials. NETWORK-COMPUTATION IN NEURAL SYSTEMS 9, R53–R78.

Lipina, T., Labrie, V., Weiner, I., Roder, J., 2005. Modulators Of The Glycine Site On NMDA Receptors, D-Serine And ALX 5407, Display Similar Beneficial Effects To Clozapine In Mouse Models Of Schizophrenia. PSYCHOPHARMACOLOGY 179, 54–67.

Lu, J., Nelson, L.E., Franks, N., Maze, M., Chamberlin, N.L., Saper, C.B., 2008. Role Of Endogenous Sleep-Wake And Analgesic Systems In Anesthesia. JOURNAL OF COMPARATIVE NEUROLOGY 508, 648–662.

Manoach, D.S., Demanuele, C., Wamsley, E.J., Vangel, M., Montrose, D.M., Miewald, J., Kupfer, D., Buysse, D., Stickgold, R., Keshavan, M.S., 2014. Sleep Spindle Deficits In Antipsychotic-Naive Early Course Schizophrenia And In Non-Psychotic First-Degree Relatives. FRONTIERS IN HUMAN NEUROSCIENCE 8.

Manoach, D.S., Pan, J.Q., Purcell, S.M., Stickgold, R., 2016. Reduced Sleep Spindles In Schizophrenia: A Treatable Endophenotype That Links Risk Genes To Impaired Cognition? BIOLOGICAL PSYCHIATRY 80, 599–608.

Manoach, D.S., Stickgold, R., 2019. Abnormal Sleep Spindles, Memory Consolidation, And Schizophrenia, In: Widiger, T., Cannon, T. (Eds.), ANNUAL REVIEW OF CLINICAL PSYCHOLOGY, VOL 15, Annual Review Of Clinical Psychology. Pp. 451–479.

Mason, O., Wakerley, D., 2012. The Psychotomimetic Nature Of Dreams: An Experimental Study. SCHIZOPHRENIA RESEARCH AND TREATMENT 2012.

Moghaddam, B., Adams, B., Verma, A., Daly, D., 1997. Activation Of Glutamatergic Neurotransmission By Ketamine: A Novel Step In The Pathway From NMDA Receptor Blockade To Dopaminergic And Cognitive Disruptions Associated With The Prefrontal Cortex. JOURNAL OF NEUROSCIENCE 17, 2921–2927.

Monti, J., Monti, D., 2005. Sleep Disturbance In Schizophrenia.

INTERNATIONAL REVIEW OF PSYCHIATRY 17, 247–253.

MORUZZI, G., MAGOUN, H., 1949. BRAIN STEM RETICULAR FORMATION AND ACTIVATION OF THE EEG. ELECTROENCEPHALOGRAPHY AND CLINICAL NEUROPHYSIOLOGY 1, 455–473.

Mota, N.B., Resende, A., Mota-Rolim, S.A., Copelli, M., Ribeiro, S., 2016. Psychosis And The Control Of Lucid Dreaming. FRONTIERS IN PSYCHOLOGY 7.

Mrzljak, L., Bergson, C., Pappy, M., Huff, R., Levenson, R., Goldmanrakic, P., 1996. Localization Of Dopamine D4 Receptors In Gabaergic Neurons Of The Primate Brain. NATURE 381, 245–248.

MULLE, C., MADARIAGA, A., DESCHENES, M., 1986. MORPHOLOGY AND ELECTROPHYSIOLOGICAL PROPERTIES OF RETICULARIS THALAMI NEURONS IN CAT - INVIVO STUDY OF A THALAMIC PACEMAKER. JOURNAL OF NEUROSCIENCE 6, 2134–2145.

Munk, M., Roelfsema, P., Konig, P., Engel, A., Singer, W., 1996. Role Of Reticular Activation In The Modulation Of Intracortical Synchronization. SCIENCE 272, 271–274.

Nugent, A.C., Ballard, E.D., Gould, T.D., Park, L.T., Moaddel, R., Brutsche, N.E., Zarate, C.A., Jr., 2019. Ketamine Has Distinct Electrophysiological And Behavioral Effects In Depressed And Healthy Subjects. MOLECULAR PSYCHIATRY 24, 1040–1052.

Paxinos, G., Watson, C., 1998. The Rat Brain - In Stereotaxic Coordinates - Preface: Fourth Edition, In: RAT BRAIN IN STEREOTAXIC COORDINATES, FOURTH ED. P. Ix+.

Pinault, D., 2011. Dysfunctional Thalamus-Related Networks In Schizophrenia. SCHIZOPHRENIA BULLETIN 37, 238–243.

Pinault, D., 2008. N-Methyl D-Aspartate Receptor Antagonists Ketarnine And MK-801 Induce Wake-Related Aberrant,Gamma Oscillations In The Rat Neocortex. BIOLOGICAL PSYCHIATRY 63, 730–735.

Pinault, D., 2005. A New Stabilizing Craniotomy-Duratomy Technique For Single-Cell Anatomo-Electrophysiological Exploration Of Living Intact Brain Networks. JOURNAL OF NEUROSCIENCE METHODS 141, 231–242.

Pinault, D., 2004. The Thalamic Reticular Nucleus: Structure, Function And Concept. BRAIN RESEARCH REVIEWS 46, 1–31.

Pinault, D., 1996. A Novel Single-Cell Staining Procedure Performed In Vivo Under Electrophysiological Control: Morpho-Functional

Features Of Juxtacellularly Labeled Thalamic Cells And Other Central Neurons With Biocytin Or Neurobiotin. JOURNAL OF NEUROSCIENCE METHODS 65, 113–136.

Pinault, D., Deschenes, M., 1998. Anatomical Evidence For A Mechanism Of Lateral Inhibition In The Rat Thalamus. EUROPEAN JOURNAL OF NEUROSCIENCE 10, 3462–3469.

PINAULT, D., DESCHENES, M., 1992a. CONTROL OF 40-HZ FIRING OF RETICULAR THALAMIC CELLS BY NEUROTRANSMITTERS. NEUROSCIENCE 51, 259–268.

PINAULT, D., DESCHENES, M., 1992b. VOLTAGE-DEPENDENT 40-HZ OSCILLATIONS IN RAT RETICULAR THALAMIC NEURONS INVIVO. NEUROSCIENCE 51, 245–258.

PINAULT, D., DESCHENES, M., 1992c. MUSCARINIC INHIBITION OF RETICULAR THALAMIC CELLS BY BASAL FOREBRAIN NEURONS. NEUROREPORT 3, 1101–1104.

Pinault, D., Slezia, A., Acsady, L., 2006. Corticothalamic 5-9 Hz Oscillations Are More Pro-Epileptogenic Than Sleep Spindles In Rats. JOURNAL OF PHYSIOLOGY-LONDON 574, 209–227.

Pinault, D., Vergnes, M., Marescaux, C., 2001. Medium-Voltage 5-9-Hz Oscillations Give Rise To Spike-And-Wave Discharges In A Genetic Model Of Absence Epilepsy: In Vivo Dual Extracellular Recording Of Thalamic Relay And Reticular Neurons. NEUROSCIENCE 105, 181–201.

Pitsikas, N., Boultadakis, A., Sakellaridis, N., 2008. Effects Of Sub-Anesthetic Doses Of Ketamine On Rats' Spatial And Non-Spatial Recognition Memory. NEUROSCIENCE 154, 454–460.

Poulin, J., Daoust, A., Forest, G., Stip, E., Godbout, R., 2003. Sleep Architecture And Its Clinical Correlates In First Episode And Neuroleptic-Naive Patients With Schizophrenia. SCHIZOPHRENIA RESEARCH 62, 147–153.

Pratt, J.A., Morris, B.J., 2015. The Thalamic Reticular Nucleus: A Functional Hub For Thalamocortical Network Dysfunction In Schizophrenia And A Target For Drug Discovery. JOURNAL OF PSYCHOPHARMACOLOGY 29, 127–137.

Ramyead, A., Kometer, M., Studerus, E., Koranyi, S., Ittig, S., Gschwandtner, U., Fuhr, P., Riecher-Roessler, A., 2015. Aberrant Current Source-Density And Lagged Phase Synchronization Of Neural Oscillations As Markers For Emerging Psychosis. SCHIZOPHRENIA BULLETIN 41, 919–929.

Rivolta, D., Heidegger, T., Scheller, B., Sauer, A., Schaum, M., Birkner, K., Singer, W., Wibral, M., Uhlhaas, P.J., 2015. Ketamine Dysregulates The Amplitude And Connectivity Of High-Frequency Oscillations In Cortical-Subcortical Networks In Humans: Evidence From Resting-State Magnetoencephalography-Recordings. SCHIZOPHRENIA BULLETIN 41, 1105–1114.

ROY, R., STULKEN, E., 1981. ELECTROENCEPHALOGRAPHIC EVIDENCE OF AROUSAL IN DOGS FROM HALOTHANE AFTER DOXAPRAM, PHYSOSTIGMINE, OR NALOXONE. ANESTHESIOLOGY 55, 392–397.

Scarone, S., Manzone, M.L., Gambini, O., Kantzas, I., Limosani, I., D'Agostino, A., Hobson, J.A., 2008. The Dream As A Model For Psychosis: An Experimental Approach Using Bizarreness As A Cognitive Marker. SCHIZOPHRENIA BULLETIN 34, 515–522.

Schwieler, L., Linderholm, K.R., Nilsson-Todd, L.K., Erhardt, S., Engberg, G., 2008. Clozapine Interacts With The Glycine Site Of The NMDA Receptor: Electrophysiological Studies Of Dopamine Neurons In The Rat Ventral Tegmental Area. LIFE SCIENCES 83, 170–175.

SHERMAN, S., KOCH, C., 1986. THE CONTROL OF RETINOGENICULATE TRANSMISSION IN THE MAMMALIAN LATERAL GENICULATE-NUCLEUS. EXPERIMENTAL BRAIN RESEARCH 63, 1–20.

SITARAM, N., WYATT, R., DAWSON, S., GILLIN, J., 1976. REM-SLEEP INDUCTION BY PHYSOSTIGMINE INFUSION DURING SLEEP. SCIENCE 191, 1281–1283.

Sleigh, J., Harvey, M., Voss, L., Denny, B., 2014. Ketamine - More Mechanisms Of Action Than Just NMDA Blockade. TRENDS IN ANAESTHESIA AND CRITICAL CARE 4, 76–81.

Slovik, M., Rosin, B., Moshel, S., Mitelman, R., Schechtman, E., Eitan, R., Raz, A., Bergman, H., 2017. Ketamine Induced Converged Synchronous Gamma Oscillations In The Cortico-Basal Ganglia Network Of Nonhuman Primates. JOURNAL OF NEUROPHYSIOLOGY 118, 917–931.

Snyder, M.A., Gao, W.-J., 2020. NMDA Receptor Hypofunction For Schizophrenia Revisited: Perspectives From Epigenetic Mechanisms. SCHIZOPHRENIA RESEARCH 217, 60–70.

Spencer, K., Nestor, P., Perlmutter, R., Niznikiewicz, M., Klump, M., Frumin, M., Shenton, M., Mccarley, R., 2004. Neural Synchrony Indexes Disordered Perception And Cognition In Schizophrenia. PROCEEDINGS OF THE NATIONAL

ACADEMY OF SCIENCES OF THE UNITED STATES OF AMERICA 101, 17288–17293.

STERIADE, M., DESCHENES, M., DOMICH, L., MULLE, C., 1985. ABOLITION OF SPINDLE OSCILLATIONS IN THALAMIC NEURONS DISCONNECTED FROM NUCLEUS RETICULARIS THALAMI. JOURNAL OF NEUROPHYSIOLOGY 54, 1473–1497.

STERIADE, M., MCCORMICK, D., SEJNOWSKI, T., 1993. THALAMOCORTICAL OSCILLATIONS IN THE SLEEPING AND AROUSED BRAIN. SCIENCE 262, 679–685.

Steullet, P., 2020. Thalamus-Related Anomalies As Candidate Mechanism-Based Biomarkers For Psychosis. SCHIZOPHRENIA RESEARCH 226, 147–157.

Tieges, Z., Mcgrath, A., Hall, R.J., Maclullich, A.M.J., 2013. Abnormal Level Of Arousal As A Predictor Of Delirium And Inattention: An Exploratory Study. AMERICAN JOURNAL OF GERIATRIC PSYCHIATRY 21, 1244–1253.

Tsekou, H., Angelopoulos, E., Paparrigopoulos, T., Golemati, S., Soldatos, C.R., Papadimitriou, G.N., Ktonas, P.Y., 2015. Sleep EEG And Spindle Characteristics After Combination Treatment With Clozapine In Drug-Resistant Schizophrenia: A Pilot Study. JOURNAL OF CLINICAL NEUROPHYSIOLOGY 32, 159–163.

Vukadinovic, Z., 2014. NMDA Receptor Hypofunction And The Thalamus In Schizophrenia. PHYSIOLOGY & BEHAVIOR 131, 156–159.

Wamsley, E.J., Tucker, M.A., Shinn, A.K., Ono, K.E., Mckinley, S.K., Ely, A.V., Goff, D.C., Stickgold, R., Manoach, D.S., 2012. Reduced Sleep Spindles And Spindle Coherence In Schizophrenia: Mechanisms Of Impaired Memory Consolidation? BIOLOGICAL PSYCHIATRY 71, 154–161.

Woodward, N.D., Heckers, S., 2016. Mapping Thalamocortical Functional Connectivity In Chronic And Early Stages Of Psychotic Disorders. BIOLOGICAL PSYCHIATRY 79, 1016–1025.

Young, A., Wimmer, R.D., 2017. Implications For The Thalamic Reticular Nucleus In Impaired Attention And Sleep In Schizophrenia. SCHIZOPHRENIA RESEARCH 180, 44–47.

Zanini, M.A., Castro, J., Cunha, G.R., Asevedo, E., Pan, P.M., Bittencourt, L., Coelho, F.M., Tufik, S., Gadelha, A., Bressan, R.A., Brietzke, E., 2015. Abnormalities In Sleep Patterns In Individuals At Risk For Psychosis And Bipolar Disorder. SCHIZOPHRENIA RESEARCH 169, 262–267.

Zanos, P., Moaddel, R., Morris, P.J., Riggs, L.M., Highland, J.N., Georgiou, P., Pereira, E.F.R., Albuquerque, E.X., Thomas, C.J., Zarate, C.A., Jr., Gould, T.D., 2018. Ketamine And Ketamine Metabolite Pharmacology: Insights Into Therapeutic Mechanisms. PHARMACOLOGICAL REVIEWS 70, 621–660.

Supplementary

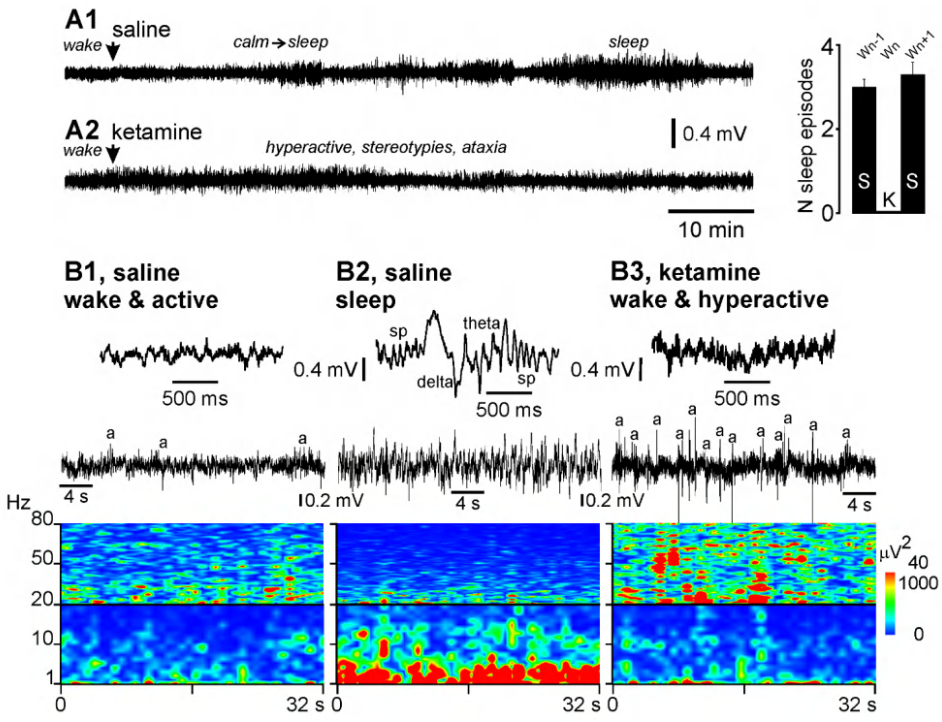

Fig. S1. Ketamine prevents the occurrence of natural sleep episodes in free-behaving rats. (A1-A2) Two typical 80-min recording sessions (cortical EEG, bandpass: 1-800 Hz, recording cable-induced artifacts withdrawn) performed in a freely moving rat with one week interval under the saline (A1) and ketamine (A2) conditions. Saline (1 ml/kg) or ketamine (2.5 mg/kg, 1 ml/kg) was subcutaneously injected a few min after the beginning of the recording session (arrow). At the very beginning of the session, the rat is usually active with a cortical EEG displaying, prominently, low-amplitude (17 Hz) oscillations (B1). Under control (saline) condition, the rat usually becomes calm (quiet immobile wakefulness) then, after toileting, goes into slow-wave sleep episodes. Non-REM sleep episodes were identified on the basis of the occurrence of delta (1-4 Hz)- , theta (5-9 Hz)- and spindle (sp, 10-16 Hz)-frequency oscillations (B2). Under the ketamine condition, the rat becomes quickly hyperactive (erratic behavior with stereotypies and ataxia) associated with a cortical EEG characterized by an abnormally excessive and persistent amplification of ongoing beta- and gamma-frequency (18- 29 and 30-80 Hz, respectively) oscillations (B3) with a partial recovery at the end of the recording session. No one sleep episode was identified during the 80-min recording session. The histogram on the right illustrates the number of non-REM sleep episodes during the 80-min recording session under the control (S or saline; N = 3.0±0.2, 18 recordings sessions), one week before (Wn-1) the ketamine challenge, or under the ketamine (K, 0.0±0.0, 15 recordings sessions) conditions. One week later (Wn+1), the ketamine-treated rats retrieve their sleep episodes under the saline condition (n = 3.3±0.3, 11 recording sessions). (B1-B3) Top traces: short bouts of desynchronized (during wake state, B1) and synchronized (during non-REM sleep, B2) cortical EEG recorded under saline condition, and of "hyper-desynchronized" cortical EEG under ketamine condition (B3, 7 minutes after injection). Middle traces: 32-s bouts of wake-related desynchronized (during wake state, B1) and non-REM sleep-related synchronized (B2) cortical EEG recorded under saline condition, and of ketamine-induced "hyper-desynchronized" cortical EEG (B3,

7 minutes after injection). Under the ketamine condition (B3), the rat behavioral hyperactivity generated many artifacts (a) in the cortical EEG due to intense electromyographic activities and cable artifacts. Bottom: Time-frequency spectral analysis (resolution: 0.03 Hz, hamming, 50% overlap) of a 32-s recording episode for each condition.

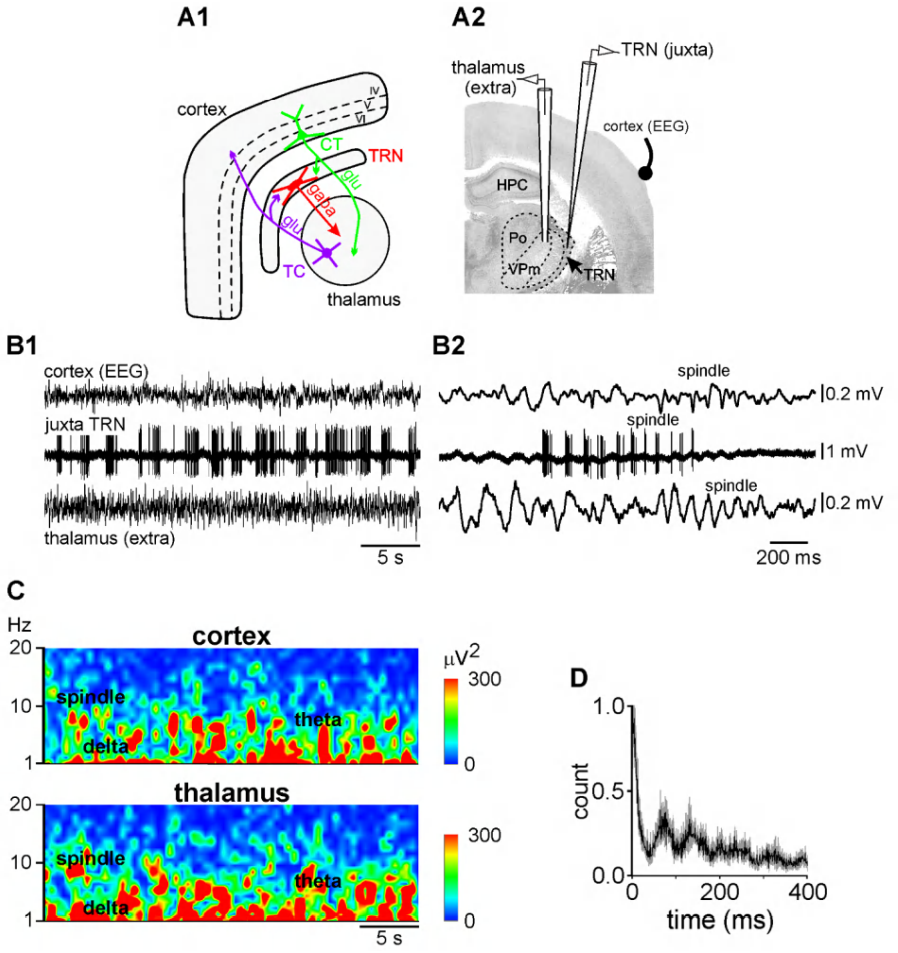

Fig. S2: Sleep-like activity patterns under the analgesic pentobarbital sedation. (A1) The hodology of the layer VI CT-TRN-TC circuit, the common circuit to all nuclei of the dorsal thalamus and the leading circuit in the generation of spindles. (A2) Location of the cortical (EEG), thalamic (extracellular configuration), and of the TRN (juxtacellular configuration) electrodes in the somatosensory system. (B1) A 32-s trace recorded in a pentobarbital sedated rat. Both the cortical EEG and the thalamic extracellular activities are prominently synchronized. During this synchronized state, the TRN cell fires rhythmic high-frequency bursts of APs at the delta- (1-4 Hz), theta- (5-9 Hz) and spindle- (10-16 Hz) frequency bands. (B2) A short-lasting trace showing spindle network (Cx EEG and thalamus extracellular) and cellular (TRN) activities. (C) Time-frequency spectral analysis of the 32-s cortical and thalamic records (resolution: 1 Hz, hamming, 50% overlap) of the B1 trace. (D) Averaged autocorrelogram (resolution: 1 ms, from ten 2-s traces ±SEM in grey) of the firing of a representative juxtacellularlyrecorded TRN neuron.

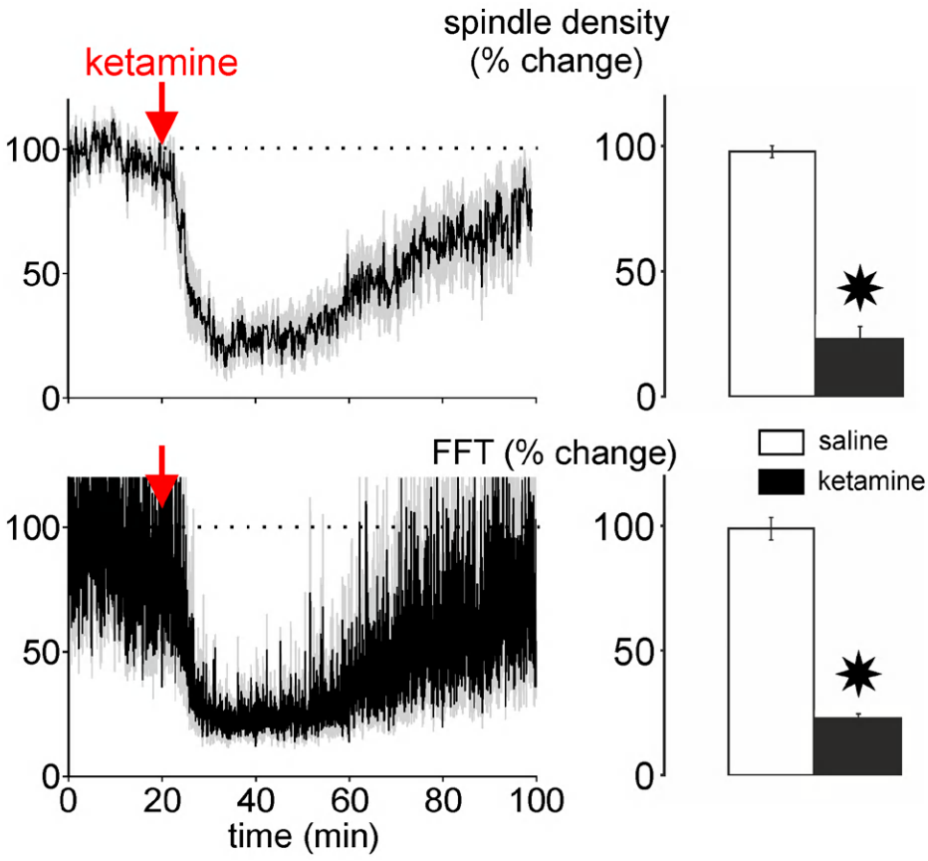

Fig. S3A: Ketamine decreases the density and the power of spindles in the thalamocortical system. (upper graph) Time course of the density (% change relative to the saline condition, grand average (black) ± SEM (grey) from 8 rats) of cortical spindles before and after the subcutaneous administrations of saline (at 0 min) and ketamine (at 20 min). In the histogram, each column represents the average (± SEM) of a 10-minute period (density resolution: 10 s; 60 values x 8 rats). (bottom graph) Time course of the power (% change relative to the saline condition, grand average (black) ± SEM (grey) from 8 rats) of spindles (from non-filtered records) before and after the subcutaneous administrations of saline (at 0 min) and ketamine (at 20 min). In the histogram, each column represents the average (± SEM) of a 10-minute period (FFT resolution: 0.5 Hz; 300 values x 8 rats). Paired t-test relative to saline condition (star when $p < 0.01$). Saline condition: 5-15 min; ketamine condition: 30-40 min.

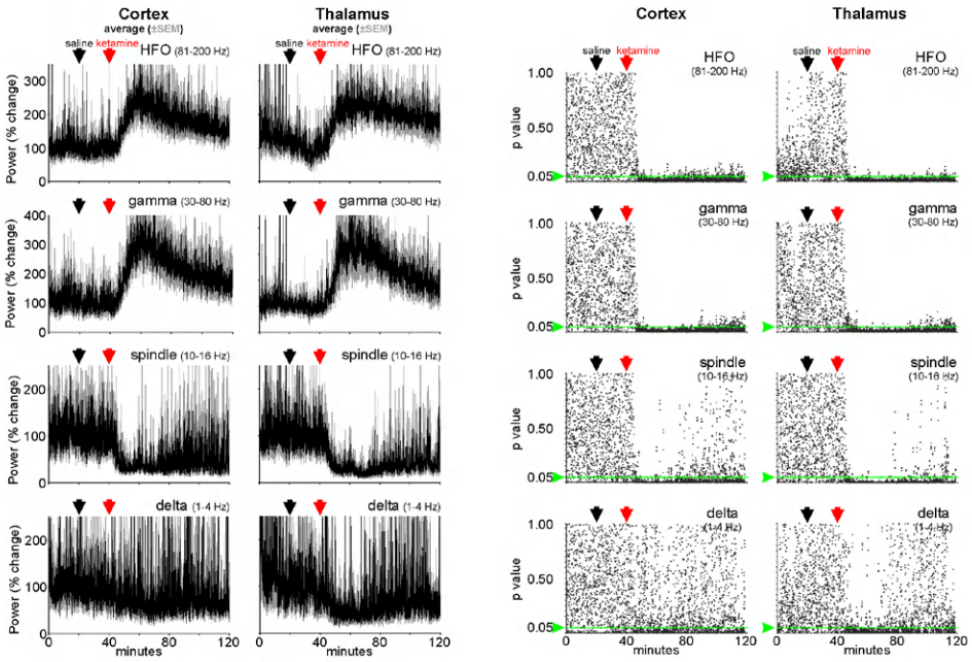

Fig. S3B: Ketamine significantly decreases the power of spindles and deltafrequency oscillations and increases that of gamma- and higher-frequency oscillations in the somatosensory thalamocortical system. (left panel) Time course of the power (% change relative to the saline condition, grand average (black) ± SEM (grey) from 6 rats with simultaneous cortical and thalamic recordings) of neural oscillations before and after the subcutaneous administrations of saline (at 20 min) and ketamine (at 40 min). (right panel) Each dot is a Student's paired t-Test (one test ketamine relative to saline (100%) every 2 seconds). The 100% corresponds to the average of all the values (n=300 per rat) obtained during the 10 min period that precedes the ketamine administration. The pvalue 0.05 is indicated by the green line. The smaller the p-value, the higher the significance. HFO, high-frequency oscillations.

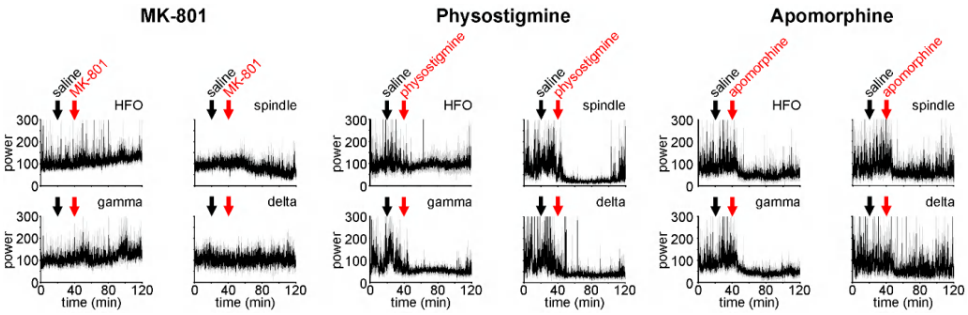

Fig. S4a: MK-801 mimics the ketamine effects better than physostigmine and apomorphine. Time course of the power (% change relative to the saline condition, mean (in black) ±SEM (in grey), 4 rats per condition, each rat being its own control) of cortical EEG oscillations (all frequency bands) before and after the subcutaneous administrations of saline (at 20 min) and (at 40 min) either MK-801 (0.1 mg/kg), physostigmine (0.5 mg/kg), or apomorphine (1 mg/kg).

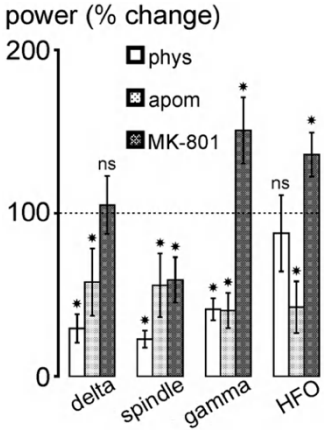

Fig. S4b: MK-801 mimics the ketamine effects better than physostigmine and apomorphine. The histogram illustrates the drug-induced percent changes (at 20-60 min postinjection, relative to the saline condition, each animal being its own control) in power of the four frequency bands in the cortical EEG (4 rats per drug; mean±SEM). Student t-test: (*) p< 0.001; ns, not significant.

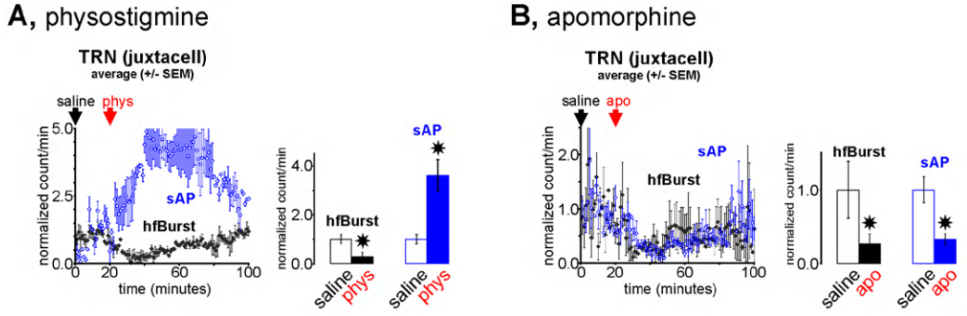

Fig. S4c: Physostigmine or apomorphine decreases the hfBurst density in juxtacellularly recorded thalamic reticular nucleus neurons. The density (number per minute, ±SEM, 2 TRN cells from 2 rats) of hfBursts and of sAPs under the saline (A or B), physostigmine (A) or apomorphine (B) conditions. In the histograms, the normalized values are from the time period of 20-60 min postinjection (phys or apo), that is, 40-80 min in the charts. Note that, like ketamine, physostigmine increases the sAP density and decreases the hfBurst density.

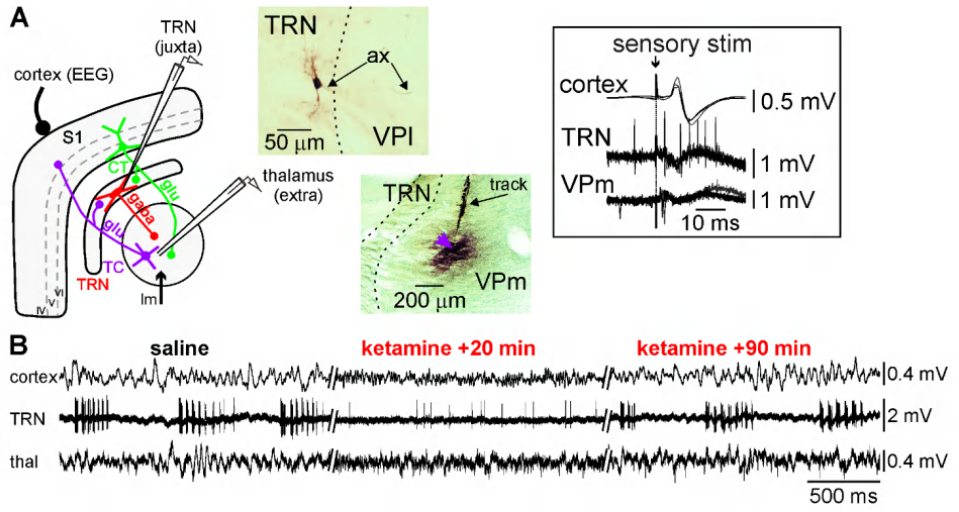

Fig. S5: Ketamine switches the firing pattern of thalamic reticular nucleus (TRN) neurons from the hfBurst mode to the sAP mode. (A) Experimental design showing the location of the recording glass micropipettes, a sharp one (tip diameter ~1µm) to record juxtacellularly (juxta) a single thalamic reticular nucleus (TRN) neuron, a semi-micropipette (tip diameter: 5-7 µm) to record the extracellular activities of a subpopulation of TC neurons in the somatosensory system (VPm, medial part of the ventral posterior nucleus). These intrathalamic recordings are done along with the cortical EEG of the related primary somatosensory cortex (S1). Is also shown, the hodology of the somatosensory 3-neuron layer VI CT-TRN-TC circuit, the principal leading cicuit in the generation of spindles. In the somatosensory system, the lemniscal (lm) input being the principal prethalamic input of the VPm. The corticothalamic (CT) and TC neurons are glutamatergic while the TRN neuron is GABAergic. At the end of the recording session, the location and the structure of the recorded neurons are labelled with the neuronal tracer Neurobiotine. The top microphotograph shows part of the somatodendritic complex and the main axon (ax) of a juxtacellularly recorded TRN neuron; the bottom microphotograph shows the extracellular labelling (methyl green counterstaining) of the recording site and electrode track in the VPm, the head arrow indicating the location of the extracellular recording site. In the frame is shown the functional identification of the recorded somatosensory neurons at the beginning of the recording session, that is, short-latency sensory-evoked activities simultaneously recorded in the cortical EEG and in thalamic relay (VPm) and reticular (TRN) neurons. (B) Typical simultaneous recordings of the S1 cortex (EEG), the somatosensory TRN (single-unit juxtacellular configuration) and related thalamus (extracellular configuration). Under the saline (control) condition, both the cortex and the thalamus exhibit a synchronized state, characterized by the occurrence of lowfrequency (1-16 Hz) oscillations, including spindles, and the TRN cell exhibits three series of rhythmic robust highfrequency bursts of action potentials (300-500 APs/s). Under the ketamine condition (here, 15 minutes post-ketamine injection), the TC system displays a more desynchronized state, characterized by the prominent occurrence of faster activities (>16 Hz), which include gamma-frequency oscillations, and the TRN cell fires more in the single AP mode than in the

burst mode. Ninety minutes after the subcutaneous administration of low-dose ketamine, the sleep state of the TC system is back in the CT-TRN-TC system.

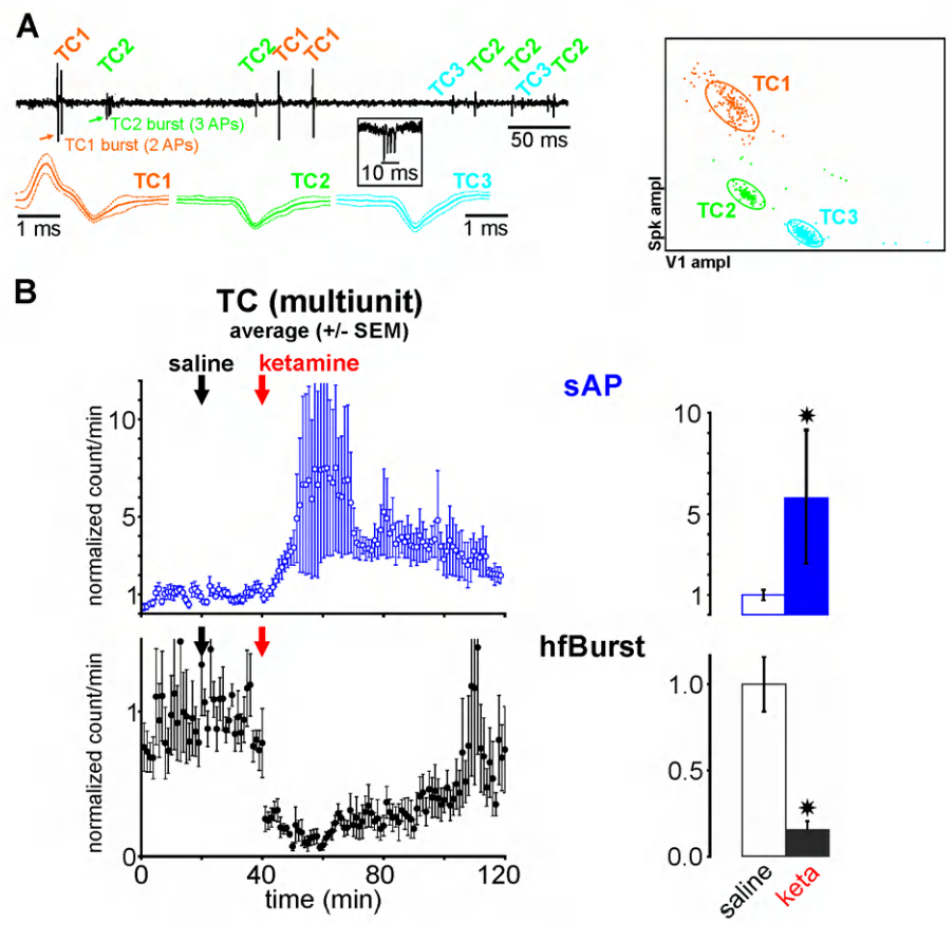

Fig. S6: Ketamine decreases the high-frequency burst (hfBurst) density and increases the single AP (sAP) density in extracellularly recorded thalamocortical (TC) neurons. (A) A typical example of a spike sorting of 3 TC cells (TC1, TC2 and TC3) from an extracellular multiunit recording. In the recording bout (high-pass filter cut at 100 Hz), the three TC cells are visually well distinguishable, TC1 exhibiting a hfBurst of 2 APs then sAPs, TC2 a hfBurst of 3 APs then sAPs, and TC3 only sAPs. A typical extracellular hfBurst is shown in the frame. The mean±SD of 50 APs of the three detected TC neurons are shown. Three clusters are well distinguishable on the basis of the amplitude of the spike and valley components (spk ampl and V1 ampl, respectively) of the APs. (B) Grand average (±SEM, N=16, from 6 rats) of the relative changes of the density (normalized count per minute, 1 being the control value under the saline condition) of the sAPs and of the hfBursts. On the right, the histograms show the average values corresponding to 20-40 minutes ketamine postinjection. Asterisk when significant (paired t-test, $p<0.01$).

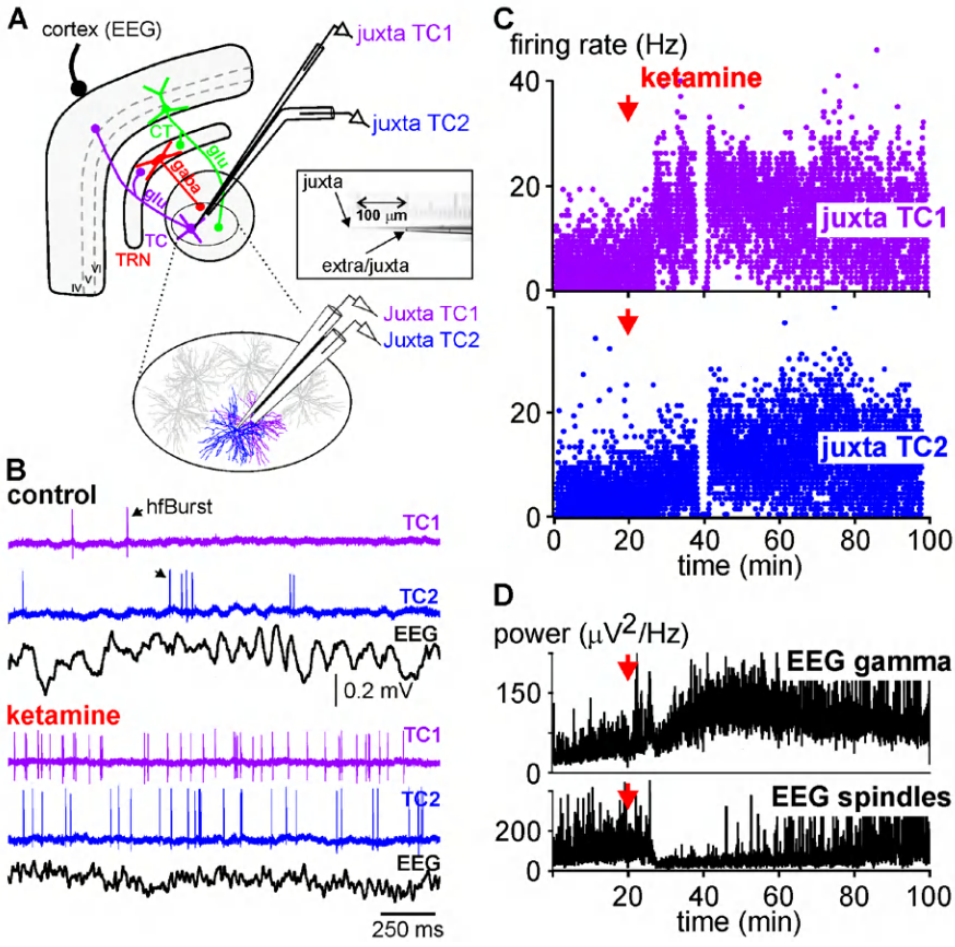

Fig. S7: Ketamine increases the firing frequency band similarly in two juxtacellularly recorded nearby TC neurons. (A) Experimental design showing the location of the recording EEG electrode on the primary somatosensory cortex and of the combined juxtacellular (tip diameter: 1 µm) and extracellular (tip diameter: 5 µm) glass micropipettes (intertip distance: 100 µm, see microphotograph in the frame). In this experiment, the latter electrodes are located in the posterior group of the thalamus (the upper lip being the receptive field for the juxtacellular micropipette). (B) Each of the two combined micropipettes records juxtacellularly a single TC neuron. Under the control (saline) condition, the cortical EEG displays sleep oscillations, including spindles, whereas both TC1 and TC2 neurons fire sAPs and hfBursts. Four to 5 minutes after a subcutaneous administration of low-dose ketamine (2.5 mg/kg), the cortical EEG exhibits less spindles/slower oscillations and more higher-frequency (>16 Hz) oscillations, including especially gamma oscillations, and the two adjacent TC neurons fire more sAPs than hfBursts. (C) Ratemeter of the simultaneously juxtacellularly recorded TC1 and TC2 neurons under saline then ketamine conditions. Each dot corresponds to the number of inter-AP intervals per second. At 40 minutes, no available data for a short while because of the sudden occurrence of artifacts that prevented accurate AP detection. (D) Time course of the power of gamma oscillations (top) and of spindles (bottom) recorded simultaneously in the somatosensory cortex before and after subcutaneous administrations of saline and ketamine (at 0 and 20 min, respectively).

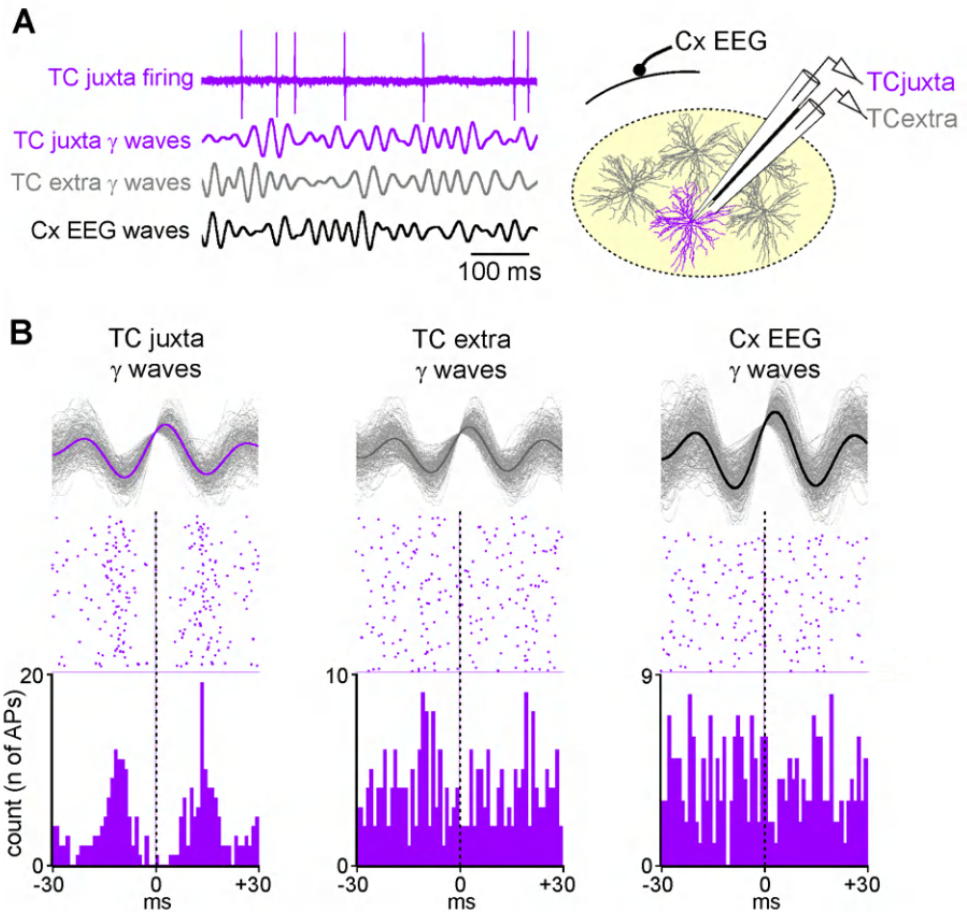

Fig. S8: Time relationship between the APs of a single TC neurons and the related juxtacellular, extracellular and cortical gamma waves. (A) Simultaneous dual juxtacellular-extracellular recording of a single TC neuron along with the EEG of the related cortex of the somatosensory system. A schematic drawing of the experimental design is shown on the right. From top to bottom: Juxtacellular firing of a single TC neuron (bandpass: 1-6000 Hz); juxtacellular TC gamma oscillations (25-55 Hz); extracellular (100 µm distant from the neuron) TC gamma oscillations (25-55 Hz); cortical EEG gamma oscillations (25-55 Hz). (B) Peri-event (gamma wave) time histogram (1-ms resolution) of the TC firing (cumulative count) under the ketamine condition. Every gamma wave (TC juxta, TC extra (inter-tip distance = 100 µm, see drawing), and Cx EEG) is an average of 100 filtered (25-55 Hz) individual gamma (γ) waves. Time "0" corresponds to the time at which gamma waves were detected. Two hundreds sweeps, each dot representing a detected AP.

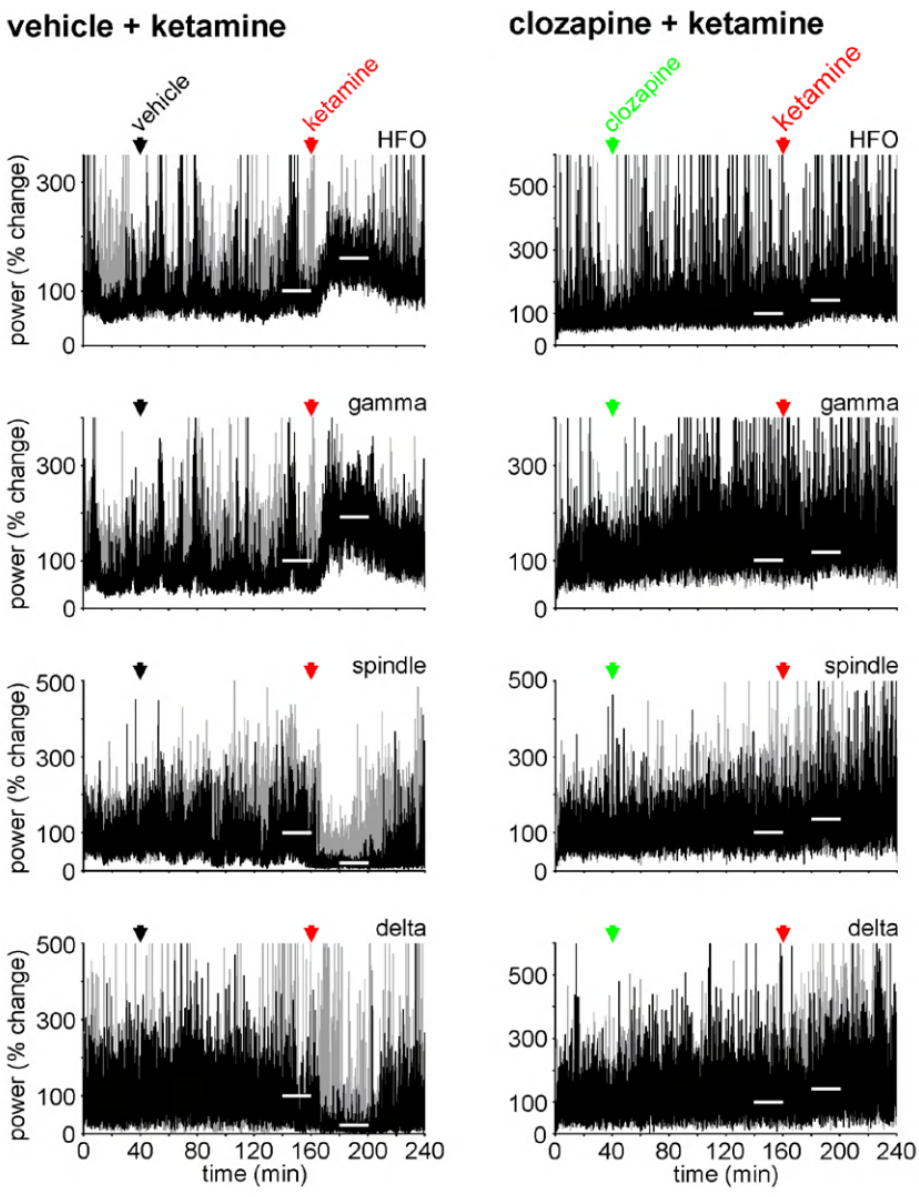

Fig. S10: Clozapine prevents the ketamine effects on sleep TC oscillations. Each chart shows, for a given frequency band oscillation, the time course (1 FFT value/2 seconds) of the drug effects (% change in power) on the cortical EEG in 2 individuals (grey and black) during a 240 min recording session, the ketamine challenge being done at 160 minutes under the control (left panel) and clozapine (right panel) conditions. The horizontal white bars indicate the time periods used for statistical comparisons (paired t-test). Left panel: Ketamine (2.5 mg/kg) was administered 120 minutes after the vehicle (NaCl/HCl 0.1N) administration (subcutaneous, 1 ml/kg). Right panel: Ketamine (2.5 mg/kg) was administered 120 minutes after the clozapine (dissolved in NaCl/HCl 0.1N) administration (subcutaneous, 5 mg/kg, 1 ml/kg). HFO, high-frequency oscillations (81-200 Hz).

Chapter 3

The psychotomimetic ketamine disrupts the transfer of late sensory information in the corticothalamic network

Yi Qin, Ali Mahdavi, Marine Bertschy, Paul M. Anderson, Sofya Kulikova, Didier Pinault

European Journal of Neuroscience. 2023 Feb;57(3):440-455.

Abstract

In prodromal and early schizophrenia, disorders of attention and perception are associated with structural and chemical brain abnormalities and with dysfunctional corticothalamic networks exhibiting disturbed brain rhythms. The underlying mechanisms are elusive. The non-competitive NMDA receptor antagonist ketamine simulates the symptoms of prodromal and early schizophrenia, including disturbances in ongoing and task & sensory-related broadband beta−/gamma-frequency (17–29 Hz/30–80 Hz) oscillations in corticothalamic networks. In normal healthy subjects and rodents, complex integration processes, like sensory perception, induce transient, large-scale synchronised beta/gamma oscillations in a time window of a few hundred ms (200–700 ms) after the presentation of the object of attention (e.g., sensory stimulation). Our goal was to use an electrophysiological multisite network approach to investigate, in lightly anesthetised rats, the effects of a single psychotomimetic dose (2.5 mg/kg, subcutaneous) of ketamine on sensory stimulus-induced oscillations. Ketamine transiently increased the power of baseline beta/gamma oscillations and decreased sensory-induced beta/gamma oscillations. In addition, it disrupted information transferability in both the somatosensory thalamus and the related cortex and decreased the sensory-induced thalamocortical connectivity in the broadband gamma range. The present findings support the hypothesis that NMDA receptor antagonism disrupts the transfer of perceptual information in the somatosensory cortico-thalamo-cortical system.

1 INTRODUCTION

In many neuropsychiatric illnesses, including schizophrenia, sleep disorders and deficits in attention-related sensorimotor and cognitive integration processes are common. These disorders insidiously start to occur during the prodromal phase (Lunsford-Avery et al., 2013; Manoach et al., 2014; Mayeli et al., 2021; McGhie & Chapman, 1961; Zanini et al., 2015). Administration of the non-competitive NMDA receptor antagonist ketamine at a subanaesthetic dose can induce a psychosis-relevant mental state in healthy humans (Anticevic et al., 2015; Grent-'t-Jong et al., 2018; Hetem et al., 2000; Hoflich et al., 2015; Krystal et al., 1994; Rivolta et al., 2015) and other species, including rodents (Chrobak et al., 2008; Ehrlichman et al., 2009; Hakami et al., 2009; Kocsis, 2012; Pinault, 2008; Pitsikas et al., 2008). The ketamine-induced psychosis-relevant mental state is reminiscent of both the prodromal phase of schizophrenia and the psychotic transition.

Sensory-related perception is a very complex and relatively long-lasting (~2 s) process, which involves early (<200 ms) and late (>200 ms) stages. These two-time stages represent a continuum through highly distributed systems involving diverse cortical areas during the perceptual process (Portella et al., 2012, 2014; Saradjian et al., 2019). The dynamics of the cortico-thalamo-cortical (CTC) network in the late stage of perception remain little known in psychotic disorders. Literature suggests the existence of a link between late sensory-related activities and perception. In a visual perception task, participants show sensory perception-related gamma activity increases in two separate components, early and late (Rodriguez et al., 1999). Likewise, in a study conducted in humans and mice two response activities (early: < 300 ms and late: > 300 ms) are recorded after visual stimulation, the latter response believed to be involved in visual perception (Funayama et al., 2015).

In schizophrenia patients, deficits in perception are associated with a reduction of phase synchrony in beta/gamma-frequency (20–60 Hz) oscillations in the late period (Uhlhaas et al., 2013). These results suggest a decrease in induced sensory-related gamma oscillations during the late period of perception. There is a line of evidence showing a decrease in induced-gamma oscillations in individuals with a clinically at-risk mental state for psychotic transition (Haenschel et al., 2009; Reilly et al., 2018). The decrease in power and synchrony of task & sensory-induced gamma oscillations may be due to the abnormal amplification of basal gamma oscillations recorded in such patients (Ramyead et al., 2015). Indeed, in the acute rodent ketamine model, early sensory-evoked gamma oscillations decrease whereas ongoing gamma oscillations increase, supporting the hypothesis of a

reduction in the signal-to-noise ratio (Anderson et al., 2017; Hakami et al., 2009; Kulikova et al., 2012).

We wanted to study whether and how late sensory-induced beta/gamma oscillations (17–29 Hz/30–80 Hz) are disturbed by NMDA receptor antagonism. To do so, we investigated the effects of low-dose ketamine in the somatosensory thalamocortical (TC) system during the late sensory stimulus-related period (200–700 ms post-sensory stimulation), involving highly distributed CTC systems (Alitto & Usrey, 2003; Briggs & Usrey, 2008; Homma et al., 2017; Urbain et al., 2015). Since sensory-induced gamma oscillations can be recorded in anesthetised rats (Neville & Haberly, 2003), the experiments were conducted in the pentobarbital-sedated rat. Spectral analysis and coherence connectivity were used in an attempt to estimate, respectively, the level of synchronisation and the functional connectivity between the recording sites (Kam et al., 2013). Unlike amplitude measures, coherence measurements show the synchronisation level between two signals based on the phase consistency (Srinivasan et al., 2007). EEG and extracellular signals are relatively complex as they are generated by multiple interacting cortical and subcortical oscillators. The complexity of such signals, related to functional aspects of the corresponding neural networks, can be assessed with non-linear analyses such as the multiscale entropy analysis (MSE) (Costa et al., 2005; Miskovic et al., 2019). The MSE has been applied to EEG from psychiatric patients (Fernandez et al., 2013). Higher MSE can indicate increases in the complexity of time-varying signals and may represent disruptions in long-range temporal connectivity or temporal integration (Breakspear & Stam, 2005). So, in an attempt to measure the dynamical complexity in the TC system at multiple timescales, MSE was applied to the extracellular local field potential (LFP) recordings. The present findings show that, in the somatosensory CTC system, ketamine disrupts the information transfer of sensory-induced gamma oscillations.

2 MATERIAL AND METHODS

Animals and drugs

Seven adult (3–6-month-old, 285–370 g), Wistar male rats were used. All animal care procedures were performed with the approval of the Ministère de l'Education Nationale, de l'Enseignement Supérieur et de la Recherche. Animals were housed and kept under controlled environmental conditions (temperature: 22 ± 1°C; humidity: 55 ± 10%; 12 h/12 h light/dark cycle; lights on at 7:00 am) with food and water available ad libitum. Every precaution was taken to minimise stress and the number of animals used for each series

of experiments. Ketamine (Imalgene 1000, MERIAL), pentobarbital sodique (CEVA santé animale) and fentanyl (Fentadon@ DECHRA) were from CENTRAVET.

Surgery under deep narco-analgesia

Narcosis was initiated with an intraperitoneal injection of pentobarbital (60 mg/kg). An additional dose (10–15 mg/kg) was administered as soon as there was a nociceptive reflex. Analgesia was achieved with a subcutaneous injection of fentanyl (7.5 µg/kg) every 30 min. The depth of the surgical narco-analgesia was continuously monitored using an electrocardiogram, watching the rhythm and breathing and assessing the nociceptive withdrawal reflex. The rectal temperature was maintained at 36.5°C (peroperative and protective hypothermia) using a thermoregulated pad. The trachea was cannulated and connected to a ventilator (50% air–50% O2, 60 breaths/min). Under local anaesthesia (lidocaine), an incision of the skin on the skull was made, and the periosteum was removed to set the skullcap bare and to perform the stereotaxic positioning of the recording electrodes on the frontoparietal skull. The deep narco-analgesia lasted about 2.5 h, the time needed to complete all the surgical procedures.

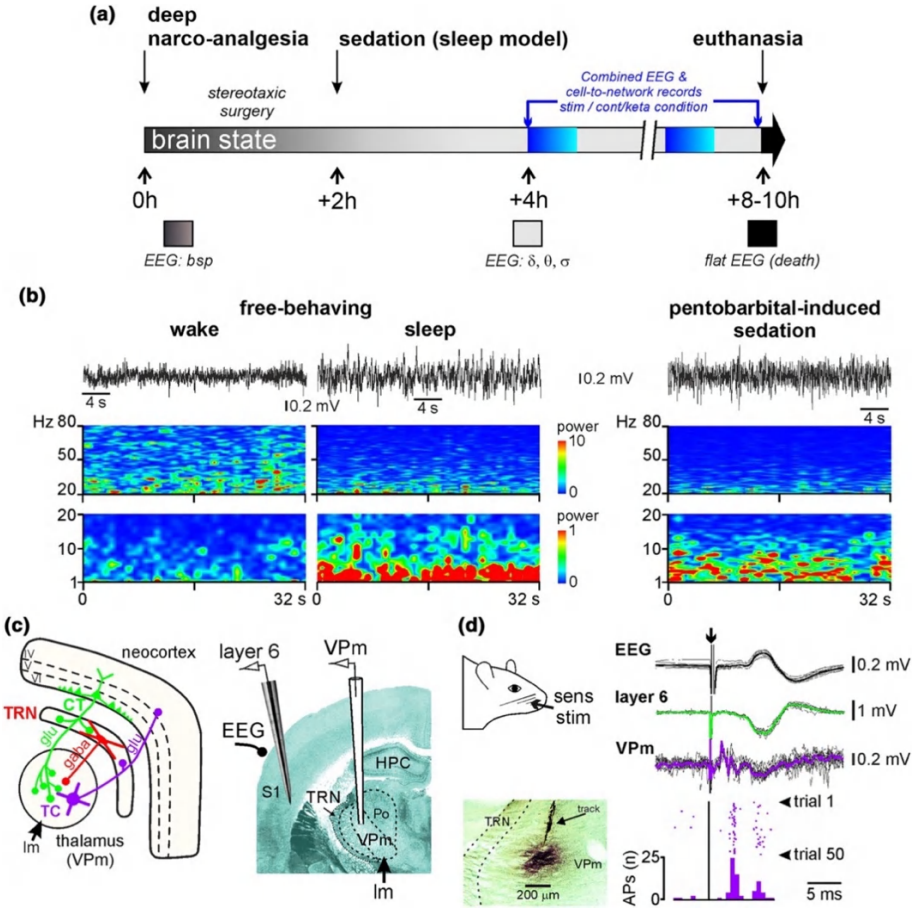

Figure 1. Experimental design. (a) Timeline illustrating the key events during the experimental procedure with repeated measures in one animal. One to three low-dose ketamine challenges can be done during one animal-experiment. At the bottom, the colour code of the brain state is dark grey for deep narco-analgesia, light grey for sedation (light narco-analgesia) and dark for death. During deep narco-analgesia, the EEG is characterised by a burst suppression pattern (bsp) and, during the sedation, principally by delta- (1–4 Hz), theta- (5–9 Hz) and sigma- (10–17 Hz) frequency oscillations (δ, θ and σ, respectively). (b) Cortical EEG oscillations in the free-behaving (left panel) or pentobarbital sedated (right) rat. Top: 32-s bouts of desynchronised, during wake state, and synchronised, during non-REM sleep, cortical EEG recorded in a free-behaving rat during a 90-minutes recording session; the right trace is from a pentobarbital-sedated rat. Bottom: Time-frequency spectral analysis (resolution: 0.03 Hz, hamming, 50% overlap) of a 32-s recording episode for each condition. The power scale (z scale in colour) is not the same for the two frequency bands 1–20 Hz (×1) and 20–80 Hz (×10). The records from the free-behaving rat are from the study performed by Pinault (biol psychiatry, 2008). (c) Simplified hodology of the thalamocortical (TC, in blue purple) and corticothalamic (CT, in green) pathways of the somatosensory system linked to the vibrissae. This involves the inhibitory afferents originating from the thalamic reticular nucleus (TRN, red). CT and TC neurons are glutamatergic and TRN neurons GABAergic. The right panel shows multi-site recordings within the thalamus (VPm) and neocortex (layer VI and cortical EEG) within the rat

somatosensory system. The VPm receives lemniscal afferents (lm). (d) the teguments of the vibrissae are electrically stimulated every 15 seconds (Sens stim). Sensory evoked potentials are recorded simultaneously within the cortex and the thalamus. For each recording site are shown an overlay of 15 recordings and their averaging. Extracellular field potentials can be accompanied by cellular discharges. The action potentials were identified using the spike sorting methods. In this example, the number of action potentials from the recordings within the VPm are shown (50 trials). At the end of the recording session, the location of the recorded neurons are labelled (extracellular iontophoresis) with the neuronal tracer Neurobiotin. The microphotograph shows the corresponding extracellular labelling (methyl green counterstaining) of the recording site and electrode track in the VPm,. HPC: Hippocampus; Po: Posterior nucleus of the thalamus.

Pentobarbital-induced sedation

At the end of the surgery, the body temperature was set to and maintained at 37.2°C. The analgesic pentobarbital-induced sedation (light narco-analgesia) was initiated about 2 h after the induction of the surgical narco-analgesia (Figure 1a) and was maintained by a continuous intravenous infusion of the following regimen (average quantity given per kg and per hour): Pentobarbital (7.2 ± 0.1 mg), fentanyl (2.4 ± 0.2 µg) and glucose (48.7 ± 1.2 mg). In order to help maintain the ventilation stable and to block muscle tone and tremors, a neuromuscular blocking agent was used (d-tubocurarine chloride: 0.64 ± 0.04 mg/kg/h). The cortical EEG and heart rate were under continuous monitoring to adjust, when necessary, the infusion rate to maintain the sedation. The EEG recordings began 2 hours after the beginning of the infusion of the sedative regimen. During the recording session and every 2 hours, drops of the local anaesthetic lidocaine were applied to the surgical wounds.

Under the pentobarbital-induced slow-wave sleep (ketamine-free) condition, the EEG recordings principally displayed oscillations in the delta-frequency band (1–4 Hz or slow-waves) accompanied by oscillations in the sigma band (10–17 Hz or 'spindle-like' activities) (Mahdavi et al., 2020; Pinault et al., 2006). These oscillations were qualitatively similar to slow-wave sleep with spindles recorded in free-behaving rats in stage II sleep (Figure 1b). The slow-wave sleep-type oscillations were sometimes interspersed with smaller and faster oscillations, including, among others, broadband gamma- and higher-frequency oscillations.

Electrophysiology-anatomy

For the EEG recordings of the frontoparietal somatosensory cortex (stereotaxic coordinates relative to bregma (Paxinos & Watson, 1998): posterior 2.3 mm, lateral 5 mm), the section of the Ag/AgCl wires (diameter 150 µm), insulated with Teflon, was placed on the inner plate of the bone. Extracellular field potential and multi-unit activities were

recorded in the somatosensory thalamus, especially in the medial part of the ventral posterior nucleus (VPm, bregma −2.8 mm, lateral 2.8 mm), and in the medial part of the posterior group (PoM, bregma −2.8 mm, lateral 2.8 mm, depth 5.6 mm) using glass micropipettes (tip diameter of 5–10 µm) filled with artificial cerebrospinal fluid and 1.5% Neurobiotin). Semi-micro quartz/platinum-iridium electrodes (Thomas Recording, GmbH, Giessen, Germany) were used for recordings in the layer 6 (depth 1.6–2.0 mm) of the related somatosensory cortex (Figure 1c). All regions of interest were recorded simultaneously, and the electrophysiological signals were sampled at a rate of 20 kHz (Digidata 1440A with pCLAMP 10 Software, Molecular Devices). The recording electrodes were moved down until the electrophysiological identification of the receptive field (Figure 1d). The anatomical identification of the recording site was validated following extracellular iontophoresis of the neuronal tracer Neurobiotin (Figure 1d), which was revealed using a standard histological procedure (Pinault, 1996). Sensory-evoked potentials were recorded after electrical stimulation of the vibrissae teguments using a pair of subcutaneous needles (duration: 75 µs; intensity: 50–60% of the intensity that gives maximal amplitude evoked potential, 1.0 to 1.5 mA; frequency: 0.06 Hz). Every trial contained recorded signals after one stimulation (10 trials/rat).

Pharmacology and repeated measures in one animal

During the recording session under the sedation condition, every rat was under its own control. Saline (vehicle, NaCl 0.9%) and ketamine (2.5 mg/kg) were subcutaneously administered (1 ml/kg). As long as the pentobarbital-induced sedation is stable (4–6 hours) and knowing that, under the present experimental conditions, the ketamine effect (peaking at 15–20 min) lasts significantly less than 90 min (Anderson et al., **2017**; Mahdavi et al., **2020**), two to three conditions (20–40-minute saline condition followed by one or two ketamine challenges) could be performed in one animal (Figure **1a**).

Data analysis

Data analyses were performed with Clampfit 10, SciWorks (Datawave Technologies) and MATLAB softwares. Spectral analysis was done with 2 Hz resolution, hamming windowing and no overlay. Recorded signals were analysed in five frequency bands: delta (1–4 Hz), theta (5–9 Hz), sigma (10–16 Hz), beta (17–29 Hz) and gamma (30–80 Hz). Sensory stimulus-induced gamma power was calculated by subtracting the evoked and basal power from the total power.

2.6.1 Total power spectral

In total, data of 40 trials (10 × 4 rats) were acquired. The total power in a given frequency range *v* was the sum of powers across the defined spectral range. We consider the 500 ms period before each stimulus the baseline. The baseline power for each trial is denoted as P_{b1}, P_{b2}, P_{b3}, … P_{b40}; stimulus-related power for each 200–700 ms post-stimulus 500-ms epoch is denoted as P_{e1}, P_{e2}, P_{e3}, … P_{e40}. Therefore, the average normalised power P_v for the frequency *v* range is computed as:

$$Pv = \sum_{i=1}^{N=40} (\frac{P_{e_i}}{P_{b_i}})/N$$

Similarly, in ketamine conditions, Pkbi and Pkei stand for the baseline and stimulus-related power, respectively for each trial i. Thus, the average normalised ketamine power Pkv is computed as:

$$P_{kv} = \sum_{i=1}^{N=40} (\frac{P_{ke_i}}{P_{kb_i}})/N$$

2.6.2 Multi-scale entropy (MSE)

The information complexity of extracellular LFP beta- and gamma-frequency oscillations (raw LFP filtered at 17–29 Hz and 30–80 Hz, respectively) was measured by MSE. Although the definition of complexity is various, it is associated with 'meaningful structural richness' and 'information randomness' (Costa et al., 2005; Hager et al., 2017). The MSE is calculated in two steps. First, coarse-graining is applied to the time series {x1, …, xi, …, xN}. It is constructed by averaging data points from non-overlapping time-windows of interest, τ. Every coarse-grained time series, yjτ, is calculated as:

$$y_j^\tau = \sum_{i=(j-1)\tau+1}^{j\tau} x_i/\tau 1 \leq j \leq N/\tau$$

where N/τ is the length of each resulting coarse-grained time series. Then the sample entropy is calculated for each series yj$^\tau$ and plotted as function of the scale factor. When τ equals one, yj^1 is equivalent to the original time series. The higher scale factor is, the longer temporal range it is. The MSE values for low scales reflect short-range temporal irregularity, while high scales reflect long-range temporal irregularity. Other parameters

for MSE calculations were adopted from previous studies (Lake et al., **2002**; Richman et al., **2004**; Takahashi et al., **2010**).

2.6.3 Coherence connectivity

Coherence was calculated by the MATLAB mscohere function.

2.6.4 Statistics

All statistics tests were calculated using MATLAB or Graphpad Prism 9. For comparing the baseline and stimulus-related activities in different frequency bands, we used a one-way ANOVA test with Holm-Šidák's multiple comparisons test as post-hoc analysis. For comparing normalised gamma total power under ketamine and saline conditions, paired t-tests were applied to each group, with each animal being its own control. For testing the effect of ketamine on induced gamma oscillations, we computed whether there was a significant interaction using a two-way ANOVA for time and condition (saline or ketamine). When assessing the coherence between recording sites, we used the Wilcoxon matched pairs signed-rank test.

3 RESULTS

Ketamine increases baseline and decreases induced beta/gamma oscillations

A representative example of multisite cortical (EEG and layer 6) and thalamic (VPm and PoM) recordings, filtered at the beta/gamma frequency band, is shown in figure 2. It reveals the ongoing (baseline) and sensory-related oscillations 2-s before and 2-s after the stimulation (0 s), respectively. It is striking that ketamine increased the power of ongoing beta/gamma oscillations in the cortex and thalamus (Figure 3a and b) as demonstrated in previous studies (Hakami et al., 2009; Kocsis, 2012; Pinault, 2008). Immediately and later after the sensory stimulation, the amplitude of the beta/gamma oscillations was modulated. During the 200–700 ms post-stimulus period, the induced beta/gamma oscillations significantly decreased in power at all recorded cortical and thalamic sites following ketamine administration (Figure 3c and d).

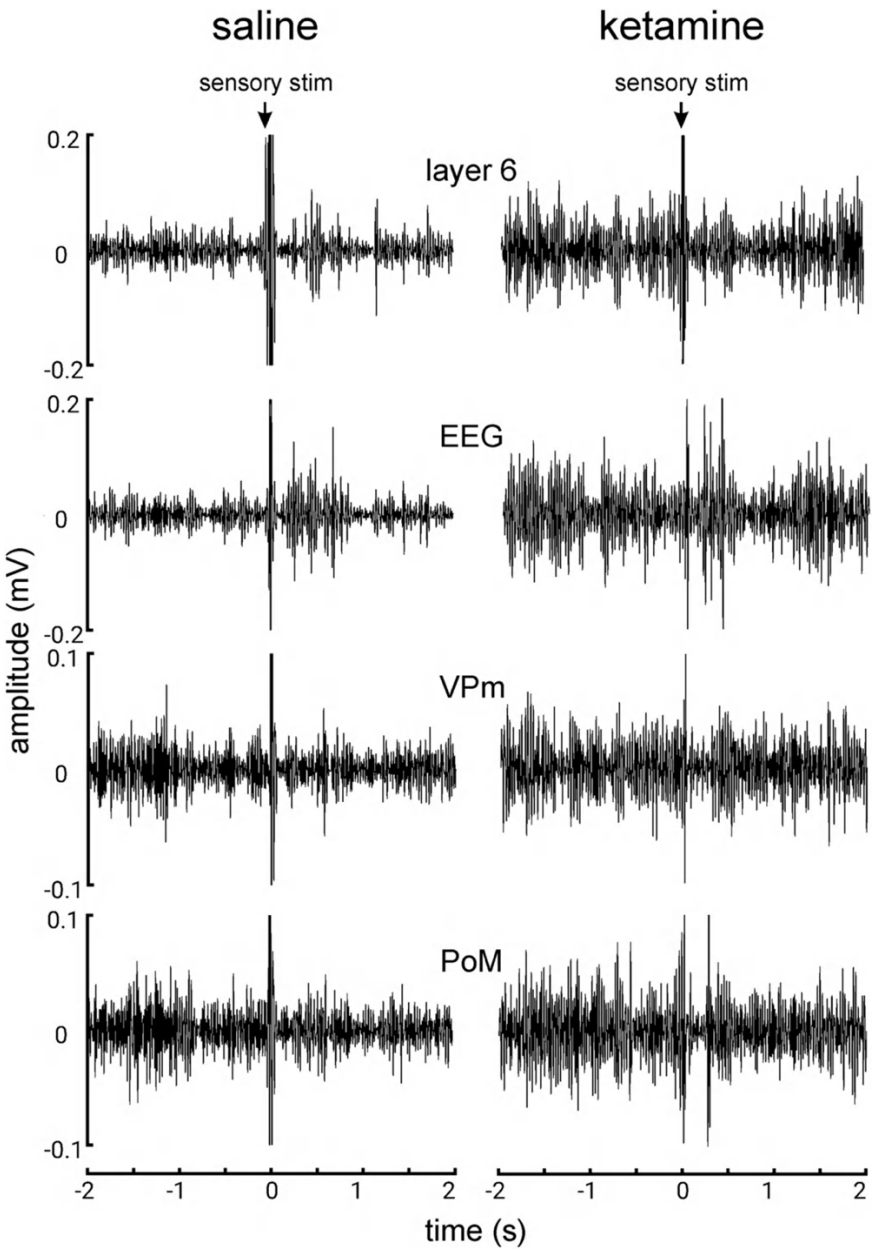

Figure 2. Simultaneous cortical (EEG & layer 6) and thalamic (VPm & PoM) recordings under saline and ketamine conditions from a lightly anaesthetised rat. They are filtered in the beta/gamma frequency band (25–50 Hz). Each trace (sweep) shows the 2-s pre-stimulus and 2-s post-stimulus periods. The teguments of the vibrissae are stimulated (sensory stim). The traces under the saline condition were recorded 10 minutes before the ketamine administration. The ketamine traces were recorded 20 minutes after the subcutaneous administration of ketamine at a subanaesthetic low-dose (2.5 mg/kg).

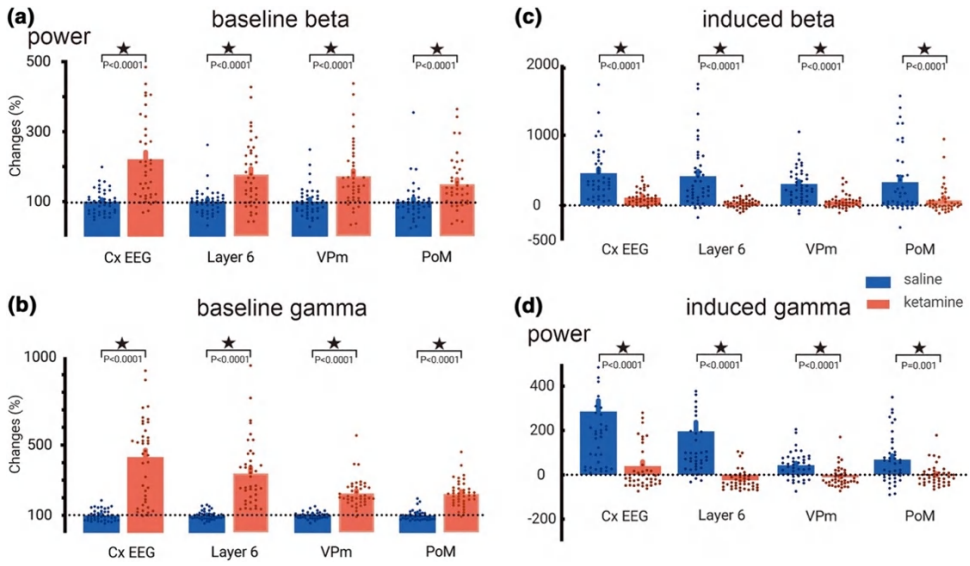

Figure 3. Ketamine increases baseline beta/gamma (a/b) oscillations, and decreases sensory-induced beta/gamma (c/d) oscillations. (a, b) each column stands for the average (± SEM, from 40 values, 10 per rats, 4 rats) of the normalised total power of gamma oscillations relative to saline baseline. Asterisks when significant (paired t-test, all P value < 0.0001, check supplement for statistic details). (c, d) the power of the induced gamma oscillations was obtained when subtracting the power of the baseline gamma from the power of the sensory-elicited total gamma. Each value (± SEM, from 40 values, 10 per rats, 4 rats) is the % change relative to the baseline gamma recorded before the sensory stimulation. Asterisks when significant (< 0.05, two-way ANOVA, corrected with holm-Sidak, check supplement for details).

Ketamine disrupts information transferability in the corticothalamic (CT) network

The post-stimulation time lapse of 200–700 ms is long enough to encode, integrate and perceive the incoming sensory signal (Rodriguez et al., 1999). We hypothesised that ketamine could interrupt information processing during this period. To test this, we measured the uncertainty of information based on MSE in the gamma band during the 200–700 ms post-stimulus period (Figure 4). The measurement of entropy can be used as an estimation of 'complexity' in physiological systems. Higher entropy means the system is likely in a more 'complex/dynamic' state (Costa et al., 2005; Hager et al., 2017). In Figure 4, it is shown that the entropy of the VPm and that of layer 6 were significantly increased along different time scales. This indicates that the information contained in the VPm and layer 6 extracellular potential was biased toward a random or 'noisy' state. No difference was observed in the PoM (Paired t-test, $p < 0.05$). Also, no significant difference was observed on MSE for the beta band in both the cortex (layer 6) and the thalamus (VPm and PoM) (Figure S1).

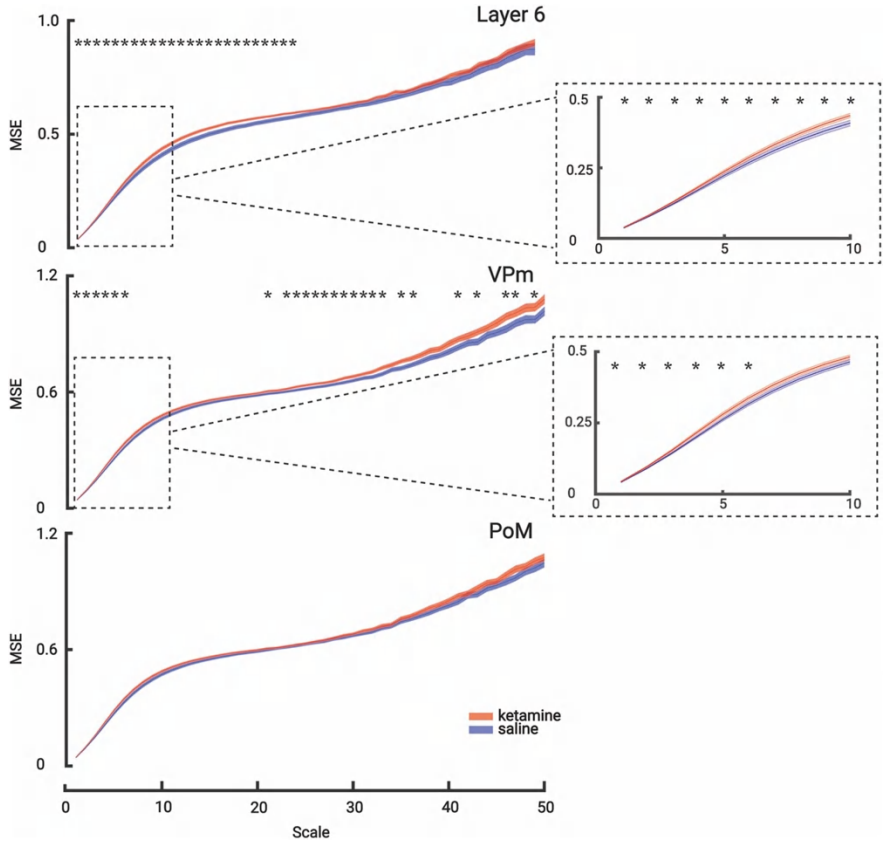

Figure 4. Ketamine increases multi-scale entropy in the gamma band between the VPm and layer 6. Comparison of the multi-scales entropies of saline (blue) and ketamine (red) conditions at all recording sites in the gamma band during the 200–700 ms post-stimulus period. Layer 6 and VPm show a significant increase in entropy. Each scale point is the average entropy (± SEM, from 40 values, 10 per rats, 4 rats). Asterisks when significant (< 0.05, paired t-test). Mean values: Layer 6: T(39) = 2.5509 ($p < 0.05$); VPm: T(39) = 2.2930 ($p < 0.05$).

The present study shows that ketamine had a strong effect on information in the specific thalamic nucleus (VPm) and in the related layer 6 in the gamma band, indicating that the gamma connectivity in the whole network might also be dysfunctional. So, we used the coherence coefficient to measure the induced connectivity in the beta and gamma bands between the cortex and thalamus. We applied magnitude-squared coherence to measure similarities between two signals during the 200–700 ms post-stimulus period. Ketamine elicited a non-significant decrease (~25%) of the coherence coefficient between layer 6 and the related thalamus (VPm) in the beta band connectivity (Figure **5a**). On the other hand, in the gamma band connectivity, ketamine dramatically decreased (nearly 40%) the coherence between layer 6 and the VPm (Figure **5b**). Furthermore, no significant change

in coherence was observed between PoM and VPm, or layer 6 and PoM in both the beta and gamma connectivity (Figur**e 5a,b,** Wilcoxon matched-pairs signed-rank test).

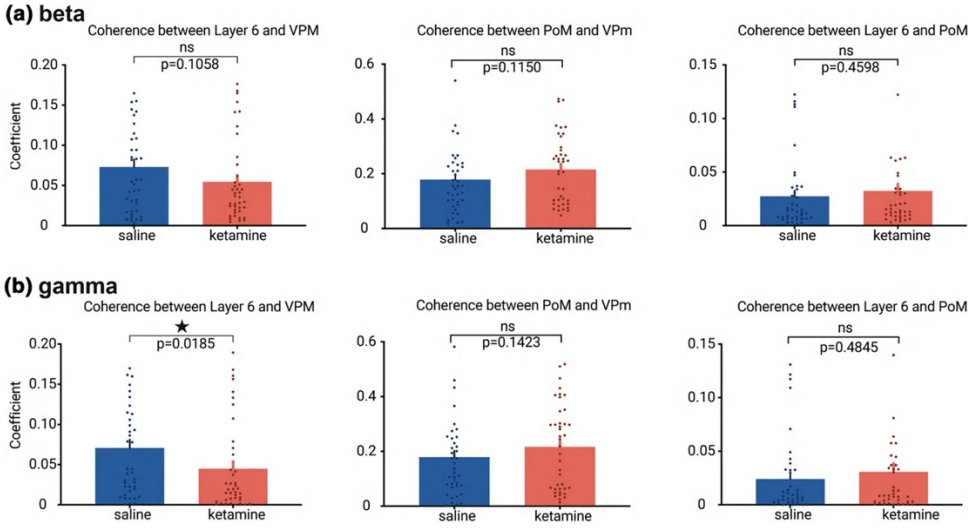

Figure 5. **Ketamine decreases coherence connectivity in the beta/gamma band between layer 6 and VPm**. Comparison of coherences connectivity of beta/gamma bands within CT-TC network under saline and ketamine conditions. Blue and red columns stand for the average coefficients (± SEM, from 40 values, 10 per rats, 4 rats) of the coherences of beta (a)/gamma (b) oscillation in the saline and ketamine conditions, respectively. Asterisks when significant (< 0.05), Wilcoxon test.

DISCUSSION

The findings presented here demonstrate that the parietal CTC system significantly contributes to sensory stimulus-induced thalamic beta/gamma frequency oscillations, which occur at the late post-stimulus stage (200–700 ms), and that the administration of the NMDA receptor antagonist ketamine disrupts the transfer of perceptual information in the system.

Low-dose ketamine decreases the signal-to-noise ratio

The present study analysed beta (17–29 Hz) and gamma (30–80 Hz) oscillations separately. Following the subcutaneous administration of ketamine, spontaneously occurring beta and gamma oscillations increased in amplitude and power in the CT system. Furthermore, the sensory-induced beta and gamma oscillations were significantly decreased in power at all recorded cortical and thalamic sites; ketamine increased the MSE in the specific CT system (Layer 6-VPm) in the gamma but not in the beta frequency band; ketamine

decreased the coherence between layer 6 and VPm in both the beta (not significant) and gamma (significant) frequencies. These findings suggest that beta and gamma oscillations have a common functionality, which is supported by a previous study demonstrating that, in the cerebral cortex, both frequency bands share cellular and biophysical mechanisms (Compte et al., 2008). Along these lines, intracellular recordings of TRN neurons demonstrated that the frequency of the intrinsically generated membrane potential oscillations responsible for generating gamma frequency (25–60 Hz) firing can drop up to 18 Hz (Pinault & Deschenes, 1992).

In the lightly-anesthetised rat, vibrissae stimulation generates a wide-band frequency response in extracellular recordings simultaneously in the VPm, PoM, and in the related somatosensory cortex (layer 6). Sensory-induced beta- and gamma-frequency oscillations were significantly decreased in a smaller post-stimulus time window (200–700 ms). The ketamine-induced obliteration of the sensory stimulus-induced beta/gamma oscillations at 200–700 ms may be the result of the ketamine-elicited abnormally and diffusely amplified basal gamma oscillations, which lead to disruption of beta/gamma-related information transferability in the somatosensory CTC system as assessed in the present study by an increase in MSE and a decrease in coherence connectivity in the specific CT system.

The fact that ketamine aberrantly and diffusely amplifies ongoing beta/gamma oscillations at all the recorded cortical and thalamic sites supports a conception of NMDA receptor hypofunction-related beta and gamma hyper-synchronies as an aberrant generalised diffuse network noise. This NMDA receptor hypofunction would induce a noise state, which would contribute to disrupting the ability of neural networks to encode and integrate input signals. In other words, NMDA receptor antagonism decreases the signal-to-noise ratio (Anderson et al., 2017; Gandal et al., 2012; Hakami et al., 2009; Kulikova et al., 2012). The disruption of the transfer of sensory information would start to occur at least during the very first stages (up to ~15 ms) of information processing, at the gate of cognitive processes (Anderson et al., 2017; Briggs & Usrey, 2008; Homma et al., 2017; Kulikova et al., 2012). The aberrant diffuse network beta/gamma noise may be a potential electrophysiological correlate of a psychosis-relevant state as increased gamma synchrony has been recorded in patients during somatic and visual hallucinations (Baldeweg et al., 1998; Becker et al., 2009; Behrendt, 2003; Spencer et al., 2004) and, importantly, in clinically at-risk mental state patients for psychosis transition and naïve in antipsychotic medication (Perrottelli et al., 2021; Ramyead et al., 2015).

Ketamine-induced increase in randomness or complexity in a signal

Our MSE results show that the specific thalamic nucleus (VPm) and related layer 6 somatosensory cortex have increased sample entropy (i.e. complexity) following ketamine administration, which is consistent with previous studies on human patients with schizophrenia (Takahashi et al., 2010). Of particular interest is that both layer 6 and the VPm showed increased MSE in the lower time scale factors, meaning those with the most detailed temporal information (i.e., with more high-frequency information incorporated in the complexity measure at these time scales). Interestingly, there is a tendency for younger, medication-free patients with higher positive symptoms to display higher levels of complexity in EEG (Fernandez et al., 2013), a finding that matches our interpretation of ketamine administration to model a psychotic-like state. It has further been suggested that these increases in neural complexity measures are evidence for the 'disconnection hypothesis' (Friston et al., 2016) whereby disruption (aberrant or reduced) in connectivity increases EEG signal complexity (Takahashi et al., 2010). In healthy humans submitted to a cognitive-visual task, ketamine increases the power of broadband gamma oscillations and disrupts feedforward and feedback signalling, leading to hypo- and hyper-connectivity in CTC networks (Grent-'t-Jong et al., 2018).

Increased entropy may also be interpreted as an increase in 'randomness' in a signal (with a truly random signal having maximal entropy (Ahmed & Mandic, 2011). Applying such an interpretation to our present results would reflect ketamine administration adding 'noise' to the system increasing ongoing beta/gamma power and resulting in a more random signal. The increased ongoing gamma power reflects an aberrant and pathological increase in non-relevant beta/gamma activity that effectively attenuates sensory-related induced beta/gamma interfering with its sensory transmission. This decreases the overall beta/gamma signal-to-noise ratio in the CTC system, disconnecting these areas and impairing sensory perception. Accompanying this disconnection hypothesis, we also observed a functional disconnection of phase coherence measures in the gamma frequency band between layer 6 and VPm but not between PoM and layer 6 or VPm. This result supports the interpretation that sensory-generated gamma activity has been disrupted between the cortex and thalamus under the ketamine condition. Disorders in the intrinsic properties (amplitude, noise and complexity) and spatial dynamics (coherence) of gamma oscillations somehow reflect a fundamental disturbance of basic integrated brain network activities.

Possible underlying mechanisms

The CTC system is involved in multiple integrative functions, including sensory, perceptual and attentional processing (Pinault, 2004; Van Essen, 2005; Wolff et al., 2021). Sensory-to-perceptual responses of the CTC system result from dynamic interactions between TC (bottom-up) and CT (top-down) processing (Alitto & Usrey, 2003; Briggs & Usrey, 2008; Homma et al., 2017). Both the TC and CT pathways are glutamatergic. In thalamic neurons, the response pattern depends on the brain state (Castro-Alamancos, 2002; Urbain et al., 2015) and on thalamic GABAergic inhibition that is mediated principally by the external source thalamic reticular nucleus (TRN) (Pinault, 2004). Under the present experimental sleep conditions, almost all the thalamic glutamatergic and GABAergic neurons are hyperpolarised and fire in the burst mode (Mahdavi et al., 2020; Pinault et al., 2006), and the arousal promoting effect of ketamine switches the spontaneous firing pattern of both the glutamatergic TC and the GABAergic TRN neurons from the burst to the tonic mode (Mahdavi et al., 2020).

The post-inhibitory rebound excitation is a cellular intrinsic property that occurs during physiological and pathological brain oscillations or following the activation of prethalamic (e.g., sensory) or cortical inputs. For instance, during slow-wave sleep, a long-lasting hyperpolarisation gives rise, in the thalamic relay and reticular neurons, to a rebound excitation caused by a low-threshold calcium-dependent potential, de-inactivated by membrane hyperpolarisation, and can be topped by a high-frequency burst of action potentials (Deschenes et al., 1984; Grenier et al., 1998; Jahnsen & Llinas, 1984; Llinas, 1988; Urbain et al., 2019). Such a post-inhibitory rebound excitation is also recorded under anaesthesia in TC neurons following the activation of prethalamic or cortical inputs (Deschenes et al., 1984; Grenier et al., 1998). There is evidence that TC bursting may serve as a 'wake-up call' in the initiation of perceptual/attentional processes (Sherman, 2001; Swadlow & Gusev, 2001). Two potential mechanisms for the effect of the NMDA receptor antagonist ketamine could be responsible alone or in combination: 1) reduced TRN-mediated inhibition (see discussion by Mahdavi et al., 2020), and 2) a reduction of the hyperpolarisation-activated cationic current Ih (Kim & Johnston, 2020). Of course, ketamine also acts on multiple cortical and subcortical structures, and there is increasing evidence that it suppresses the activity of GABAergic interneurons leading to disinhibition of glutamatergic neurons (Ali et al., 2020; Homayoun & Moghaddam, 2007). Although ketamine acts at many other receptors, including dopaminergic, serotoninergic, opioid and GABAergic receptors (Kapur & Seeman, 2002; Lewis et al., 2008; Sarton et al., 2001; Seeman & Lasaga, 2005), it is generally believed that most of its effects are accounted for by NMDA receptor antagonism.

The late (200–700 ms post-stimulus) sensory-induced beta/gamma oscillations were, on average, measurable in the sedated rat. These late response activities would be involved in the perceptual process (Funayama et al., 2015). In sedated rats, the level of perception and the underlying neural activities are expected to be attenuated because of the presence of rhythmic GABAergic-mediated inhibitions at least in the delta- and sigma-frequency bands (slow-wave sleep with spindles). Ketamine, by reducing the slow waves, spindles and burst activities, depolarises and switches the burst firing pattern to the irregular tonic mode (Mahdavi et al., 2020). This means that ketamine brings a persistent depolarising pressure to the membrane potential (persistent UP state) of the glutamatergic and GABAergic neurons, which is expected to disrupt the tonic firing pattern associated with a sensory-perceptual process. Moreover, it was demonstrated that, in the rat, NMDA receptor antagonism disrupts synchronisation of action potential firing in the prefrontal cortex, which would lead to a disruption of the transfer of information processing dependent on the timing of action potentials (Molina et al., 2014).

Limitations of the study

The experiments were performed on the pentobarbital-sedated rat (non-REM sleep model). The present findings do not allow drawing definitive conclusions. However, the combined two models, one for the brain state (sleep model) and one for the ketamine psychosis-relevant challenge (Mahdavi et al., 2020), provide interesting tools to conceptually and mechanistically advance our understanding of the neurobiology of psychotic disorders. The major requirement of the present study was to have the equivalent of a stationary stage II non-REM sleep, during which we could perform repeated measures. Furthermore, under the present experimental conditions, a single systemic administration of ketamine at a psychotomimetic dose (2.5 mg/kg, estimated from a study conducted in free-behaving rats (Pinault, 2008) induces most of the oscillopathies (especially basal gamma hyperactivity and delta/spindle hypoactivity) recorded in patients having psychotic disorders (Mahdavi et al., 2020). One advantage of the pentobarbital-induced sedation was its relative stability over time, allowing repeated measures.

Under the present experimental conditions, the degree of perception and attention would have been weakened because the pentobarbital induces a slow-wave sleep with spindle-like activities by increasing the GABAergic neurotransmission (Maldifassi et al., 2016). In short, the experimental conditions, which promote cortical slow waves (Knyazev, 2012; Murphy et al., 2009; Pinault et al., 2006; Urbain et al., 2019), would have prevented or attenuated the full corticalisation of sensory-perception processing and, subsequently,

the full implication of the CT (feedback) and cortico-cortical (feedforward) pathways. However, the CTC system, which includes the TRN (Pinault, 2004), is functionally polyvalent in a state-dependent way as it is involved in sensory-perception processing (Saalmann & Kastner, 2011), wake–sleep brain oscillations (Steriade et al., 1993) and attention-sensory processes (Chen et al., 2015; Wimmer et al., 2015). So, it is not surprising that the highly distributed CTC systems play a central role in the disorders of sleep integrity, sensorimotor, perception and attentional processes observed in patients with psychotic disorders (Chen et al., 2015; Ferrarelli & Tononi, 2011; Pinault, 2011; Shipp, 2004; Steriade et al., 1993; Wolff et al., 2021).

Ketamine exerts a wide range of dose-dependent effects (dissociative anaesthesia, sedation, psychotomimetic, antidepressant, analgesic so on). So, we should not exclude the analgesic effect of low-dose ketamine (Laskowski et al., 2011; Zanos et al., 2018). Pain involves the somatosensory CTC system among many other brain regions (amygdala, insula, S2, ACC and PFC). By examining the role of the auditory system in pain processing, it was demonstrated that the information to VPm and PoM is disrupted by the auditory CT pathway (Zhou et al., 2022). So, the ketamine-induced disruption of sensory information transfer in the CT network may be a common part of the mechanisms underlying the analgesic and psychotomimetic effects of ketamine.

Conclusion and perspectives

The present results provide anatomo-functional relevance to understanding the neural dynamics underlying ketamine-induced impairment of encoding processes (Hetem et al., 2000), perception-related (feedforward and feedback) dysconnectivity and abnormal amplification of gamma oscillations in human CTC systems (Anticevic et al., 2014; Driesen et al., 2013; Grent-'t-Jong et al., 2018; Hoflich et al., 2015; Rivolta et al., 2015). The NMDA receptor hypofunction-related gamma hyper-synchronies (power increases) are neurophysiological abnormalities that may represent a core biological feature of the psychotic transition. Although the interpretation of measures using complexity estimators (like MSE) of neural signals is not simple, in recent years there is accumulating evidence that increased and abnormal complexity may also be a hallmark of psychosis (Fernandez et al., 2013; Ibanez-Molina et al., 2018; Yang et al., 2015). Abnormal and diffuse amplification of spontaneously-occurring broadband gamma oscillations in neural networks (gamma noise) associated with reductions in sensory-related, evoked and induced gamma-band responses (gamma signal) are potentially predictive translational biomarkers of psychosis transition (Anderson et al., 2017; Gandal et al., 2012; Hakami et al., 2009; Kulikova et al., 2012). The sensory-evoked potential is also an appropriate index

to evaluate the expression of the plasticity of neural circuits (Kulikova et al., 2012). Because of their spatio-temporal structure and stereotyped pattern, sensory-evoked and induced gamma oscillations represent potential reliable and suitable variables (Hong et al., 2010; Leicht et al., 2016; Reilly et al., 2018; Spencer et al., 2008; Tada et al., 2016) for the development of innovative therapies preventing the psychotic transition.

ACKNOWLEDGEMENTS

The present work was supported by INSERM, the French National Institute of Health and Medical Research (Institut National de la Santé et de la Recherche Médicale, 2013-), l'Université de Strasbourg, Unistra (2013-), and Neurex. The funders of this project are INSERM, the Université de Strasbourg, and the NeuroTime Erasmus+ program of the European Commission (2015-2020: YQ and AM). This publication reflects the views only of the authors, and the European Commission cannot be held responsible for any use, which may be made of the information contained therein. The authors thank Damaris Cornec for her technical assistance, and Christiaan Levelt for critical reading of the manuscript.

Supplementary

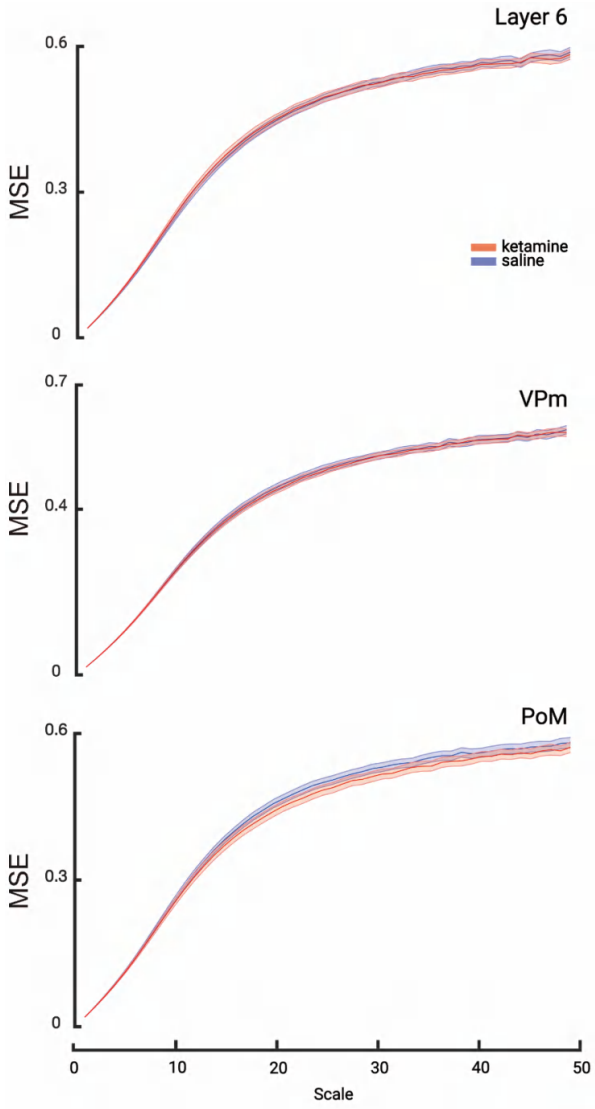

Figure S1: Ketamine does not change the multi-scale entropy in the beta band between the cortex and thalamus. Comparison of the multi-scales entropies of saline (blue) and ketamine (red) conditions at all recording sites in the beta band during the 200-700 ms post-stimulus period. Layer 6 and VPm show a significant increase in entropy. Each scale point is the average entropy (± SEM, from 40 values, 10 per rats, 4 rats). The statistical test does not reveal any significant difference between the saline and ketamine conditions ($p > 0.05$, paired t-test)

References

Ahmed MU, Mandic DP (2011) Multivariate Multiscale Entropy: A Tool For Complexity Analysis Of Multichannel Data. PHYSICAL REVIEW E 84.

Ali F, Gerhard DM, Sweasy K, Pothula S, Pittenger C, Duman RS, Kwan AC (2020) Ketamine Disinhibits Dendrites And Enhances Calcium Signals In Prefrontal Dendritic Spines. NATURE COMMUNICATIONS 11.

Alitto H, Usrey W (2003) Corticothalamic Feedback And Sensory Processing. CURRENT OPINION IN NEUROBIOLOGY 13:440–445.

Anderson PM, Jones NC, O'Brien TJ, Pinault D (2017) The N-Methyl D-Aspartate Glutamate Receptor Antagonist Ketamine Disrupts The Functional State Of The Corticothalamic Pathway. CEREBRAL CORTEX 27:3172–3185.

Anticevic A, Cole MW, Repovs G, Murray JD, Brumbaugh MS, Winkler AM, Savic A, Krystal JH, Pearlson GD, Glahn DC (2014) Characterizing Thalamo-Cortical Disturbances In Schizophrenia And Bipolar Illness. CEREBRAL CORTEX 24:3116–3130.

Baldeweg T, Spence S, Hirsch S, Gruzelier J (1998) Gamma-Band Electroencephalographic Oscillations In A Patient With Somatic Hallucinations. LANCET 352:620–621.

Becker C, Gramann K, Mueller HJ, Elliott MA (2009) Electrophysiological Correlates Of Flicker-Induced Color Hallucinations. CONSCIOUSNESS AND COGNITION 18:266–276.

Behrendt R (2003) Hallucinations: Synchronisation Of Thalamocortical Gamma Oscillations Underconstrained By Sensory Input. CONSCIOUSNESS AND COGNITION 12:413–451.

Breakspear M, Stam C (2005) Dynamics Of A Neural System With A Multiscale Architecture. PHILOSOPHICAL TRANSACTIONS OF THE ROYAL SOCIETY B-BIOLOGICAL SCIENCES 360:1051–1074.

Briggs F, Usrey WM (2008) Emerging Views Of Corticothalamic Function. CURRENT OPINION IN NEUROBIOLOGY 18:403–407.

Castro-Alamancos M (2002) Different Temporal Processing Of Sensory Inputs In The Rat Thalamus During Quiescent And Information Processing States In Vivo. JOURNAL OF PHYSIOLOGY-LONDON 539:567–578.

Chen Z, Wimmer RD, Wilson MA, Halassa MM (2016) Thalamic Circuit Mechanisms Link Sensory

Processing In Sleep And Attention. FRONTIERS IN NEURAL CIRCUITS 9.

Chrobak JJ, Hinman JR, Sabolek HR (2008) Revealing Past Memories: Proactive Interference And Ketamine-Induced Memory Deficits. JOURNAL OF NEUROSCIENCE 28:4512–4520.

Compte A, Reig R, Descalzo VF, Harvey MA, Puccini GD, Sanchez-Vives MV (2008) Spontaneous High-Frequency (10-80 Hz) Oscillations During Up States In The Cerebral Cortex In Vitro. JOURNAL OF NEUROSCIENCE 28:13828–13844.

Costa M, Goldberger A, Peng C (2005) Multiscale Entropy Analysis Of Biological Signals. PHYSICAL REVIEW E 71.

Deschenes M, Paradis M, Roy J, Steriade M (1984) Electrophysiology Of Neurons Of Lateral Thalamic Nuclei In Cat - Resting Properties And Burst Discharges. JOURNAL OF NEUROPHYSIOLOGY 51:1196–1219.

Ehrlichman RS, Gandal MJ, Maxwell CR, Lazarewicz MT, Finkel LH, Contreras D, Turetsky BI, Siegel SJ (2009) N-Methyl-D-Aspartic Acid Receptor Antagonist-Induced Frequency Oscillations In Mice Recreate Pattern Of Electrophysiological Deficits In Schizophrenia. NEUROSCIENCE 158:705–712.

Fernandez A, Gomez C, Hornero R, Jose Lopez-Ibor J (2013) Complexity And Schizophrenia. PROGRESS IN NEURO-PSYCHOPHARMACOLOGY & BIOLOGICAL PSYCHIATRY 45:267–276.

Ferrarelli F, Tononi G (2011) The Thalamic Reticular Nucleus And Schizophrenia. SCHIZOPHRENIA BULLETIN 37:306–315.

Friston K, Brown HR, Siemerkus J, Stephan KE (2016) The Dysconnection Hypothesis (2016). SCHIZOPHRENIA RESEARCH 176:83–94.

Funayama K, Minamisawa G, Matsumoto N, Ban H, Chan AW, Matsuki N, Murphy TH, Ikegaya Y (2015) Neocortical Rebound Depolarization Enhances Visual Perception. PLOS BIOLOGY 13.

Gandal MJ, Edgar JC, Klook K, Siegel SJ (2012) Gamma Synchrony: Towards A Translational Biomarker For The Treatment-Resistant Symptoms Of Schizophrenia. NEUROPHARMACOLOGY 62:1504–1518.

Grenier F, Timofeev I, Steriade M (1998) Leading Role Of Thalamic Over Cortical Neurons During Postinhibitory Rebound Excitation. PROCEEDINGS OF THE NATIONAL ACADEMY OF SCIENCES OF THE UNITED STATES OF AMERICA 95:13929–13934.

Haenschel C, Bittner RA, Waltz J, Haertling F, Wibral M, Singer W, Linden DEJ, Rodriguez E (2009) Cortical Oscillatory Activity Is Critical For Working Memory As Revealed By Deficits In Early-Onset Schizophrenia. JOURNAL OF NEUROSCIENCE 29:9481–9489.

Hager B, Yang AC, Brady R, Meda S, Clementz B, Pearlson GD, Sweeney JA, Tamminga C, Keshavan M (2017) Neural Complexity As A Potential Translational Biomarker For Psychosis. JOURNAL OF AFFECTIVE DISORDERS 216:89–99.

Hakami T, Jones NC, Tolmacheva EA, Gaudias J, Chaumont J, Salzberg M, O'Brien TJ, Pinault D (2009) NMDA Receptor Hypofunction Leads To Generalized And Persistent Aberrant Gamma Oscillations Independent Of Hyperlocomotion And The State Of Consciousness. PLOS ONE 4.

Hetem L, Danion J, Diemunsch P, Brandt C (2000) Effect Of A Subanesthetic Dose Of Ketamine On Memory And Conscious Awareness In Healthy Volunteers. PSYCHOPHARMACOLOGY 152:283–288.

Homayoun H, Moghaddam B (2007) NMDA Receptor Hypofunction Produces Opposite Effects On Prefrontal Cortex Interneurons And Pyramidal Neurons. JOURNAL OF NEUROSCIENCE 27:11496–11500.

Homma NY, Happel MFK, Nodal FR, Ohl FW, King AJ, Bajo VM (2017) A Role For Auditory Corticothalamic Feedback In The Perception Of Complex Sounds. JOURNAL OF NEUROSCIENCE 37:6149–6161.

Hong LE, Summerfelt A, Buchanan RW, O'Donnell P, Thaker GK, Weiler MA, Lahti AC (2010) Gamma And Delta Neural Oscillations And Association With Clinical Symptoms Under Subanesthetic Ketamine. NEUROPSYCHOPHARMACOLOGY 35:632–640.

Ibanez-Molina AJ, Lozano V, Soriano MF, Aznarte J I, Gomez-Ariza CJ, Bajo MT (2018) EEG Multiscale Complexity In Schizophrenia During Picture Naming. FRONTIERS IN PHYSIOLOGY 9.

Jahnsen H, LLINAS R (1984) Electrophysiological Properties Of Guinea-Pig Thalamic Neurons - AN INVITRO STUDY. JOURNAL OF PHYSIOLOGY-LONDON 349:205-.

Kam JWY, Bolbecker AR, O'Donnell BF, Hetrick WP, Brenner CA (2013) Resting State EEG Power And Coherence Abnormalities In Bipolar Disorder And Schizophrenia. JOURNAL OF PSYCHIATRIC RESEARCH 47:1893–1901.

Kapur S, Seeman P (2002) NMDA Receptor Antagonists Ketamine And PCP Have Direct Effects On The Dopamine D-2 And Serotonin 5-HT2 Receptors - Implications For Models Of Schizophrenia. MOLECULAR PSYCHIATRY 7:837–844.

Kim CS, Johnston D (2020) Antidepressant Effects Of (S)-Ketamine Through A Reduction Of Hyperpolarization-Activated Current I-H. ISCIENCE 23.

Knyazev GG (2012) EEG Delta Oscillations As A Correlate Of Basic Homeostatic And Motivational Processes. NEUROSCIENCE AND BIOBEHAVIORAL REVIEWS 36:677–695.

Kocsis B (2012) Differential Role Of NR2A And NR2B Subunits In N-Methyl-D-Aspartate Receptor Antagonist-Induced Aberrant Cortical Gamma Oscillations. BIOLOGICAL PSYCHIATRY 71:987–995.

Krystal J, KARPER L, SEIBYL J, FREEMAN G, DELANEY R, BREMNER J, HENINGER G, BOWERS M, CHARNEY D (1994) SUBANESTHETIC EFFECTS OF THE NONCOMPETITIVE NMDA ANTAGONIST, KETAMINE, IN HUMANS - PSYCHOTOMIMETIC, PERCEPTUAL, COGNITIVE, AND NEUROENDOCRINE RESPONSES. ARCHIVES OF GENERAL PSYCHIATRY 51:199–214.

Kulikova SP, Tolmacheva EA, Anderson P, Gaudias J, Adams BE, Zheng T, Pinault D (2012) Opposite Effects Of Ketamine And Deep Brain Stimulation On Rat Thalamocortical Information Processing. EUROPEAN JOURNAL OF NEUROSCIENCE 36:3407–3419.

Lake D, Richman J, Griffin M, Moorman J (2002) Sample Entropy Analysis Of Neonatal Heart Rate Variability. AMERICAN JOURNAL OF PHYSIOLOGY-REGULATORY INTEGRATIVE AND COMPARATIVE PHYSIOLOGY 283:R789–R797.

Laskowski K, Stirling A, Mckay WP, Lim HJ (2011) A Systematic Review Of Intravenous Ketamine For Postoperative Analgesia. CANADIAN JOURNAL OF ANESTHESIA-JOURNAL CANADIEN D ANESTHESIE 58:911–923.

Leicht G, Vauth S, Polomac N, Andreou C, Rauh J, Mussmann M, Karow A, Mulert C (2016) EEG-Informed Fmri Reveals A Disturbed Gamma-Band-Specific Network In Subjects At High Risk For Psychosis. SCHIZOPHRENIA BULLETIN 42:239–249.

Lewis DA, Cho RY, Carter CS, Eklund K, Forster S, Kelly MA, Montrose D (2008) Subunit-Selective Modulation Of GABA Type A Receptor Neurotransmission And Cognition In Schizophrenia.

AMERICAN JOURNAL OF PSYCHIATRY 165:1585–1593.

LLINAS R (1988) THE INTRINSIC ELECTROPHYSIOLOGICAL PROPERTIES OF MAMMALIAN NEURONS - INSIGHTS INTO CENTRAL NERVOUS-SYSTEM FUNCTION. SCIENCE 242:1654–1664.

Lunsford-Avery JR, Orr JM, Gupta T, Pelletier-Baldelli A, Dean DJ, Watts AKS, Bernard J, Millman ZB, Mittal VA (2013) Sleep Dysfunction And Thalamic Abnormalities In Adolescents At Ultra High-Risk For Psychosis. SCHIZOPHRENIA RESEARCH 151:148–153.

Mahdavi A, Qin Y, Aubry A-S, Cornec D, Kulikova S, Pinault D (2020) A Single Psychotomimetic Dose Of Ketamine Decreases Thalamocortical Spindles And Delta Oscillations In The Sedated Rat. SCHIZOPHRENIA RESEARCH 222:362–374.

Maldifassi MC, Baur R, Sigel E (2016) Functional Sites Involved In Modulation Of The GABA(A) Receptor Channel By The Intravenous Anesthetics Propofol, Etomidate And Pentobarbital. NEUROPHARMACOLOGY 105:207–214.

Manoach DS, Demanuele C, Wamsley EJ, Vangel M, Montrose DM, Miewald J, Kupfer D, Buysse D, Stickgold R, Keshavan MS (2014) Sleep Spindle Deficits In Antipsychotic-Naive Early Course Schizophrenia And In Non-Psychotic First-Degree Relatives. FRONTIERS IN HUMAN NEUROSCIENCE 8.

Mayeli A, Lagoy A, Donati FL, Kaskie RE, Najibi SM, Ferrarelli F (2021) Sleep Abnormalities In Individuals At Clinical High Risk For Psychosis. JOURNAL OF PSYCHIATRIC RESEARCH 137:328–334.

MCGHIE A, CHAPMAN J (1961) DISORDERS OF ATTENTION AND PERCEPTION IN EARLY SCHIZOPHRENIA. BRITISH JOURNAL OF MEDICAL PSYCHOLOGY 34:103-.

Molina LA, Skelin I, Gruber AJ (2014) Acute NMDA Receptor Antagonism Disrupts Synchronization Of Action Potential Firing In Rat Prefrontal Cortex. PLOS ONE 9.

Murphy M, Riedner BA, Huber R, Massimini M, Ferrarelli F, Tononi G (2009) Source Modeling Sleep Slow Waves. PROCEEDINGS OF THE NATIONAL ACADEMY OF SCIENCES OF THE UNITED STATES OF AMERICA 106:1608–1613.

Neville K, Haberly L (2003) Beta And Gamma Oscillations In The Olfactory System Of The Urethane-Anesthetized Rat. JOURNAL OF NEUROPHYSIOLOGY 90:3921–3930.

Paxinos G, Watson C (1998) The Rat Brain - In Stereotaxic Coordinates - Preface: Fourth Edition. In: RAT BRAIN IN STEREOTAXIC COORDINATES, FOURTH ED., Pp Ix+.

Perrottelli A, Giordano GM, Brando F, Giuliani L, Mucci A (2021) EEG-Based Measures In At-Risk Mental State And Early Stages Of Schizophrenia: A Systematic Review. FRONTIERS IN PSYCHIATRY 12.

Pinault D (1996) A Novel Single-Cell Staining Procedure Performed In Vivo Under Electrophysiological Control: Morpho-Functional Features Of Juxtacellularly Labeled Thalamic Cells And Other Central Neurons With Biocytin Or Neurobiotin. JOURNAL OF NEUROSCIENCE METHODS 65:113–136.

Pinault D (2004) The Thalamic Reticular Nucleus: Structure, Function And Concept. BRAIN RESEARCH REVIEWS 46:1–31.

Pinault D (2008) N-Methyl D-Aspartate Receptor Antagonists Ketarnine And MK-801 Induce Wake-Related Aberrant,Gamma Oscillations In The Rat Neocortex. BIOLOGICAL PSYCHIATRY 63:730–735.

Pinault D (2011) Dysfunctional Thalamus-Related Networks In Schizophrenia. SCHIZOPHRENIA BULLETIN 37:238–243.

PINAULT D, DESCHENES M (1992) VOLTAGE-DEPENDENT 40-HZ OSCILLATIONS IN RAT RETICULAR THALAMIC NEURONS INVIVO. NEUROSCIENCE 51:245–258.

Pinault D, Slezia A, Acsady L (2006) Corticothalamic 5-9 Hz Oscillations Are More Pro-Epileptogenic Than Sleep Spindles In Rats. JOURNAL OF PHYSIOLOGY-LONDON 574:209–227.

Pitsikas N, Boultadakis A, Sakellaridis N (2008) Effects Of Sub-Anesthetic Doses Of Ketamine On Rats' Spatial And Non-Spatial Recognition Memory. NEUROSCIENCE 154:454–460.

Portella C, Machado S, Arias-Carrion O, Sack AT, Silva JG, Orsini M, Araujo Leite MA, Silva AC, Nardi AE, Cagy M, Piedade R, Ribeiro P (2012) Relationship Between Early And Late Stages Of Information Processing: An Event-Related Potential Study. NEUROLOGY INTERNATIONAL 4:71–77.

Portella C, Machado S, Paes F, Cagy M, Sack AT, Sandoval-Carrillo A, Salas-Pacheco J, Silva AC, Piedade R, Ribeiro P, Nardi AE, Arias-Carrion O (2014) Differences In Early And Late Stages Of Information Processing Between Slow Versus Fast Participants. International Archives Of Medicine 7:49.

Ramyead A, Kometer M, Studerus E, Koranyi S, Ittig S, Gschwandtner U,

Fuhr P, Riecher-Roessler A (2015) Aberrant Current Source-Density And Lagged Phase Synchronization Of Neural Oscillations As Markers For Emerging Psychosis. SCHIZOPHRENIA BULLETIN 41:919–929.

Reilly TJ, Nottage JF, Studerus E, Rutigliano G, De Micheli AI, Fusar-Poli P, Mcguire P (2018) Gamma Band Oscillations In The Early Phase Of Psychosis: A Systematic Review. NEUROSCIENCE AND BIOBEHAVIORAL REVIEWS 90:381–399.

Richman J, Lake D, Moorman J (2004) Sample Entropy. In: NUMERICAL COMPUTER METHODS, PT E (Johnson M, Brand L, Eds), Pp 172–184 Methods In Enzymology.

Rivolta D, Heidegger T, Scheller B, Sauer A, Schaum M, Birkner K, Singer W, Wibral M, Uhlhaas PJ (2015) Ketamine Dysregulates The Amplitude And Connectivity Of High-Frequency Oscillations In Cortical-Subcortical Networks In Humans: Evidence From Resting-State Magnetoencephalography-Recordings. SCHIZOPHRENIA BULLETIN 41:1105–1114.

Rodriguez E, George N, Lachaux J, Martinerie J, Renault B, Varela F (1999) Perception's Shadow: Long-Distance Synchronization Of Human Brain Activity. NATURE 397:430–433.

Saalmann YB, Kastner S (2011) Cognitive And Perceptual Functions Of The Visual Thalamus. NEURON 71:209–223.

Saradjian AH, Teasdale N, Blouin J, Mouchnino L (2019) Independent Early And Late Sensory Processes For Proprioceptive Integration When Planning A Step. CEREBRAL CORTEX 29:2353–2365.

Sarton E, Teppema L, Olievier C, Nieuwenhuijs D, Matthes H, Kieffer B, Dahan A (2001) The Involvement Of The Mu-Opioid Receptor In Ketamine-Induced Respiratory Depression And Antinociception. ANESTHESIA AND ANALGESIA 93:1495–1500.

Seeman P, Lasaga M (2005) Dopamine Agonist Action Of Phencyclidine. SYNAPSE 58:275–277.

Sherman S (2001) A Wake-Up Call From The Thalamus. NATURE NEUROSCIENCE 4:344–346.

Shipp S (2004) The Brain Circuitry Of Attention. TRENDS IN COGNITIVE SCIENCES 8:223–230.

Spencer K, Nestor P, Perlmutter R, Niznikiewicz M, Klump M, Frumin M, Shenton M, Mccarley R (2004) Neural Synchrony Indexes Disordered Perception And Cognition In Schizophrenia. PROCEEDINGS OF THE NATIONAL ACADEMY OF SCIENCES OF THE

UNITED STATES OF AMERICA 101:17288–17293.

Spencer KM, Niznikiewicz MA, Shenton ME, Mccarley RW (2008) Sensory-Evoked Gamma Oscillations In Chronic Schizophrenia. BIOLOGICAL PSYCHIATRY 63:744–747.

Srinivasan R, Winter WR, Ding J, Nunez PL (2007) EEG And MEG Coherence: Measures Of Functional Connectivity At Distinct Spatial Scales Of Neocortical Dynamics. JOURNAL OF NEUROSCIENCE METHODS 166:41–52.

STERIADE M, MCCORMICK D, SEJNOWSKI T (1993) THALAMOCORTICAL OSCILLATIONS IN THE SLEEPING AND AROUSED BRAIN. SCIENCE 262:679–685.

Swadlow H, Gusev A (2001) The Impact Of `Bursting' Thalamic Impulses At A Neocortical Synapse. NATURE NEUROSCIENCE 4:402–408.

Takahashi T, Cho RY, Mizuno T, Kikuchi M, Murata T, Takahashi K, Wada Y (2010) Antipsychotics Reverse Abnormal EEG Complexity In Drug-Naive Schizophrenia: A Multiscale Entropy Analysis. NEUROIMAGE 51:173–182.

Uhlhaas PJ, Roux F, Singer W (2013) Thalamocortical Synchronization And Cognition: Implications For Schizophrenia? NEURON 77:997–999.

Urbain N, Fourcaud-Trocme N, Laheux S, Salin PA, Gentet LJ (2019) Brain-State-Dependent Modulation Of Neuronal Firing And Membrane Potential Dynamics In The Somatosensory Thalamus During Natural Sleep. CELL REPORTS 26:1443+.

Urbain N, Salin PA, Libourel P-A, Comte J-C, Gentet LJ, Petersen CCH (2015) Whisking-Related Changes In Neuronal Firing And Membrane Potential Dynamics In The Somatosensory Thalamus Of Awake Mice. CELL REPORTS 13:647–656.

Van Essen D (2005) Corticocortical And Thalamocortical Information Flow In The Primate Visual System. In: CORTICAL FUNCTION: A VIEW FROM THE THALAMUS (Casagrande V, Guillery R, Sherman S, Eds), Pp 173–185 Progress In Brain Research.

Wimmer RD, Schmitt LI, Davidson TJ, Nakajima M, Deisseroth K, Halassa MM (2015) Thalamic Control Of Sensory Selection In Divided Attention. NATURE 526:705–709.

Wolff M, Morceau S, Folkard R, Martin-Cortecero J, Groh A (2021) A Thalamic Bridge From Sensory Perception To Cognition. NEUROSCIENCE AND

BIOBEHAVIORAL REVIEWS 120:222–235.

Yang AC, Hong C-J, Liou Y-J, Huang K-L, Huang C-C, Liu M-E, Lo M-T, Huang NE, Peng C-K, Lin C-P, Tsai S-J (2015) Decreased Resting-State Brain Activity Complexity In Schizophrenia Characterized By Both Increased Regularity And Randomness. HUMAN BRAIN MAPPING 36:2174–2186.

Zanini MA, Castro J, Cunha GR, Asevedo E, Pan PM, Bittencourt L, Coelho FM, Tufik S, Gadelha A, Bressan RA, Brietzke E (2015) Abnormalities In Sleep Patterns In Individuals At Risk For Psychosis And Bipolar Disorder. SCHIZOPHRENIA RESEARCH 169:262–267.

Zanos P, Moaddel R, Morris PJ, Riggs LM, Highland JN, Georgiou P, Pereira EFR, Albuquerque EX, Thomas CJ, Zarate CA Jr, Gould TD (2018) Ketamine And Ketamine Metabolite Pharmacology: Insights Into Therapeutic Mechanisms. PHARMACOLOGICAL REVIEWS 70:621–660

Zhou W, Ye C, Wang H, Mao Y, Zhang W, Liu A, Yang C-L, Li T, Hayashi L, Zhao W, Chen L, Liu Y, Tao W, Zhang Z (2022) Sound Induces Analgesia Through Corticothalamic Circuits. SCIENCE 377:198+.

Chapter 4

Thalamic regulation of ocular dominance plasticity in adult visual cortex

Yi Qin[1,4], Mehran Ahmadlou[2], Samuel Suhai[1], Paul Neering[1], Leander de Kraker[1], J. Alexander Heimel[2] & Christiaan N. Levelt[1,3]

[1]Molecular Visual Plasticity Group, Netherlands Institute for Neuroscience, Royal Netherlands Academy of Arts and Sciences, Meibergdreef 47, 1105 BA Amsterdam, the Netherlands

[2]Circuits, Structure and Function Group, Netherlands Institute for Neuroscience, Royal Netherlands Academy of Arts and Sciences, Meibergdreef 47, 1105 BA Amsterdam, the Netherlands[2]

[3]Department of Molecular and Cellular Neurobiology, Center for Neurogenomics and Cognitive Research, VU University Amsterdam, de Boelelaan 1085, 1081 HV, the Netherlands. [4]University of Strasbourg, Strasbourg, France.

eLife, under review

Summary

Experience-dependent plasticity in the adult visual system is generally thought of as a cortical process. However, several recent studies have shown that perceptual learning or monocular deprivation can also induce plasticity in the adult dorsolateral geniculate nucleus (dLGN) of the thalamus. How plasticity in the thalamus and cortex interact in the adult visual system is ill understood. To assess the influence of thalamic plasticity on plasticity in primary visual cortex (V1), we made use of our previous finding that during the critical period, ocular dominance (OD) plasticity occurs in dLGN and requires thalamic synaptic inhibition. Using multielectrode recordings we find that this is also true in adult mice, and that in the absence of thalamic inhibition and plasticity, OD plasticity in adult V1 is absent. To study the influence of V1 on thalamic plasticity we silenced V1 and show that during the critical period, but not in adulthood, the OD shift in dLGN is partially caused by feedback from V1. We conclude that during adulthood, the thalamus plays an unexpectedly dominant role in experience-dependent plasticity in V1. Our findings highlight the importance of considering the thalamus as a potential source of plasticity in learning events that are typically thought of as cortical processes.

Introduction

Experience-dependent plasticity in the adult visual system is largely thought of as a cortical process (Gilbert et al., 2009; Gilbert and Wiesel, 1992). However, several recent studies have demonstrated that plasticity also occurs in the adult dorsal lateral geniculate nucleus (dLGN) of the thalamus of human subjects during perceptual learning (Yu et al., 2016) and mice upon monocular deprivation (MD) (Huh et al., 2020; Jaepel et al., 2017). How plasticity in adult dLGN is regulated and whether plasticity in dLGN and V1 influence each other has barely been studied.

In this study, we addressed these questions using ocular dominance (OD) plasticity in mice as a model. OD is the property that neurons preferentially respond to visual stimuli presented to one eye versus the other (Wiesel and Hubel, 1963a). Visual experience affects OD and a period of MD results in an OD shift in V1 neurons due to weakened responses to the deprived eye and strengthened responses to the non-deprived eye (Hensch and Stryker, 1996; Wiesel and Hubel, 1963a). OD plasticity is most prominent during a critical period of development (Gordon and Stryker, 1996; Wiesel and Hubel, 1963a) but can also be induced in young adult mice (Heimel et al., 2007; Hofer et al., 2006; Lehmann and Löwel, 2008; Sato and Stryker, 2008; Sawtell et al., 2003). This requires a longer period of deprivation, however, and the shift is smaller and less persistent and is mediated predominantly by strengthening of responses to the non-deprived eye (Frenkel and Bear, 2004; Heimel et al., 2007; Hofer et al., 2006; Lehmann and Löwel, 2008; Sato and Stryker, 2008).

Previously, we demonstrated that during the critical period, extensive OD plasticity can be induced in dLGN and that this requires synaptic inhibition in the thalamus (Sommeijer et al., 2017). Multielectrode recordings revealed that OD plasticity in dLGN is strongly reduced in mice in which thalamic synaptic inhibition is inactivated by deleting the gene encoding the GABA receptor alpha1 subunit (*Gabra1*) selectively in the dorsal thalamus (Gabra1$^{fl\text{-}hom}$ x Olig3-cre^{+} mice, hereafter referred to as “KO mice”). Interestingly, OD plasticity induced by long-term monocular deprivation (MD) is also reduced in V1 of these mice due to the absence of ipsilateral eye response strengthening (Sommeijer et al., 2017), suggesting that during the critical period, thalamic plasticity contributes to plasticity in V1. Here, we investigated how dLGN and V1 influence each other during OD plasticity in adulthood. We find that in adult mice lacking thalamic synaptic inhibition, OD plasticity is absent in both dLGN and V1. Silencing V1 of adult wild-type (WT) mice does not affect the OD shift in dLGN, showing that it does not depend on feedback from V1. In contrast, we

find that during the critical period, the OD shift in dLGN is partially depends on activity in V1. Together, our findings show that thalamocortical interactions underlying OD plasticity change with age and suggest that the thalamus may be an important source of plasticity in adult learning events that have generally been considered cortical processes.

Results

Visual responses in adult dLGN of WT and KO mice

Previous work showed that during the critical period, visual responses of dLGN neurons in Gabra1^{flhom} x olig3-cre^{+} KO mice were less sustained due to the lack of thalamic synaptic inhibition, while average response strengths and basic receptive field properties seemed surprisingly unaffected (Sommeijer et al., 2017).

To assess whether this situation remained similar in adulthood, we measured visual responses in dLGN using a 16-channel silicon probe in anesthetized KO mice and Gabra1^{fl-hom} x olig3-cre^{-} (WT) siblings. Recordings were performed in the ipsilateral projection zone of dLGN (Fig. 1A). Receptive field sizes and positions were determined by presenting white squares (5 deg) at random positions on a black background (Fig. 1B). We only included recordings from channels with receptive fields corresponding to the central 30^{o} of the visual field. We observed no differences in receptive field sizes in KO and WT mice (Fig. 1C). As receptive field sizes in dLGN are known to become smaller between eye opening and critical period onset (Tschetter et al., 2018), this observation suggests that dLGN develops surprisingly normally in the absence of synaptic inhibition. To investigate this further, we analyzed the numbers, densities and sizes of inhibitory and cholinergic boutons, which are also known to increase during the same developmental window (Bickford et al., 2010, Sommeijer et al. 2017, Sokhadze et al., 2018). Again, in adult WT and KO mice we observed no differences (Suppl. Fig. 1).

To record visual responses of dLGN neurons to the contra- or ipsilateral eye separately, the other eye was closed and visual stimuli (full screen, full contrast black/white reversals, at 3s intervals) were presented (Fig. 1B). We selected single units from non-deprived WT and KO mice and assessed their responses to the contra- and ipsilateral eye. Examples of monocular and binocular single units are shown in Figure 1D. To assess whether the temporal profile of visual responses differed in adult WT and KO mice, we compared the areas under the curve (AUC) of the peristimulus time histogram (PSTH) during different time bins (Fig. 1E). This revealed that in KO mice, visual responses attenuated faster than in wild-type siblings: responses were weaker during the second 150 ms after visual stimulation but a trend towards stronger responses was observed during the first 150 ms (P=0.095). Thus, while average response strength in KO mice was similar to that in WT mice, the attenuation index was increased. These results show that like the situation during the critical period (Sommeijer et al., 2017), visual responses in dLGN neurons in

adult KO and WT mice mostly differ in their temporal profile, while average response strengths and receptive fields sizes are hardly changed.

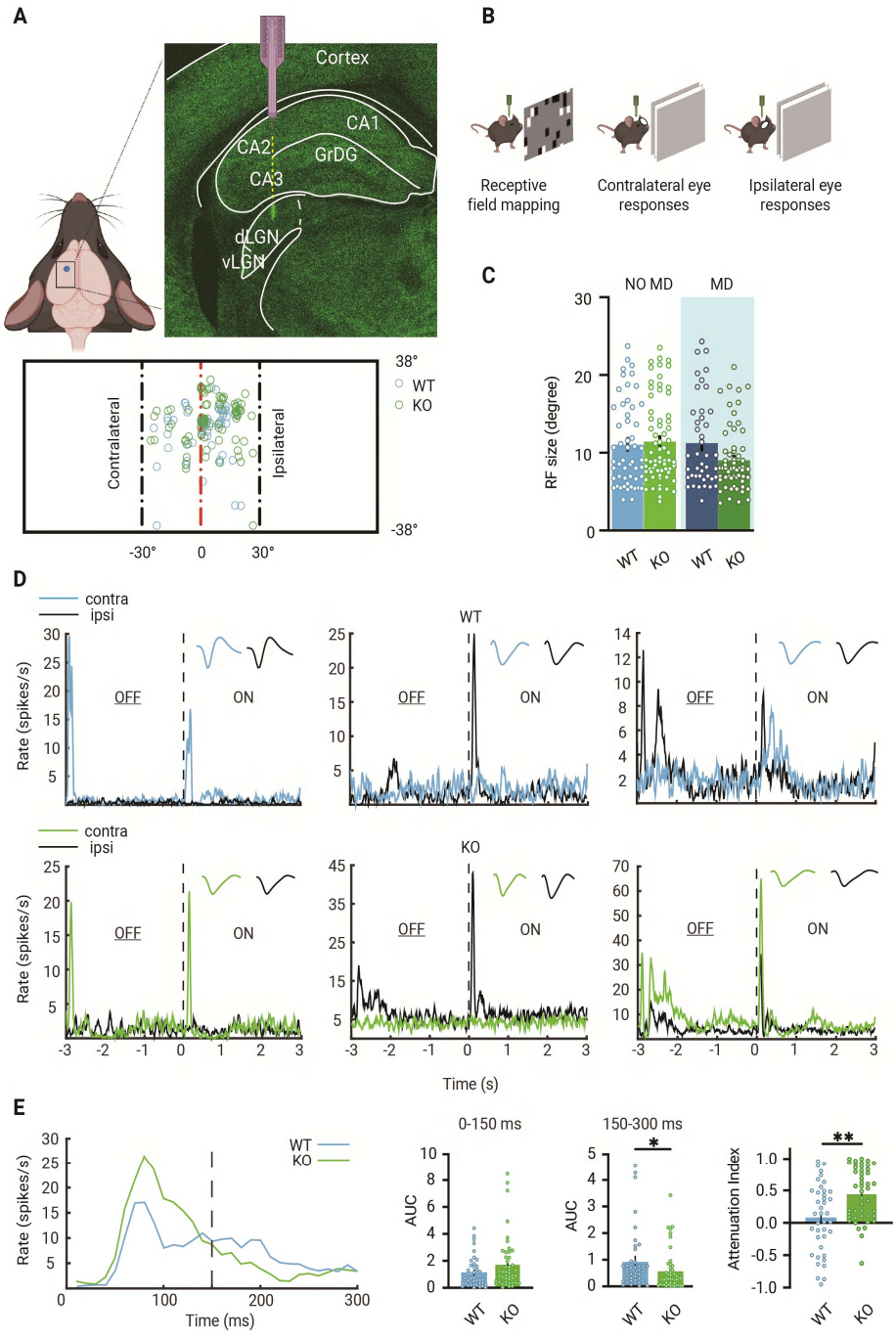

Fig. 1 | Visual responses of dLGN neurons in mice lacking thalamic Gabra1. A, Recording electrodes were placed in the ipsilateral projection zone of dLGN (see green fluorescent trace of actual electrode penetration in dLGN).

All receptive field centers of multi-units recorded in wild-type (WT, blue) and knockout (KO, green) mice (n=61 units from 13 non-deprived or monocularly deprived (MD) mice and n=80 units from 18 NO MD or MD mice). Nose position is at 0 degrees horizontally and vertically. The black dashed lines indicate -30 degree and +30 degree horizontal angles. **B,** Experimental setup to measure receptive field (RF) and single eye responses. **C**, RF sizes of multi-units in NO MD and MD (shaded area) KO and WT mice do not differ (interaction of genotype with MD: two-way ANOVA, P=0.07). **D,** Examples of dLGN neuron responses to full screen OFF-ON flash stimuli in WT (blue) and KO (green) mice. Colored and black lines indicate responses of contra- and ipsilateral eyes, respectively. Waveforms of each unit responding to the contra- or ipsilateral eye are shown in the upper right corner. **E,** Left, average responses of contralateral eye in WT (blue) and KO (green) mice. Middle, areas under curve (AUC) of early (0-150ms, left) and late responses (150-300ms, mid). Right, attenuation index of visual responses in WT and KO mice.

OD plasticity in dLGN is reduced in adult mice lacking thalamic synaptic inhibition

We then continued experiments to assess OD plasticity in the dLGN of WT and KO mice. We monocularly deprived adult WT and KO mice for 7 days, long enough to induce an OD shift in adult V1 (Frenkel and Bear, 2004; Heimel et al., 2007; Hofer et al., 2006; Lehmann and Löwel, 2008; Sato and Stryker, 2008), by suturing one eye closed. We recorded responses to the ipsi- and contralateral eye in dLGN neurons (Fig. 2A) and calculated the OD index (ODI) of all units recorded in monocularly deprived and non-deprived KO and WT mice and averaged them to obtain an OD score (Fig. 2B). We found that after one week of MD, a significant OD shift occurred in dLGN of adult WT mice. This was predominantly caused by a significant increase in the responses to the non-deprived ipsilateral eye (Fig. 2C). In KO mice, no OD shift could be induced in dLGN (Fig. 2B) and no significant changes were observed in the responses to the ipsi- or contralateral eye (Fig, 2D). Together, these results show that also in adulthood, OD plasticity in dLGN depends on thalamic synaptic inhibition.

OD plasticity in adult V1 is reduced in mice lacking thalamic synaptic inhibition

During the critical period, OD plasticity in V1 is partially deficient in KO mice. Brief MD induces a normal OD shift, but longer MD does not cause the OD shift to strengthen further (Sommeijer et al., 2017). This suggests that the critical period opens normally in V1 of KO mice, but that the second, homeostatic phase of the OD shift depends on thalamic inhibition and plasticity. Residual OD plasticity in adult V1 has various similarities with the second phase of OD plasticity during the critical period and also requires long term MD. We were therefore investigated whether OD plasticity in V1 was deficient in adult KO mice.

To address this question, we monocularly deprived WT and KO mice for 7 days, after which we recorded visual responses from single units in V1 of these mice and of normally sighted siblings (Fig. 3A). Again, we only included channels with receptive fields within the central 30° of the visual field to ascertain we recorded from binocular V1. Like in dLGN, receptive field sizes did not differ between KO and WT mice and were not affected by a week of MD (Fig. 3B).

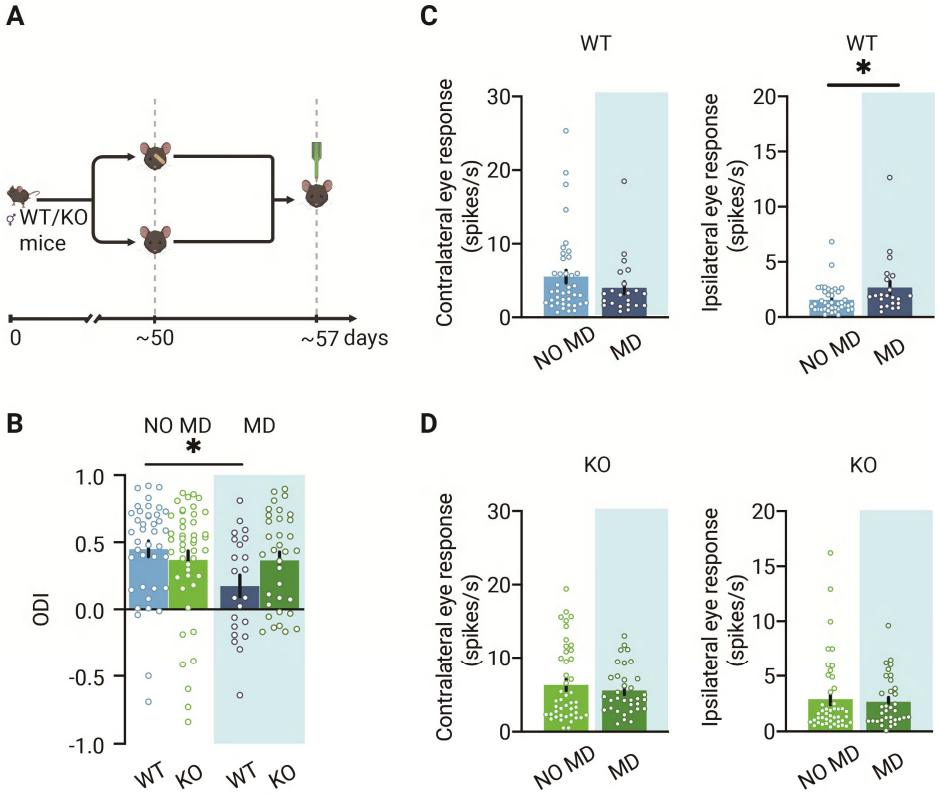

Fig. 2| Reduced OD plasticity in dLGN of mice lacking thalamic synaptic inhibition. A, Illustration of the experiment design. In experiments, four groups of animals were used: deprived (MD) or non-deprived (NO MD) wild-type and knockout mice. Mice in the MD group had the eyelids of the eye contralateral to the recording side sutured 7 for days. **B,** 7 days of MD reduces the ODI in WT mice but not in KO animals (interaction of genotype with MD: two-way ANOVA, P=0.046, Tukey's post-hoc test; WT NO MD vs. WT MD, P=0.040; WT NO MD, n=40 units, 7 mice; WT MD, n=22 units, 6 mice; KO NO MD, n=45 units, 9 mice; KO MD, n=34 units, 9 mice). **C,** In WT mice, responses to the ipsilateral eye are significantly increased after 7-d MD. Responses to the contralateral eye are unchanged (Mann-Whitney; contralateral, NO MD vs. MD, P=0.29; ipsilateral, NO MD vs. MD, P=0.032). **D,** In KO mice, MD causes no significant changes in responses to either the contralateral or the ipsilateral eye (Mann-Whitney; contralateral, NO MD vs. MD, P=0.73; ipsilateral, NO MD vs. MD, P=0.59).

Visual responses to the contra- or ipsilateral eye were recorded in the same way as for dLGN, using the same visual stimuli (examples shown in Fig. 3C). Like in dLGN, visual responses in V1 were more attenuated in KO mice than in WT mice (Fig. 3D). Next, we calculated the OD index from all single units in the four groups (Fig. 3E). A clear OD shift was induced in V1 of monocularly deprived WT mice. As expected, the OD shift involved an increase in open, ipsilateral eye responses (Fig. 3F). We also found a significant decrease of deprived, contralateral eye responses (Fig. 3F). While several studies have provided evidence that a loss of contralateral eye responses contributes less to adult OD plasticity than during the critical period (Frenkel and Bear, 2004; Kalogeraki et al., 2017; Sato and Stryker, 2008), others have shown that it still occurs in adulthood (Rose et al., 2016). Possibly, the OD shift and the loss of deprived eye responses are more pronounced in our recordings due to them being limited to the center of the visual field or the use of flash stimuli instead of moving gratings.

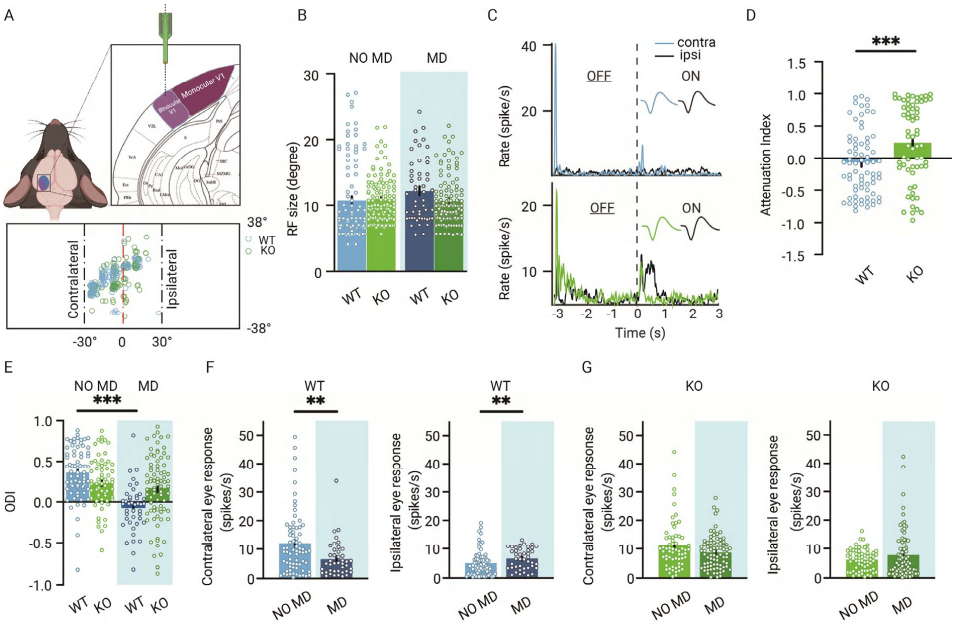

Fig. 3| Reduced OD plasticity in adult V1 lacking thalamic OD plasticity. A, Recording electrodes are located in binocular V1. All receptive field centers of multi-units recorded in WT (blue) and KO (green) mice (n=112 units from 13 NO MD or MD mice and n=138 units from 18 NO MD or MD mice). Nose position is at 0 degrees horizontally and vertically. The black dashed lines indicate -30 degree and +30 degree horizontal angles. **B**, RF sizes of units in KO and KO mice do not differ (interaction of genotype with MD: two-way ANOVA, P=0.07). **C,** Two examples of single unit responses in V1 of a WT (blue) and KO (green) mouse to the contra- and ipsilateral eyes to ON and OFF visual stimuli. Each stimulus lasted 3s. Colored and black lines indicate contra- and ipsilateral eye responses, respectively. **D**, Attenuation index of contralateral eye responses in V1 of WT and KO mice. **E,** 7 days of MD reduces the ODI in WT but not KO mice (interaction of genotype with MD: two-way ANOVA, P<0.001,

Tukey's post-hoc test; WT NO MD vs. WT MD, P<0.001; WT NO MD, n=71 units, 7 mice; WT MD, n=42, 6 mice; KO NO MD, n=63 units, 9 mice; KO MD, n=78 units, 9 mice). **F,** In WT mice, responses to the contralateral eye are significantly reduced after 7-d MD, while those to the ipsilateral eye are significant increased (Mann-Whitney; contralateral, NO MD vs. MD, P=0.0043; ipsilateral, NO MD vs. MD, P=0.0062). **G,** In KO mice, MD causes no significant changes in responses to either the contralateral or the ipsilateral eye (MannWhitney; contralateral, NO MD vs. MD, P=0.17; ipsilateral, NO MD vs. MD, P=0.66.).

In adult KO mice, the OD shift after 7 days of MD was negligible and significantly smaller than in WT mice (Fig. 3G). The contra- and ipsilateral eye responses in V1 of non-deprived KO mice were of comparable strength as those observed in WT mice, despite the lack of synaptic inhibition in the thalamus. After 7 days of monocular deprivation, no significant strengthening of ipsilateral eye responses or weakening of deprived eye responses occurred (Fig. 3F). We conclude that in adult mice, absence of synaptic inhibition in the thalamus reduces OD plasticity in V1.

Effect of feedback from V1 to dLGN responses in the presence or absence of thalamic synaptic inhibition

These results so far show that OD plasticity in dLGN affects the OD shift in V1. OD plasticity in V1 may also influence the OD shift in dLGN. Apart from the retinal input dLGN relay cells receive, they are also strongly innervated by excitatory feedback connections from layer 6 cells in V1. Additionally, dLGN neurons receive bisynaptic inhibitory feedback from V1 via the thalamic reticular nucleus (TRN) and local interneurons (Fig. 4A). Depending on whether excitatory or inhibitory feedback dominates, responses of dLGN relay cells to the ipsi- or contralateral eye in dLGN may be strengthened or inhibited by V1 feedback (Denman and Contreras, 2015; Howarth et al., 2014; Jaepel et al., 2017; Kirchgessner et al., 2020; Olsen et al., 2012). These feedback inputs from V1 can thus influence the OD of relay cells in dLGN.

To investigate how dLGN responses were influenced by V1 feedback and how synaptic thalamic inhibition affected this, we silenced V1 of WT and KO mice with the GABA-receptor agonist muscimol while recording from dLGN. Muscimol injections effectively silenced V1 (Fig. 4A). On average, silencing V1 did not alter responses to the contra- or ipsilateral eye in individual units in dLGN of adult WT mice (Fig. 4B-D). In KO mice, V1 silencing also did not significantly affect responses to the contralateral eye (Fig. 4E-G). Responses to the ipsilateral eye showed a trend towards weakening after silencing V1, but this did not reach significance (P=0.094). Thus, also in the absence of synaptic inhibition in the thalamus, V1 feedback has relatively little influence on dLGN responses to the contra- or ipsilateral eye.

Feedback from V1 does not affect the OD shift in adult dLGN

Finally, we investigated whether feedback from V1 influenced the OD shift in dLGN of adult WT and KO mice. In non-deprived mice, the OD index did not change after silencing V1 of WT mice (Fig. 5A), as expected considering that contra- and ipsilateral eye response strengths were not affected by V1 feedback (Fig. 4C, D). Similarly, the OD index in non-deprived KO mice did not change upon silencing V1 (Fig. 5B), which was also expected based on the small changes in contra- and lateral eye responses that we observed (Fig. 4F, G).

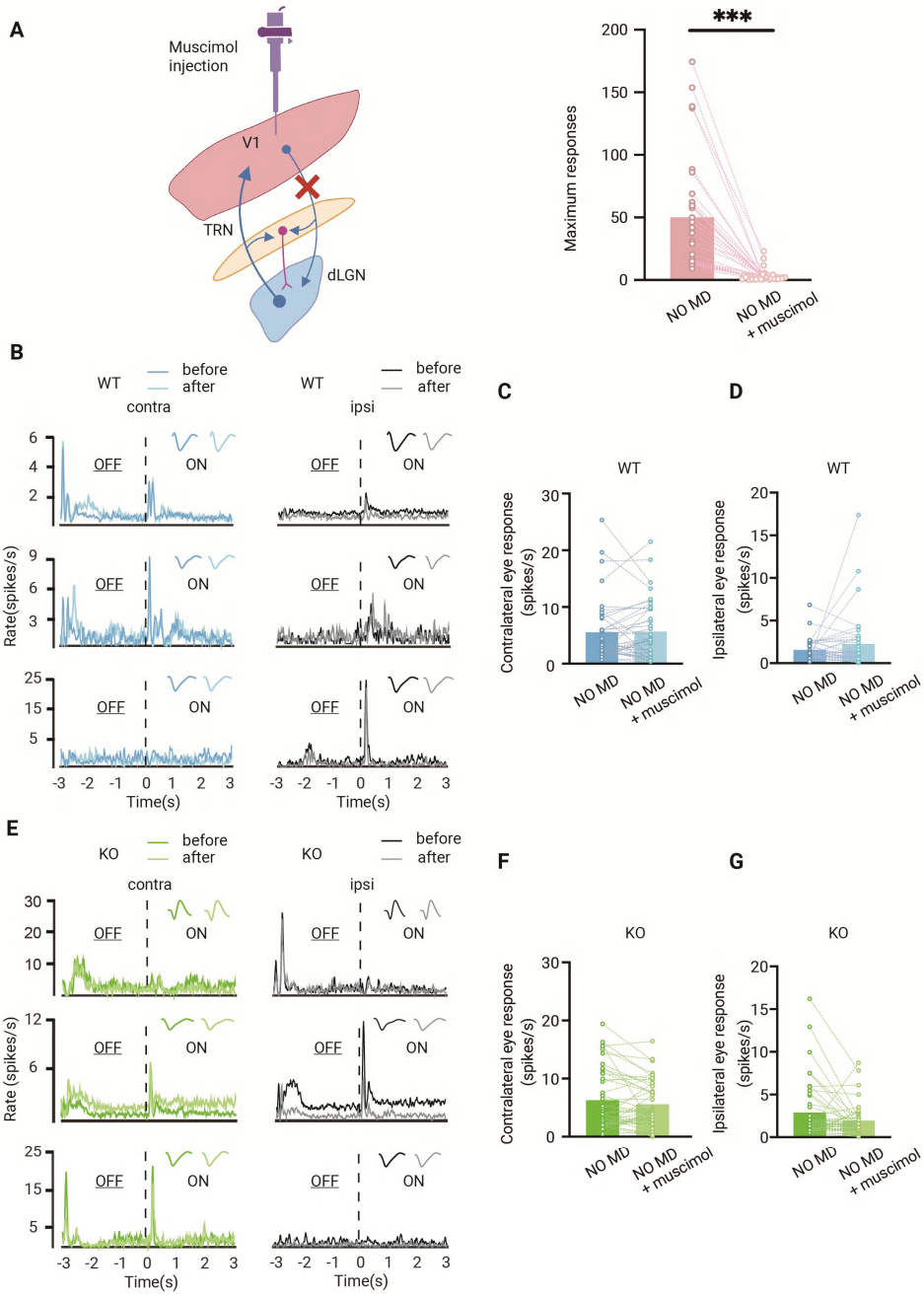

Fig. 4| Effect of feedback from V1 to dLGN responses. A, Left, illustration of corticothalamic-thalamocortical feedback network. dLGN is innervated by V1 and receives glutamatergic feedback. All these projections send excitatory colaterals to the thalamic reticular nucleus (TRN) which sends inhibitory inputs to dLGN. By muscimol injection in V1, corticothalamic projections are silenced. Right, V1 is effectively silenced by muscimol injection (Wilcoxon signed rank, P<0.001, n=31 mice). **B,** Examples of dLGN responses before and after muscimol injection

in V1 of non-deprived WT mice. Waveforms of each unit are shown in upper right corner. Left and right panels correspond to contralateral and ipsilateral eye responses respectively. Dark and light lines represent responses before and after muscimol injection respectively. **C & D,** Silencing V1 feedback has no significant effect on contralateral (**C**) or ipsilateral (**D**) responses in WT mice (Wilcoxon signed rank; contralateral, WT NO MD vs. WT NO MD with muscimol, P=0.62; ipsilateral, WT NO MD vs. WT NO MD with muscimol, P=0.94, n=40 units, 7 mice). **E,** Examples of dLGN responses before and after muscimol injection in V1 of non-deprived KO mice. Waveforms of each unit are shown in upper right corner. Left and right panels correspond to contralateral and ipsilateral eye responses respectively. Dark and light lines represent responses before and after muscimol injection respectively. **F & G,** There is no significant effect of V1 silencing on contralateral (**F**) or ipsilateral (**G**) eye responses in KO mice, but a trend towards decreased ipsilateral eye responses is present (Wilcoxon signed rank; contralateral, KO NO MD vs. KO NO MD with muscimol, P=0.19; ipsilateral, KO NO MD vs. KO NO MD with muscimol, P=0.059, n=45 units, 9 mice).

Despite the considerable OD shift we observed in V1 of adult WT mice, silencing V1 did not affect the OD measured in dLGN (Fig. 5C). Also, average responses to the two eyes were not altered in the absence of cortical feedback (Fig. 5D, E). This confirms that the OD shift in adult dLGN is not inherited from V1 (Jaepel et al., 2017) and supports the idea that dLGN plasticity involves the plasticity of retinogeniculate afferents. Interestingly, when we repeated this experiment in (C57Bl/6JRj) WT mice during the critical period, we found that silencing V1 also did not affect ipsi- or contralateral eye responses in non-deprived mice (Suppl. Fig. 2A, B), but selectively reduced ipsilateral eye responses in monocularly deprived mice (Fig. 5G-H). Consequently, silencing V1 significantly reduced the OD shift in these animals (Fig 5I). Thus, during the critical period, corticothalamic connections strengthen the OD shift in dLGN, while they do not in adulthood.

In monocularly deprived adult KO mice (Fig. 5I-K), silencing V1 did not affect responses to the contralateral eye, but significantly reduced those to the ipsilateral eye (Fig.5J, K), similarly to what we observed in WT mice during the critical period. However, despite this effect of V1 silencing, the average ODI in monocularly deprived KO mice was not significantly altered by it (Fig. 5I). We conclude that feedback from V1 does not affect OD in the dLGN of adult mice, independently of whether they are monocularly deprived or lack synaptic inhibition in the thalamus. During the critical period, however, V1 silencing does reduce the OD shift observed in dLGN.

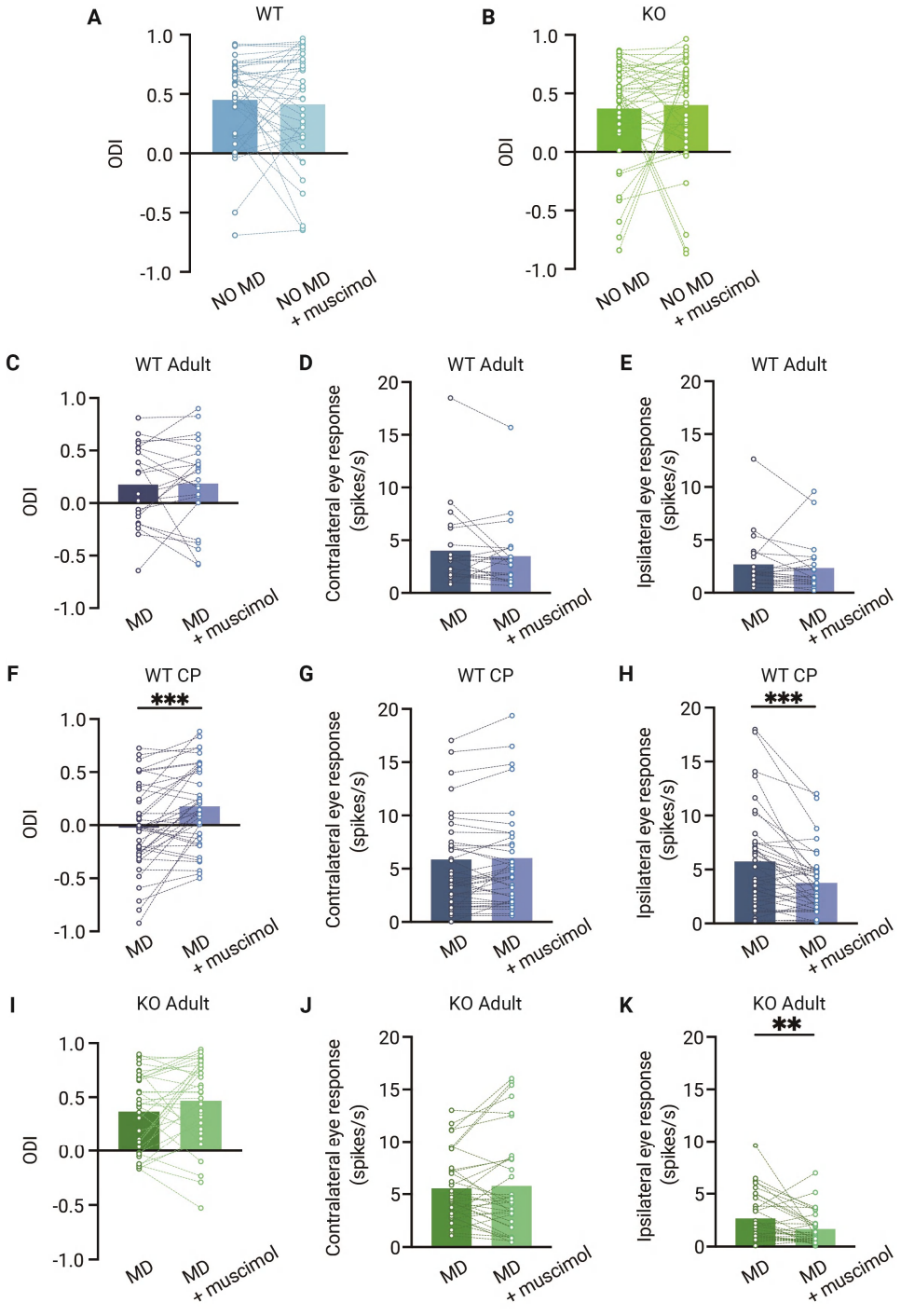

Fig. 5| The OD shift in dlGN is independent from V1 feedback in adult mice but not in critical period mice. A

& B, Muscimol injection in V1 has no effect on the ODI in dLGN of adult non-deprived WT (**A**) and KO (**B**) mice (Wilcoxon signed rank; WT NO MD vs. WT NO MD with muscimol, P=0.86, n=40 units, 7 mice; KO NO MD vs. KO NO MD with muscimol, P=0.45, 45 units, 9 mice). **C, D & E,** Muscimol injection in V1 has no significant effect on the ODI (**C**), or contralateral (**D**) or ipsilateral (**E**) eye responses in dLGN of monocularly deprived WT mice (Wilcoxon signed rank; ODI, WT MD vs. WT MD with muscimol, P=0.89; contralateral, WT MD vs. WT MD with muscimol, P=0.21; ipsilateral, WT MD vs. WT MD with muscimol, P=0.10, n=22 units, 6 mice). **F, G & H,** During the critical period, V1 silencing has a significant influence on the ODI (**F**) and ipsilateral eye responses (**H**) in dLGN of monocularly deprived WT mice, but not on contralateral eye responses in these mice (**G**) (Wilcoxon signed rank; ODI, WT MD vs. WT MD with muscimol, P<0.001; contralateral, WT MD vs. WT MD with muscimol, P=0.46; ipsilateral, WT MD vs. WT MD with muscimol, P=0.003, n=41 units, 10 mice). **I, J & K,** Muscimol injection in V1 has no significant influence on the ODI and contralateral eye responses in KO MD mice, but significantly modulates dLGN ipsilateral eye responses (Wilcoxon signed rank; ODI, KO MD vs. KO MD with muscimol, P=0.13; contralateral, KO MD vs. KO MD with muscimol, P=0.97; ipsilateral, KO MD vs. KO MD with muscimol, P=0.004, n=34 units, 9 mice).

Discussion

In summary, we show that OD plasticity in dLGN is reduced in adult mice lacking thalamic synaptic inhibition. In these mice, OD plasticity in V1 is absent, suggesting that it requires thalamic plasticity. We do not find evidence that feedback from V1 affects the thalamic OD shift in adult mice. This differs from the situation during the critical period, in which the OD shift in dLGN is partially inherited from V1.

How does inactivation of synaptic inhibition and OD plasticity in dLGN interfere with the OD shift in V1? It seems likely that MD-induced changes in dLGN relay cell responses to inputs from the two eyes will directly alter binocular responses in V1, and that reduced plasticity in dLGN will thus diminish the OD shift in V1. Additionally, the strengthening of responses to the non-deprived eye in dLGN neurons may provide their axons with a competitive advantage during OD plasticity in V1, further enhancing the OD shift in V1. We cannot rule out the possibility, however, that OD plasticity in V1 is also affected by the more attenuated nature of dLGN responses that we observe in mice lacking thalamic synaptic inhibition (Sommeijer et al., 2017), for example by altering spike-timing dependent plasticity in V1.

The main substrate of plasticity in adult dLGN appears to be the retinogeniculate synapse, as silencing V1, the other main source of visual input to dLGN, does not affect the OD shift. Recent work has shown that while many relay cells in dLGN receive binocular inputs (Rompani et al., 2017), synapses from the non-dominant eye are often silent and dominated by NMDA receptors (Bauer et al., 2021). Because silent synapses contribute

strongly to OD plasticity in V1, it is interesting to speculate that OD plasticity in dLGN also involves the unsilencing and strengthening of these synapses (Huang et al., 2015; Yusifov et al., 2021). Indeed, the OD shift in adult mice involves many contralateral eye-selective neurons to become binocular (Jaepel et al., 2017).

The plasticity deficits we observe in KO mice during adulthood are similar to what we observed during the critical period. At first glance, this phenotype is reminiscent of that in heterozygous GAD65-deficient mice, in which synaptic GABA release is diminished and OD plasticity is reduced during the critical period and in adulthood. It is believed that in these mice, development of V1 is halted in a pre-critical period-like stage. This is not the case in mice lacking thalamic synaptic inhibition, however, as in these mice the critical period in V1 opens normally. In contrast to GAD65deficient mice, brief MD during the critical period results in a normal OD shift in KO mice. Whether reduced plasticity in dLGN of adult KO mice is caused by halted thalamic development remains unclear. So far, we did not find evidence to support this. Receptive fields of dLGN relay cells become smaller between eye opening and critical period onset, and in WT and KO mice, receptive field sizes are the same. Furthermore, there is a substantial increase in inhibitory and cholinergic boutons during this developmental stage, but again, WT and KO mice are not different in this respect. The primary difference between WT and KO mice in dLGN thus appears to be the lack of synaptic inhibition. Together, our results indicate that thalamic inhibition and plasticity play a crucial role in OD plasticity in adult V1, regardless of the developmental contribution to the plasticity deficit in dLGN.

The study by Bauer et al (Bauer et al., 2021) also showed that binocularity in mouse dLGN may be lower than suggested by the current study and earlier work (Howarth et al., 2014; Sommeijer et al., 2017) that involved multi-electrode recordings in dLGN. Although this difference may be caused by technical limitations of single unit recordings or calcium imaging, we think it is most likely explained by the fact that studies employing electrophysiological recording in dLGN targeted the frontal ipsilateral projection zone of dLGN, which is its most binocular region (Bauer et al., 2021). Recording in this region is essential when studying OD plasticity or binocularity in dLGN, but will strongly bias towards binocularly-responding relay cells. When using two-photon imaging of dLGN boutons in V1 (Bauer et al., 2021; Huh et al., 2020; Jaepel et al., 2017), neurons from other parts of dLGN including the monocular shell- and caudal regions are also sampled.

It is unknown whether adult thalamic OD plasticity also occurs in species in which retinal inputs from the two eyes are organized in more strictly separated layers in dLGN, such as

cats or primates. Studies in cats consistently found that upon MD or squint during the critical period, the layers responding to the affected eye were thinner (Hickey et al., 1977; Wiesel and Hubel, 1963b) and that the neuronal responses in these layers were slower or weaker (Eysel et al., 1979; Ikeda and Wright, 1976; Sestokas and Lehmkuhle, 1986; Wiesel and Hubel, 1963b). Also in human amblyopes it was noted that dLGN responses to the amblyopic eye were weaker (Hess et al., 2009). So far, studies on dLGN plasticity by prolonged visual deprivation in adulthood are missing, though it was noted that in human subjects that suffered from glaucoma, the dLGN layers representing the affected eye were thinner (Yücel et al., 2001). Future research will need to establish whether plasticity in dLGN in humans contributes to amblyopia, and whether it can be enhanced to treat the disorder. That enhancement of thalamic plasticity is in principle possible is shown by experiments in mice, demonstrating that inactivation of the nogo-66 receptor in thalamus allows recovery of reduced acuity in adult mice that were monocularly deprived during development (Stephany et al., 2018).

Despite extensive monosynaptic excitatory feedback and bisynaptic inhibitory feedback (through TRN) from V1, we found that feedback does not affect the average strength of response to ipsi- or contralateral eye stimulation and thus neither the measured OD shift in dLGN of adult mice. The absence of V1 on the OD shift in adult mice was also reported previously (Jaepel et al., 2017). However in that study, silencing V1 with muscimol reduced the imaged calcium responses in boutons of dLGN axons projecting to V1, suggesting that dLGN neurons became less responsive to inputs from both eyes. A possible explanation for this apparent discrepancy may be that muscimol also has a direct inhibitory effect on thalamocortical inputs (Wang et al., 2019), which may reduce calcium responses in synaptic boutons of dLGN neurons without actually reducing their spiking activity at the soma.

Studies involving optogenetic stimulation of layer 6 neurons find that feedback from V1 suppresses dLGN responses (Denman and Contreras, 2015; Kirchgessner et al., 2020; Olsen et al., 2012), though this differs per cell and changes with stimulus strength and frequency (Kirchgessner et al., 2020). When V1 feedback is silenced, however, the average strength of dLGN responses is not reduced in most studies (Denman and Contreras, 2015; Howarth et al., 2014; Kirchgessner et al., 2020). This suggests that broad optogenetic stimulation of layer 6 predominantly recruits inhibitory feedback, while visual stimulation provides either more balanced or more limited excitatory and inhibitory feedback to dLGN. In line with these previous studies, we find that silencing V1 does not significantly alter dLGN responses to either eye in WT mice. If the lack of effect of V1

silencing is due to balanced excitatory and inhibitory feedback, one would expect that in KO mice lacking thalamic synaptic inhibition, silencing V1 would cause a reduction of dLGN responses. However, such an effect in KO mice was only observed in dLGN responses to the ipsilateral eye, and reached significance only in monocularly deprived mice. This suggests that V1 feedback affects dLGN responses to the ipsilateral eye more strongly than those to the contralateral eye, possibly through a pathway involving callosal inputs to V1 that are fed back to dLGN (Cerri et al., 2010). In addition, extrasynaptic GABA (A) and GABA (B)-mediated inhibition are likely to be intact (Leresche and Lambert, 2018) in KO mice and could partially balance excitatory and inhibitory feedback to dLGN.

We found that during the critical period, the influence of V1 feedback on the OD shift in dLGN was much stronger. Possibly, inhibition in dLGN is weaker during the critical period, resulting in a stronger decrease of ipsilateral eye responses upon V1 silencing, similarly to the situation in adult KO mice. Additionally, a strong OD shift occurs in V1 during the critical period, adding to the strength of the cortical feedback representing the ipsilateral eye. During the critical period, an experiencedependent phase of retinogeniculate refinement takes place, probably optimizing direction-selective inputs from the retina (Hooks and Chen, 2020; Rompani et al., 2017; Thompson et al., 2017). This experience-dependent refinement, like OD plasticity in dLGN, also depends on feedback from V1 (Thompson et al., 2017, 2016). It is thus possible that refinement of binocular inputs and directionselective inputs in dLGN are one and the same process.
We conclude that dLGN retains a high level of plasticity in adulthood and has considerable influence on cortical plasticity. This plasticity may not be restricted to binocular responses, but could also be relevant for other forms of perceptual learning (Yu et al., 2016). The findings stress that a thalamic involvement needs to be considered in amblyopia and learning disabilities. Additionally, the results may help understanding brain disorders that are thought to involve dysfunctional thalamocortical circuits, ranging from attention deficit disorder (Wells et al., 2016) to schizophrenia (Benoit et al., 2022; Pinault, 2011; Pratt et al., 2017). Future experiments focusing on changes in thalamic responses and their interaction with the cortex may provide exciting new insights in how the brain learns.

Methods

Animals

All mice used to assess OD plasticity in adulthood were bred from homozygous conditional Gabra1deficient mice ($Gabra1^{fl\text{-}hom}$) (Vicini et al., 2001) crossed with homozygous Gabra1-deficient, heterozygous Olig3-cre knockin mice (Vue et al., 2009) ($Gabra1^{fl\text{-}hom}$ Olig3-cre^{+}). Before crossbreading the lines, $Gabra1^{fl\text{-}hom}$ mice had been backcrossed to C57Bl/6JRj mice (Janvier) for at least 6 generations. Olig3-cre^{-} mice were crossed to C57Bl/6JRj mice for at least 2 generations, but should be considered mixed background. All animals were tested for unintended germline recombination of the $Gabra1^{fl}$ locus, and such mice were excluded from breeding or experiments. In our experiments, we used 4 groups of animals: monocularly deprived or non-deprived $Gabra1^{fl\text{-}hom}$ Olig3-cre^{-} mice and monocularly deprived or non-deprived $Gabra1^{fl\text{-}hom}$ Olig3-cre^{+} siblings (P45-P90). The experimenter was blind to the genotype of the mice until the end of the experiment. Mice used for OD plasticity experiments during the critical period were C57Bl/6JRj mice. All mice were housed in a 12h/ 12h dark/light cycle. Both male and female mice were used. Mice housing conditions were according to
Dutch law. All experiments were approved by the institutional animal care and use committee of the Royal Netherlands Academy of Arts and Sciences.

Immunohistochemistry

Age-matched mice were anesthetized with 0.1 ml/g body weight Nembutal (Janssen) and perfused with 4% paraformaldehyde (PFA) in PBS (~50 ml per mouse) and post-fixed for 2-6 h. Post fixation time was consistent between compared groups. Sections from dLGN of 50 µm were made by using a vibratome (Leica VT1000S). Mouse-α-GAD67 (1:500, Chemicon, MAB5406) was used to label inhibitory boutons and and guinea pig-α-VaChT (1:500, SySy 139105) to label cholinergic boutons. Primary antibodies were visualized using Fluor 594 Goat-α-mouse (1:1000, Invitrogen, A11032 and Alexa Fluor 488 Goat-α-Guinea pig (1:1000, Invitrogen, A11073). Free-floating sections were briefly washed in PBS followed by 1-2 h blocking in PBS containing 5% normal goat serum and 0.1% Triton X100 at room temperature. Primary antibody incubation was performed overnight at 4 °C in fresh blocking solution. Next, the sections were washed three times for 10 min in PBS with 0.1% Tween-20 (PBST) followed by secondary antibody incubation in fresh blocking solution for 1.5-2 h at RT. After washing three times for 10 min in TBST the sections were mounted on glass slides using Mowiol (Calbiochem/ MerckMillipore), glass covered and stored at 4°C.

Confocal microscopy and data analysis

Sections were imaged using a confocal microscopy (Leica SP5) with constant gain and laser power across compared samples. Care was taken that no signal clipping was present. For quantification of GAD67 and VAChT puncta, and images were taken with a 40x objective (2048 x 2048 resolution). Background fluorescence was subtracted with ImageJ. VAChT and GAD67 puncta were quantified using the 'SynQuant' ImageJ plugin (Wang et al., 2020), creating ROIs corresponding to synaptic puncta. For each image we calculated the average size of identified puncta, the number of puncta per unit of area and the percentage of image area identified as part of punctum.

Monocular deprivation

The eyelids of the eye contralateral to the recording side were sutured for MD. The surgery was performed under isoflurane anesthesia (5% induction, 1.5-2% maintenance in 0.7 l/min O_2). The eye was rinsed with saline. The eyelids were sutured together with 7.0 Ethilon thread. Eyes were checked for infection in the following days and reopened during recording. Only mice with healthy eye conditions were included.

Electrophysiology recordings, visual stimulation and V1 silencing

Mice were anesthetized by intraperitoneal injection of urethane (Sigma; 20% solution in saline, 1.2g/kg body weight), supplemented by intraperitoneal injection of chlorprothixene (Sigma; 2.0mg/ml in saline, 8mg/kg body weight), followed by subcutaneous injection of atropine (Sigma; 1mg/ml, 6mg/kg body weight), and head-fixed by ear- and bite bars. The temperature was measured with a rectal probe and maintained at 36.5 °C. The craniotomies for dLGN (2.0 mm lateral, 2.5 mm posterior from bregma) and V1 (2.95 mm lateral, 0.45 mm anterior from lambda) recording windows were made using a dental drill. During recordings of V1 or dLGN responses to input from one eye, the other eye was covered with a double layer of black cloth and black tape.

Using a linear silicon microelectrode (A1x16-5mm-25-177-A16, 16 channels spaced 50 µm apart, Neuronexus), extracellular recordings from V1 and dLGN were performed separately. Visual stimuli were projected by a gamma-corrected projector (PLUS U2-X1130 DLP) on a back-projection screen (Macada Innovision, covering a 60X42 cm area) positioned 17.5 cm in front of the mouse. The visual stimuli were programmed using the MATLAB (MathWorks) scripts package Psychophysics Toolbox 3 (Brainard, 1997). V1 was first recorded at a depth of approximately 800 µm from the cortical surface. Receptive field position was checked by showing white squares (5 deg) at random positions on a black background. If the receptive field was not within 30° from the center, we relocated

the electrode and checked again. ODI was measured by presenting alternating white and gray full-screen stimuli to each eye in turn. Each stimulus lasted 3s. Both white and gray screens were presented with 100 repetitions. When the V1 recording was finished, we relocated the electrode to dLGN at a depth of 2700-3000 µm from bregma. The receptive field and ODI measurement procedures were repeated in dLGN. We then silenced V1 by injecting muscimol (Sigma; 10 mM; ~150 µL per mouse), a selective agonist for $GABA_A$ receptors, in V1 and measured the ODI again in dLGN. After recording, we moved electrode back to V1 to verify that muscimol had silenced V1.

The extracellular signals were amplified and bandpass filtered at 500 Hz-10 kHz and digitized at 24 kHz using a Tucker-Davis Technologies RX5 Pentusa base station. The spike detection was done by a voltage thresholder at 3x s.d. online per recording, or offline using the open-source sorting package KiloSort (Pachitariu et al., 2016). Spikes were sorted and clustered by either principle component analysis-based custom-written MATLAB scripts or integrated template matching-based KiloSort scripts.

Analysis of electrophysiological data

Data analysis was done using custom-made MATLAB scripts (http://github.com/heimel/inVivoTools). For each 3 s stimulus related activity, we treated the last 500ms of the previous trail as baseline. Therefore, we defined the visual responses as the difference between the first 500ms of the stimulus and the mean of the last 500ms activities of the previous stimulus. The peak visual responses of stimuli were considered as the maximum firing rates in first 300ms of visual related responses. The visual responses were calculated as average responses of 300ms. ODI was calculated as $(R_{contra}-R_{ipsi})/(R_{contra}+R_{ipsi})$, where the R_{contra} is the average firing rate of the unit when contralateral eye was open and ipsilateral eye was covered; R_{ipsi} is opposite. For receptive field mapping, we computed the spike - triggered average of the random sparse squares stimulus. The peak rate threshold was set to 5 Hz when the patch was within the receptive field. The actual position and size of visual field were computed and corrected for the actual distance between stimuli and animal.

Statistics

For testing the interaction between genotype with MD on OD plasticity and RF size in V1 and dLGN, we used a two-way ANOVA test with post-hoc Tukey-Kramer tests. Quantitation of immunohistochemical analyses were performed using using Student's t-test. All other tests were done with non-parametric tests. Statistical analyses of the

response changes of V1 and dLGN units in WT and KO mice, were done by non-parametric Mann-Whitney U tests. For testing the significance of the effect of silencing V1 on adult and critical period dLGN responses, on the OD in adult deprived and non-deprived KO mice and WT mice, on the OD in critical period deprived WT mice, and the effects of muscimol injection on V1 responses, Wilcoxon signed rank tests were used.

Acknowledgements

The authors thank Emma Ruimschotel for technical assistance, Robin Haak and Huub Terra for help with spike sorting, Huub Terra for providing feedback on the manuscript and the Mechatronics department and Animal facilities of the NIN for their services. Figures 1A&B, 2A, 3A and 4A were created with BioRender.com (2022). This project has received funding from the NeuroTime Erasmus+ program of the European Commission and the European Union's Horizon 2020 Research and Innovation Programme under Grant Agreements No.785907 (HBP SGA2) and 945539 (HBP SGA3).

Supplementary data

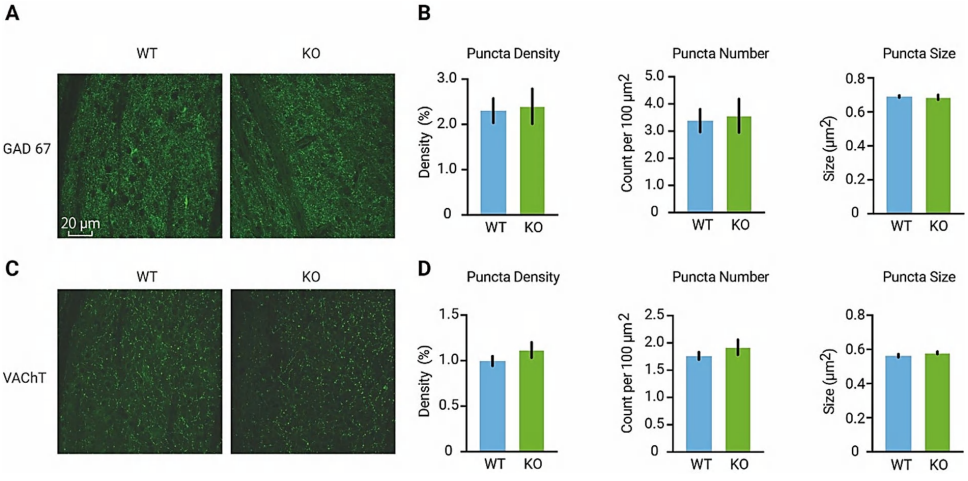

Supplementary Figure 1. A, Examples of immunohistochemical staining for GAD67 in dLGN of adult WT and KO mice. **B**, Quantification of the density, number, and sizes of GAD67 puncta (putative inhibitory boutons). No differences were detected between WT and KO mice (T-test; puncta density, P=0.85; puncta number, P=0.82; puncta size, P=0.80. n=3 mice per group, 3 slices were imaged per mouse). **C,** Examples of immunohistochemical staining for VAChT puncta (putative cholinergic boutons) in dLGN of adult WT and KO mice. **D,** Quantification of the density, number, and sizes of VAChT. No differences were detected between WT and KO mice (T-test; puncta density, P=0.29; puncta number, P=0.35; puncta size, P=0.22. n=3 mice per group, 3 slices were imaged per mouse).

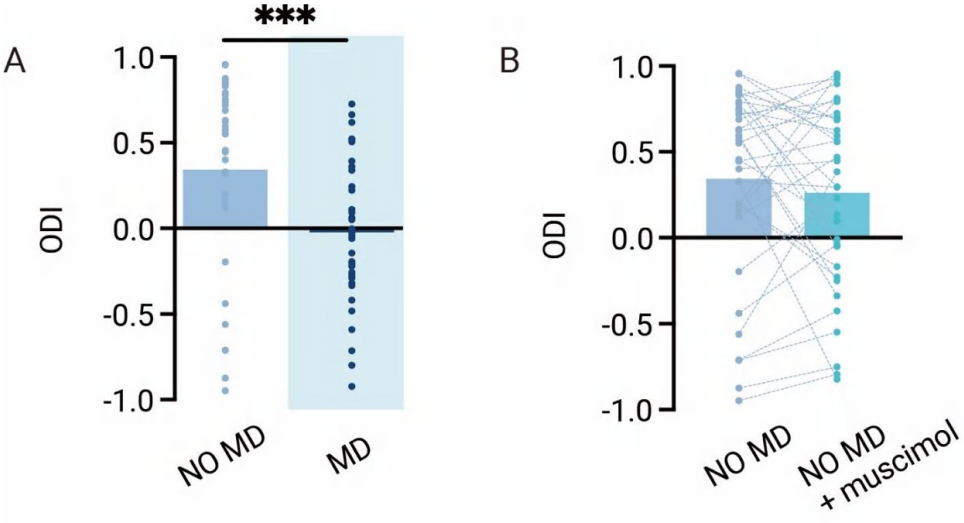

Supplementary Figure 2. A, MD induces ocular dominance plasticity in dLGN of WT mice during the critical period (Mann-Whitney; WT NO MD vs. WT MD, P=0.0015; WT NO MD, n=36, 10 mice; WT MD, n=41, 10 mice). **B,** During the critical period, V1 feedback has no effect on OD in non-deprived WT mice (Wilcoxon signed rank; ODI, WT NO MD vs. WT MD with muscimol, P=0.20).

References

Bauer J, Weiler S, Fernholz MHP, Laubender D, Scheuss V, Hübener M, Bonhoeffer T, Rose T (2021) Limited functional convergence of eye-specific inputs in the retinogeniculate pathway of the mouse. Neuron 109:2457–2468.

Benoit LJ, Canetta S, Kellendonk C (2022) Thalamocortical Development: A Neurodevelopmental Framework for Schizophrenia. Biol Psychiatry 92:491–500.

Bickford ME, Slusarczyk A, Dilger EK, Krahe TE, Kucuk C, Guido W (2010) Synaptic Development of the Mouse Dorsal Lateral Geniculate Nucleus. J Comp Neurol 518:622–635.

Brainard DH (1997) The Psychophysics Toolbox. Spat Vis 10:433–436.

Cerri C, Restani L, Caleo M (2010) Callosal contribution to ocular dominance in rat primary visual cortex. Eur J Neurosci 32:1163–1169.

Denman DJ, Contreras D (2015) Complex Effects on In Vivo Visual Responses by Specific Projections from Mouse Cortical Layer 6 to Dorsal Lateral Geniculate Nucleus. J Neurosci 35:9265–9280.

Eysel UT, Grüsser OJ, Hoffmann KP (1979) Monocular deprivation and the signal transmission by X- and Y-neurons of the cat lateral geniculate nucleus. Exp brain Res 34:521–539.

Frenkel MY, Bear MF (2004) How monocular deprivation shifts ocular dominance in visual cortex of young mice. Neuron 44:917–923.

Gilbert CD, Li W, Piech V (2009) Perceptual learning and adult cortical plasticity. J Physiol 587:2751.

Gilbert CD, Wiesel TN (1992) Receptive field dynamics in adult primary visual cortex. Nature 356:152.

Gordon A, Stryker P (1996) Experience-Dependent Plasticity of Binocular Responses in the Primary Visual Cortex of the Mouse. J Neurosci 76:3274–3286.

Heimel JA, Hartman RJ, Hermans JM, Levelt CN (2007) Screening mouse vision with intrinsic signal optical imaging. Eur J Neurosci 25:795–804.

Hensch TK, Stryker MP (1996) Ocular dominance plasticity under metabotropic glutamate receptor blockade. Science 272:554–557.

Hess RF, Thompson B, Gole G, Mullen KT (2009) Deficient responses from the lateral geniculate nucleus in humans with amblyopia. Eur J Neurosci 29:1064–1070.

Hickey TL, Spear PD, Kratz KE (1977) Quantitative studies of cell size in

the cat's dorsal lateral geniculate nucleus following visual deprivation. J Comp Neurol 172:265–281.

Hofer SB, Mrsic-Flogel TD, Bonhoeffer T, Hübener M (2006) Prior experience enhances plasticity in adult visual cortex. Nat Neurosci 9:127–132.

Hooks BM, Chen C (2020) Circuitry Underlying Experience-Dependent Plasticity in the Mouse Visual System. Neuron 106:21–36.

Howarth M, Walmsley L, Brown TM (2014) Binocular integration in the mouse lateral geniculate nuclei. Curr Biol 24:1241–1247.

Huang X, Stodieck SK, Goetze B, Cui L, Wong MH, Wenzel C, Hosang L, Dong Y, Löwel S, Schlüter OM (2015) Progressive maturation of silent synapses governs the duration of a critical period. Proc Natl Acad Sci 112:E3131-E3140.

Huh CYL, Abdelaal K, Salinas KJ, Gu D, Zeitoun J, Figueroa Velez DX, Peach JP, Fowlkes CC, Gandhi SP (2020) Long-term Monocular Deprivation during Juvenile Critical Period Disrupts Binocular Integration in Mouse Visual Thalamus. J Neurosci 40:585–604.

Ikeda H, Wright MJ (1976) Properties of LGN cells in kittens reared with convergent squint: a neurophysiological demonstration of amblyopia. Exp brain Res 25:63–77.

Jaepel J, Hübener M, Bonhoeffer T, Rose T (2017) Lateral geniculate neurons projecting to primary visual cortex show ocular dominance plasticity in adult mice. Nat Neurosci 20:1708–1714.

Kalogeraki E, Pielecka-Fortuna J, Löwel S (2017) Environmental enrichment accelerates ocular dominance plasticity in mouse visual cortex whereas transfer to standard cages resulted in a rapid loss of increased plasticity. PLoS One 12:e0186999.

Kirchgessner MA, Franklin AD, Callaway EM (2020) Context-dependent and dynamic functional influence of corticothalamic pathways to first- And higher-order visual thalamus. Proc Natl Acad Sci USA 117:13066–13077.

Lehmann K, Löwel S (2008) Age-Dependent Ocular Dominance Plasticity in Adult Mice. PLoS One 3:e3120.

Leresche N, Lambert RC (2018) GABA receptors and T-type Ca 2+ channels crosstalk in thalamic networks. Neuropharmacology 136:37–45.

Olsen B SR, DS A, H S, M. (2012) Gain control by layer six in cortical circuits of vision. Nature 483:47–54.

Pachitariu M, Steinmetz N, Kadir S, Carandini M, HK D (2016) Kilosort: realtime spike-sorting for extracellular electrophysiology with hundreds of channels. bioRxiv 061481.

Pinault D (2011) Dysfunctional thalamus-related networks in schizophrenia. Schizophr Bull 37:238–243.

Pratt J, Dawson N, Morris BJ, Grent-'t-Jong T, Roux F, Uhlhaas PJ (2017) Thalamo-cortical communication, glutamatergic neurotransmission and neural oscillations: A unique window into the origins of ScZ? Schizophr Res 180:4–12.

Rompani SB, Müllner FE, Wanner A, Zhang C, Roth CN, Yonehara K, Roska B (2017) Different Modes of Visual Integration in the Lateral Geniculate Nucleus Revealed by Single-Cell-Initiated Transsynaptic Tracing. Neuron 93:767–776.

Rose T, Jaepel J, Hübener M, Bonhoeffer T (2016) Cell-specific restoration of stimulus preference after monocular deprivation in the visual cortex. Science 352:1319–1322.

Sato M, Stryker MP (2008) Distinctive Features of Adult Ocular Dominance Plasticity. J Neurosci 28:10278–10286.

Sawtell NB, Frenkel MY, Philpot BD, Nakazawa K, Tonegawa S, Bear MF (2003) NMDA receptordependent ocular dominance plasticity in adult visual cortex. Neuron 38:977–985.

Sestokas A, Lehmkuhle S (1986) The effects of monocular deprivation on the visual latency of geniculate X- and Y-cells in the cat. Brain Res 395:93–95.

Sokhadze G, Seabrook TA, Guido W (2018) The absence of retinal input disrupts the development of cholinergic brainstem projections in the mouse dorsal lateral geniculate nucleus. Neural Dev 13.

Sommeijer J-PP, Ahmadlou M, Saiepour MH, Seignette K, Min R, Heimel JA, Levelt CN (2017) Thalamic inhibition regulates critical-period plasticity in visual cortex and thalamus. Nat Neurosci 1.

Stephany C-É, Ma X, Dorton HM, Wu J, Solomon AM, Frantz MG, Qiu S, McGee AW (2018) Distinct Circuits for Recovery of Eye Dominance and Acuity in Murine Amblyopia. Curr Biol 28:1914–1923.

Thompson A, Gribizis A, Chen C, Crair MC (2017) Activity-dependent development of visual receptive fields. Curr Opin Neurobiol 42:136–143.

Thompson AD, Picard N, Min L, Fagiolini M, Chen C (2016) Cortical Feedback Regulates Feedforward Retinogeniculate Refinement. Neuron 91:1021–1033.

Tschetter WW, Govindaiah G, Etherington IM, Guido W, Niell CM (2018) Refinement of Spatial Receptive Fields in the Developing Mouse Lateral Geniculate Nucleus Is Coordinated with Excitatory and Inhibitory Remodeling. J Neurosci 38:4531–4542.

Vicini S, Ferguson C, Prybylowski K, Kralic J, Morrow AL, Homanics GE (2001) GABA(A) receptor alpha1 subunit deletion prevents developmental changes of inhibitory synaptic currents in cerebellar neurons. J Neurosci 21:3009–3016.

Vue TY, Bluske K, Alishahi A, Yang LL, Koyano-Nakagawa N, Novitch B, Nakagawa Y (2009) Sonic hedgehog signaling controls thalamic progenitor identity and nuclei specification in mice. J Neurosci 29:4484–4497.

Wang L, Kloc M, Maher E, Erisir A, Maffei A (2019) Presynaptic GABAA Receptors Modulate Thalamocortical Inputs in Layer 4 of Rat V1. Cereb Cortex 29:921–936.

Wang Y, Wang C, Ranefall P, Broussard GJ, Wang Y, Shi G, Lyu B, Wu CT, Wang Y, Tian L, Yu G (2020) SynQuant: an automatic tool to quantify synapses from microscopy images. Bioinformatics 36:1599–1606.

Wells MF, Wimmer RD, Schmitt LI, Feng G, Halassa MM (2016) Thalamic reticular impairment underlies attention deficit in Ptchd1(Y/-) mice. Nature 532:58–63.

Wiesel TN, Hubel DH (1963a) EFFECTS OF VISUAL DEPRIVATION ON MORPHOLOGY AND PHYSIOLOGY OF CELLS IN THE CATS LATERAL GENICULATE BODY. J Neurophysiol 26:978–993.

Wiesel TN, Hubel DH (1963b) SINGLE-CELL RESPONSES IN STRIATE CORTEX OF KITTENS DEPRIVED OF VISION IN ONE EYE. J Neurophysiol 26:1003–1017.

Yu Q, Zhang P, Qiu J, Fang F (2016) Perceptual Learning of Contrast Detection in the Human Lateral Geniculate Nucleus. Curr Biol 26:3176–3182.

Yücel YH, Zhang Q, Weinreb RN, Kaufman PL, Gupta N (2001) Atrophy of relay neurons in magno-and parvocellular layers in the lateral geniculate nucleus in experimental glaucoma. Investig Ophthalmol Vis Sci 42:3216–3222.

Yusifov R, Tippmann A, Staiger JF, Schlüter OM, Löwel S (2021) Spine dynamics of PSD-95-deficient neurons in the visual cortex link silent synapses to structural cortical plasticity. Proc Natl Acad Sci U S A 118.

Chapter 5

Astrocyte CB1 receptors are required for inhibitory maturation and ocular dominance plasticity in the mouse visual cortex

Rogier Min[1,2,3,*], **Yi Qin**[1], Sven Kerst[1,2,3], Mohammad Hadi Saiepour[1], Mariska van Lier[1], Beat Lutz[4], Giovanni Marsicano[5] and Christiaan N. Levelt[1,6,*]

[1]Department of Molecular Visual Plasticity, Netherlands Institute for Neuroscience, an Institute of the Royal Netherlands Academy of Arts and Sciences, Amsterdam, The Netherlands.

[2]Department of Child Neurology, Amsterdam Leukodystrophy Center, Emma Children's Hospital, Amsterdam University Medical Centers, location Vrije Universiteit Amsterdam, Amsterdam Neuroscience, Amsterdam, The Netherlands.

[3]Department of Integrative Neurophysiology, Center for Neurogenomics and Cognitive Research, Vrije Universiteit Amsterdam, Amsterdam Neuroscience, The Netherlands.

[4]Institute of Physiological Chemistry, University Medical Center of the Johannes Gutenberg University Mainz, Mainz, GermanyNetherlands Institute for Neuroscience

[5]INSERM, U1215 NeuroCentre Magendie, 146 rue Léo Saignat, 33077 Bordeaux Cedex, France

[6]Department of Molecular and Cellular Neuroscience, Center for Neurogenomics and Cognitive Research, Vrije Universiteit Amsterdam, Amsterdam Neuroscience, The Netherlands.

Summary and Introduction

Neuronal circuits are shaped by experience. This happens much more readily in the young compared to the adult brain. The unique learning capacity of the young brain is regulated through postnatal critical periods, during which the ability of neuronal networks to re-wire is greatly enhanced (Hensch, 2005). Endocannabinoids, signaling through the cannabinoid CB1 receptor (CB1R), regulate several forms of neuronal plasticity (Chevaleyre et al., 2006). In the developing neocortex, CB1Rs play a key role in the maturation of inhibitory circuits. For example, interfering with CB1R signaling during development disrupts inhibitory maturation in the prefrontal cortex(Cass et al., 2014). In developing primary visual cortex (V1), endocannabinoid-mediated plasticity at inhibitory synapses regulates the maturation of inhibitory synaptic transmission, shifting synapses from an immature state characterized by strong short-term depression to a mature state with reduced short-term depression (Jiang et al., 2010; Sun et al., 2015). This maturation step correlates with the timing of the critical period. While CB1Rs were originally thought to reside mainly on presynaptic axon terminals, recent studies have highlighted an unexpected role for astrocytic CB1Rs in endocannabinoid mediated plasticity (Navarrete and Araque, 2008; Han et al., 2012; Min and Nevian, 2012). Here, we investigate the impact of genetically removing CB1Rs from interneurons or astrocytes on development of inhibitory synapses and network plasticity of V1. We show that removing CB1Rs from astrocytes interferes with maturation of inhibitory synaptic transmission in V1. In addition, it strongly reduces ocular dominance (OD) plasticity during the critical period. In contrast, removing interneuron CB1Rs leaves these processes intact. Our results reveal an unexpected role of astrocytic CB1Rs in critical period plasticity in V1, and highlight the involvement of glial cells in the plasticity and synaptic maturation of sensory circuits.

Results and discussion

Removal of astrocyte vs interneuron CB1 receptors

Inhibitory synapses in primary visual cortex (V1) undergo a CB1 receptor (CB1R)-dependent maturation step during postnatal development: they shift from an immature state characterized by strong short-term synaptic depression towards a state with reduced short-term depression (Jiang et al., 2010; Sun et al., 2015). This process is complete around P28, corresponding to the peak of the critical period for OD plasticity in mouse (Gordon and Stryker, 1996)10/25/23 6:05:00 PM. Furthermore, inhibitory maturation is absent in full CB1R knockout mice (Sun et al., 2015). CB1Rs are traditionally thought to reside on presynaptic axon terminals. However, the parvalbumin positive fast-spiking interneurons that undergo developmental maturation(Jiang et al., 2010; Huang and Kirkwood, 2020) are thought to express no or only low levels of CB1Rs (Bodor et al., 2005; Hill et al., 2007; Wedzony and Chocyk, 2009). Furthermore, it was previously shown that astrocytes also express CB1Rs (Navarrete and Araque, 2008; Min and Nevian, 2012), which are involved in plasticity of developing sensory circuits (Min and Nevian, 2012). To investigate how removal of CB1Rs from different cell types (astrocytes vs interneurons) affects inhibitory maturation in V1, we made use of conditional knockout mice lacking CB1Rs in either astrocytes or interneurons. We crossed mice containing a floxed CB1R gene (Marsicano et al., 2003) with different Cre-driver lines. For interneuron-specific recombination we used GAD2-Cre mice (Taniguchi et al., 2011), while for astrocyte specific recombination we used GLAST-CreERT2 mice (JAX stock #012586). The resulting mice lacked CB1Rs either in astrocytes (“GLAST-CB1R-KO mice”) or interneurons (“GAD2-CB1R-KO mice”).

Conditional recombination in GLAST-CreERT2 mice requires induction by tamoxifen injection. For our experiments, astrocyte-specific recombination needed to be induced at a young age, before the start of the critical period. A potential problem with early tamoxifen injection may be that recombination occurs in neuronal precursor cells, leading to recombination in neurons. We therefore tested at which age, GLAST-CreERT2 induction was specific for glial cell types. Using a TdTomato Cre-reporter line crossed to GLAST-CreERT2 mice, we found that a single intraperitoneal (ip) tamoxifen injection at P1 indeed resulted in recombination in a small number of neocortical neurons (Fig. 1A). In contrast, a single injection between P3 and P5 resulted in efficient and specific recombination in glial cells, with no neuronal recombination in V1. 80% of V1 astrocytes showed recombination, while 77% of recombined cells were astrocytes (Fig. 1B,C), the rest being

other glial cells (oligodendrocytes, oligodendrocyte precursor cells and NG2 cells; Fig. 1D,E). Because astrocytes are the main glial cell type expressing CB1Rs (Allen Brain Atlas; www.brain-map.org), any phenotypic changes observed in GLAST-CB1R-KO mice that are treated with tamoxifen at P3-5 are most likely due to loss of CB1R expression in astrocytes.

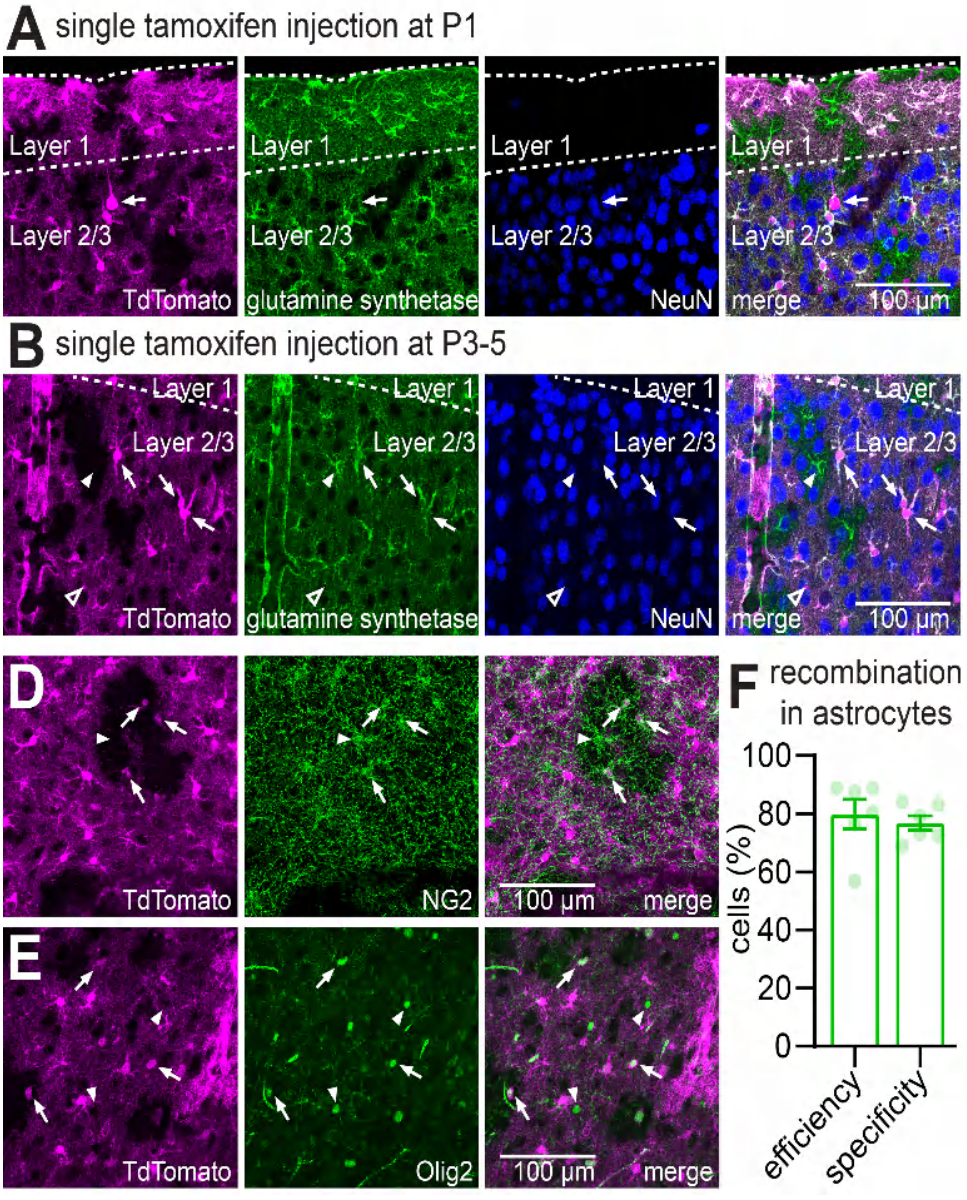

Figure 1. Early astrocytic recombination in GLAST-CreERT2 mice. (A) GLAST-CreERT2 TdTomato mice received a single ip injection of tamoxifen at P1. Slices containing V1 were prepared at P28-35, processed for immunofluorescence imaging and visualized using confocal microscopy. Recombination (indicated by TdTomato expression, magenta) was observed in astrocytes (visualized using a glutamine synthetase antibody, green), but also in sparse neurons (visualized using NeuN antibody, blue). An example neuron with pyramidal morphology is indicated by the arrow. (B) Changing the tamoxifen injection regime to a single injection at P3-5 abolished neuronal recombination in V1, while astrocyte recombination was efficient (~80%). Arrows indicate TdTomato expressing astrocytes, arrowheads indicate TdTomato negative astrocytes. (C,D) Specificity of recombination was high for astrocytes, but some non-neuronal recombination was seen in glial cells positive for NG2 positive cells (C, green, arrows) or Olig2 positive cells (D, green, arrows). Arrowheads indicate TdTomato negative NG2 and Olig2 positive cells. (E) Quantification of efficiency and specificity of recombination in astrocytes in mice receiving a single tamoxifen ip injection at P3-5, based on TdTomato and glutamine synthetase positivity.

Loss of astrocytic CB1Rs interferes with inhibitory synaptic maturation

To investigate how loss of CB1Rs from specific cell types affected inhibitory synaptic maturation we assessed short-term dynamics of inhibitory synapses in acute brain slices of P28-35 mice. Whole cell patch-clamp recordings were made from L2/3 pyramidal neurons, and evoked inhibitory postsynaptic currents (IPSCs) were measured upon repetitive extracellular stimulation (10 pulses at 25 Hz; see methods for recording details). V1 inhibitory synapses onto L2/3 pyramidal neurons normally mature towards a state characterized by less pronounced short-term synaptic depression at P28-35. This inhibitory maturation is absent in full CB1R knockout mice, with inhibitory synapses maintaining an immature state characterized by stronger short-term depression (Sun et al., 2015). We found that short-term dynamics of inhibitory synapses in P28-35 GAD2-CB1R-KO mice did not differ from that in wildtype littermates (Fig. 2A; normalized steady state IPSC amplitude: wildtype: 0.42±0.05, n=16; GAD2-CB1R-KO: 0.45±0.05, n=19; P=0.71; Mann-Whitney test), suggesting normal inhibitory maturation in the absence of interneuron CB1Rs. In contrast, GLAST-CB1R-KO mice showed more pronounced short-term depression when compared to wildtype littermates (Fig. 2B; normalized steady state IPSC amplitude: wildtype: 0.48±0.03, n=11; GAD2-CB1R-KO: 0.33±0.03, n=14; P=0.008; Mann-Whitney test). This suggests that loss of CB1Rs on astrocytes, but not on interneurons, interferes with the maturation of inhibitory synaptic transmission.

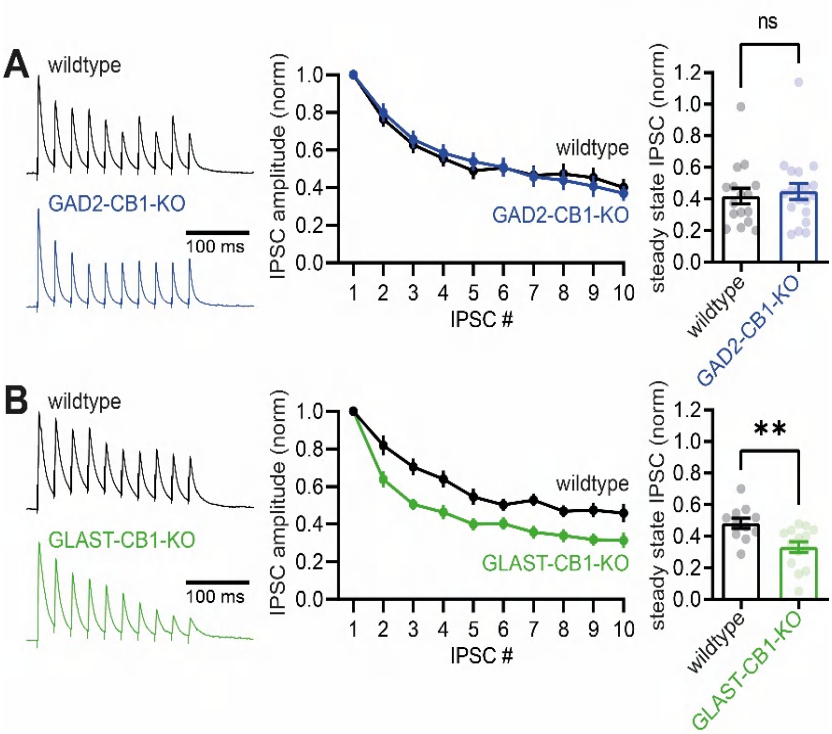

Figure 2. Impaired inhibitory synaptic maturation upon loss of astrocyte CB1 receptors. (A) Left: example traces showing the dynamics of inhibitory synaptic transmission in acute brain slices from GAD2-CB1R-KO mice (blue) and their wildtype littermates (black). Middle: averaged IPSC amplitude normalized to the first, for each of the 10 IPSCs in the train. Right: Steady state IPSC amplitude (averaged normalized amplitude of the last three IPSCs in the train) for all individual recorded neurons (dots). Bars show mean. (B) Same as in A, but for GLAST-CB1R-KO mice (green) and their wildtype littermates (black). Error bars indicate SEM.

Long-term depression of inhibitory synapses is intact upon removal of interneuron or astrocyte CB1Rs

Inhibitory synapses in V1 can undergo endocannabinoid-mediated long-term depression (iLTD) at early developmental stages, but this form of plasticity is lost during maturation. iLTD is blocked by CB1R antagonists, and absent in full CB1R knockout mice (Jiang et al., 2010; Sun et al., 2015). To investigate how iLTD was effected by cell-type specific CB1R removal we prepared acute brain slices from young mice (P14-21), and performed whole cell patch-clamp recordings from L2/3 pyramidal neurons. Evoked IPSCs were recorded for a baseline period of 10 minutes, followed by iLTD induction using a theta-burst protocol (see methods for additional details). In wildtype mice this led to a significant reduction in IPSC amplitude, indicating robust iLTD expression (iLTD: 17.0±2.9%, n=29, IPSC amplitude

baseline vs after iLTD induction: P=0.0002, paired t-test). iLTD was abolished in the presence of the CB1R antagonist AM251 (10 µM; iLTD: 0.0±4.2% iLTD, n=12, IPSC amplitude baseline vs after iLTD induction: P=0.92; % iLTD control vs +AM251: P=0.002, unpaired t-test).

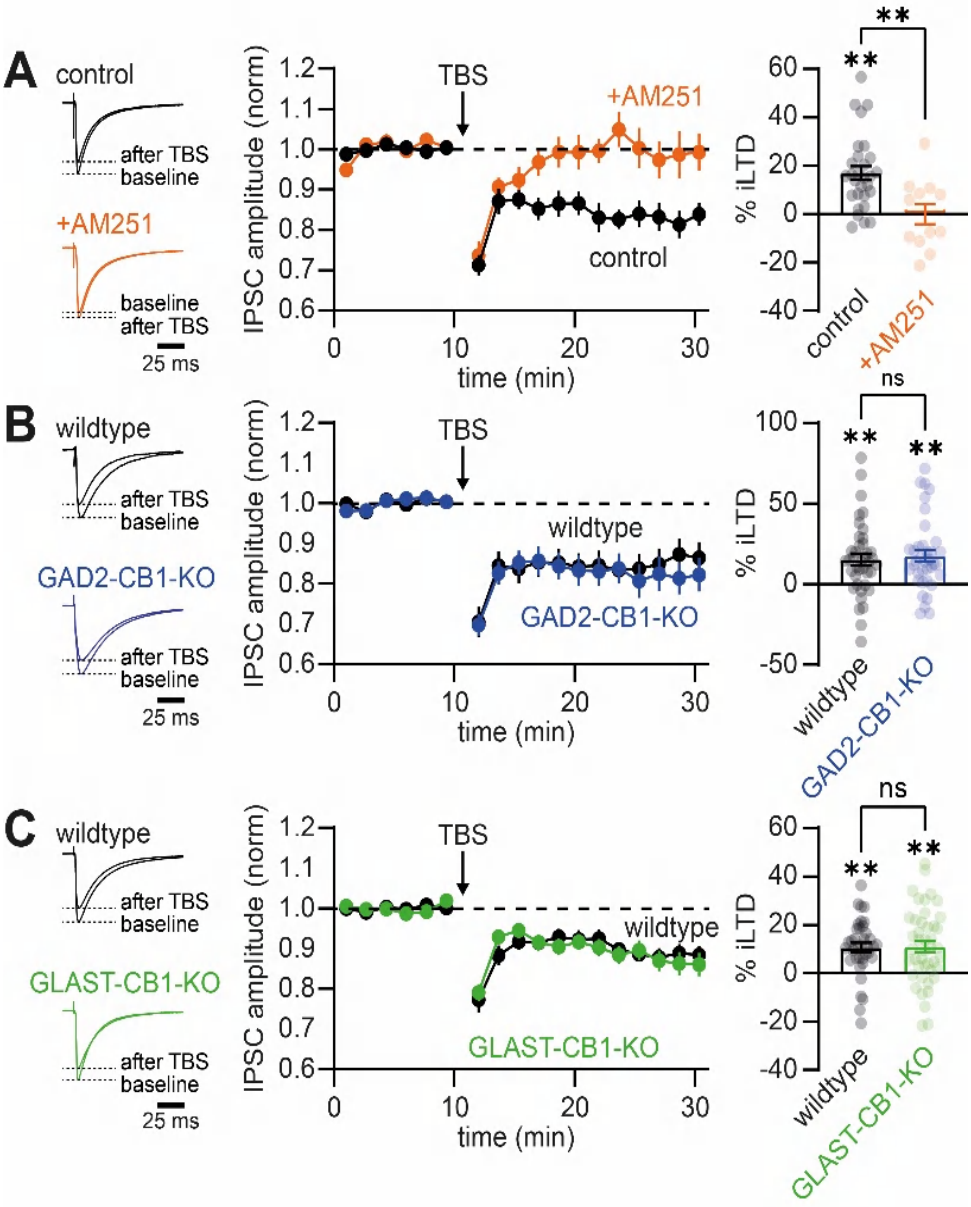

Figure 3. iLTD is unaffected by removal of astrocyte or interneuron CB1 receptors. (A) Left: example traces showing the averaged IPSC during the 10 minutes of baseline recording and 10-20 minutes after iLTD induction by TBS. Black traces are from a control experiment, orange in the presence of the CB1 receptor antagonist AM251.

Middle: Averaged time course of the IPSC amplitude normalized to baseline for all experiments under control conditions (black) and in the presence of AM251 (orange). Right: Averaged amount of iLTD (% reduction of the IPSC amplitude after TBS) for all individual recorded neurons (dots). Bars show mean. (B) Same as in A, but now for GAD2-CB1R-KO mice (blue) and their wildtype littermates (black). (C) Same as in A and B, but now for GLAST-CB1R-KO mice (green) and their wildtype littermates (black). Error bars indicate SEM.

Next, we investigated how iLTD was influenced by cell-type specific removal of CB1Rs. Surprisingly, we found that neither removal of interneuron CB1Rs, nor of astrocyte CB1Rs, affected the magnitude of iLTD (Fig. 3B,C). iLTD did not significantly differ between interneuron CB1R knockouts and wildtype littermates (GAD2-CB1R-KO iLTD: 17.7±3.7%, n=37, IPSC amplitude baseline vs after iLTD induction: P=0.0002, paired t-test; wildtype littermates iLTD: 15.3±3.6% iLTD, n=40, IPSC amplitude baseline vs after iLTD induction: P<0.0001; % iLTD wildtype vs GAD2-CB1R-KO: P=0.65, unpaired t-test; Fig. 3B). The same was true for astrocyte CB1R knockouts (GLAST-CB1R-KO iLTD: 11.1±2.3%, n=44, IPSC amplitude baseline vs after iLTD induction: P<0.0001, paired t-test; wildtype littermates iLTD: 10.7±1.9% iLTD, n=37, IPSC amplitude baseline vs after iLTD induction: P<0.0001; % iLTD wildtype vs GAD2-CB1R-KO: P=0.91, unpaired t-test; Fig. 3B). Therefore, while inhibitory synaptic maturation relies on astrocyte CB1Rs, iLTD surprisingly is independent of both astrocyte and interneuron CB1Rs.

Loss of astrocytic CB1Rs disrupts OD plasticity

The maturation of inhibitory synaptic transmission is known to be critical for the occurrence of OD plasticity during the critical period[1]. Therefore, we assessed OD plasticity in mice in which CB1R expression was disrupted in astrocytes or interneurons. Using optical imaging of intrinsic signal (Heimel et al., 2007), we measured responses to stimulation of the two eyes in the binocular region of V1, calculated the OD index (ODI; see methods), and compared mice that were reared normally (non-deprived) with mice that were monocularly deprived for three days starting around P28 (3 days MD). In wildtype littermates of both GAD2-CB1R-KO mice and GLAST-CB1R-KO mice 3 days MD caused a robust OD shift (GAD2-CB1R littermates: ODI non-deprived: 0.34±0.04, n=5; 3 days MD: 0.07±0.05, n=6; GLAST-CB1R littermates: ODI non-deprived: 0.33±0.04, n=6; 3 days MD 0.02±0.06, n=7; Fig. 4A,B). This OD shift was also observed upon interneuron specific CB1R removal (GAD2-CB1R-KO: ODI non-deprived: 0.31±0.04, n=5; 3 days MD: 0.03±0.05, n=5; Fig. 4A). Statistical analysis yielded no interaction between genotype and molecular deprivation for GAD2-CB1R-KO mice (two-way ANOVA; interaction of genotype with OD shift P=0.93; Tukey's post-hoc test: wildtype non-deprived vs 3 days MD: P=0.002; GAD2-CB1R-KO non-deprived vs 3 days MD: P=0.003; wildtype 3 days MD vs GAD2-CB1R-

KO 3 days MD: *P*=0.95). In contrast, no significant OD shift was observed upon removal of astrocyte CB1Rs (GLAST-CB1R-KO: ODI non-deprived: 0.31±0.04, n=7; 3 days MD: 0.22±0.04, n=8; two-way ANOVA; interaction of genotype with OD shift *P*=0.022; Tukey's post-hoc test: wildtype non-deprived vs 3 days MD: *P*=0.006; GLAST-CB1R-KO non-deprived vs 3 days MD: *P*=0.54; wildtype 3 days MD vs GLAST-CB1R-KO 3 days MD: *P*=0.021; Fig. 4B). Therefore, CB1Rs on astrocytes, not on interneurons, are required for OD plasticity during the critical period.

OD plasticity is disrupted in deep cortical layers upon loss of astrocytic CB1Rs

Previous studies that described effects of pharmacological CB1R blockade on OD plasticity revealed that the effect of acute CB1R blockade on OD plasticity is layer specific, with OD plasticity in layer 2/3 of V1 being sensitive to treatment with a CB1R antagonist, while deeper layers show normal OD plasticity upon CB1R antagonist treatment (Liu et al., 2008; Frantz et al., 2020). To investigate whether the disruption of OD plasticity upon developmental loss of astrocytic CB1Rs was equally layer specific, we performed electrophysiological recordings using laminar probes in GLAST-CB1R-KO mice. Analyzing OD plasticity over all cortical layers confirmed the disruption of OD plasticity that we observed using intrinsic signal optical imaging. Upon removal of astrocyte CB1Rs OD plasticity was still observed, but in significantly reduced from (wildtype: ODI non-deprived: 0.32±0.03, n=162/11; 3 days MD: -0.04±0.03, n=104/7; GLAST-CB1R-KO: non-deprived: 0.31±0.03, n=139/10; 3 days MD: 0.15±0.03, n=121/8; two-way ANOVA; interaction of genotype with OD shift *P*=0.002; Tukey's post-hoc test: wildtype non-deprived vs 3 days MD: *P*<0.0001; GLAST-CB1R-KO non-deprived vs 3 days MD: *P*=0.0006; wildtype 3 days MD vs GLAST-CB1R-KO 3 days MD: *P*<0.0001; Fig. 4C). Next, we specifically looked at OD plasticity in deeper cortical layers, by separately analyzing units in layer 4 and layer 5/6, based on depth. We found that loss of astrocytic CB1Rs reduced OD plasticity in deep cortical layers (Fig. 4D; L4: wildtype: ODI non-deprived: 0.32±0.06, n=33/11; 3 days MD: -0.06±0.06, n=21/7; GLAST-CB1R-KO: non-deprived: 0.25±0.07, n=30/10; 3 days MD: 0.14±0.05, n=24/8; two-way ANOVA; interaction of genotype with OD shift *P*=0.033; L5/6: wildtype: ODI non-deprived: 0.28±0.04, n=69/11; 3 days MD: -0.09±0.05, n=44/7; GLAST-CB1R-KO: non-deprived: 0.31±0.04, n=56/10; 3 days MD: 0.11±0.03, n=56/8; two-way ANOVA; interaction of genotype with OD shift *P*=0.048). Therefore, genetic removal of astrocytic CB1Rs during development has a different and broader effect on OD plasticity than acute pharmacological CB1R blockade.

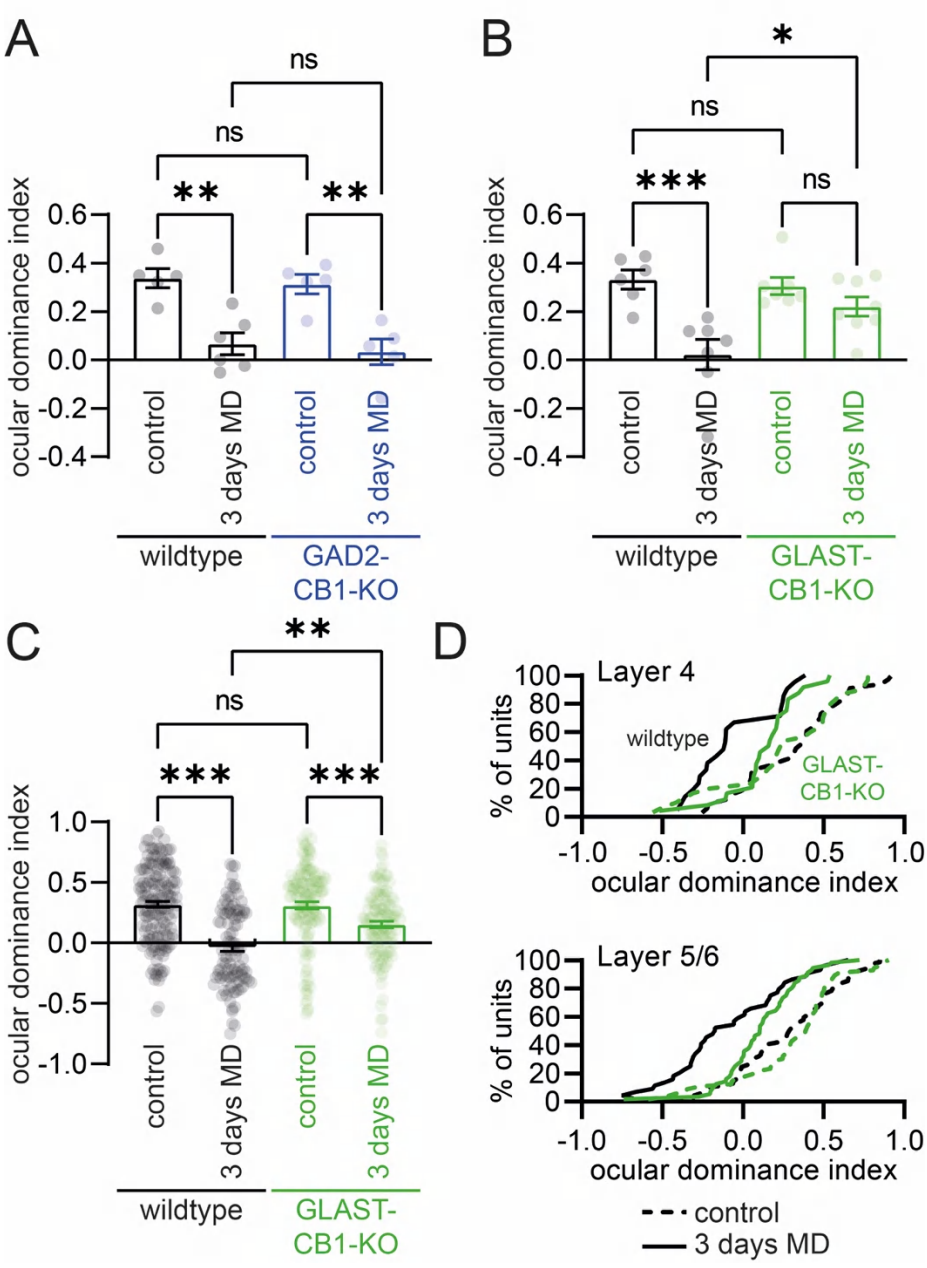

Figure 4. Ocular dominance plasticity is disrupted upon loss of astrocyte CB1 receptors. (A) Summary graphs of the ocular dominance index, as assessed using optical imaging of the intrinsic signal. Data is shown for GAD2-CB1R-KO mice (blue) and their wildtype littermates (black), both under control conditions and after three days of monocular deprivation (3 days MD). Dots indicate recorded ocular dominance index for individual mice, bars show means. (B) Same as in A, but now for GLAST-CB1R-KO mice (green) and their wildtype littermates (black). (C) Same as in A and B, but here ocular dominance index was assessed using *in vivo* electrophysiology. Dots

represent individual single units, bars show means. (D) Cumulative distribution of ocular dominance index against % of units, for deep cortical layers (L4 and L5/6). Dotted lines represent undeprived controls, solid lines represent 3 days monocular deprivation. Green lines show data from GLAST-CB1R-KO mice, black lines from wildtype littermates.

Discussion

In conclusion, we show that astrocytic CB1Rs contribute to the maturation of inhibitory synapses and affect OD plasticity in the developing V1. It is well known that the maturation of inhibitory synapses in V1 is required for the onset of the critical period of OD plasticity (Hensch et al., 1998; Hanover et al., 1999; Fagiolini and Hensch, 2000; Hensch, 2005). Our finding thus supports the idea that the deficit in OD plasticity we observe in astrocytic CB1R deficient mice is caused by deficient maturation of inhibitory synapses affecting critical period onset.

During maturation of V1, inhibitory innervation changes extensively. During the first week after eye opening (p14-p21) the number and size of inhibitory synapses increase resulting in stronger inhibition(Huang et al., 1999). The causal link between inhibitory maturation and opening of the critical period of OD plasticity is well established: In mice with reduced GABA-release due to the absence of GAD65, a protein involved in GABA synthesis, the critical period does not start (Hensch et al., 1998; Fagiolini and Hensch, 2000). Increasing GABAergic transmission in these mice by intraventricular benzodiazepine infusion rescues the phenotype and initiates the critical period (Fagiolini and Hensch, 2000). In addition to the general increase in synaptic strength, synaptic release and short-term depression decrease with development, resulting in more reliable and precise inhibition (Morales et al., 2002; Jiang et al., 2005; Tang et al., 2007). At inhibitory synapses formed by parvalbumin positive fast-spiking interneurons the maturation of inhibitory synaptic strength and dynamics depends on CB1R signaling, since both processes are blocked by CB1R antagonist treatment or by genetic CB1R knockout (Jiang et al., 2010; Sun et al., 2015; Huang and Kirkwood, 2020). This has been puzzling, since parvalbumin positive interneurons express no or only low levels of CB1Rs (Bodor et al., 2005; Hill et al., 2007; Wedzony and Chocyk, 2009). Our findings that inhibitory synaptic transmission is intact upon interneuron CB1R removal, but that it is disrupted when astrocyte CB1Rs are removed, provide an explanation for this apparent discrepancy. Furthermore, we show that interfering with CB1R dependent maturation of inhibition disrupts OD plasticity.

The mechanism underlying CB1R mediated inhibitory synapse maturation is not clear yet. In previous studies, CB1R inactivation resulted in a reduction of both i-LTD and synapse

maturation, and therefore these processes were considered to be causally related (Jiang et al., 2010; Sun et al., 2015). Our observation that in GLAST-CB1R-KO mice inhibitory synapse maturation is affected, while i-LTD is still intact, is puzzling. One possible explanation is that recombination in GLAST-CB1R-KO mice is incomplete, leading to residual CB1R expression in some astrocytes. Experiments with TdTomato reporter mice (Figure 1) reveal recombination in ~80% of astrocytes upon a single early postnatal tamoxifen injection. Since full genetic CB1R removal from an astrocyte requires bi-allelic recombination, it is expected that 60-70% of astrocytes in GLAST-CB1R-KO mice lack CB1Rs. i-LTD induced by strong electrophysiological stimulation of a large number of inhibitory synapses might be resilient to such incomplete CB1R inactivation, with CB1R activation on the remaining astrocytes being sufficient for i-LTD induction. Alternatively, i-LTD could rely on CB1Rs in both inhibitory neurons and astrocytes. The physiological maturation of inhibitory synapses, which would involve molecular mechanisms overlapping with those of i-LTD may then be more sensitive to astrocytic CB1R removal.

Previous work has shown that acute pharmacological blocking of CB1Rs during the critical period reduces OD plasticity. In those experiments, OD plasticity was only affected in the superficial layers, while an OD shift could still be induced in layers 4-6 (Liu et al., 2008; Frantz et al., 2020). LTD of excitatory synapses in layer 2/3 of sensory cortex is dependent on CB1Rs, while excitatory LTD in deeper layers is CB1R independent (Crozier et al., 2007; Banerjee et al., 2009). It is therefore believed that the effect of acute CB1R blockage on OD plasticity is caused by selective interference with e-LTD in layer 2/3. We find that in astrocytic CB1R-deficient animals, OD plasticity is reduced in all layers of V1. This suggests that CB1Rs regulate OD plasticity through multiple mechanisms: acutely by mediating LTD at excitatory synapses in layer 2/3 neurons and indirectly by driving the development of inhibitory synapses in all cortical layers (Sun et al., 2015). We do not know whether inactivating CB1Rs in astrocytes will also acutely affect OD plasticity by an acute effect on excitatory LTD. But several studies have shown that astrocyte CB1Rs can regulate plasticity at excitatory synapses (Min and Nevian, 2012), for instance by driving D-serine release necessary for NMDA receptor activation (Robin et al., 2018). One would need to inactivate CB1Rs in astrocytes at a later age to dissociate developmental and acute astrocyte CB1R effects.

In GLAST-CB1R-KO mice, astrocyte CB1Rs are not only inactivated in V1, but also in the rest of the brain. We can therefore not rule out that the observed reduction of OD plasticity is caused by the absence of astrocytic CB1Rs in other brain structures, such as the dorsal lateral geniculate nucleus (dLGN) providing input to V1. We have recently

shown that OD plasticity also occurs in the thalamus, and that thalamic synaptic inhibition is essential for OD plasticity both in dLGN and in V1 (Sommeijer et al., 2017). However, in the absence of thalamic inhibition, OD plasticity was predominantly affected after 7 days of MD, while after 3 days of MD, the OD shift was barely reduced (Sommeijer et al., 2017). In our current study, we saw a strong decrease of OD plasticity already after 3 days of MD in GLAST-CB1R mice, suggesting that reduced thalamic inhibition is not the main cause of this plasticity deficit.

Taken together, we show that astrocytic CB1Rs are crucial for critical period plasticity in V1. These findings add to a larger body of research that reveal a role for astrocytes in regulating critical periods in the brain (Ackerman et al., 2021; Ribot et al., 2021). Interestingly, transplanting astrocytes from kittens into V1 of adult cats reopens the critical period of OD plasticity (Muller and Best, 1989). A more recent study found that transplanting immature astrocytes in V1 of adult mice reopens the critical period through degradation of the extracellular matrix (Ribot et al., 2021). Adult astrocytes no longer have the ability to re-open the critical period due to decreased metalloprotease 9 activity. Whether the expression of CB1Rs on immature astrocytes also contributes to their ability to alter critical period plasticity remains unclear. Future experiments involving the transplantation of astrocytes from young mice lacking CB1Rs may provide an answer.

Methods

Animals

Experimental procedures involving mice were in strict compliance with animal welfare policies of the Dutch government and were approved by the Institutional Animal Care and Use Committee of the Netherlands Institute for Neuroscience. Transgenic mice were bred on a C57Bl6/J background. For generation of conditional CB1R knockout mice, mice homozygous for a loxP-site flanked CB1R gene (Marsicano et al., 2003) and heterozygous for either Gad2-IRES-Cre (GAD2-Cre mice; Jax Stock No: 019022) (Taniguchi et al., 2011) or GLAST-CreERT2 (Jax Stock No: 012586) were bred. To assess efficacy and specificity of recombination in GLAST-CreERT2 mice these were crossed with ROSA-TdTomato reporter mice (Madisen et al., 2010), in which a Cre-dependent transgene encoding the tdTomato fluorescent protein is inserted in the ROSA26 locus (Jax Stock No: 007908). Experiments were performed on mice of either sex. Animals were housed on a 12 h light/dark cycle with unlimited access to standard lab chow and water.

Tamoxifen injection

Mouse pups received a single intraperitoneal (i.p.) tamoxifen injection to induce Cre mediated recombination in the GLAST-CreERT2 line. Tamoxifen was dissolved in corn oil at a final concentration of 5 mg/ml. Dissolving of the tamoxifen was aided by placing the Eppendorf tube in an ultrasonic water bath, heated to 30°C, for ~1 hour. 20-25 µl tamoxifen was injected using a thin insulin needle. To assess specificity and efficacy of recombination injections were performed either at P1 or between P3-P5. For all further experiments, a single injection between P3-P5 was used.

Monocular deprivation

Surgery for monocular deprivation (MD) was performed as follows: Mice were anesthetized using isoflurane (5% induction, 1.5–2% maintenance in 0.7 l/min O2). Edges of the upper and lower eyelids of the right eye (contralateral to the side on which recordings were performed) were carefully removed. Antibiotic ointment (Cavasan) was applied. Eyelids were sutured together with 2–3 sutures using 7.0 Ethilon thread during isoflurane anesthesia. Postoperative lidocaine ointment was applied to the closed eyelid. Eyes were checked for infection or opacity once reopened 3 days later, and only mice with clear corneas were included.

Intrinsic signal optical imaging and electrophysiology

Mice were anesthetized by intraperitoneal injection of urethane (20% solution in saline, 1.2 g/kg body weight), supplemented by a subcutaneous injection of chlorprothixene (2.0 mg/ml in saline, 8 mg/kg body weight). Sometimes a supplement of about 10% of the original dose of urethane was necessary. Injection of anesthetic was immediately followed by a subcutaneous injection of atropine sulfate (50 µg/ml in saline, 1 µg/10g body weight) to reduce secretions from mucous membranes and facilitate breathing. Anesthesia reached sufficient depth after 45–60 min. Body temperature was monitored with a rectal probe and maintained at a temperature at 36.5 °C using a heating pad. The animal was fixated by ear bars with conical tips prepared with lidocaine ointment. A bite rod was positioned behind the front teeth, 4 mm lower than the ear bars. A continuous flow of oxygen was provided close to the nose. For analgesia of the scalp, xylocaine ointment (lidocaine HCl) was applied before resection of a part of the scalp to expose the skull.

OD measurements was performed as previously described (Heimel et al., 2007). In brief, the exposed skull was illuminated with 700 ± 30 nm light and the intensity of reflected light was measured. Responses were acquired with an Imager 3001 system (Optical Imaging, Israel). A gamma corrected computer screen was placed in front of the mouse, covering an area of the mouse visual field ranging from − 15 to 75 degrees horizontally and − 45 to 45 degrees vertically. First the retinotopic representation of V1 was mapped. Full contrast, square wave gratings of 0.05 cycles per degree (cpd), moving at 2 Hz and changing direction every 0.6 s were shown every 9 s for 3 s in a pseudorandomly chosen quadrant while the rest of the screen was a constant gray. Fifteen stimuli in each quadrant were sufficient to construct a robust retinotopic map of V1. To subsequently measure OD, shutters were placed in front of both eyes. Either shutter opened independently at preset intervals, for a period of 6 seconds. After full opening of the shutter, the visual stimuli described above were presented in the upper nasal quadrant of the screen for a period of 3 seconds. Fifty responses to stimulation were recorded for each eye. For quantification, the response of a defined region of interest within the binocular part of V1 (as determined by retinotopic mapping) was normalized to the response seen in a region of reference (ROR) outside of V1, which lacked a stimulus specific response. The negative ratio of ROI over ROR signal was taken, normalized to the stimulus onset and averaged from the first frame after stimulus onset until 2s after stimulus offset. The Ocular Dominance Index (ODI) was calculated as (contralateral response − ipsilateral response)/(contralateral response + ipsilateral response).

For *in vivo* electrophysiology, a craniotomy was prepared over V1, 2.95 mm lateral and 0.45 mm anterior to lambda. Mice were placed in front of a gamma-corrected projector (PLUS U2-X1130 DLP), which projected visual stimuli onto a back-projection screen (Macada Innovision, the Netherlands; 60X42 cm area) positioned 17.5 cm in front of the mouse. One eye was covered with a double layer of black fabric and black tape while neuronal responses to stimulation of the other eye were recorded. Visual stimuli were created with the MATLAB (MathWorks) software package Psychophysics Toolbox 3(Brainard, 1997). The position of the receptive field was determined by displaying white squares (5 degrees) at random locations on a black background. The ODI was calculated by presenting each eye with alternating white and gray full-screen stimuli. Each stimulation lasted 3 seconds. There were 100 repetitions of both white and gray screens. Extracellular recordings from V1 were made using a linear silicon microelectrode (A1x16-5mm-25-177-A16, 16 channels spaced 50 m apart, Neuronexus, USA). Extracellular signals were amplified and bandpass filtered at 500 Hz-10 kHz before being digitized at 24 kHz using a RX5 Pentusa base station (Tucker-Davis Technologies, USA). A voltage thresholder

at 3x standard deviation was used to detect spikes online. Custom-written MATLAB programs (http://github.com/heimel/inVivoTools) were used to analyze the data. We computed the spike - triggered average of the random spare square stimulus for receptive field mapping. The actual position and size of the visual field were calculated and corrected for the distance between the stimulus and the animal. We used the last 500ms of the previous trail as the baseline for each 3 s stimulus-related activity. As a result, we characterized visual responses as the difference between the first 500ms of the stimulus and the mean of the prior stimulus's last 500ms activities. The greatest firing rates in the first 300ms of visual related reactions were regarded the peak visual responses to stimuli. The visual responses were calculated as 300ms average multi-unit responses. ODI was calculated as $\left(R_{contra} - R_{ipsi}\right)/\left(R_{contra} + R_{ipsi}\right)$, where the R_{contra} is the average multi-unit firing rate of the unit when contralateral eye was open and ipsilateral eye was covered; R_{ipsi} is opposite.

Slice electrophysiology

For acute brain slice preparation, animals aged between P14-35 were briefly anesthetized using isoflurane, followed by decapitation. Brains were removed and placed in ice-cold slicing medium. For most experiments sucrose based slicing medium was used, containing (in mM): 212.7 sucrose, 26 NaHCO3, 3 KCl, 1.25 NaH2PO4, 1 CaCl2, 3 MgCl2 and 10 D(+)-glucose (carboxygenated with 5% CO2/95% O2; osmolarity 300-310 mOsm). For some early experiments choline chloride based slicing medium was used, containing (in mM): 110 choline chloride, 7 MgCl2, 0.5 CaCl2, 2.5 KCl, 11.6 Na-ascorbate, 3.10 Na-pyruvate, 1.25 NaH2PO4, 25 D-glucose and 25 NaHCO3 (carboxygenated with 5% CO2/95% O2; osmolarity 300-310 mOsm). Quality of slices and properties of recorded neurons were indistinguishable for both solutions. Coronal slices (350 µm) containing V1 were prepared using a vibratome. Within each slice, the hemispheres were separated with a scalpel at the middle axis to be used for individual recordings. The slices were transferred to a holding chamber and left to recover for at least 30 min at 35°C in carboxygenated artificial cerebrospinal fluid (ACSF), containing (mM): 124 NaCl, 26 NaHCO3, 3 KCl, 1.25 NaH2PO4, 2 CaCl2, 1 MgCl2 and 10 D(+)-glucose (carboxygenated with 5% CO2/95% O2; osmolarity 300-310 mOsm). After recovery the holding chamber was moved to room temperature and slices were kept until recording (up to 8 hours after slice preparation).

For recording, slices were transferred to the stage of an upright microscope, where they were continuously perfused with heated (30-32°C) ACSF. NMDA receptor and AMPA receptor mediated glutamatergic synaptic responses were blocked by addition of D-AP5 (50 µM) and DNQX (10 µM) to the recording ACSF. Whole cell patch-clamp recordings from

pyramidal neurons in Layer 2/3 of V1 were made using a Multiclamp 700B amplifier in voltage clamp mode and PClamp software (Molecular Devices, USA). Cells were patched with borosilicate glass electrodes with tip resistances of ~3.5 MOhm, and filled with intracellular solution containing (mM): 120 CsCl, 8 NaCl, 10 HEPES, 2 EGTA, 10 Na-phosphocreatine, 4 Mg-ATP, 0.5 Na-GTP and 5 QX-314 (pH: 7.4; osmolarity ~285 mOsm). IPSCs were evoked with an ACSF filled glass electrode with a broken tip or with a concentric bipolar stimulation electrode, placed in Layer 4. Intensity of the stimulation pulse was adjusted to obtain a reliable and stable IPSC response.

For experiments in which iLTD was evoked, IPSCs were evoked every 20 seconds until a stable baseline was established. Next, iLTD was induced using theta burst stimulation (TBS), consisting of 8-10 thetaburst epochs delivered every 5 seconds. Each theta-burst epoch consisted of 10 trains of 5 pulses at 100 Hz, with the trains being delivered at 5 Hz (adapted from[4,5]). In a small subset of experiments, the strength of extracellular stimulation was doubled during TBS delivery. Because this did not affect the magnitude or dynamics of iLTD, all experiments were grouped for final analysis. AM251 was diluted in DMSO, and the stock solution was added to ACSF to obtain a final concentration of 10 µM (final DMSO concentration: 0.1%).

IPSC amplitude was analysed using custom scripts in IGOR pro (WaveMetrics, USA). For iLTD analysis, magnitude of iLTD was determined by comparing the IPSC amplitude during the 10 minute baseline to the IPSC amplitude 10-20 minutes after TBS. Recordings were excluded if the IPSC amplitude differed >12.5% between the first and the last 6 responses of the baseline, if input resistance increased >25% between baseline and iLTD window, if access resistance increased to >20 MOhm, or if leak current reached lower than -500 pA.

Immunohistochemistry

Mice were anesthetized with an overdose of pentobarbital (100 mg/kg i.p.), followed by transcardial perfusion with 4% paraformaldehyde (PFA) in phosphate buffered saline (PBS). Brains were isolated and post-fixated for >2 hours in PFA at 4°C. After changing to PBS, coronal slices (50 µm thickness) were prepared. Slices were incubated for 2 hours in 500 µl blocking solution (0.1% Triton X-100, 5% NGS in PBS) on a rotary shaker at room temperature. Afterwards, slices were incubated with primary antibody containing solution and left overnight at 4°. The next day primary antibody solution was discarded, and slices were washed three times for 10 min at room temperature on the rotary shaker with 500

µl of washing solution (0.1% Tween in PBS). 250 µl of secondary antibody solution was added per well and slices were incubated for 1 h at room temperature on the rotary shaker. Next, slices were again washed three times for 10 min at room temperature on the rotary shaker with washing solution. Stained slices were mounted on glass slides using mowiol. The following antibodies were used: Glutamine Synthetase (monoclonal mouse, MAB302, Merck Millipore, USA), NeuN (monoclonal mouse, 1:1000, MAB377, Merck Millipore, USA), NG2 (polyclonal rabbit, 1:250, AB5320, Merck Millipore, USA) and Olig2 (monoclonal mouse, 1:250, MABN50, Merck Millipore, USA). Secondary antibody conjugated with Alexa-488 was used (1:250 or 1:500, ThermoFisher, USA). Imaging of the immunostained sections was done using a Leica TCS SP5 Confocal microscope (Leica, Germany).

Statistics

Data representation and statistical analysis were performed using GraphPad Prism 9.0 (GraphPad Software, USA). The used tests are indicated in the text. Statistically significant differences were defined as $P \leq 0.05$. Data are represented as mean ± SEM.

References

Ackerman SD, Perez-Catalan NA, Freeman MR, Doe CQ (2021) Astrocytes close a motor circuit critical period. Nature 592:414–420.

Banerjee A, Meredith RM, Rodriguez-Moreno A, Mierau SB, Auberson YP, Paulsen O (2009) Double dissociation of spike timing-dependent potentiation and depression by subunit-preferring NMDA receptor antagonists in mouse barrel cortex. Cereb Cortex 19:2959–2969.

Bodor AL, Katona I, Nyiri G, Mackie K, Ledent C, Hajos N, Freund TF (2005) Endocannabinoid signaling in rat somatosensory cortex: laminar differences and involvement of specific interneuron types. J Neurosci 25:6845–6856.

Brainard DH (1997) The Psychophysics Toolbox. Spat Vis 10:433–436.

Cass DK, Flores-Barrera E, Thomases DR, Vital WF, Caballero A, Tseng KY (2014) CB1 cannabinoid receptor stimulation during adolescence impairs the maturation of GABA function in the adult rat prefrontal cortex. Mol Psychiatry 19:536–543.

Chevaleyre V, Takahashi KA, Castillo PE (2006) Endocannabinoid-mediated synaptic plasticity in the CNS. Annu Rev Neurosci 29:37–76.

Crozier RA, Wang Y, Liu CH, Bear MF (2007) Deprivation-induced synaptic depression by distinct mechanisms in different layers of mouse visual cortex. Proc Natl Acad Sci U S A 104:1383–1388.

Fagiolini M, Hensch TK (2000) Inhibitory threshold for critical-period activation in primary visual cortex. Nature 404:183–186.

Frantz MG, Crouse EC, Sokhadze G, Ikrar T, Stephany CE, Nguyen C, Xu X, McGee AW (2020) Layer 4 Gates Plasticity in Visual Cortex Independent of a Canonical Microcircuit. Curr Biol 30:2962-2973 2965.

Gordon JA, Stryker MP (1996) Experience-dependent plasticity of binocular responses in the primary visual cortex of the mouse. J Neurosci 16:3274–3286.

Han J, Kesner P, Metna-Laurent M, Duan T, Xu L, Georges F, Koehl M, Abrous DN, Mendizabal-Zubiaga J, Grandes P (2012) Acute cannabinoids impair working memory through astroglial CB1 receptor modulation of hippocampal LTD. Cell 148:1039–1050.

Hanover JL, Huang ZJ, Tonegawa S, Stryker MP (1999) Brain-derived

neurotrophic factor overexpression induces precocious critical period in mouse visual cortex. J Neurosci 19, RC40.

Heimel JA, Hartman RJ, Hermans JM, Levelt CN (2007) Screening mouse vision with intrinsic signal optical imaging. Eur J Neurosci 25:795–804.

Hensch TK (2005) Critical period plasticity in local cortical circuits. Nat Rev Neurosci 6:877–888.

Hensch TK, Fagiolini M, Mataga N, Stryker MP, Baekkeskov S, Kash SF (1998) Local GABA circuit control of experience-dependent plasticity in developing visual cortex. Science 282:1504–1508.

Hill EL, Gallopin T, Ferezou I, Cauli B, Rossier J, Schweitzer P, Lambolez B (2007) Functional CB1 receptors are broadly expressed in neocortical GABAergic and glutamatergic neurons. J Neurophysiol 97:2580–2589.

Huang S, Kirkwood A (2020) Endocannabinoid Signaling Contributes to Experience-Induced Increase of Synaptic Release Sites From Parvalbumin Interneurons in Mouse Visual Cortex. Front Cell Neurosci 14:571133.

Huang ZJ, Kirkwood A, Pizzorusso T, Porciatti V, Morales B, Bear MF, Maffei L, Tonegawa S (1999) BDNF regulates the maturation of inhibition and the critical period of plasticity in mouse visual cortex. Cell 98:739–755.

Jiang B, Huang S, Pasquale R, Millman D, Song L, Lee HK, Tsumoto T, Kirkwood A (2010) The maturation of GABAergic transmission in visual cortex requires endocannabinoid-mediated LTD of inhibitory inputs during a critical period. Neuron 66:248–259.

Jiang B, Huang ZJ, Morales B, Kirkwood A (2005) Maturation of GABAergic transmission and the timing of plasticity in visual cortex. Brain Res Brain Res Rev 50:126–133.

Liu CH, Heynen AJ, Shuler MG, Bear MF (2008) Cannabinoid receptor blockade reveals parallel plasticity mechanisms in different layers of mouse visual cortex. Neuron 58:340–345.

Madisen L, Zwingman TA, Sunkin SM, Oh SW, Zariwala HA, Gu H, Ng LL, Palmiter RD, Hawrylycz MJ, Jones AR (2010) A robust and high-throughput Cre reporting and characterization system for the whole mouse brain. Nat Neurosci 13:133–140.

Marsicano G, Goodenough S, Monory K, Hermann H, Eder M, Cannich A, Azad SC, Cascio MG, Gutierrez SO, Stelt M (2003) CB1 cannabinoid receptors and on-demand

defense against excitotoxicity. Science 302:84–88.

Min R, Nevian T (2012) Astrocyte signaling controls spike timing-dependent depression at neocortical synapses. Nat Neurosci 15:746–753.

Morales B, Choi SY, Kirkwood A (2002) Dark rearing alters the development of GABAergic transmission in visual cortex. J Neurosci 22:8084–8090.

Muller CM, Best J (1989) Ocular dominance plasticity in adult cat visual cortex after transplantation of cultured astrocytes. Nature 342:427–430.

Navarrete M, Araque A (2008) Endocannabinoids mediate neuron-astrocyte communication. Neuron 57:883–893.

Ribot J, Breton R, Calvo CF, Moulard J, Ezan P, Zapata J, Samama K, Moreau M, Bemelmans AP, Sabatet V (2021) Astrocytes close the mouse critical period for visual plasticity. Science 373:77–81.

Robin LM, Cruz JF, Langlais VC, Martin-Fernandez M, Metna-Laurent M, Busquets-Garcia A, Bellocchio L, Soria-Gomez E, Papouin T, Varilh M (2018) Astroglial CB1 Receptors Determine Synaptic D-Serine Availability to Enable Recognition Memory. Neuron 98:935-944 935.

Sommeijer JP, Ahmadlou M, Saiepour MH, Seignette K, Min R, Heimel JA, Levelt CN (2017) Thalamic inhibition regulates critical-period plasticity in visual cortex and thalamus. Nat Neurosci 20:1715–1721.

Sun W, Wang L, Li S, Tie X, Jiang B (2015) Layer-specific endocannabinoid-mediated long-term depression of GABAergic neurotransmission onto principal neurons in mouse visual cortex. Eur J Neurosci 42:1952–1965.

Tang AH, Chai Z, Wang SQ (2007) Dark rearing alters the short-term synaptic plasticity in visual cortex. Neurosci Lett 422:49–53.

Taniguchi H, He M, Wu P, Kim S, Paik R, Sugino K, Kvitsiani D, Fu Y, Lu J, Lin Y (2011) A resource of Cre driver lines for genetic targeting of GABAergic neurons in cerebral cortex. Neuron 71:995–1013.

Wedzony K, Chocyk A (2009) Cannabinoid CB1 receptors in rat medial prefrontal cortex are colocalized with calbindin- but not parvalbumin- and calretinin-positive GABA-ergic neurons. Pharmacol Rep 61:1000–1007.

Chapter 6

Discussion

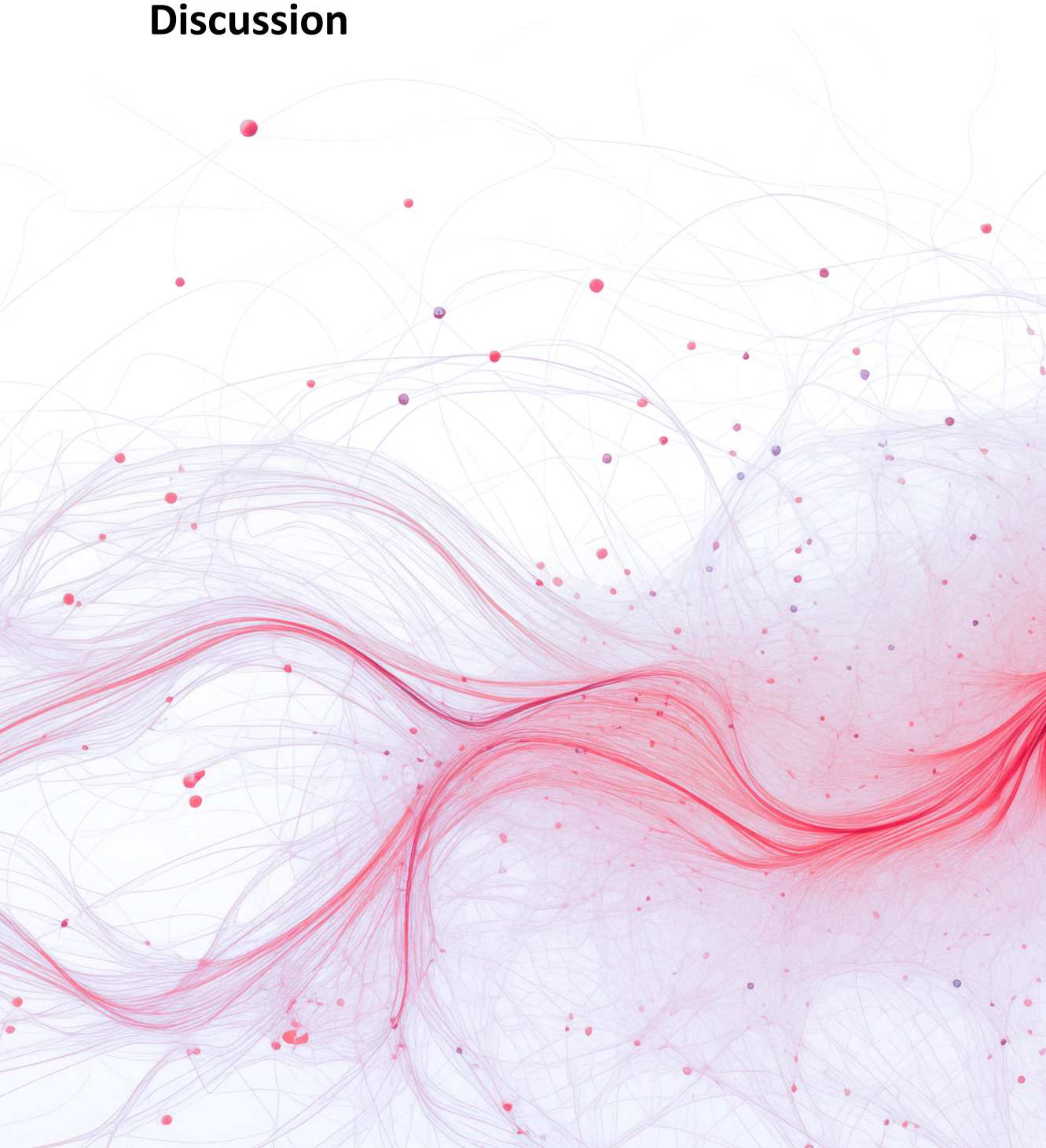

Proper neural firing pattern in CTC is essential for arousal level and spindle

In Chapter 2, we found that a low dose of ketamine induces a decrease in spindle activity in the CTC system and an increase in gamma and higher frequency oscillations. These results are in line with previous arousal-promoting effects of ketamine detected in awake, freely moving animals[1–3]. Additionally, these activity patterns are reminiscent of oscillatory activity during natural REM sleep[4]. Previous researchers have suggested that REM sleep and especially dreaming are natural forms of psychosis[5–9]. The ketamine-induced desynchronized state we observe may thus be interpreted as a pathological REM-sleep-like arousal level.

In thalamic neurons, the burst-firing mode is a reliable hallmark of sleep oscillations. During sleep, membrane hyperpolarization causes the deinactivation of T-type calcium channels. Subsequent depolarization of the neuron, caused by synaptic inputs, then results in burst firing[10]. Since ketamine increases the arousal level of the animal, the cortical and thalamic neurons are expected to be less hyperpolarized. This is thus expected to result in less burst firing and more AP firing, which is exactly what we observed: in the ketamine condition, the single AP density is substantially increased in TC and TRN neurons. Also, the interaction between TC and TRN neurons and intrinsic properties of TRN are key to generate thalamic spindle activities[11,12]. Therefore, disrupting the firing mode of these neurons is expected to cause deficits in spindle oscillation, which is what we demonstrated in chapter 2. Interestingly, disrupted T-type calcium channel activity may be involved in schizophrenia[13]. Ketamine may mimic this effect by causing the membrane potential to be less hyperpolarized, thus keeping the T-type calcium channels in an inactivated state.

Since we found that both TC and TRN neurons switch from burst to tonic AP firing upon ketamine administration, it is possible that these effects are caused by a common input that contributes to sustained excitation and depolarization of both regions. This source may well be cortical feedback, as TRN and TC neurons are innervated by axonal branches from the same CT neurons[14,15]. Since cortical GABAergic interneurons are highly sensitive to NMDA receptor antagonists[16], CT neurons may become disinhibited in the presence of ketamine. Thus, the sustained thalamic gamma hyperactivity[15,17,18] and increased gamma-frequency of TRN cells[19,20] induced by ketamine, may be an indirect effect caused by disinhibition of CT neurons innervating both TRN and TC cells.

In conclusion, we find that ketamine can induce changes in arousal levels and decrease spindle activity, possibly due to alterations in the firing pattern within the strongly reciprocally connected CTC system.

Disrupted sensory information from local to network

In the preceding section, we explored the impact of ketamine on the cortico-thalamo-cortical (CTC) network under baseline conditions. Previous research on human subjects has shown that gamma activity increases in two distinct components, early and late, during perceptual tasks[21]. This suggests that the sensory perception process may consist of both early (<200ms) and late (>200ms) stages, with different cortical areas involved in each stage[22–24]. However, the dynamics of the CTC network during the late stage of perception remain poorly understood in psychotic disorders. Therefore, in Chapter 3, we investigated the effects of ketamine on the late stage of sensory responses during sedation.

We first demonstrated that ketamine increases the baseline thalamic beta (17-29 Hz) and gamma (30-80 Hz) oscillatory activity at all recorded cortical and thalamic sites (VPM, POM, layer VI of somatosensory cortex, and frontoparietal somatosensory cortex), while decreasing the sensory-induced gamma and beta activity. Since induced activity is defined as the relative response (absolute response minus baseline activity) and contains sensory information, our finding implies that the sensory information may be submerged in the abnormally high background noise.

Furthermore, it is worth noting that schizophrenia patients exhibit a similar reduction in beta/gamma-frequency activity during the late stages of perception, which is linked to performance deficits in a perception task[25]. Earlier research has also reported that NMDA receptor agonists decrease the signal-to-noise ratio during the first stage of perception (<200ms)[17,26–28]. Since we discovered a similar deficit in the late stage, the disruption of sensory information induced by ketamine may be long-lasting.

After finding a reduction in the signal-to-noise ratio in the ketamine condition, which could potentially impair sensory information processing, we employed multi-scale entropy (MSE) analysis to quantify changes in information. MSE is an information-theoretic index that estimates the complexity of signal information. In mathematical information theory developed by Claude Shannon, the term "complexity of information" or "entropy" can be understood as the "randomness" of a signal. Thus, increased entropy can be interpreted

as an increase in the randomness of the signal, with maximal entropy being achieved in a truly random signal[29].

Our MSE results demonstrate that neural activity in VPM and layer 6 of the somatosensory cortex exhibited increased complexity following ketamine administration. This finding is consistent with previous studies of schizophrenia patients that observed increased MSE of EEG[30]. Furthermore, clinical studies have found that medication-free patients with higher levels of positive symptoms tend to display higher levels of complexity in EEG[31]. Given that increased entropy or complexity can be interpreted as an increase in the randomness of a signal[29], our MSE results suggest that ketamine administration introduced more noise into the system.

Additionally, we observed that ketamine reduced functional connectivity (coherence) between layer 6 and VPM, but we did not find any changes in the connectivity between layer 6 - POm and VPM - POm. Taken together with the finding that MSE increased upon ketamine treatment, this result may indicate that information transfer is less efficient due to higher noise levels in the system.

It is worth noting that the late period of perception we focused on overlaps with the post-inhibitory rebound activity period. This suggests that the abnormal late-stage activity we observed may reflect deficits in post-inhibitory rebound activity. In the thalamus, this rebound excitation is caused by a low-threshold calcium-independent potential that leads to burst firing[32–36]. Therefore, the impairment of rebound activity could result from abnormal burst firing. Our results of the ketamine state may be due to ketamine interrupting the firing pattern of the thalamus. Notably, burst firing in the thalamocortical (TC) pathway may serve as an initiation signal for perception[37,38]. Thus, impairment of burst firing could lead to perception dysfunction.

In addition, our findings in Chapter 2 revealed that ketamine converts neurons from burst to tonic firing, suggesting that the information deficits (signal-to-noise ratio, MSE) might share the same mechanism as described in Chapter 3. The timing of neural firing that carries information is altered by ketamine.

In conclusion, Chapters 2 and 3 demonstrated that ketamine exerts a persistent depolarizing pressure on the membrane potential of TC and thalamic reticular nucleus (TRN) neurons, which is expected to disrupt the firing pattern associated with sensory-

perceptual processes and spindle activities. This suggests that a similar mechanism may exist in patients with schizophrenia symptoms.

Thalamic inhibition regulates plasticity in the CTC network

In Chapter 4, we demonstrate that synaptic inhibition is essential for OD plasticity in dLGN and V1 of adult mice. Although the mechanism behind it is not clear, we notice that dLGN neurons in mice lacking thalamic synaptic inhibition ("KO mice") attenuate more strongly than in wild-type mice. Combined with previous results in KO mice obtained during the critical period, which also showed transient thalamic responses[39], it is possible that this change in the firing properties of thalamic neurons alters spike-timing dependent plasticity. This could affect OD plasticity in both dLGN and V1.

Due to the absence of synaptic inhibition in the thalamus, the thalamocortical (TC) neurons may be in a more depolarized state. This could cause TC neurons in KO mice to have more tonic than burst mode firing. However, there may also be a paradoxical effect: reduced fast synaptic inhibition may cause stronger dLGN activation, resulting in stronger activation of TRN, and consequently, stronger GABA-release in dLGN. This, in turn, can activate extrasynaptic GABA(B) receptors which are slower and cause stronger an longer-lasting inhibition of TC neurons. It is thus possible that in the absence of thalamic synaptic inhibition, dLGN is dominated by burst firing. Currently, experiments are being performed to understand which of the two scenarios apply, and how information processing is affected in the absence of synaptic thalamic inhibition.

We also assessed how corticothalamic (CT) feedback affected the OD shift in dLGN. After inducing OD plasticity, we silenced primary visual cortex (V1) during the recordings of eye-specific responses in dLGN. We found that silencing V1, and thus CT feedback to dLGN, does not affect the OD shift in dLGN of adult mice. This result is in accordance with previous work[40]. Feedback from V1 to dLGN can result in increased dLGN responses, but V1 to TRN feedback may instead result in dLGN inhibition. Previous studies using optogenetics to activate layer 6 neurons in the primary visual cortex (V1) have shown that feedback from V1 suppresses responses in dLGN[41–43]. However, these effects vary depending on the strength and frequency of stimulation. In most studies in which V1 is silenced, the average strength of dLGN responses in not reduced, suggesting that excitatory and (indirect) inhibitory feedback from V1 to dLGN are balanced.

We observed that in KO mice lacking thalamic synaptic inhibition, dLGN responses to the ipsilateral eye were selectively reduced upon silencing of V1. This suggests that V1 feedback predominantly strengthens dLGN responses to the ipsilateral eye in these mice. A possible explanation for this is that V1 does not only receive ipsilateral eye input directly from dLGN, but also indirectly through callosal connections from contralateral V1. These two sources of ipsilateral eye inputs to V1 may result in relatively stronger ipsilateral eye feedback to dLGN. With reduced inhibition in dLGN, the effect of V1 silencing may thus affect ipsilateral eye responses in dLGN than responses to the contralateral eye.

Interestingly, during the critical period, we do find an effect of V1 feedback on the OD shift in dLGN. Like in adult KO mice, silencing V1 predominantly affects dLGN responses to the ipsilateral eye. Possibly, during the critical period, inhibition in dLGN is weaker (like it is in V1). Notably, an experience-dependent retinogeniculate refinement also takes place in this period, resulting in the reduction of the number of retinal ganglion cells providing inputs to each dLGN TC cell[44–46]. This process also depends on V1 feedback[46,47] and may thus involve the same plasticity mechanisms. If silencing feedback from V1 has an acute effect on binocular responses in dLGN during the critical period, it may have a larger effect on OD plasticity in dLGN when silenced during the entire process. Future research may reveal the importance of recurrent activity in the CTC loop during developmental plasticity.

In conclusion, these results show that the CTC system is much more important for plasticity in the adult and developing cortex than anticipated. This may have important consequences for understanding developmental disorders, as observed changes in cortical organization, function or plasticity may have a thalamic origin and reversely, deficits in thalamic organization may a cortical origin.

Astrocyte CB1 regulates plasticity in V1

In Chapter 5, we investigated how CB1 receptors on astrocytes affect critical period regulation and plasticity in V1. Because maturation of inhibitory innervation is one of the key factors regulating the onset and closure of the critical period[48–51], we first measured the IPSCs from L2/3 pyramidal neurons and found that inhibitory synaptic maturation requires astrocytic CB1 receptors but not interneuron CB1 receptors. We discovered that the absence of astrocytic CB1 receptors did not affect endocannabinoid-mediated long-term depression (iLTD). This is surprising as it is generally believed that the changes in synaptic transmission that were absent in mice lacking astrocytic CB1Rs might be mediated through iLTD[52,53]. A possible explanation is that CB1R deficiency in our mice was

not complete. This partial deficit may not be sufficient to interfere with iLTD induced by powerful stimulation in a slice electrophysiology experiment, but may still interfere with the more protracted synapse maturation process that occurs during normal cortical development. Whether iLTD would be abolished by removing CB1R more efficiently from astrocytes or whether that would also require deletion of CB1R from interneurons remains to be investigated.

We also demonstrated that CB1 receptors in astrocytes, but not in interneurons, are necessary for OD plasticity in V1. Animals lacking astrocytic CB1 receptors exhibited reduced plasticity in all layers of V1. Previous work has shown that acute pharmacological blocking of CB1 receptors also interferes with OD plasticity, but only in the superficial layers of V1[54,55]. It is thought that this plasticity deficit is caused by diminished CB1R-dependent LTD of excitatory connections (eLTD)[56,57]. We believe that the early CB1R removal from astrocytes affects OD plasticity in all layers by interfering with the development of inhibitory synapses[52], which is required for critical period opening.

It is important to note that CB1 receptors in GLAST-CB1R-KO mice are not only inactivated in astrocytes in V1 but in the entire brain. This could include the removal of CB1 receptors in dLGN. In the previous section, we demonstrated that thalamic synaptic inhibition is essential for OD plasticity in both dLGN and V1[58]. Therefore, the CTC network may also contribute to the OD plasticity deficit in mice lacking astrocytic CB1 receptors. However, given that in juvenile mice lacking thalamic synaptic inhibition, OD plasticity in V1 is unaffected during the first 3 days of monocular deprivation[58], while in mice lacking astrocytic CB1 receptors the deficit is already present during that period, it is unlikely that the reduction of thalamic inhibition is the primary cause of this plasticity deficit.

Neural plasticity, CB1 receptors and schizophrenia

Previous studies have shown that structural and functional changes in the brain can occur before the onset of symptoms of schizophrenia. Schizophrenia typically begins in late adolescence and these changes may be a result of pathological neurodevelopmental processes that can lead to psychotic symptoms during adolescence or young adulthood[59].

Adolescence is a critical period in brain development, characterized by fast functional and structural changes. During this time, there is significant synapse pruning, reduction in gray matter, and enhanced myelination in the human frontal brain[60]. Long-term MRI studies

have shown that while gray matter volumes rise during childhood, they begin to fall in the cortex during human adolescence[61].

Neurotransmitter systems, including GABAergic and glutamatergic transmission, also undergo substantial structural alterations, particularly in the frontal lobe. For instance, in the primate GABAergic system, the density of PV-positive axons of basket neurons steadily increases in the cortex[62]. Additionally, mRNAs encoding GABAa receptor α1 and α2 subunits in both human and primate dorsolateral prefrontal cortex (DLPFC) exhibit opposite trajectories, with α1 levels increasing and α2 decreasing[63]. This could be functionally significant, as increased α1 subunit expression is important for generating gamma oscillations in the cortex, which are associated with working memory and perception[64].

In the glutamatergic circuit, the expression of NMDAR subunit GluN3A, which plays a crucial role in unitary NMDAR current conductance, decreases from childhood to adulthood in the human prefrontal cortex[65]. Moreover, previous in vitro mouse studies have shown that the frequency of excitatory postsynaptic currents (EPSCs) on pyramidal output neurons remains relatively stable from adolescence to adulthood in prefrontal cortex (PFC). However, inhibitory postsynaptic currents (IPSCs) increase sharply during this period[66].

Furthermore, research on mouse models of sensory systems has demonstrated that the maturation of the GABAergic inhibitory circuitry is the key to the onset of the critical period. Taken together, the studies underscore the rapid increase in GABAergic innervation of PFC from adolescence to adulthood, possibly leading to a reduction in the general excitation: inhibition (E: I) ratio[67]. This, in turn, may eventually result in an increase in the signal-to-noise ratio by suppressing spontaneous activity[68] and triggering the onset of the critical period.

Besides these anatomical changes, functional maturation of neural oscillations and synchrony also occurs during this period. For example, changes in resting-state oscillatory activity are well known to occur between adolescence and adulthood[69,70]. In adult cortex, resting-state activity is characterized by alpha oscillations and attenuated low and high frequencies. However, in adolescence, the amplitudes in the delta and theta band are reduced, while alpha and beta range are more prominent[69,70]. Also, in perception-related tasks, like the Mooney faces test, the phase synchrony of gamma band oscillations increases gradually from early childhood to adulthood. However, there is a substantial

reduction during late adolescence (even lower than childhood level), suggesting that cortical networks might reorganize during the transition from adolescence to adulthood[71]. Researchers suggest that cortical networks increasingly express high-frequency oscillations along with enhanced long-range synchronization between different regions during the adolescent period[72]. All these studies indicate that the brain goes through a process of functional and anatomical restructuring from adolescence to adulthood. Notably, while these rapid changes are crucial for proper brain function in adulthood, they may also make adolescents more vulnerable to psychotic disorders[73].

During adolescence, the normal development of neural synchrony and cortical networks can be disrupted by various pathological changes. For instance, increased myelination during adolescence can decrease conduction times and reduce the response latency[74]. Thus, abnormal development of white matter pathways can impair the synchrony of neural activity[72]. Additionally, aberrant pruning during this stage may increase synchrony, leading to pathological coactivation of different brain regions and the development of psychotic symptoms[75]. Finally, abnormal modifications in GABAergic neurotransmission can be a potential pathological factor. The increase in gamma oscillations during the transition from adolescence to adulthood, which is closely linked with perceptual and cognitive processes, is likely due to changes in GABAa receptor composition[76]. Therefore, alterations to the GABAergic system during adolescence could potentially affect normal maturation and neural synchrony.

Endocannabinoids are imortant for normal brain maturation during adolescence and may also be involved in the developpment of schizophrenia. Adolescent tetrahydrocannabinol (THC) exposure will significantly impact CB1R expression and functionality. Previous studies demonstrated that high doses of THC decrease CB1R levels in PFC, striatum, hippocampus and thalamus in rat[77]. CB1Rs are widely distributed presynaptically and the activation of endocannabinoids can affect both glutamatergic and GABAergic synapses[78]. In rats, chronic exposure to THC significantly downregulates GAD67 in PFC, the enzyme for GABA synthesis, which could reduce GABAergic level in adulthood[79]. THC exposure during adolescence could also increase the expression of multiple glutamatergic receptors in PFC, such as NMDA receptor subunits GluN2A and GluN2B, and the AMPA receptor GluA1 subunit in rats[80,81]. Notably, these changes can lead to maturation issues in adulthood. For example, GluN2B expression, which normally declines from adolescence into adulthood, remains high due to earlier THC exposure. Moreover, rat adolescent THC exposure also reduces endocannabinoid- mediated LTD in PFC layer 5 pyramidal cells[82] and reduces dendritic spines and arborizations in layer 2/3 pyramidal neurons even after

low-dose THC exposure[83]. This evidence suggests that adolescent THC exposure could lead to deficits in maturation and pruning. These adolescent THC-induced alterations could impact the excitatory-inhibitory balance and affect signal-to-noise ratio and may underlie psychotic events. Notably, previous work demonstrated that the activation of GABAa receptors in PFC can reverse psychotic behavior induced by THC in rat[79]. This might indicate the link between CB1 receptor and schizophrenia could be mediated by the GABAergic system.

Although there is not enough direct cellular evidence to link deficits in CB1R-mediated changes in inhibition with psychotic disorders, many studies indicate that GABAergic dysfunction might be related to schizophrenia. For example, in schizophrenia patients, decreased GAD67 mRNA is observed in PV neurons in PFC[84]. Mice with a homozygous deletion of the *Gad67* gene in PV neurons or a heterozygous deletion in cortical and hippocampal interneurons show schizophrenia-like negative symptoms and reduced inhibitory synaptic transmission[85,86]. The concentration of GABA in the cerebrospinal fluid is also significantly reduced in patients experiencing their first episode of schizophrenia[87].

Until now, it is difficult to tell whether all schizophrenia symptoms are consequences of one decisive factor, but based on all evidence above and my research in this thesis, schizophrenia could result from an abnormal inhibition-excitation balance. This imbalance could start with CB1-related maturation deficits of the GABAergic system, as we described in Chapter 5, which may lead to impairment of neural plasticity and pruning during development. It may become further aggravated to abnormal network connectivity and deficits in information transfer in perception, as we mentioned in Chapter 3. Eventually, all these structural and functional disturbances are behaviorally presented as schizophrenia symptoms.

References

1. Ahnaou, A., Huysmans, H., Van de Casteele, T. & Drinkenburg, W. H. I. M. Cortical high gamma network oscillations and connectivity: a translational index for antipsychotics to normalize aberrant neurophysiological activity. *Transl Psychiatry* **7**, 1–14 (2017).
2. Hakami, T. *et al.* NMDA receptor hypofunction leads to generalized and persistent aberrant γ oscillations independent of hyperlocomotion and the state of consciousness. *PLoS ONE* **4**, e6755 (2009).
3. Pinault, D. N-Methyl d-Aspartate Receptor Antagonists Ketamine and MK-801 Induce Wake-Related Aberrant γ Oscillations in the Rat Neocortex. *Biological Psychiatry* **63**, 730–735 (2008).
4. Kocsis, B. State-dependent increase of cortical gamma activity during REM sleep after selective blockade of NR2B subunit containing NMDA receptors. *Sleep* **35**, 1011–1016 (2012).
5. Dresler, M. *et al.* Neural correlates of insight in dreaming and psychosis. *SLEEP MEDICINE REVIEWS* **20**, 92–99 (2015).
6. Hobson, J. Dreaming as delirium: A mental status analysis of our nightly madness. *SEMINARS IN NEUROLOGY* **17**, 121–128 (1997).
7. Mason, O. & Wakerley, D. The Psychotomimetic Nature of Dreams: An Experimental Study. *SCHIZOPHRENIA RESEARCH AND TREATMENT* **2012**, (2012).
8. Mota, N. B., Resende, A., Mota-Rolim, S. A., Copelli, M. & Ribeiro, S. Psychosis and the Control of Lucid Dreaming. *FRONTIERS IN PSYCHOLOGY* **7**, (2016).
9. Scarone, S. *et al.* The dream as a model for psychosis: An experimental approach using bizarreness as a cognitive marker. *SCHIZOPHRENIA BULLETIN* **34**, 515–522 (2008).
10. Crunelli, V., Cope, D. W. & Hughes, S. W. Thalamic T-type Ca2+ channels and NREM sleep. *CELL CALCIUM* **40**, 175–190 (2006).
11. STERIADE, M., DESCHENES, M., DOMICH, L. & MULLE, C. ABOLITION OF SPINDLE OSCILLATIONS IN THALAMIC NEURONS DISCONNECTED FROM NUCLEUS RETICULARIS THALAMI. *JOURNAL OF NEUROPHYSIOLOGY* **54**, 1473–1497 (1985).
12. STERIADE, M., MCCORMICK, D. & SEJNOWSKI, T. THALAMOCORTICAL OSCILLATIONS IN THE SLEEPING

AND AROUSED BRAIN. *SCIENCE* **262**, 679–685 (1993).

13. Andrade, A. *et al.* A rare schizophrenia risk variant of CACNA1I disrupts Ca(V)3.3 channel activity. *SCIENTIFIC REPORTS* **6**, (2016).
14. BOURASSA, J., PINAULT, D. & DESCHENES, M. CORTICOTHALAMIC PROJECTIONS FROM THE CORTICAL BARREL FIELD TO THE SOMATOSENSORY THALAMUS IN RATS - A SINGLE-FIBER STUDY USING BIOCYTIN AS AN ANTEROGRADE TRACER. *EUROPEAN JOURNAL OF NEUROSCIENCE* **7**, 19–30 (1995).
15. Golshani, P., Liu, X. & Jones, E. Differences in quantal amplitude reflect GluR4-subunit number at corticothalamic synapses on two populations of thalamic neurons. *PROCEEDINGS OF THE NATIONAL ACADEMY OF SCIENCES OF THE UNITED STATES OF AMERICA* **98**, 4172–4177 (2001).
16. Grunze, H. *et al.* NMDA-dependent modulation of CA1 local circuit inhibition. *JOURNAL OF NEUROSCIENCE* **16**, 2034–2043 (1996).
17. Anderson, P. M., Jones, N. C., O'Brien, T. J. & Pinault, D. The N-Methyl D-Aspartate Glutamate Receptor Antagonist Ketamine Disrupts the Functional State of the Corticothalamic Pathway. *CEREBRAL CORTEX* **27**, 3172–3185 (2017).
18. Crandall, S. R., Cruikshank, S. J. & Connors, B. W. A Corticothalamic Switch: Controlling the Thalamus with Dynamic Synapses. *Neuron* **86**, 768–782 (2015).
19. PINAULT, D. & DESCHENES, M. MUSCARINIC INHIBITION OF RETICULAR THALAMIC CELLS BY BASAL FOREBRAIN NEURONS. *NEUROREPORT* **3**, 1101–1104 (1992).
20. PINAULT, D. & DESCHENES, M. VOLTAGE-DEPENDENT 40-HZ OSCILLATIONS IN RAT RETICULAR THALAMIC NEURONS INVIVO. *NEUROSCIENCE* **51**, 245–258 (1992).
21. Rodriguez, E. *et al.* Perception's shadow: Long-distance synchronization of human brain activity. *Nature* **397**, 430–433 (1999).
22. Portella, C. *et al.* Relationship between early and late stages of information processing: An event-related potential study. *Neurology International* **4**, 71–77 (2012).
23. Portella, C. *et al.* Differences in early and late stages of information processing between slow versus fast participants. *International Archives of Medicine* **7**, 49 (2014).
24. Saradjian, A. H., Teasdale, N., Blouin, J. & Mouchnino, L. Independent Early and Late Sensory Processes

for Proprioceptive Integration When Planning a Step. *Cerebral Cortex* **29**, 2353–2365 (2019).

25. Uhlhaas, P. J. Dysconnectivity, large-scale networks and neuronal dynamics in schizophrenia. *Current Opinion in Neurobiology* **23**, 283–290 (2013).
26. Briggs, F. & Usrey, W. M. Emerging views of corticothalamic function. *CURRENT OPINION IN NEUROBIOLOGY* **18**, 403–407 (2008).
27. Homma, N. Y. *et al.* A Role for Auditory Corticothalamic Feedback in the Perception of Complex Sounds. *JOURNAL OF NEUROSCIENCE* **37**, 6149–6161 (2017).
28. Kulikova, S. P. *et al.* Opposite effects of ketamine and deep brain stimulation on rat thalamocortical information processing. *European Journal of Neuroscience* **36**, 3407–3419 (2012).
29. Ahmed, M. U. & Mandic, D. P. Multivariate multiscale entropy: A tool for complexity analysis of multichannel data. *PHYSICAL REVIEW E* **84**, (2011).
30. Takahashi, T. *et al.* Antipsychotics reverse abnormal EEG complexity in drug-naive schizophrenia: A multiscale entropy analysis. *NeuroImage* **51**, 173–182 (2010).
31. Fernandez, A., Gomez, C., Hornero, R. & Jose Lopez-Ibor, J. Complexity and schizophrenia. *PROGRESS IN NEURO-PSYCHOPHARMACOLOGY & BIOLOGICAL PSYCHIATRY* **45**, 267–276 (2013).
32. DESCHENES, M., PARADIS, M., ROY, J. & STERIADE, M. ELECTROPHYSIOLOGY OF NEURONS OF LATERAL THALAMIC NUCLEI IN CAT - RESTING PROPERTIES AND BURST DISCHARGES. *JOURNAL OF NEUROPHYSIOLOGY* **51**, 1196–1219 (1984).
33. Grenier, F., Timofeev, I. & Steriade, M. Leading role of thalamic over cortical neurons during postinhibitory rebound excitation. *Proc. Natl. Acad. Sci. U. S. A.* **95**, 13929–34 (1998).
34. JAHNSEN, H. & LLINAS, R. ELECTROPHYSIOLOGICAL PROPERTIES OF GUINEA-PIG THALAMIC NEURONS - AN INVITRO STUDY. *JOURNAL OF PHYSIOLOGY-LONDON* **349**, 205-(1984).
35. LLINAS, R. THE INTRINSIC ELECTROPHYSIOLOGICAL PROPERTIES OF MAMMALIAN NEURONS - INSIGHTS INTO CENTRAL NERVOUS-SYSTEM FUNCTION. *SCIENCE* **242**, 1654–1664 (1988).
36. Urbain, N. *et al.* Whisking-Related Changes in Neuronal Firing and Membrane Potential Dynamics in the Somatosensory Thalamus of

Awake Mice. *Cell Reports* **13**, 647–656 (2015).

37. Sherman, S. A wake-up call from the thalamus. *NATURE NEUROSCIENCE* **4**, 344–346 (2001).
38. Swadlow, H. & Gusev, A. The impact of `bursting' thalamic impulses at a neocortical synapse. *NATURE NEUROSCIENCE* **4**, 402–408 (2001).
39. Sommeijer, J. P. *et al.* Thalamic inhibition regulates critical-period plasticity in visual cortex and thalamus. *Nature Neuroscience* **20**, 1716–1721 (2017).
40. Jaepel, J., Hübener, M., Bonhoeffer, T. & Rose, T. Lateral geniculate neurons projecting to primary visual cortex show ocular dominance plasticity in adult mice. *Nature Neuroscience* **20**, 1708–1714 (2017).
41. Olsen, S. R., Bortone, D. S., Adesnik, H. & Scanziani, M. Gain control by layer six in cortical circuits of vision. *Nature* **483**, 47–54 (2012).
42. Kirchgessner, M. A., Franklin, A. D. & Callaway, E. M. Context-dependent and dynamic functional influence of corticothalamic pathways to first-And higher-order visual thalamus. *Proceedings of the National Academy of Sciences of the United States of America* **117**, 13066–13077 (2020).
43. Denman, D. J. & Contreras, D. Complex effects on In Vivo visual responses by specific projections from mouse cortical layer 6 to dorsal lateral geniculate nucleus. *Journal of Neuroscience* **35**, 9265–9280 (2015).
44. Hooks, B. M. & Chen, C. Circuitry Underlying Experience-Dependent Plasticity in the Mouse Visual System. *Neuron* **106**, 21–36 (2020).
45. Rompani, S. B. *et al.* Erratum: Different Modes of Visual Integration in the Lateral Geniculate Nucleus Revealed by Single-Cell-Initiated Transsynaptic Tracing (Neuron (2017) 93(4) (767–776.e6) (S0896627317300521) (10.1016/j.neuron.2017.01.028)). *Neuron* **93**, 1519 (2017).
46. Thompson, A., Gribizis, A., Chen, C. & Crair, M. C. Activity-dependent development of visual receptive fields. *Current Opinion in Neurobiology* **42**, 136–143 (2017).
47. Thompson, A. D. A Role for Corticothalamic Feedback in Developmental Refinement at the Retinogeniculate Synapse. (2016).
48. Hensch, T. K. Critical period plasticity in local cortical circuits. *Nat Rev Neurosci* **6**, 877–888 (2005).
49. Fagiolini, M. & Hensch, T. K. Inhibitory threshold for critical-period activation in primary visual

cortex. *Nature* **404**, 183–186 (2000).

50. Hensch, T. K. *et al.* Local GABA circuit control of experience-dependent plasticity in developing visual cortex. *Science* **282**, 1504–1508 (1998).
51. Huang, Z. J. *et al.* BDNF regulates the maturation of inhibition and the critical period of plasticity in mouse visual cortex. *Cell* **98**, 739–755 (1999).
52. Sun, W., Wang, L., Li, S., Tie, X. & Jiang, B. Layer-specific endocannabinoid-mediated long-term depression of GABAergic neurotransmission onto principal neurons in mouse visual cortex. *Eur J Neurosci* **42**, 1952–1965 (2015).
53. Jiang, B. *et al.* The maturation of GABAergic transmission in visual cortex requires endocannabinoid-mediated LTD of inhibitory inputs during a critical period. *Neuron* **66**, 248–259 (2010).
54. Liu, C. H., Heynen, A. J., Shuler, M. G. & Bear, M. F. Cannabinoid receptor blockade reveals parallel plasticity mechanisms in different layers of mouse visual cortex. *Neuron* **58**, 340–345 (2008).
55. Frantz, M. G. *et al.* Layer 4 Gates Plasticity in Visual Cortex Independent of a Canonical Microcircuit. *Curr Biol* **30**, 2962-2973 2965 (2020).
56. Crozier, R. A., Wang, Y., Liu, C. H. & Bear, M. F. Deprivation-induced synaptic depression by distinct mechanisms in different layers of mouse visual cortex. *Proc Natl Acad Sci U S A* **104**, 1383–1388 (2007).
57. Banerjee, A. *et al.* Double dissociation of spike timing-dependent potentiation and depression by subunit-preferring NMDA receptor antagonists in mouse barrel cortex. *Cereb Cortex* **19**, 2959–2969 (2009).
58. Sommeijer, J. P. *et al.* Thalamic inhibition regulates critical-period plasticity in visual cortex and thalamus. *Nat Neurosci* **20**, 1715–1721 (2017).
59. Weinberger, D. R. & Lipska, B. K. Cortical maldevelopment, anti-psychotic drugs, and schizophrenia: a search for common ground. *Schizophr Res* **16**, 87–110 (1995).
60. Arain, M. *et al.* Maturation of the adolescent brain. *Neuropsychiatr Dis Treat* **9**, 449–461 (2013).
61. Gogtay, N. *et al.* Dynamic mapping of human cortical development during childhood through early adulthood. *Proc Natl Acad Sci U S A* **101**, 8174–8179 (2004).
62. Hoftman, G. D. & Lewis, D. A. Postnatal Developmental Trajectories of Neural Circuits in the Primate Prefrontal Cortex:

Identifying Sensitive Periods for Vulnerability to Schizophrenia. *Schizophr Bull* **37**, 493–503 (2011).

63. Fillman, S. G., Duncan, C. E., Webster, M. J., Elashoff, M. & Weickert, C. S. Developmental co-regulation of the β and γ GABAA receptor subunits with distinct α subunits in the human dorsolateral prefrontal cortex. *International Journal of Developmental Neuroscience* **28**, 513–519 (2010).
64. Howard, M. W. *et al.* Gamma Oscillations Correlate with Working Memory Load in Humans. *Cerebral Cortex* **13**, 1369–1374 (2003).
65. Henson, M. A. *et al.* Developmental Regulation of the NMDA Receptor Subunits, NR3A and NR1, in Human Prefrontal Cortex. *Cerebral Cortex* **18**, 2560–2573 (2008).
66. Caballero, A., Orozco, A. & Tseng, K. Y. Developmental regulation of excitatory-inhibitory synaptic balance in the prefrontal cortex during adolescence. *Seminars in Cell & Developmental Biology* **118**, 60–63 (2021).
67. Larsen, B. *et al.* A developmental reduction of the excitation:inhibition ratio in association cortex during adolescence. *Sci Adv* **8**, eabj8750 (2022).
68. Toyoizumi, T. *et al.* A theory of the transition to critical period plasticity: inhibition selectively suppresses spontaneous activity. *Neuron* **80**, 51–63 (2013).
69. Gasser, T., Jennen-Steinmetz, C., Sroka, L., Verleger, R. & Möcks, J. Development of the EEG of school-age children and adolescents II. Topography. *Electroencephalography and Clinical Neurophysiology* **69**, 100–109 (1988).
70. Whitford, T. J. *et al.* Brain maturation in adolescence: Concurrent changes in neuroanatomy and neurophysiology. *Human Brain Mapping* **28**, 228–237 (2007).
71. Uhlhaas, P. J. *et al.* Neural synchrony in cortical networks: history, concept and current status. *Front Integr Neurosci* **3**, 17 (2009).
72. Uhlhaas, P. J. & Singer, W. The development of neural synchrony and large-scale cortical networks during adolescence: relevance for the pathophysiology of schizophrenia and neurodevelopmental hypothesis. *Schizophr Bull* **37**, 514–523 (2011).
73. Spear, L. P. Neurobehavioral Changes in Adolescence. *Curr Dir Psychol Sci* **9**, 111–114 (2000).
74. Salami, M., Itami, C., Tsumoto, T. & Kimura, F. Change of conduction

velocity by regional myelination yields constant latency irrespective of distance between thalamus and cortex. *Proc Natl Acad Sci U S A* **100**, 6174–6179 (2003).

75. Keshavan, M. S. *et al.* Sleep and suicidality in psychotic patients. *Acta Psychiatrica Scandinavica* **89**, 122–125 (1994).
76. Hashimoto, T. *et al.* Protracted developmental trajectories of GABAA receptor α1 and α2 subunit expression in primate prefrontal cortex. *Biological psychiatry* **65**, 1015–1023 (2009).
77. Rubino, T. *et al.* Adolescent exposure to THC in female rats disrupts developmental changes in the prefrontal cortex. *Neurobiol Dis* **73**, 60–69 (2015).
78. Freund, T. F. Interneuron Diversity series: Rhythm and mood in perisomatic inhibition. *Trends Neurosci* **26**, 489–495 (2003).
79. Renard, S. B. *et al.* Unique and Overlapping Symptoms in Schizophrenia Spectrum and Dissociative Disorders in Relation to Models of Psychopathology: A Systematic Review. *Schizophr Bull* **43**, 108–121 (2017).
80. Zamberletti, E. *et al.* Long-term hippocampal glutamate synapse and astrocyte dysfunctions underlying the altered phenotype induced by adolescent THC treatment in male rats. *Pharmacological Research* **111**, 459–470 (2016).
81. Prini, P., Penna, F., Sciuccati, E., Alberio, T. & Rubino, T. Chronic Δ^8-THC Exposure Differently Affects Histone Modifications in the Adolescent and Adult Rat Brain. *Int J Mol Sci* **18**, 2094 (2017).
82. Cuccurazzu, B. *et al.* Adult Cellular Neuroadaptations Induced by Adolescent THC Exposure in Female Rats Are Rescued by Enhancing Anandamide Signaling. *Int J Neuropsychopharmacol* **21**, 1014–1024 (2018).
83. Miller, M. L. *et al.* Adolescent exposure to Δ9-tetrahydrocannabinol alters the transcriptional trajectory and dendritic architecture of prefrontal pyramidal neurons. *Mol Psychiatry* **24**, 588–600 (2019).
84. Blum, B. P. & Mann, J. J. The GABAergic system in schizophrenia. *International Journal of Neuropsychopharmacology* **5**, 159–179 (2002).
85. Kolata, S. M. *et al.* Neuropsychiatric Phenotypes Produced by GABA Reduction in Mouse Cortex and Hippocampus. *Neuropsychopharmacol.* **43**, 1445–1456 (2018).

86. Fujihara, K. *et al.* Glutamate Decarboxylase 67 Deficiency in a Subset of GABAergic Neurons Induces Schizophrenia-Related Phenotypes. *Neuropsychopharmacol* **40**, 2475–2486 (2015).

87. Orhan, F. *et al.* CSF GABA is reduced in first-episode psychosis and associates to symptom severity. *Mol Psychiatry* **23**, 1244–1250 (2018).

Summary

The work presented in this thesis aimed at investigating the function and mechanism of corticothalamic-thalamocortical network in schizophrenia and experience-dependent plasticity, further discussed their possible connection.

In Chapter 2, we investigated the effects of ketamine on the corticothalamic circuit (CTC) system. The study found that a low dose of ketamine caused a decrease in spindle activity in the CTC system and an increase in gamma and higher frequency oscillations. These activity patterns are similar to those seen during natural REM sleep and may be interpreted as a pathological REM-sleep-like arousal level. The study also found that ketamine caused thalamic neurons to switch from burst-firing to tonic AP firing, which possibly disrupted the firing mode of these neurons and caused deficits in spindle oscillation. This effect may be caused by the less hyperpolarized membrane potential of the neurons, which keeps the T-type calcium channels in an inactivated state. Furthermore, the study suggests that the sustained thalamic gamma hyperactivity induced by ketamine may be an indirect effect caused by disinhibition of cortical neurons innervating both thalamic reticular nucleus (TRN) and thalamocortical (TC) cells. Overall, the study concludes that ketamine can induce changes in arousal levels and decrease spindle activity, possibly due to changes in the firing pattern in the CTC system.

In Chapter 3, we investigated the effects of ketamine on the late stage of sensory responses during sedation. The study found that ketamine increased the baseline thalamic beta and gamma oscillatory activity while decreasing the sensory-induced gamma and beta activity. The disruption of sensory information induced by ketamine may be long-lasting and impair sensory information processing dude to low signal noise ratio. The study used multi-scale entropy (MSE) analysis to quantify changes in information and found that neural activity in VPM and layer 6 somatosensory cortex exhibited increased complexity following ketamine administration. This result may indicate that information transfer is less efficient due to higher noise levels in the system. Additionally, ketamine reduced functional connectivity between layer 6 and VPM. The abnormal late-stage activity observed in the study may reflect deficits in post-inhibitory rebound activity caused by abnormal burst firing.

In Chapter 4, we discussed the role of thalamic synaptic inhibition in regulating ocular dominance (OD) plasticity in the dLGN and V1 of adult mice. We found that thalamic synaptic inhibition is crucial for OD plasticity, and its absence possibly causes changes in the firing properties of thalamic neurons, affecting spike-timing dependent plasticity in both dLGN and V1. We also studied how corticothalamic (CT) feedback affected thalamic OD plasticity and found that silencing primary visual cortex (V1) did not affect the OD shift in dLGN of adult mice, although it did have an effect during the critical period. We suggest that these findings have important implications for understanding developmental disorders as changes in cortical organization, function, or plasticity may have a thalamic origin, and deficits in thalamic organization may have a cortical origin.

In Chapter 5, studied how CB1 receptors on astrocytes affect critical period regulation and plasticity in the primary visual cortex (V1). We found that astrocytic CB1 receptors are necessary for inhibitory synaptic maturation in L2/3 pyramidal neurons, which is an important factor in regulating the onset and closure of the critical period. The absence of astrocytic CB1 receptors surprisingly did not affect endocannabinoid-mediated long-term depression (iLTD). We also demonstrated that CB1 receptors in astrocytes, but not in interneurons, are necessary for ocular dominance (OD) plasticity in V1. Animals lacking astrocytic CB1 receptors exhibited reduced plasticity in all layers of V1. We concluded the early CB1R removal from astrocytes affects OD plasticity in all layers by interfering with the development of inhibitory synapses, which is required for critical period opening.

NEDERLANDSE SAMENVATTING

Het werk dat in dit proefschrift wordt gepresenteerd is gericht op het onderzoeken van de functies en het mechanismen van het corticothalamus-thalamocorticale netwerk in schizofrenie en ervaringsafhankelijke plasticiteit, waarbij hun mogelijke verband verder wordt besproken.

In hoofdstuk 2 onderzochten we de effecten van ketamine op het corticothalamus circuit (CTC) systeem. Uit het onderzoek bleek dat een lage dosis ketamine een afname van de spindelactiviteit in het CTC-systeem en een toename van gamma- en hogerfrequente oscillaties veroorzaakt. Deze activiteitspatronen zijn vergelijkbaar met die tijdens de natuurlijke REM-slaap en kunnen worden geïnterpreteerd als een pathologisch REM-slaap-achtig alertheidsniveau. Uit het onderzoek bleek ook dat ketamine ervoor zorgt dat thalamische neuronen van burst-vuren overschakelen naar tonisch aktiepotentiaal (AP)-vuren. Mogelijk verstoort dit de vuurpatronen van deze neuronen veroorzaakt het een afname van spindeloscillaties. Deze effecten zijn mogelijk het gevolg van een minder gehyperpolariseerde membraanpotentiaal van de neuronen, waardoor de T-type calciumkanalen in een geïnactiveerde toestand blijven. Verder suggereert het onderzoek dat de aanhoudende thalamus gamma hyperactiviteit geïnduceerd door ketamine, een indirect effect kan zijn, veroorzaakt door disinhibitie van corticale neuronen die zowel de thalamus reticulaire nucleus (TRN) als thalamocorticale (TC) cellen innerveren. Over het geheel genomen concludeert het onderzoek dat ketamine veranderingen in alertheidsniveaus kan induceren en spindelactiviteit kan verminderen, mogelijk door veranderingen in het vuurpatroon van het CTC-systeem.

In hoofdstuk 3 onderzochten we de effecten van ketamine op de late fase van sensorische reacties tijdens sedatie. Uit het onderzoek bleek dat ketamine de baseline thalamus bèta- en gamma-oscillatoire activiteit verhoogt, terwijl het de sensorisch-geïnduceerde gamma- en bèta-activiteit vermindert. De verstoring van sensorische informatie veroorzaakt door ketamine kan langdurig zijn en de sensorische informatieverwerking schaden door een lage signaalruisverhouding. Voor het onderzoek werd gebruik gemaakt van multischaal entropie (MSE) analyse om veranderingen in informatie te kwantificeren. Dit maakte duidelijk dat neurale activiteit in de ventrale posteromediale kern van de thalamus (VPM) en in laag 6 van de somatosensorische cortex een verhoogde complexiteit vertoonde na toediening van ketamine. Dit resultaat kan erop wijzen dat informatieoverdracht minder

efficiënt is door hogere ruisniveaus in het systeem. Bovendien vermindert ketamine de functionele connectiviteit tussen laag 6 en VPM. De abnormale late-fase activiteit (>200 ms) die wij waarnamen in de studie kan duiden op een afname van post-inhibitory rebound activiteit veroorzaakt door abnormaal burst vuren.

In hoofdstuk 4 bestudeerden we de rol van thalamische synaptische inhibitie in het reguleren van oculaire dominantie (OD) plasticiteit in de dorsolaterale geniculate kern (dLGN) van de thalamus en de primaire visuele schors (V1) van volwassen muizen. We ontdekten dat thalamische synaptische inhibitie cruciaal is voor OD plasticiteit in beide structuren. De afwezigheid van deze inhibitie veroorzaakt veranderingen van de temporele eigenschappen van de activiteit van thalamische neuronen. Mogelijk beinvloedt dit de spike-timing afhankelijke plasticiteit in zowel dLGN als V1. We bestudeerden ook hoe corticothalamische (CT) feedback OD plasticiteit in de thalamus beïnvloedt en ontdekten dat het uitschakelen van de primaire visuele cortex (V1) geen effect heeft op de OD verschuiving in dLGN van volwassen muizen, hoewel het wel een effect heeft tijdens de kritieke periode. We verwachten dat deze bevindingen belangrijke implicaties hebben voor het begrijpen van ontwikkelingsstoornissen van het brein. Ze tonen aan dat veranderingen in de corticale organisatie, functie of plasticiteit een thalamische oorsprong kunnen hebben, en afwijkingen in de thalamische organisatie een corticale oorsprong kunnen hebben.

In Hoofdstuk 5 bestudeerden we hoe de cannabinoïde receptor type 1 (CB1 receptor) op astrocyten de regulatie van de kritieke periode en plasticiteit kan beïnvloeden in de primaire visuele cortex (V1). We ontdekten dat astrocytaire CB1 receptoren nodig zijn voor de rijping van remmende synapsen op piramidaalcellen in lagen 2 en 3 van V1. Deze inhibitoire synapsen zijn een belangrijke factor bij het reguleren van het begin en einde van kritische perioden tijdens de ontwikkeling van V1. We ontdekten dat de afwezigheid van astrocytaire CB1-receptoren verrassend genoeg geen invloed heeft op endocannabinoïde-gemedieerde lange-termijn depressie (iLTD). We toonden ook aan dat CB1 receptoren op astrocyten, maar niet op inhibitoire interneuronen, noodzakelijk zijn voor OD plasticiteit in V1. Dieren zonder astrocytaire CB1 receptoren vertonen verminderde OD plasticiteit in alle lagen van V1. We concluderen dat de vroege verwijdering van CB1R uit astrocyten de OD-plasticiteit beïnvloedt door het verstoren van de ontwikkeling van remmende synapsen, die nodig zijn voor de opening van de kritischre periode.

List of publications

Mahdavi A[1], **Qin Y[1]**, Aubry AS, Cornec D, Kulikova S, Pinault D. A single psychotomimetic dose of ketamine decreases thalamocortical spindles and delta oscillations in the sedated rat. ***Schizophrenia Research***. 2020; Aug; 222:362-374. **(Co-first author)**.

Qin Y, Mahdavi A, Bertschy M, Anderson PM, Kulikova S, Pinault D. The psychotomimetic ketamine disrupts the transfer of late sensory information in the corticothalamic network. ***European Journal of Neuroscience***. 2022 Oct 13.

Qin Yi, Ahmadlou Mehran, Suhai Samuel, Neering Paul, de Kraker Leander, Heimel J. Alexander, Levelt Christiaan N. (2023) Thalamic regulation of ocular dominance plasticity in adult visual cortex. ***eLife*** 12:RP88124.

Rogier Min, **Yi Qin**, Sven Kerst, Mohammad Hadi Saiepour, Mariska van Lier, Beat Lutz, Giovanni Marsicano and Christiaan N. Levelt. Astrocyte CB1 receptors are required for inhibitory maturation and ocular dominance plasticity in the mouse visual cortex. (in preparation)

van Lier M, Saiepour MH, Kole K, Cheyne JE, Zabouri N, Blok T, **Qin Y**, Ruimschotel E, Heimel JA, Lohmann, C, Levelt CN. Disruption of Critical Period Plasticity in a Mouse Model of Neurofibromatosis Type 1. ***Journal of Neuroscience***. 2020 Jul 8;40(28):5495-5509.

Xing Y, **Qin Y**, Jing W, Zhang Y, Wang Y, Guo D, Xia Y, Yao D. Exposure to Mozart music reduces cognitive impairment in pilocarpine-induced status epilepticus rats. ***Cognitive Neurodynamics***. 2016 Feb;10(1):23-30.

Portfolio

Name PhD student: Yi Qin PhD period: September 2015 – December 2023 Names of PhD supervisor(s) & co-supervisor(s): Diddier Pinault; Pieter Roelfsema; Christiaan Levelt		
1. PhD training Courses		
	Year	ECTS
Dutch Language Course (KNAW)	2020	1
Scientific writing in English (KNAW)	2019	0.5
Laboratory animal science (KNAW)	2016	3.6
Technical advances in RNA biology- challenges and opportunities (Strasbourg)	2016	0.16
L'Hyglene et a le securite des noveaux entrants a l'IGBMC (Strasbourg)	2015	0.2
Sensitisation to entrepreneurship or the thesis work viewed from the entrepreneurship point of view (Strasbourg)	2016	0.5
Workshop ' The attentive brain, the deluded brain - what is reality' (Strasbourg)	2015	0.9

2. Seminars and conferences		
	Year	ECTS
Weekly Journal Club	2015-2023	7
Weekly lab meeting	2015-2023	7
Neuroscience Symposium (NIN)	2015-2023	7
European Visual Cortex Meeting	2019	1
Fens Forum	2018	1

Résumé étendu en français

Le travail présenté dans ce mémoire consistait à étudier avec des modèles murins les propriétés fonctionnelles et dysfonctionnelles du circuit cortico-thalamo-cortical (CTC) afin de comprendre certains aspects des mécanismes qui sous-tendent la schizophrénie (Strasbourg) ainsi que la plasticité neuronale dépendante de l'expérience visuelle (Amsterdam). Leurs possible liens sont discutés.

Dans les troubles psychotiques, comme la schizophrénie, sont fréquents des troubles du sommeil, des comportements anormaux, des déficits cognitifs, des anomalies moléculaires et génétiques et des oscillations neurales aberrantes (ou oscillopathies). Par exemple, les oscillations électro-encéphalographiques ou EEG du sommeil (fuseaux et ondes delta) sont diminuées. Les oscillations neurales sont des électro-biomarqueurs de l'état de connectivité au sein de systèmes hautement distribués, qui incluent les voies corticothalamiques (CT) et thalamocorticales (TC). Les oscillopathies peuvent être enregistrées dès la phase prodromique. Grâce à ses propriétés bioélectriques de type oscillatoire, le thalamus joue un rôle central dans le processus et le transfert d'informations spécifiques (sensorielles et motrices) et contextuelles lors des traitements sensori-moteurs, cognitifs et émotionnels ascendants et descendants (connexions fonctionnelles mutuelles entre les structures corticales et sous-corticales). Le traitement et le transfert des informations sont affectés dans la maladie. La plasticité corticale visuelle est, elle-aussi, altérée. De nombreuses évidences cliniques et expérimentales s'accumulent au fil des ans soutenant à la fois l'implication du thalamus et des transmissions glutamatergiques (récepteurs au glutamate de type NMDA) et GABAergiques dans les troubles psychiatriques et la plasticité neuronale. Les modèles pharmacologiques et génétiques de l'antagonisme des récepteurs NMDA reproduisent les symptômes et les oscillopathies enregistrés chez les patients psychiatriques. Une administration systémique unique à une dose subanesthésique de kétamine, un antagoniste non compétitif des récepteurs NMDA du glutamate, reproduit transitoirement, chez l'homme et le rongeur, les oscillopathies avec un tableau clinique rappelant la transition psychotique. Un tel modèle pharmacologique aigu pourrait aider la recherche et le développement de traitements innovants chez des patients avec un état mental à haut risque vers une conversion psychotique.

Chapitre 2 : En combinant des enregistrements EEG et cellulaires durant le sommeil à ondes lentes chez le rat adulte, nous avons étudié l'effet psychotomimétique de la kétamine sur les réponses du circuit CTC à une stimulation sensorielle. Une dose subanesthésique de kétamine entraîne une diminution des fuseaux EEG du sommeil et une augmentation de la puissance des oscillations gamma (30-80 Hz) et des oscillations à plus haute fréquence. Ces patrons d'activités rapides (hyperactivité gamma) et persistant rappellent ceux observés dans la schizophrénie ainsi que ceux associés au sommeil paradoxal naturel. Parallèlement, la kétamine change le mode de décharge des neurones thalamiques, du mode courte (20-30 ms) rafale à haute fréquence (200-500ms) (mode phasique) de potentiels d'action au mode potentiel d'action isolé (mode tonique et irrégulier). Cet effet est dû à une variation du potentiel de membrane qui devient moins hyperpolarisé sous l'influence de la kétamine. En effet, l'hyperpolarisation (< -60 mV), naturellement très dominante durant le sommeil, dé-inactive les courants calciques de type T qui sont à l'origine du mode phasique. Cette hyperactivité gamma thalamique persistante induite par la kétamine pourrait être un effet indirect causé par la désinhibition des neurones CT qui innervent à la fois les neurones GABAergiques du noyau réticulaire thalamique (TRN) et les neurones TC glutamatergiques. Ces résultats soutiennent l'hypothèse selon laquelle un hypofonctionnement des récepteurs NMDA est impliqué dans la réduction des oscillations du sommeil (fuseaux et oscillations delta) observée dans la schizophrénie. La conversion rapide induite par la kétamine des activités TC-TRN impliquerait à la fois le système réticulaire ascendant et la voie CT.

Chapitre 3 : Dès la phase prodromique de la schizophrénie, les déficits de perception sensorielle observés sont associés à une réduction de la synchronisation de phase des oscillations dans la large bande de fréquence bêta-gamma (20-60 Hz). Cela suggère une diminution en puissance des oscillations induites par une stimulation sensorielle durant la période tardive (> 200 ms), celle qui est associée au processus perceptuel. De nombreuses observations indiquent une diminution des oscillations bêta-gamma induites chez les individus présentant un état mental cliniquement à risque de transition vers la psychose. La diminution de la puissance et de la synchronisation des oscillations gamma induites par une tâche

cognitive ou une stimulation sensorielle peuvent être dues à l'amplification anormale des oscillations gamma basales (ou spontanées) enregistrées chez ces patients. En effet, dans notre modèle kétamine murin, les oscillations bêta-gamma évoquées à courte latence (< 100 ms, ou précoces) par une stimulation sensorielle diminuent alors que les oscillations gamma spontanées – survenant plusieurs secondes avant ou après toute stimulation sensorielle - augmentent, confortant l'hypothèse d'une réduction du rapport signal (réponse)/bruit (oscillations basales). Ces résultats soutiennent l'hypothèse selon laquelle le dysfonctionnement du réseau CTC induit par la kétamine entraîne un brouillage de l'information sensorielle.

C'est pourquoi nous avons étudié les effets du blocage des récepteurs NMDA par la kétamine au sein du système CTC sur les oscillations bêta-gamma induites, c'est-à-dire tardives (survenant 200 à 700 ms après une stimulation sensorielle). Les oscillations gamma induites étaient enregistrées chez des rats légèrement anesthésiés. Dans ces conditions, des enregistrements EEG étaient combinés avec des enregistrements extracellulaires multisites (cortex et thalamus) au sein du système somatosensoriel (vibrisses). L'analyse spectrale et la cohérence de connectivité ont été utilisées pour estimer, respectivement, le niveau de synchronisation et la connectivité fonctionnelle entre les sites d'enregistrement. La mesure de cohérence montre le niveau de synchronisation entre deux signaux en fonction de la cohérence de phase. Les signaux EEG et extracellulaires sont relativement complexes car ils sont générés par plusieurs oscillateurs corticaux et sous-corticaux en interaction. La complexité de ces signaux, liée aux aspects fonctionnels des réseaux neuronaux correspondants, peut être évaluée avec des analyses non linéaires telles que l'analyse entropique multi-échelle (MSE). La MSE a déjà été appliquée à l'EEG de patients psychiatriques. Une MSE plus élevé indique une augmentation de la complexité des signaux variant dans le temps, suggérant ainsi des perturbations dans la connectivité temporelle durant les processus d'intégration temporelle au sein des circuits hautement distribués comme les systèmes CTC. Ainsi, pour tenter de mesurer la complexité dynamique du système TC à plusieurs échelles de temps, la MSE a été appliquée aux enregistrements extracellulaires. Nos résultats montrent que, dans le système somatosensoriel CTC, la kétamine augmentait de manière transitoire la puissance des oscillations gamma basale et diminuait les oscillations gamma induites par la stimulation sensorielle. En outre, elle perturbait la transférabilité des

informations à la fois dans le thalamus somatosensoriel et dans le cortex associé et diminuait la connectivité TC dans la bande de fréquence bêta-gamma induite par le stimulus. En conclusion, nos résultats soutiennent l'hypothèse selon laquelle l'antagonisme des récepteurs NMDA perturbe le transfert d'informations associé à un processus perceptuel dans le système CTC somatosensoriel.

Chapitre 4 : Dans le système visuel adulte, la plasticité dépendante de l'expérience est généralement considérée comme un processus cortical. La façon dont la plasticité dans le thalamus et le cortex interagit dans le système visuel adulte est mal comprise. Ici, nous avons exploré le rôle du réseau CT dans la plasticité dépendante de l'expérience. Nous cherchons à comprendre comment la plasticité dans le thalamus et le cortex interagit dans le système visuel adulte. Pour évaluer l'influence de la plasticité thalamique sur la plasticité de V1 (aire visuelle primaire) chez les animaux adultes, nous avons utilisé des enregistrements multi-électrodes dans V1 et dans le dLGN (noyau thalamique visuel) chez des souris adultes WT et des souris KO à sous-unité GABA alpha1 thalamique. Nous avons également réduit au silence V1 pendant les enregistrements thalamiques pour étudier le rôle de V1 dans la plasticité thalamique de l'OD (dominance oculaire).

C'est pourquoi nous avons examiné le rôle de l'inhibition synaptique thalamique dans la régulation de la plasticité de l'OD dans le dLGN et V1 de souris adultes. Nous avons mis en évidence que l'inhibition synaptique thalamique est cruciale pour la plasticité de l'OD et que son absence peut entraîner des changements dans les propriétés de déclenchement des neurones thalamiques, affectant la plasticité dépendante de la synchronisation des décharges à la fois dans le dLGN et dans V1. Nous avons également étudié comment le feedback (CT) affectait la plasticité thalamique de l'OD et nous avons constaté que la mise sous silence du cortex visuel primaire (V1) n'affectait pas le déplacement de l'OD dans le dLGN de souris adultes, bien qu'elle ait eu un effet pendant la période critique. Nous pensons que ces résultats ont des implications importantes pour la compréhension des troubles du développement, car les changements dans l'organisation, la fonction ou la plasticité corticale peuvent avoir une origine thalamique, et les déficits dans l'organisation thalamique peuvent avoir une origine corticale.

Chapitre 5 : Les circuits neuronaux sont façonnés par l'expérience. Les endocannabinoïdes, par l'intermédiaire du récepteur cannabinoïde CB1 (CB1R), régulent plusieurs formes de plasticité neuronale. Dans le néocortex en cours de développement, les CB1R jouent un rôle clé dans la maturation des circuits inhibiteurs. Dans ce chapitre, nous étudions le rôle des endocannabinoïdes dans la plasticité neuronale dépendante de l'expérience. Des études antérieures ont mis en évidence le rôle inattendu des CB1R astrocytaires dans la plasticité. Nous examinons donc l'impact de la suppression des CB1R des interneurones ou des astrocytes pendant la période critique de la plasticité de l'OD dans V1. Afin d'explorer comment la perte des CB1Rs selon le type cellulaire affecte la maturation synaptique inhibitrice, nous évaluons la dynamique de la transmission à court terme et de la dépression à long terme dans des tranches de cerveau en phase aiguë. En outre, nous évaluons la plasticité OD par couche chez des souris avec et sans CB1R astrocytaires.

Nous avons donc étudié comment les récepteurs CB1 des astrocytes affectent la régulation de la période critique et la plasticité dans V1. Nous avons découvert que les récepteurs CB1 astrocytaires sont nécessaires à la maturation synaptique inhibitrice des neurones pyramidaux L2/3, ce qui est un facteur important dans la régulation du début et de la fin de la période critique. L'absence de récepteurs CB1 astrocytaires n'a étonnamment pas affecté la dépression à long terme médiée par les endocannabinoïdes. Nous avons également démontré que les récepteurs CB1 dans les astrocytes, mais pas dans les interneurones, sont nécessaires pour la plasticité de l'OD dans V1. Les animaux dépourvus de récepteurs CB1 astrocytaires présentent une plasticité réduite dans toutes les couches de V1. Ces résultats nous ammènent à conclure que l'élimination précoce des CB1R des astrocytes affecte la plasticité de la dominance oculaire dans toutes les couches en interférant avec le développement des synapses inhibitrices, ce qui est nécessaire pour l'ouverture de la période critique.

Mots clés :

Thalamus, ketamine, schizophrenia, ocular dominance, CB1, visiual cortex

Acknowledgement

Eight years ago, as I stood alone at the plane's hatch, preparing to fly from China to Europe, I paused for a moment, feeling a mixture of excitement and nervousness. I knew that my life would never be the same again. Looking back now, I can confidently say I made the right decision, and it has been an incredible journey of my PhD in neuroscience. This experience has been a transformative and enriching chapter in my life, and I credit my success to the support and encouragement of many remarkable individuals.

First and foremost, I would like to express my heartfelt gratitude to my devoted supervisors, Christiaan and Didier. Their unwavering guidance, intellectual insights, and dedication to my research have been instrumental in shaping my academic growth. But they did more than that; they extended their support to many aspects of my life in Europe, providing me with a sense of belonging and security in a foreign land. Their mentorship has left an indelible mark on my academic journey, and for that, I am truly thankful.

I extend my sincere appreciation to the members of my defense committee, Prof. Roelfsema, Prof. Wierenga, Prof. Pennartz, Dr. Olcese, Prof. Uhlhaas, Dr. Kaufling, Prof. Veinante, Dr. Darbon, for their insightful feedback and rigorous examination of my thesis. Your expertise and constructive criticism have added immense value to my research and have contributed to the quality of this work.

I would also like to thank my exceptional lab colleagues from France and the Netherlands, who shared this academic adventure with me. To me, you guys are more than colleagues but also my friends in Europe. Marine and Ali, I will always remember the happy lunch hours we spent together in Strasbourg. Koen, Leander, Laura, Valentina, Paul, Huub, Emma, Mariska, Hadi, Prem, Leonie, Robbin, Rasa, and Jorrit, you guys' companionship is the best gift for me in these eight years. You opened my eyes to understanding European culture. The intellectual camaraderie, collaborative spirit, and the countless discussions we shared have greatly enriched my research and personal growth. Your friendship and support have been invaluable. Special thanks to Alexander and Merhan, you are my saviors in Matlab and electrophysiology!

I would also like to thank all my Chinese PhD friends in the Netherlands, who shared this academic 'journey to the west' with me: Lihui, Yulan, Yuting, Feng, Ziting, XinYu, Jian, and Shirong. Thanks for your support!

Special thanks to my best friends in the Netherlands: Miki, Huiying, Zora, Xiangru, and Angus. I will never forget the weekends we spent together! Also, my friends faraway in China: Nan, Mingyang, Agnes, Hongye, Wei, Lengyao, Manqian, Shuyu, Luotuo, Yoko Neko, Wakey Wakey, Starman, Cuicui-shark.

At last, I would like to thank my beloved mother, father, and all family members. Thanks for all you have done for me throughout my life.

This thesis is dedicated to my grandma and uncle in the heaven.
谨以此书献给在我留学期间离世而未见上最后一面的奶奶和舅舅。

Université de Strasbourg

Yi QIN

École doctorale Sciences de la vie et de la santé | ED 414
Université de Strasbourg

La symphonie thalamocorticale : comment le thalamus et le cortex s'accordent ensemble dans la schizophrénie et la plasticité

Résumé

La thèse explore la fonction et le mécanisme du réseau corticothalamique-thalamocortical dans la schizophrénie et la plasticité dépendante de l'expérience. Nos résultats révèlent que la kétamine induit des oscillations anormales dans le système CTC et des déficits de perception sensorielle dans la schizophrénie. Nous avons également exploré la plasticité dépendante de l'expérience, en soulignant le rôle de l'inhibition synaptique thalamique dans la plasticité de la dominance oculaire et l'influence de la rétroaction corticale. Nous avons étudié l'implication des récepteurs CB1 dans la maturation synaptique inhibitrice et la plasticité de la dominance oculaire dans le cortex visuel primaire. La discussion générale soulève la possibilité d'un lien entre la plasticité neuronale et la schizophrénie, en particulier pendant la phase de transformation de l'adolescence, lorsque le cerveau subit des changements significatifs.

Résumé en anglais

The thesis explores the function and mechanism of corticothalamic-thalamocortical network in schizophrenia and experience-dependent plasticity. Our findings reveal that ketamine induces abnormal oscillations in the CTC system and sensory perception deficits in schizophrenia. We also explored experience-dependent plasticity, highlighting the role of thalamic synaptic inhibition in ocular dominance plasticity and the influence of cortical feedback. We investigated the involvement of CB1 receptors in inhibitory synaptic maturation and ocular dominance plasticity within the primary visual cortex. The general discussion raises the possibility of a link between neural plasticity and schizophrenia, particularly during the transformative phase of adolescence when the brain undergoes significant changes.